

# **CONSOLIDATION CHARACTERISTICS OF NON-HOMOGENEOUS CLAY LAYERS UNDER TIME DEPENDENT LOADING**

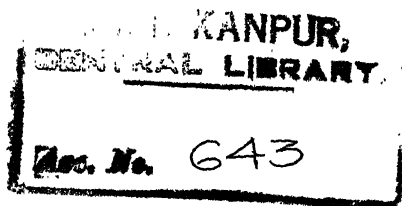


**A THESIS SUBMITTED**

In Partial Fulfilment of the Requirements

FOR THE DEGREE OF

**DOCTOR OF PHILOSOPHY**



**CE-1970-D-KUP-CON**

*By*  
**T. KUPPUSAMY**

**POST GRADUATE OFFICE**  
This thesis has been approved  
for the award of the Degree of  
Doctor of Philosophy (Ph.D.)  
in accordance with the  
regulations of the Indian  
Institute of Technology Kanpur  
Dated: 9/1/71

**to the**

**DEPARTMENT OF CIVIL ENGINEERING  
INDIAN INSTITUTE OF TECHNOLOGY KANPUR**

**SEPTEMBER 1970**

## CERTIFICATE

Certified that this work on "Consolidation Characteristics of Non-homogeneous Clay Layers under Time Dependent Loading", has been carried out under my supervision and that this has not been submitted elsewhere for a degree.

*M. Anandakrishnan*  
 ( M. ANANDAKRISHNAN )  
 Professor  
 Department of Civil Engineering

This thesis has been approved for the award of the Degree of Doctor of Philosophy in accordance with the regulations of the Indian Institute of Technology, Kanpur.

( M. ANANDAKRISHNAN )  
 Professor  
 Department of Civil Engineering

POST GRADUATE OFFICE
This thesis has been approved for the award of the Degree of Doctor of Philosophy (M. Phil.) in accordance with the regulations of the Indian Institute of Technology Kanpur.

## CERTIFICATE

Certified that Mr. T. Kuppusamy credited the following courses in partial fulfilment of the requirements for the Degree of Doctor of Philosophy.

Course Number	Name	Grade
CE 639	Theoretical Soil Mechanics	A
CE 640	Rock Mechanics	A
ME 681	Mathematical Methods in Engineering	B
CE 638	Clay Mineralogy	A
CE 650	Engineering Analysis	B
CE 615	Ground-water Hydrology	A
CE 637	Application of Soil Mechanics	A
CE 697	Special Topics in Soil Mechanics	A

He obtained a Cumulative Point Index of 9.50/10.0 in the course work and passed the Comprehensive Examination in May 1969.

*M. Anandakrishnan*  
 ( M. ANANDAKRISHNAN )  
 Professor  
 Department of Civil Engineering

## ACKNOWLEDGEMENTS

The author expresses his deep sense of gratitude to Dr. M. Anandakrishnan, Professor of Civil Engineering, Indian Institute of Technology Kanpur, for his continuous guidance, invaluable suggestions and encouragements during the entire phase of this study.

Gratitude is recorded to Dr. P.C. Dass of Mathematics Department and Dr. A.M. Richardson of Civil Engineering Department, Indian Institute of Technology Kanpur, for some of the valuable discussions. The author is indebted to Mr. N.R. Krishnaswamy for some of the useful discussions and his cheerful friendship. Sincere thanks are due to Mr. K.V. Lakshmidhar and Mr. R.P. Trivedi for their unfailing support in the laboratory.

The financial support by the Civil Engineering Department and the Computer facilities by the Computer Centre, I.I.T. Kanpur, are gratefully acknowledged. The author expresses his appreciation to Mr. R.P. Trivedi and Mr. Rameshwar Lal for typing this thesis and to Mr. J.C. Verma for preparing the drawings. Thanks are due to Mr. Venkatraman and Mr. A. Varadharajan for their help in proof reading. Sincere appreciation is recorded to Raji, the author's wife, for her cheerful assistance and co-operation.

## TABLE OF CONTENTS

	<u>Page</u>
TITLE	i
CERTIFICATE	ii
ACKNOWLEDGEMENTS	iv
TABLE OF CONTENTS	v
LIST OF FIGURES	vii
LIST OF TABLES	xvi
LIST OF SYMBOLS	xvii
SYNOPSIS	xx
CHAPTER I INTRODUCTION TO THE PROBLEM	1
CHAPTER II CONSOLIDATION OF THICK CLAY LAYER WITH VARYING PARAMETERS	12
Thick Clay Layer with Space Variation of k, m and C	13
Thick Clay Layer with General Variation of k, m and C	25
Conclusions	33
CHAPTER III CONSOLIDATION OF LAYERED SYSTEM UNDER INSTANTANEOUS LOADING	63
Two-Layer Systems	68
Three-Layer Systems	72
Conclusions	74
CHAPTER IV CONSOLIDATION OF LAYERED SYSTEMS UNDER TIME DEPENDENT CONSTRUCTION TYPE OF LOADING	100

	<u>Page</u>
Single Layer	101
Two-Layer System with Two-Way Drainage	105
Two-Layer System with One-Way Drainage	110
Comparison of Terzaghi's Method with Rigorous Analytical Solution for Single Layer	113
Three-Layer System	114
Conclusions	116
CHAPTER V      EXPERIMENTAL STUDY OF CONSOLIDATION IN LAYERED SYSTEMS	128
Experimental Set-up	129
Soils Tested	129
Testing Procedure	130
Conclusions	135
CHAPTER VI     CONCLUSIONS AND RECOMMENDATIONS	167
LIST OF REFERENCES	171
APPENDIX	176
VITA	183

## LIST OF FIGURES

<u>Figure Number</u>		<u>Page</u>
1.1	Thin Layer	10
1.2	Layered System	10
1.3	Thick Layer	10
1.4	Variation of Parameters with Depth	10
1.5	Construction Loading	11
1.6	Instantaneous Loading	11
1.7	Variation of Parameters with Pore Pressure	11
1.8	General Variation of the Parameters	11
2.1	Finite Difference Mesh	36
2.2	Case 1	36
2.3	Case 2	36
2.4	Case 3	37
2.5	Case 4	37
2.6	Case 5	37
2.7	Case 6	37
2.8	Boundaries in Consolidation Problem	37
2.9	Consolidation of Thick Layer with Two Face Drainage	38
2.10	Pore Pressure Distribution in Thick Layer	39
2.11	Consolidation of Thick Layer with Two Face Drainage	40

<u>Figure Number</u>		<u>Page</u>
2.12	Consolidation of Thick Layer with Two Face Drainage	41
2.13	Consolidation of Thick Layer with Single Face Drainage	42
2.14	Consolidation of Thick Layer with Single Face Drainage	43
2.15	Consolidation of Thick Layer with Single Face Drainage	44
2.16	Consolidation of Thick Layer with Single Face Drainage	45
2.17	Consolidation of Thick Layer under Construction Loading	46
2.18	Consolidation of Thick Layer under Construction Loading	47
2.19	Consolidation of Thick Layer under Construction Loading	48
2.20	Consolidation of Thick Layer under Construction Loading	49
2.21	Consolidation of Thick Layer under Construction Loading	50
2.22	Consolidation of Thick Layer under Construction Loading	51
2.23	Consolidation of Thick Layer under Construction Loading	52

<u>Figure Number</u>		<u>Page</u>
2.24	Consolidation of Thick Layer under Construction Loading	53
2.25	Consolidation of Thick Layer under Construction Loading	54
2.26	Average Pore Pressure Ratios under Construction Loading	55
2.27	Average Pore Pressure Ratios under Construction Loading	56
2.28	Average Pore Pressure Ratios under Construction Loading	57
2.29	Average Pore Pressure Ratios under Construction Loading	58
2.30	Effect of Individual Decrease of k and m with Pore Pressure	59
2.31	Effect of Decrease of k and m with Pore Pressure	60
2.32	Effect of General Variation of k and m with Constant C	61
2.33	Effect of General Variation of k and m	62
3.1	Finite Difference Mesh	75
3.2	Two Layer with Two Way Drainage	75
3.3	Two Layer with One Way Drainage	75
3.4	Three Layer with Two Way Drainage	75
3.5	Three Layer with One Way Drainage	75

<u>Figure Number</u>		<u>Page</u>
3.6	Consolidation of Two Layer System with Constant m	76
3.7	Consolidation of Two Layer System with Constant m	77
3.8	Consolidation of Two Layer System with Constant m	78
3.9	Consolidation of Two Layer System with Constant m	79
3.10	Consolidation of Two Layer System with Constant m	80
3.11	Consolidation of Two Layer System with Two Way Drainage	81
3.12	Consolidation of Two Layer System with Constant C	82
3.13	Consolidation of Two Layer System with Constant C	83
3.14	Consolidation of Two Layer System with One Way Drainage	84
3.15	Consolidation of Two Layer System with One Way Drainage	85
3.16	Consolidation of Two Layer System with Constant k	86
3.17	Consolidation of Two Layer System with Constant k	87

<u>Figure Number</u>		<u>Page</u>
3.18	Consolidation of Two Layer System	88
3.19	Consolidation of Two Layer System	89
3.20	Consolidation of Bottom Layer	90
3.21	Consolidation of Bottom Layer	90
3.22	Consolidation of Bottom Layer	91
3.23	Consolidation of Bottom Layer	91
3.24	Consolidation of Bottom Layer	92
3.25	Consolidation of Bottom Layer	92
3.26	Consolidation of Top Layer	93
3.27	Consolidation of Top Layer	93
3.28	Consolidation of Top Layer	94
3.29	Consolidation of Top Layer	94
3.30	Consolidation of Top Layer	95
3.31	Consolidation of Top Layer	95
3.32	Consolidation of A Three Layer System	96
3.33	Consolidation of A Three Layer System	97
3.34	Consolidation of A Three Layer System	98
3.35	Consolidation of A Three Layer System	99
4.1	Single Layer with Two Way Drainage	117
4.2	Two Layer System with Two Way Drainage	117
4.3	Two Layer System with One Way Drainage	117
4.4	Comparison of Finite Difference Solution and Analytical Solution for a Single Layer, Two Way Drainage . During Construction	118

<u>Figure Number</u>		<u>Page</u>
4.5	Comparison of Finite Difference Solution and Analytical Solution for a Single Layer, Two Way Drainage - after Construction	119
4.6	Average Pore Pressure Ratios for a Two Layer System with One Way Top Drainage During Construction	120
4.7	Average Pore Pressure Ratios for a Two Layer System with One Way Top Drainage During Post-construction Period	121
4.8	Average Pore Pressure Ratios for a Two Layer System with One Way Top Drainage During Construction	122
4.9	Average Pore Pressure Ratios for a Two Layer System with One Way Top Drainage During Post-construction Period	123
4.10	Comparison of Finite Difference Solution and Analytical Solution for Two Layer System - Two Way Drainage for Construction Loading - Layer 2	124
4.11	Comparison of Finite Difference Solution and Analytical Solution for Two Layer System - Two Way Drainage for Construction Loading - Layer 1	125

<u>Figure Number</u>		<u>Page</u>
4.12	Comparison of Terzaghi's Method for a Single Layer under Construction Loading	126
4.13	Consolidation of a Three Layer System under Construction Loading	127
5.1	Oedometer for Multilayer System	137
5.2	Consolidation Apparatus	138
5.3	Grain Size Distribution Curves	139
5.4	Coefficient of Consolidation	140
5.5	Void Ratio Pressure Curve	141
5.6	Consolidation of Single Layer under Construction Loading	142
5.7	Consolidation of Single Layer under Construction Loading	143
5.8	Consolidation of Single Layer under Construction Loading	144
5.9	Consolidation of Single Layer under Construction Loading	145
5.10	Consolidation of Single Layer under Construction Loading	146
5.11	Average Pore Pressure Ratios in a Single Layer under Construction Loading	147
5.12	Average Pore Pressure Ratios in a Single Layer under Construction Loading	148

<u>Figure Number</u>		<u>Page</u>
5.13	Average Pore Pressure Ratios in a Single Layer under Construction Loading	149
5.14	Average Pore Pressure Ratios in a Single Layer under Construction Loading	150
5.15	Consolidation of Two Layer System - Instantaneous Loading	151
5.16	Consolidation of Two Layer System - Instantaneous Loading	152
5.17	Consolidation of Two Layer System - Instantaneous Loading	153
5.18	Consolidation of Two Layer System - Instantaneous Loading	154
5.19	Consolidation of Two Layer System - Instantaneous Loading	155
5.20	Consolidation of Three Layer System - Instantaneous Loading	156
5.21	Consolidation of Three Layer System - Instantaneous Loading	157
5.22	Consolidation of Two Layer System under Construction Loading	158
5.23	Consolidation of Two Layer System under Construction Loading	159
5.24	Consolidation of Two Layer System under Construction Loading	160.

<u>Figure Number</u>		<u>Page</u>
5.25	Consolidation of Two Layer System under Construction Loading	161
5.26	Consolidation of Two Layer System under Construction Loading	162
5.27	Consolidation of Two Layer System under Construction Loading	163
5.28	Consolidation of Two Layer System under Construction Loading	164
5.29	Consolidation of Three Layer System under Construction Loading	165
5.30	Consolidation of Three Layer System under Construction Loading	166

## LIST OF TABLES

<u>Table umber</u>		<u>Page</u>
3.1	Consolidation of the Two Layers	72
5.1	Soil Properties	130
5.2	Permeability Values	131

## LIST OF SYMBOLS

Each symbol is defined when first introduced and some of the common symbols used in this thesis are listed below:

$A_i$	= Roots of the given equation
$a, a_v$	= Coefficient of compressibility (slope of void ratio - pressure curve)
$b, B$	= Arbitrary constants
$C, C_0, C_v$	= Coefficient of consolidation
$d_1, d_2$	= Constants
$D$	= Arbitrary constant
$e$	= Void ratio
$E$	= Arbitrary constant
$F_i$	= The corresponding expression with $A_i$ roots
$F$	= Arbitrary constant
$G$	= Arbitrary constant
$h, H$	= Thickness
$i, j$	= Denoting numbers
$k$	= Coefficient of permeability
$m$	= Coefficient of volume compressibility ( $= \frac{k}{C}$ )
$n$	= Integir values
$N$	= Arbitrary constant
$P$	= Non-dimensional pore pressure quantity
$p$	= Non-dimensional space variable

- $R$  = A constant  
 $S_t$  = Settlement at any time  $t$   
 $t$  = Time variable  
 $t_0$  = Construction period  
 $T$  = Time factor  
 $T_0$  = Time factor corresponding to construction period  
 period  $t_0$   
 $u$  = Point pore pressure  
 $\bar{u}_0$  = Total imposed pressure  
 $\bar{u}$  = Integrated value of point pore pressure  
 throughout the depth  
 $U$  = Consolidation ratio  
 $v_1, v_2, v_3$  = Displacement components  
 $X$  = Non-dimensional space variable  
 $Z$  = Space variable  
 $\bar{\alpha}$  = A parameter in two layer system =  $\frac{k_2}{k_1} \cdot \frac{h_1}{h_2}$   
 $\bar{\beta}$  = A parameter in two layer system =  $\frac{c_2}{c_1} \left( \frac{h_1}{h_2} \right)^2$   
 $\alpha$  = A Parameter  
 $\beta$  = A parameter  
 $\gamma$  = A parameter  
 $\mu$  = A parameter  
 $\sigma$  = A parameter  
 $\nu$  = A parameter

- $\rho_i$  = Settlement at any instant  
 $\rho_{100}$  = Total consolidation settlement  
 $\nabla$  = Operator ( $= \frac{\partial}{\partial x} + \frac{\partial}{\partial y} + \frac{\partial}{\partial z}$ )  
 $\nabla^2$  = Laplace operator ( $= \frac{\partial^2}{\partial x^2} + \frac{\partial^2}{\partial y^2} + \frac{\partial^2}{\partial z^2}$ )  
 $\nabla^4$  = Biharmonic operator ( $= \frac{\partial^4}{\partial x^4} + \frac{\partial^4}{\partial y^4} + \frac{\partial^4}{\partial z^4}$ )  
 $\phi$  = A function of T  
 $\Delta P$  = Incremental load  
 $\Delta x, \Delta z, \delta z$  = Finite difference mesh size, space variable  
 $\Delta t, \Delta T, \delta t$  = Finite difference mesh size, time variable

## SYNOPSIS

T. KUPPUSAMY, Ph.D., Indian Institute of Technology, Kanpur, September 1970, "Consolidation Characteristics of Non-homogeneous Clay Layers under Time Dependent Loading".

The present work involves the study of consolidation behaviour of soils subject to complex field conditions. Detailed analyses are presented for the theoretical consolidation characteristics of a thick layer and multi-layered systems subjected to constant as well as time-dependent loading conditions. In this work a stratum with continuous variation of consolidation parameters with respect to depth is characterised as a thick layer while discontinuous variation of parameters with respect to depth is assumed in a layered system. The time-dependent construction type of loading is assumed as a linearly varying load during the construction period and as constant thereafter. Based on the theoretical investigations of the above field situations and loading environments, comprehensive conclusions on the consolidation behaviour of soils are presented. In some cases, simplified analyses using Terzaghi's original formulation are carried out and compared with the more rigorous analyses presented here.

In a thick clay layer the effects of the variations of the consolidation parameters are studied. The influence of the location of the drainage boundary on the consolidation characteristics of a thick clay layer with single face drainage is investigated. An attempt is made to present a set of design

charts for a thick clay layer for the assumed variation of parameters under time dependent construction type of loading.

A new formulation is made for a non-homogeneous thick clay deposit consolidating with varying parameters during the process of consolidation. In this case the parameters are functions of depth and the pore pressure as consolidation progresses. The effects of the above general variation of parameters are analysed. This formulation leads to a non-linear equation, the solution of which is obtained by step by step numerical integration.

In layered systems the effects of extreme ranges of parameters of individual layers are investigated. A set of design charts in a two layer system is attempted for a possible range of parameters.

Rigorous mathematical analyses of layered systems under construction loading are presented. Closed form solutions for single and two layer system under construction loading are obtained. A three layer system is analysed by numerical method. The solutions are illustrated with examples.

A simple experimental set-up is devised for testing layered systems under construction type of loading. The experimental results of layered systems up to three layers under instantaneous as well as construction type of loading are compared with the results obtained by analytical procedures.

## CHAPTER I

### INTRODUCTION TO THE PROBLEM

#### General

Till today the essential basis of settlement analysis is the one-dimensional consolidation theory as proposed by Terzaghi (43) four decades ago. The general success of this theory in predicting the field settlements has been one of the strongest incentives in the earlier developments of the soil mechanics science. An adequate summary embodying all the further advances in the consolidation theory is not possible in view of the extensive consolidation literature. However, appropriate developments related to the present research work undertaken are reviewed in subsequent chapters. Though the state-of-art of settlement prediction has been streamlined by simplified theories, the heterogeneous nature of soil deposits still offers considerable challenge in applying the idealised theoretical models to real engineering problems. At best, most of the theories can serve as tools in arriving at a rational engineering judgement. With the developments in computation technique and improved laboratory equipments, it has now become possible to develop solutions for complex cases. These solutions can offer better insight about the consolidation behaviour of soils under field conditions than those obtained from highly simplified models. All the numerical computations in this study are done with the help of the digital computer I.B.M. 7044.

## CONSOLIDATION THEORIES

The extensive research works carried out by many research workers in the past following Terzaghi's theory can be categorised mainly as follows:

- a. Mathematical analysis
- b. Testing procedure and material properties
- c. Application to field problems

### Mathematical analysis

The overall process of consolidation consists of a fluid flow mechanism in a compressible material. From the continuity equation of compressible material, Terzaghi derived for one-dimensional case the basic differential equation for consolidation akin to the diffusion equation in heat-transfer literature as:

$$C \frac{\partial^2 u}{\partial z^2} = \frac{\partial u}{\partial t} \quad (1.1)$$

An extension of the above equation to three dimensional case leads to the equation, (27),

$$C \nabla^2 u = \frac{\partial u}{\partial t} \quad (1.2)$$

where

$$\nabla^2 = \frac{\partial^2}{\partial x^2} + \frac{\partial^2}{\partial y^2} + \frac{\partial^2}{\partial z^2}$$

Verigin (45), (46), solved three dimensional problems for different configurations of loading area using Eq. (1.2). The assumption of the constitutive Eq. (1.2) was shown to be not strictly valid by a more rational theory proposed by Biot (5). The right hand side of Eq. (1.2) is a volumetric strain rate rather than excess pore pressure rate. However, the above equation is strictly valid when reduced to one dimensional form. Biot's formulation is based on the assumption that a linearly elastic skeleton material is filled up with pore fluid. From the basic equations of the theory of elasticity the following equations are formulated:

$$G \nabla^2 v_1 + \frac{G}{1-2\mu} \frac{\partial e}{\partial x} - \frac{\partial u}{\partial x} = 0 \quad (1.3)$$

$$G \nabla^2 v_2 + \frac{G}{1-2\mu} \frac{\partial e}{\partial y} - \frac{\partial u}{\partial y} = 0 \quad (1.4)$$

$$G \nabla^2 v_3 + \frac{G}{1-2\mu} \frac{\partial e}{\partial z} - \frac{\partial u}{\partial z} = 0 \quad (1.5)$$

From the continuity equation of compressible material it is derived:

$$c \nabla^2 e = \frac{\partial e}{\partial t} \quad (1.6)$$

where  $v_1, v_2, v_3$  are displacements in x, y and z directions respectively,

$G, \mu$  are Lame's elastic constants of soil skeleton,  
 $e$  is the volumetric strain,

$C$  is the coefficient of consolidation, and  
 $u$  is the pore pressure.

The four unknowns  $v_1$ ,  $v_2$ ,  $v_3$  and  $u$  are obtained by simultaneously solving the Eqs. 1.3 to 1.6 together with the appropriate boundary conditions. The mathematical exercise is highly involved. Few plane strain problems by this method are solved, (6), (18), (19), (36). Analysis of field situations by this method is highly complex and almost impossible.

In the consolidation process the fluid flow mechanism is often coupled with visco-elastic stress-strain-time relationship in order to explain the "Secondary consolidation" effect. The effective stress-strain-time relationship can be translated into rheological models composed of Maxwell and Kelvin units. Taylor (42) combined a linear spring and dashpot to explain the viscous effects in soils. Since then many investigators worked various linear and non-linear models to simulate the time-deformation behaviour of soils during the overall process of consolidation, (16), (20), (35), (47), (48). The rheological model analysis can accommodate only the material properties. The lack of simulation of the geometric properties of consolidation problems limits the scope of such studies.

#### Testing procedure and material properties

The simple oedometer test plays an important role in the evaluation of the consolidation parameters of soils. Diversified test results are obtained if the conventional

esting procedure is not adhered to (11), (16), (40). The variations of the coefficients C, k and m during the consolidation process have been investigated by Anandakrishnan (2), Zeevaert (49). While recognising the limitations of the trends of variation of the parameters obtained in the laboratory it is believed that the same trends will hold true quantitatively for field situations. Therefore certain variations of these parameters are assumed in some of the problems analysed in this research. However, further refined testing technique may provide the true variations of the parameters.

Lambe (15) and Davis (13) gave approximate methods of computing settlements to include three dimensional effect using triaxial apparatus. By conducting drained triaxial compression test for the appropriate stress path the volumetric and axial strains can be noted. Using these values of strains the initial and final settlements can be computed from the theory of elasticity for axisymmetric as well as plane strain problems. Though the above testing method is simple, it is extremely difficult to successfully conduct the test without failing the samples as they will be near the failure conditions, (21).

#### Application to field problems

In actual field situations, the consolidation parameters k, m and C vary spatially. Stratification and layered deposition are common features in the field. Even in homogeneous thick clay layers the variation of the parameters with depth can be

envisioned, (17), (34). However, in actual application to field problems the lack of appreciation of the manner of variation of parameters, the coefficients of permeability, compressibility and consolidation  $k$ ,  $m$  and  $C$  respectively and the loading conditions resulted in resorting to oversimplified models.

Richart (28), Palmer and Brown (22), Sridharan and Nagaraj (39) have provided certain approximate method of analysing layered systems. The deviations that can result from the approximation are compared with the exact solutions in subsequent chapters.

#### OBJECT AND SCOPE OF THE PRESENT INVESTIGATION

The scope of this research is to obtain solutions to several complex field conditions and loading environments so as to arrive at certain general conclusions on the consolidation behaviour of soils subjected to these conditions and to compare with the results obtained by the simplified theory. From a review of several case studies involving layers with varying material properties it is seen that the rates of consolidation are evaluated with an almost total dependence on the coefficient of consolidation. One of the purposes of this study is to evaluate the effects of relative magnitudes of the variations in permeability,  $k$  and compressibility,  $m$  and the location of the drainage faces even though the coefficient of consolidation may still remain constant. A limited number of laboratory experiments simulating some of the above situations have been conducted and the results are compared with the analytical solutions.

For the purpose of this study the following possible field situations are considered:

#### Geometrical configuration

Most of the complex field situations can be idealised as shown in Figs. 1.1 to 1.3. The thickness of the compressible layers in these situations is small in comparison with the large loading area at the surface. One dimensional analysis is valid for these cases. The discontinuous variation of the soil properties with depth constitutes the layered system as shown in Fig. 1.2. A continuous variation of soil properties with depth constitutes a thick layer as shown in Fig. 1.3. The variations are as shown in Fig. 1.4.

#### Nature of loading

In the construction of buildings, embankments and other structures the loading always progresses gradually with respect to time. This construction type of loading is assumed as shown in Fig. 1.5. The total pressure,  $\bar{u}_o$  is imposed in a time,  $t_o$  which is the construction period. The instantaneous loading is shown in Fig. 1.6.

#### Variation of parameters during consolidation

The variation of the parameters during consolidation is assumed as function of  $(1 - \frac{u_i}{u_o})$  as shown in Fig. 1.7.

### General variation of parameters

In general, the parameters can vary with respect to depth and the pore pressure as the consolidation progresses. This is shown in Fig. 1.8.

In Chapter II, an attempt is made to analyse the consolidation characteristics of a thick layer by numerical method. Different variations of soil parameters with respect to depth are investigated so as to arrive at comprehensive conclusions. The effects of relative situations of drainage boundaries and loading nature are also studied. The deviations in the results that may occur in such cases when simplified theory is used are clearly brought out. A new formulation of consolidation theory with general variation of parameters is presented. This forms a non-linear consolidation theory of a non-homogeneous clay layer with variable coefficients. The solution of the non-linear equation is obtained by step by step numerical integration. Various regenerated cases can be derived from this general equation. The effects of the general variations of the parameters are analysed. If data regarding the variations of parameters in actual field conditions are available, the settlement analysis of such situations can be carried out by this present method only, to give reasonable estimates.

In Chapter III, layered systems under instantaneous loading are analysed. An attempt is made to study the effects of extreme ranges of parameters of individual layers. A set

of design charts in a two-layer system for a possible range of soil parameters is presented. The effects of the relative magnitudes of  $k$  and  $m$  of the individual layers and the location of the drainage faces in layered systems are analysed.

In Chapter IV, rigorous mathematical analyses of single as well as two-layer systems are attempted for time dependent construction type of loading. The solution obtained for the single layer is identical with that of Schiffman's (32), (33), obtained in a different way. The analytical solutions for a two-layer system under time dependent construction loading for single face as well as two face drainage are presented here for the first time. The above solutions are checked with the numerical solutions of the above problems. Also the analysis of a three layer system is attempted by numerical method. The solutions are illustrated with examples.

In Chapter V, an investigation is taken for laboratory consolidation tests on layered systems for instantaneous as well as construction loading. A simple method of gradually applying the load to effect construction loading is devised. Four types of soil are used to constitute the different layers in the tests. Samples with single, two and three layers are tested. The experimental results are compared with the theoretical solutions.

Chapter VI summarises the whole investigation and the important conclusions are listed.

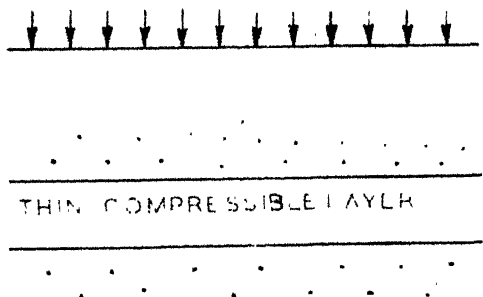


FIG.1.1 THIN LAYER

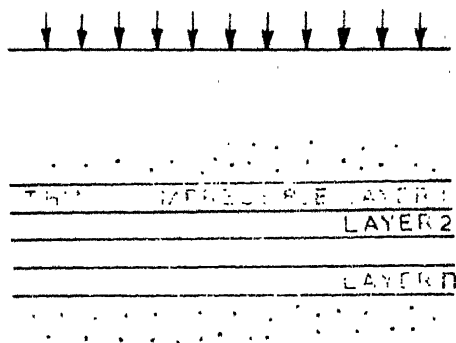


FIG.1.2 LAYERED SYSTEM

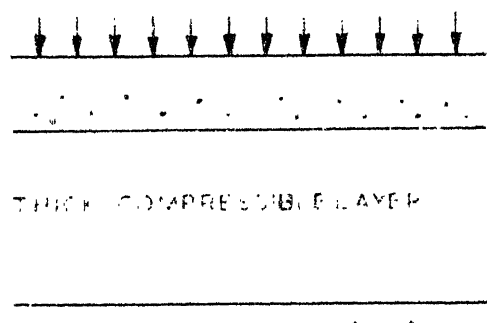


FIG.1.3 THICK LAYER

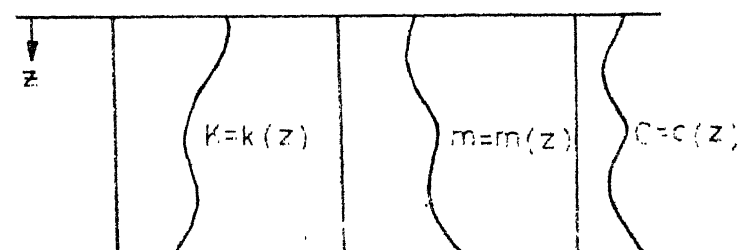


FIG.1.4 VARIATION OF PARAMETERS  
WITH DEPTH

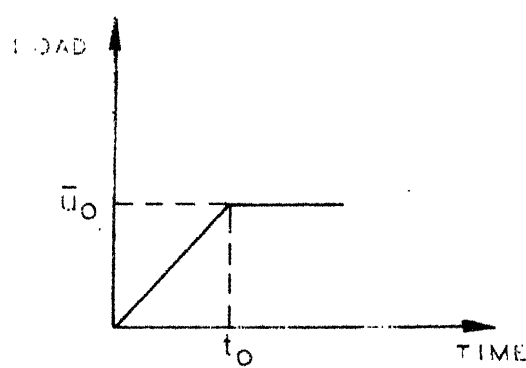


FIG. I.5 CONSTRUCTION  
LOADING

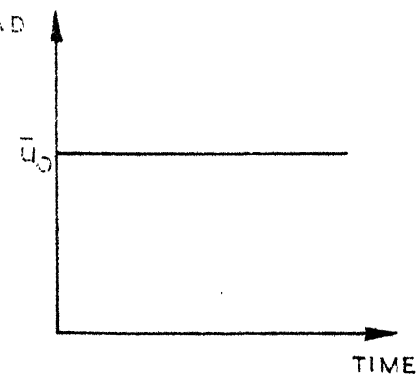


FIG. I.6 INSTANTANEOUS  
LOADING

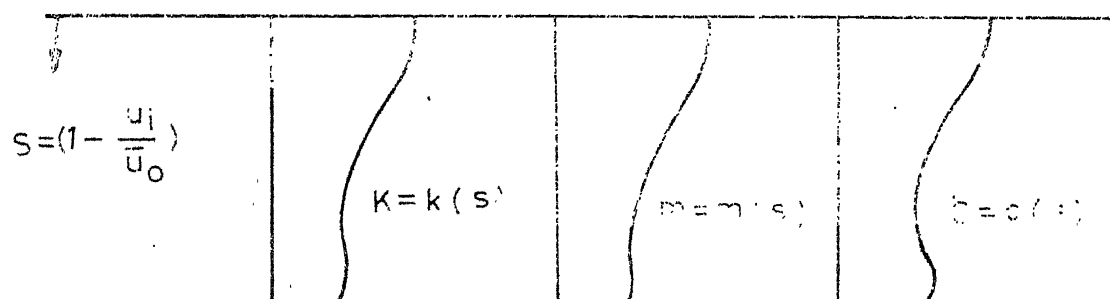


FIG. I.7 VARIATION OF PARAMETERS WITH PORE-PRESSURE

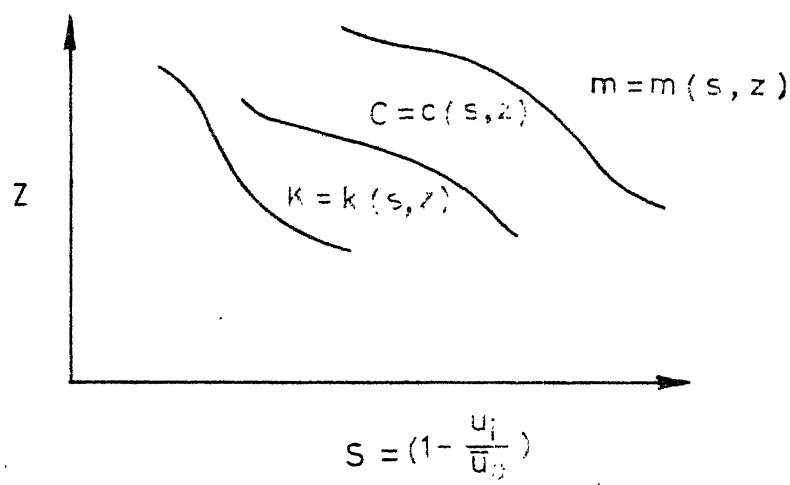


FIG. I.8 GENERAL VARIATION OF THE  
PARAMETERS

## CHAPTER II

### CONSOLIDATION OF THICK CLAY LAYER WITH VARYING PARAMETERS

#### INTRODUCTION

Demand for construction of structures on thick compressible soil is common in present-day engineering practice. The thick clay layer which is normally consolidating under its own overburden pressure will not have uniform soil properties throughout the depth. The depth dependence of hydraulic properties as discussed by Dietrich (17) and Jacobson (4) shows that a linear or a non-linear variation of  $k$  with depth can exist in field. The variation of the consolidation parameters  $k$ ,  $m$  and  $C$  in a thick clay layer can be due to the following factors:

1. Decreasing void ratios at greater depths due to higher consolidation pressures.
2. Finer materials which settle first at greater depths during sedimentation.
3. Variation of soil itself with depth due to non-homogeneity.

The variation of  $C$  with consolidation pressures are evident from laboratory test results, (41), (42). During the process of consolidation under an incremental load the void ratio changes. Therefore the parameters vary as functions

of pore pressure as consolidation progresses, (2), (31), (34), (49). It is also quite conceivable that even if the coefficient of consolidation, C is constant, different variations of k and m can exist. Hence an investigation of these factors will greatly enhance the understanding of consolidation behaviour of thick clay deposits.

#### THICK CLAY LAYER WITH SPACE VARIATION OF k, m, AND C

Schiffman and Gibson (34) studied the consolidation of non-homogeneous thick layers for two way drainage only. In view of the variations of the parameters the effects due to one-way drainage cannot be extrapolated from the two-way drainage study. The location of the drainage boundaries will exert considerable influence on consolidation characteristics. The analysis conducted in this chapter for different variations of the parameters demonstrates the extent of approximation involved in using simplified approaches for such cases. Also the extension of the analysis for construction loading is presented.

#### Formulation

The general consolidation equation for a saturated clay mass in which there is a head generation is, (32):

$$\nabla \cdot K \cdot \nabla u + K \nabla^2 u + Q_m = m \frac{\partial u}{\partial t} \quad (2,1)$$

where

$$\nabla = \left( \frac{\partial}{\partial x} + \frac{\partial}{\partial y} + \frac{\partial}{\partial z} \right),$$

$$\nabla^2 = \left( \frac{\partial^2}{\partial x^2} + \frac{\partial^2}{\partial y^2} + \frac{\partial^2}{\partial z^2} \right),$$

$$Q = \text{the rate of head generation} = \frac{d(\Delta P)}{dt},$$

$$\Delta P = \text{change in pressure,}$$

$$t = \text{time, and}$$

$$u = \text{excess pore pressure.}$$

For one dimensional case Eqn(2.1) reduces to:

$$k \frac{\partial^2 u}{\partial z^2} + \frac{dk}{dz} \cdot \frac{\partial u}{\partial z} = m \left\{ \frac{\partial u}{\partial t} - \frac{d(\Delta P)}{dt} \right\} \quad (2.2)$$

For constant k and instantaneous loading, Eq. (2.2) simplifies to Terzaghi's original equation (which will be referred to as simplified equation hereafter):

$$C \frac{\partial^2 u}{\partial z^2} = \frac{\partial u}{\partial t} \quad (2.3)$$

For constant k and time dependent loading Eq. (2.2) takes the form:

$$C \frac{\partial^2 u}{\partial z^2} + R = \frac{\partial u}{\partial t} \quad (2.4)$$

in which  $R$  can be a function of space and time variables.

Assuming the time dependent construction type of loading as shown in Fig. 1.6, the rate of imposition of excess pressure,  $R$  is equal to  $\bar{u}_o/t_o$  where  $\bar{u}_o$  is the total imposed pressure and  $t_o$  is the construction period.

For the case of thick layer with  $k$  and  $m$  varying with respect to depth alone the Eq. (2.2) is modified as:

$$k(Z) \frac{\partial^2 u}{\partial z^2} + \frac{\partial u}{\partial Z} \cdot \frac{dk(Z)}{dZ} = m(Z) \left\{ \frac{\partial u}{\partial t} - \frac{\bar{u}_o}{t_o} \right\} \quad (2.5)$$

For the following variations of  $k$  and  $m$ ,

$$k = k_o (1 \pm \alpha x) \quad \text{and}$$

$$m = m_o (1 \pm \beta x) \quad (2.6)$$

where

$$x = \text{the non-dimensionalised coordinate} = \frac{z}{H},$$

$H$  = the thickness of the layer and

$z$  = the depth

And using the following notations,

$$P = \frac{u}{\bar{u}_o}; \quad T = \frac{c_o t}{H^2}; \quad T_o = \frac{c_o t_o}{H^2};$$

$$c_o = \frac{k_o}{m_o} \quad \text{and} \quad c(z) = \frac{k(z)}{m(z)} \quad (2.7)$$

from Eq. (2.5) it is obtained:

$$\frac{(1 \pm \alpha x)}{(1 \pm \beta x)} \frac{\partial^2 P}{\partial x^2} + \frac{(\pm \alpha)}{(1 \pm \beta x)} \frac{\partial P}{\partial x} = \frac{\partial P}{\partial T} - \frac{1}{T_0} \quad (2.8)$$

The boundary conditions are:

1. Drainage at both faces

$$\begin{aligned} P(1, T) &= 0 & 0 \leq T \leq T_0 \quad \text{and} \\ P(0, T) &= 0 & \\ P(x, 0) &= 0 & 0 \leq x \leq 1 \end{aligned} \quad (2.9)$$

2. Drainage at top face only

$$\begin{aligned} P(0, T) &= 0 & 0 \leq T \leq T_0 \quad \text{and} \\ \left. \frac{\partial P}{\partial x} \right|_{(1, T)} &= 0 \\ P(x, 0) &= 0 & 0 \leq x \leq 1 \end{aligned} \quad (2.10)$$

After the construction is over the Eq. (2.8) is to be modified as:

$$\frac{(1 \pm \alpha x)}{(1 \pm \beta x)} \frac{\partial^2 P^*}{\partial x^2} + \frac{(\pm \alpha)}{(1 \pm \beta x)} \frac{\partial P^*}{\partial x} = \frac{\partial P^*}{\partial T} \quad T_0 < T < \infty \quad (2.11)$$

The boundary conditions are:

1. Drainage at both faces

$$\begin{aligned} P^*(x, T_0) &= P(x, T_0), \text{ Solution of Eq. (2.8)} \\ P^*(1, T) &= 0 & T_0 \leq T \leq \infty \\ P^*(0, T) &= 0 \end{aligned} \quad (2.12)$$

2. Drainage at top face only

$$P^*(x, T_0) = P(x, T_0), \text{ Solution of Eq. (2.8)}$$

$$\begin{aligned} P^*(0, T) &= 0 & T_0 \leq T \leq \infty \\ \frac{\partial P^*}{\partial x} \Big|_{(1, T)} &= 0 \end{aligned} \quad (2.13)$$

For the case of instantaneous loading the following equation is to be used:

$$\frac{(1 \pm \alpha x)}{(1 \pm \beta x)} \frac{\partial^2 P}{\partial x^2} + \frac{(\pm \alpha)}{(1 \pm \beta x)} \frac{\partial P}{\partial x} = \frac{\partial P}{\partial T} \quad (2.14)$$

The boundary conditions are:

1. Drainage at both faces

$$\begin{aligned} P(0, T) &= 0 & 0 \leq T \leq \infty \text{ and} \\ P(1, T) &= 0 \\ P(x, 0) &= 1.0 & 0 \leq x \leq 1 \end{aligned} \quad (2.15)$$

2. Drainage at top face only

$$\begin{aligned} P(0, T) &= 0 \\ \frac{\partial P}{\partial x} \Big|_{(1, T)} &= 0 & 0 \leq T \leq \infty \text{ and} \\ P(x, 0) &= 1.0 & 0 \leq x \leq 1 \end{aligned} \quad (2.16)$$

The differences are evident by comparing the constitutive Eq. (2.14) and the simplified Eq. (2.3). In the Eq. (2.14), the coefficients of the differential terms are functions of the independent variable,  $x$ . The extra

second term in this equation reflects the variation of  $k$ . The Eq. (2.14) can be simplified for the following cases:

For constant permeability,  $k$  (i.e.,  $\alpha = 0$ )

$$\frac{\partial^2 P}{\partial x^2} = (1 \pm \beta x) \frac{\partial P}{\partial T} \quad (2.17)$$

For constant compressibility,  $m$  (i.e.,  $\beta = 0$ )

$$(1 \pm \alpha x) \frac{\partial^2 P}{\partial x^2} \pm \alpha \frac{\partial P}{\partial x} = \frac{\partial P}{\partial T} \quad (2.18)$$

### Finite difference equations

Solutions of the Eq. (2.8) for various cases are complex by analytical approach. However, the equation is readily solvable with greater ease by using finite difference technique with the aid of a high speed digital computer. Many numerical methods are available for solving the above type of equations, (29). The following finite difference method is adopted here.

Using the finite difference mesh as shown in Fig. (2.1), Eq. (2.8) is written in the difference form as:

$$\frac{(1 \pm \alpha x)}{(1 \pm \beta x)} \frac{(P_2 - 2P_0 + P_4)}{\Delta x^2} + \frac{(\pm \alpha)}{(1 \pm \beta x)} \frac{(P_4 - P_0)}{\Delta x} = \frac{(P_1 - P_0)}{\Delta T} - \frac{1}{T_0} \quad (2.19)$$

Rearranging the terms:

$$\begin{aligned}
 P_1 &= P_4 \left\{ \frac{\Delta T}{\Delta x^2} A(x) + \frac{\Delta T}{\Delta x} B(x) \right\} + P_2 \left\{ \frac{\Delta T}{\Delta x^2} A(x) \right\} \\
 &\quad + P_0 \left\{ 1 - \frac{2 \Delta T}{\Delta x^2} A(x) - \frac{\Delta T}{\Delta x} B(x) \right\} + \frac{\Delta T}{T_0}
 \end{aligned} \tag{2.20}$$

here

$$A(x) = \frac{(1 \pm \alpha x)}{(1 \pm \beta x)} \quad \text{and}$$

$$B(x) = \frac{\pm \alpha}{(1 \pm \beta x)}$$

The boundary conditions are:

1. At the drainage boundary,  $P_1 = 0$
2. At the impervious boundary,  $P_2 = P_4$

The stability and convergence of the above procedure depend upon the following conditions (34),

$$\Delta T \leq \frac{2K(x)}{\frac{dk}{dx}} \quad \text{and}$$

$$\frac{\Delta T}{\Delta x^2} \leq \frac{1}{2C(x)} \tag{2.21}$$

## CASES STUDIED

In order to study the effects of the variations of the parameters for different boundary as well as loading conditions, the following cases are analysed.

Case 1: A tenfold increase in coefficient of permeability,  $k$  and coefficient of compressibility,  $m$  with constant coefficient of consolidation,  $C$  as shown in Fig. 2.2.

Case 2: A hundredfold increase in coefficient of permeability,  $k$  and coefficient compressibility,  $m$  with constant coefficient of consolidation,  $C$  as shown in Fig. 2.3.

Case 3: A tenfold decrease in coefficient of permeability,  $k$  and coefficient of compressibility,  $m$  with constant coefficient of consolidation,  $C$  as shown in Fig. 2.4.

Case 4: A hundredfold decrease in coefficient of permeability,  $k$  and coefficient of compressibility,  $m$  with constant coefficient of consolidation,  $C$  as shown in Fig. 2.5.

In all the above four cases the coefficient of consolidation is constant. Analysis by simplified Eq. (2.3) will be a common practice for these situations. Therefore the study of the above cases will illustrate the differences that might exist between the results using the simplified approach and the present method.

Case 5: A tenfold increase in coefficient of permeability,  $k$  and a tenfold decrease in coefficient of compressibility,  $m$  effecting a hundredfold increase in the coefficient of consolidation,  $C$  as shown in Fig. 2.6.

Case 6: A tenfold decrease in coefficient of permeability  $k$  and a tenfold increase of coefficient of compressibility,  $m$  effecting a hundredfold decrease in the coefficient of consolidation,  $C$  as shown in Fig. 2.7.

The above two cases are analysed to compare with the analysis by the simplified Eq. (2.3) using average values of the coefficients.

Some of the above cases are analysed for the following conditions:

1. Drainage at both faces
2. Drainage at a single face
3. Instantaneous loading
4. Construction type of loading

## RESULTS

### Instantaneous loading

The results of the computations for the cases studied are presented in the form of graphs in Figs. 2.9 to 2.16. The dotted curves shown in the figures are as per the simplified Eq. (2.3) whereas the other curves are as per the modified Eq. (2.14). The variations of the parameters are shown in

A clay layer draining on both faces and with constant coefficient of consolidation,  $C$  but with a ten or a hundredfold decrease of coefficients of permeability,  $k$  and compressibility,  $m$ , respectively show slower rate of consolidation by the analysis assuming space variation of the parameters  $k$  and  $m$  (Eqs 2.14) as compared with the rate of consolidation by the simplified Eq. (2.3) as seen in Fig. 2.9. The tenfold decrease consolidates faster than the hundredfold decrease. The pore pressure distribution along the depth at various times for the hundredfold decrease (Fig. 2.10) show a significant deviation from the simplified analysis. Therefore, even if the coefficient of consolidation is constant in a thick layer the estimation of the rate of settlement by the simplified equation will be in considerable error if the space variation of  $k$  and  $m$  is not considered.

For a thick clay layer draining on both faces with a tenfold increase of  $k$  and a tenfold decrease of  $m$  effecting a hundredfold increase of  $C$  with depth, the consolidation - time curve is shown in Fig. 2.11. Also the case of tenfold decrease of  $k$  and a tenfold increase of  $m$  effecting a hundredfold decrease of  $C$  with depth is shown in Fig. 2.12. Simplified analysis with average values of  $\bar{C}$  at the mid depth and the arithmetic average of the top and bottom values is done. The results of a similar analysis with a single face drainage located on the side with lower coefficient of consolidation and on the side of higher coefficient of consolidation are

shown in Figs. 2.13 and 2.14 respectively. The results by the simplified equation are considerably different from those obtained by considering the space variation of  $k$  and  $m$ . However, the simplified analysis with average  $\bar{C}$  value at mid depth shows considerably less error than that by assuming arithmetic average.

Another type of variation in  $k$  and  $m$  is visualised as a tenfold increase or a tenfold decrease of  $k$  and  $m$  but constant  $C$  with depth. A single drainage face is assumed to be located at the top only. In such a situation the drainage face is located on the side with lower values of  $k$  and  $m$  in the former case and on the side of higher values of  $k$  and  $m$  in the latter case. The results of the analysis of these two cases are shown in Fig. 2.15 along with the results by simplified equation. These are designated as curves (1), (2) and (3) respectively in the Fig. 2.15. It is interesting to note that when the drainage face is located closer to the higher values of  $k$  and  $m$  the rate of consolidation is faster than if it is located on the side of lower values. Similarly a hundredfold increase of  $k$  and  $m$  (curve (4) in Fig. 2.14) shows slower rate of consolidation than the above two cases. In these cases, it may be noted that the soil has higher compressibility farther away from the drainage face but lower permeability towards the drainage face. Thus the volume of water expelled due to larger volume change, farther from drainage face, meets with higher resistance to flow towards the drainage face due to the decreasing permeability. This causes the retardation in the rate of consolidation.

Similarly, the acceleration in the rate of consolidation is effected in a reverse situation. Incidentally, the approximation involved by simplified analysis is also brought out in this figure. Similarly for a thick clay layer with tenfold increase of  $k$  and  $m$  with depth and the single face drainage located on the higher values of  $k$  and  $m$ , the rate of consolidation is faster than if the drainage face is located on the side of lower values of  $k$  and  $m$  (Fig. 2.16). The simplified analysis for single face drainage does not bring out this difference.

#### Construction loading

The results of settlement analysis assuming construction type of loading for the various cases discussed under instantaneous loading are presented in Figs. 2.17 to 2.29. As before the analysis is carried out for thick layer assuming the different variations of  $k$  and  $m$  with depth. For all these cases the consolidation-time curves for a set of  $T_o$  ( $=C_o t_o / (F/2)^2$ ) values corresponding to the construction periods,  $t_o$ , are given in Figs. 2.17 to 2.25. These curves will serve as design charts for computation of settlements for the various situations shown. However, the range of  $T_o$  values covered is limited on account of enormous computation time required. For any intermediate construction periods within the chart, suitable interpolations can be made. Also in all these figures, the limiting conditions of instantaneous loading as well as the simplified analysis by Eq. 2.3 are shown in dotted lines for comparison.

In Figs. 2.26 to 2.29 the curves are drawn relating the average pore pressure ratios,  $\bar{u}/\bar{u}_0$ , where  $\bar{u}$  is the integrated value of pore pressure throughout the depth, and the time factor  $T$  for various values of  $T_0$ . These curves show the pore pressure build up and decay characteristics under construction loading. Here curve (1) represents the simplified case wherein  $k$ ,  $m$  and  $C$  are all constants throughout the depth. Curve (2) represents a tenfold increase while curve (3) represents a tenfold decrease of  $k$  and  $m$  with depth but having constant  $C$ . The drainage is allowed at the top only. The resistance to flow causing retardation in the rate of pore pressure decay when the drainage face is located farther from higher compressibility but closer to lower permeability is observed here also as in the case of instantaneous loading.

The simplified method shows different deviations depending upon  $T_0$  values. The building up and decay characteristics of pore pressure depend upon the construction periods also. Realistic estimations of consolidation settlements for construction loading can be made only by the analysis with the modified equations presented here.

#### THICK CLAY LAYER WITH GENERAL VARIATION OF $k$ , $m$ AND $C$

Non-linear consolidation problems have been attempted in the past with the assumption of linear  $e - \log k$  and  $e - \log P$  relations for homogeneous clay layer, (23), (24), (26). But the consolidation of non-homogeneous clay layer with variable

coefficients has not been attempted so far. In general, the parameters  $k$ ,  $m$  and  $C$  can vary with depth and pore pressure as consolidation progresses. Some simple functions of  $k$  and  $m$  are to be assumed here in order to analyse the effects of the general variation of the parameters on the consolidation phenomenon.

### Formulation

The one dimensional consolidation equation for instantaneous loading for variable coefficients from Eq. (2.1) is:

$$\frac{\partial}{\partial Z} \left( k \frac{\partial u}{\partial Z} \right) = m \frac{\partial u}{\partial t} \quad (2.22)$$

when  $k = k(u, Z)$  and

$$m = m(u, Z)$$

From Eq. (2.22) it is obtained by chain rule:

$$k \frac{\partial^2 u}{\partial Z^2} + \frac{\partial u}{\partial Z} \left\{ \frac{\partial k}{\partial u} \cdot \frac{\partial u}{\partial Z} + \frac{\partial k}{\partial Z} \right\} = m \frac{\partial u}{\partial t} \quad (2.23)$$

Putting  $x = \frac{Z}{H}$ ;  $P = \frac{u}{u_0}$ ;  $t^* = \frac{t}{H^2}$  we get

$$\frac{\partial^2 P}{\partial x^2} + \frac{1}{k} \frac{\partial k}{\partial P} \left( \frac{\partial P}{\partial x} \right)^2 + \frac{1}{k} \cdot \frac{\partial k}{\partial x} \cdot \frac{\partial P}{\partial x} = \frac{m}{k} \frac{\partial P}{\partial t^*} \quad (2.24)$$

Now the variation of  $k$  and  $m$  is assumed as:

$$k = k_0 (1 + \alpha x) \left\{ 1 - \gamma(1-P) \right\} \quad \text{and} \quad (2.25)$$

$$m = m_0 (1 + \beta x) \left\{ 1 - \mu(1-P) \right\} \quad (2.26)$$

Therefore,

$$\frac{\partial k}{\partial P} = k_0 (1 + \alpha x) \quad (2.27)$$

$$\frac{\partial k}{\partial x} = k_0 \alpha \left\{ 1 - \gamma(1-p) \right\} \quad (2.28)$$

Substituting Eqs. (2.27) and (2.28) into Eq. (2.24) and

putting  $C_0 = \frac{k_0}{m_0}$ ;  $T = \frac{C_0 t}{H^2}$

We get:

$$\begin{aligned} \frac{\partial^2 P}{\partial x^2} + \frac{k_0 \gamma (1+\alpha x)}{k_0 (1+\alpha x) \left\{ 1 - \gamma(1-P) \right\}} \left( \frac{\partial P}{\partial x} \right)^2 + \frac{k_0 \alpha \left\{ 1 - \gamma(1-P) \right\}}{k_0 (1+\alpha x) \left\{ 1 - \gamma(1-P) \right\}} \frac{\partial P}{\partial x} \\ = \frac{(1+\beta x) \left\{ 1 - \mu(1-P) \right\}}{(1+\alpha x) \left\{ 1 - \gamma(1-P) \right\}} \frac{\partial P}{\partial T} \end{aligned} \quad (2.29)$$

Simplifying we get:

$$\frac{\partial^2 P}{\partial x^2} + A(\gamma, P) \left( \frac{\partial P}{\partial x} \right)^2 + B(\alpha, x) \frac{\partial P}{\partial x} = C(\alpha, \beta, \gamma, \mu, P, x) \frac{\partial P}{\partial T} \quad (2.30)$$

Where,

$$A(\gamma, P) = \frac{\gamma}{1 - \gamma(1-P)},$$

$$B(\alpha, x) = \frac{\alpha}{(1+\alpha x)}; \text{ and}$$

$$C(\alpha, \beta, \gamma, \mu, P, x) = \frac{(1+\beta x) \{ 1-\mu(1-P) \}}{(1+\alpha x) \{ 1-\gamma(1-P) \}}$$

The above Eq. (2.30) is non-linear. Closed form solution of the equation is not possible. However, in the consolidation problems there always exists an open boundary. The values of  $P$  are specified only on the three boundaries as shown in Fig. 2.8.

1. At time  $t = 0$
2. At depth  $Z = 0$
3. At depth  $Z = H$

Taking advantage of the open boundary step-by-step numerical integration of non-linear consolidation equation is possible. However, very small intervals of integration should be chosen in order to get convergent results. Hence the computation time is large for solving such problems.

#### Finite difference equations

Using the finite difference mesh as shown in Fig. 2.1, Eq. (2.30) is written in difference form as:

$$\begin{aligned} & \frac{P_2 - 2P_0 + P_4}{\Delta x^2} + A(\gamma, P_0) \left\{ \frac{P_2 - P_0}{\Delta x} \right\}^2 + B(\alpha, x) \frac{P_2 - P_0}{\Delta x} \\ &= C(\alpha, \beta, \gamma, \mu, P_0, x) \frac{P_1 - P_0}{\Delta T} \end{aligned} \quad (2.31)$$

Therefore,

$$P_1 = \frac{\Delta T}{C(\alpha, \beta, \gamma, \mu, P_0, x)} \frac{P_2 - 2P_0 + P_4}{\Delta x^2} + A(\gamma, P_0) \left\{ \frac{P_2 - P_0}{\Delta x} \right\}^2 + B(\alpha, x) \frac{P_2 - P_0}{\Delta x} + P_0 \quad (2.32)$$

The boundary conditions are:

1. At the drainage boundary  $P_1 = 0$
2. At the impervious boundary  $P_2 = P_4$

The stability and convergence of the results depend upon the individual values of the parameters  $\alpha, \beta, \gamma, \mu, \Delta x$  and  $\Delta T$ . However, the convergence of the particular cases studied is given in the Appendix.

#### Regenerated cases

The following regenerated cases can be derived from the general Eq. (2.29).

1. Thick layer with space variation of  $k, m$  and  $C$ , which was discussed earlier.

Here  $\gamma = \mu = 0$

The Eq. (2.29) reduces to the form of Eq. (2.14).

2. A layer with varying  $k, m$  and  $C$  with respect to the pore pressure.

Here  $\alpha = \beta = 0$

The Eq. (2.29) reduces to:

$$\frac{\partial^2 P}{\partial x^2} + \frac{\gamma}{1-\gamma(1-P)} \left(\frac{\partial P}{\partial x}\right)^2 = \frac{1-\mu(1-P)}{1-\gamma(1-P)} \frac{\partial P}{\partial T} \quad (2.33)$$

3. When  $k$  alone varies as a function of pore pressure.

Here  $\mu = 0$

The Eq. (2.33) reduces to:

$$\frac{\partial^2 P}{\partial x^2} - \frac{\gamma}{1-\gamma(1-P)} \left(\frac{\partial P}{\partial x}\right)^2 = \frac{1}{1-\gamma(1-P)} \frac{\partial P}{\partial T} \quad (2.34)$$

4. When  $m$  alone varies as a function of pore pressure:

Here  $\gamma = 0$

The Eq. (2.33) reduces to:

$$\frac{\partial^2 P}{\partial x^2} = 1 - \mu(1-P) \frac{\partial P}{\partial T} \quad (2.35)$$

Schiffman (32) gave an approximate method of solving an equation similar to Eq. (2.34). Scott (31), studied similar variation of Eq. (2.35).

#### CASES STUDIED

In order to understand the effect of the general variations of the parameters, the following cases are analysed.

Case 1: A layer with variation of  $k$  alone during the process of consolidation. So here  $\alpha = \beta = \mu = 0$

Case 2: A layer with variation of  $m$  alone during the process of consolidation. So here  $\alpha = \beta = \gamma = 0$

The above two cases are taken for analysing the relative effects of the individual variation of  $k$  and  $m$ .

Case 3: A layer with  $k$  and  $m$  varying as the same functions of  $u$ . So here  $\alpha = \beta = 0$  and  $\gamma = \mu$ .

$$k = k_o \{ 1 - \gamma(1-P) \}$$

$$m = m_o \{ 1 - \mu(1-P) \} = m_o \{ 1 - \gamma(1-P) \}$$

Therefore,

$$C = \frac{k}{m} = \frac{k_o}{m_o} = C_o$$

Case 4: A thick layer with  $k$  and  $m$  varying as the same functions of the depth and pore pressure. So here  $\alpha = \beta$  and  $\gamma = \mu$ .

$$k = k_o (1 + \alpha x) \{ 1 - \gamma(1-P) \}$$

$$m = m_o (1 + \beta x) \{ 1 - \mu(1-P) \} = m_o (1 + \alpha x) \{ 1 - \gamma(1-P) \}$$

Therefore,

$$C = \frac{k}{m} = \frac{k_o}{m_o} = C_o$$

In the above cases 3 and 4 the value of  $C$  is constant throughout the depth and during consolidation. Hence, the usage of simplified approach can be studied and the results can be compared.

Case 5: A thick layer with general variation of  $k$  and  $m$ .  
 So here  $\alpha \neq \beta \neq \gamma \neq \mu$ .

A comparison of the results with the simplified analysis using average coefficient values will demonstrate the approximation involved.

All the above cases are analysed for instantaneous loading and for two way drainage.

#### RESULTS

The results of all the cases studied are presented in Figs. 2.30 to 2.33.

It is seen that the decrease in  $m$  during the process of consolidation assuming constant  $k$ , shows faster rate of pore pressure dissipation than the decrease in  $k$  during the process of consolidation assuming constant  $m$  (Fig. 2.30). These effects are obvious because the coefficient of consolidation,  $C = \frac{K}{m}$ , increases when  $m$  decreases and thus faster consolidation takes place. Similarly,  $C$  decreases when  $k$  decreases and hence slower rate of consolidation is seen. But the retardation of consolidation by a decrease in  $k$  is more than the acceleration of consolidation by the same decrease in  $m$ . This shows that the effect of the variation of  $k$  is more than that of  $m$ .

For a clay layer having the same coefficient of consolidation throughout the depth and during the consolidation

process, the decrease of  $k$  and  $m$  result in slower rates of consolidation compared to the simplified analysis (Figs. 2.31 and 2.32).

A general variation of  $k$  and  $m$  is effected by taking the following values:

$$\alpha = - .80 ; \beta = 4.0 ; \gamma = .25 \text{ and } \mu = .50$$

This shows that the permeability is decreased to one fifth and the compressibility is increased to five times the values of  $k_0$ ,  $m_0$  with respect to depth. At the end of consolidation process the permeability is reduced to three fourths and the compressibility is reduced to half the initial values,  $k(Z)$  and  $m(Z)$ . The average value of  $\bar{C}$  at the mid depth and at 50 percent consolidation is  $.233 C_0$ . Fig. 2.33 shows that the use of simplified Eq. (2.3) with average value of coefficients results in considerable variation of rate of consolidation as compared to the general variable coefficient Eq. (2.29).

#### CONCLUSIONS

The following conclusions summarise the findings of this investigation:

For a thick clay layer even though the coefficient of consolidation  $C$  is constant throughout the depth, the rate of consolidation is very much affected by the individual variation of  $k$  and  $m$  with respect to depth. A tenfold and hundredfold

decrease in  $k$  and  $m$  result in slower rates of consolidation as compared to the simplified analysis.

The location of the drainage boundary has significant influence on the consolidation process of thick clay layers with single face drainage. The consolidation is faster when the drainage boundary is located on the side of higher  $k$  and  $m$  values.

In a thick layer under construction loading the pore pressure build up during the construction and decay thereafter depend upon the construction periods also. Analysis of such cases with the modified Eq. (2.14) presented here will give better estimates of rates of consolidation.

A set of design charts for a thick layer under construction loading are presented. If appropriate field situations could be idealised under the various cases discussed here the design charts will be useful for predicting the field settlements.

A new formulation taking into account the general variation of the consolidation parameters is presented. This forms a non-linear consolidation theory of non-homogeneous thick clay deposit with variation of parameters during the process of consolidation. Various regenerated cases can be derived from this general formulation.

The effect of individual decrease of  $k$  during consolidation is found to be more than that of  $m$ .

Even though the coefficient of consolidation is constant throughout the depth and during consolidation, the rate of settlement is influenced by the individual variations of  $k$  and  $m$ .

In general, using average coefficients with the simplified Eq. (2.3) yields very approximate estimates as compared with more refined analysis.

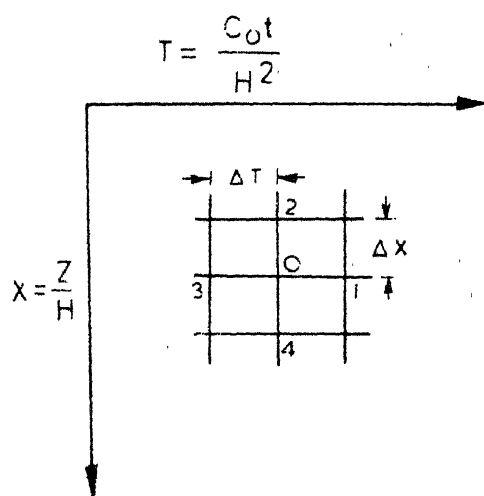


FIG. 2.1 FINITE DIFFERENCE MESH

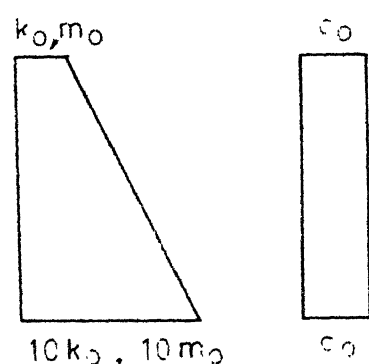


FIG. 2.2 CASE 1

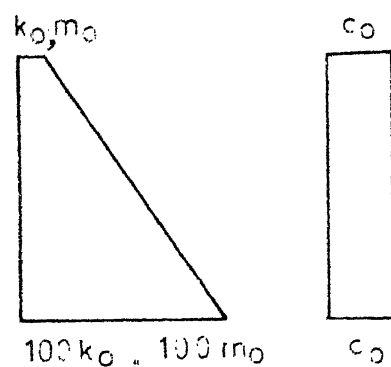


FIG. 2.3 CASE 2

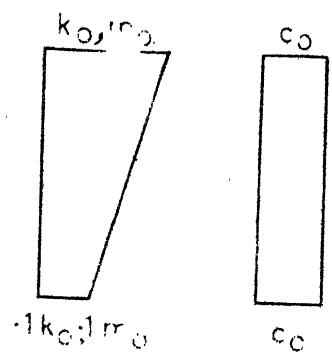


FIG.2.4 CASE 3

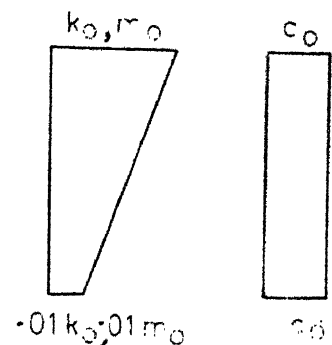


FIG.2.5 CASE 4

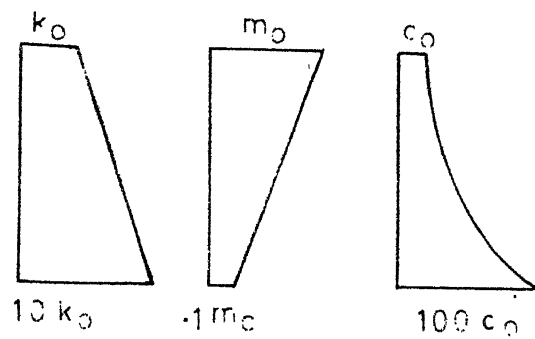


FIG.2.6 CASE 5

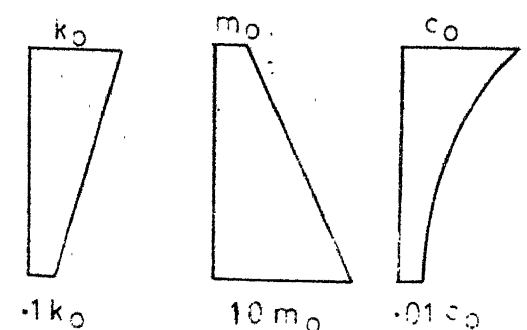


FIG.2.7 CASE 6

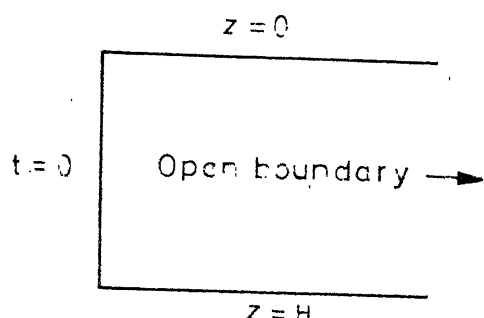


FIG.2.8 BOUNDARIES IN CONSOLIDATION PROBLEM

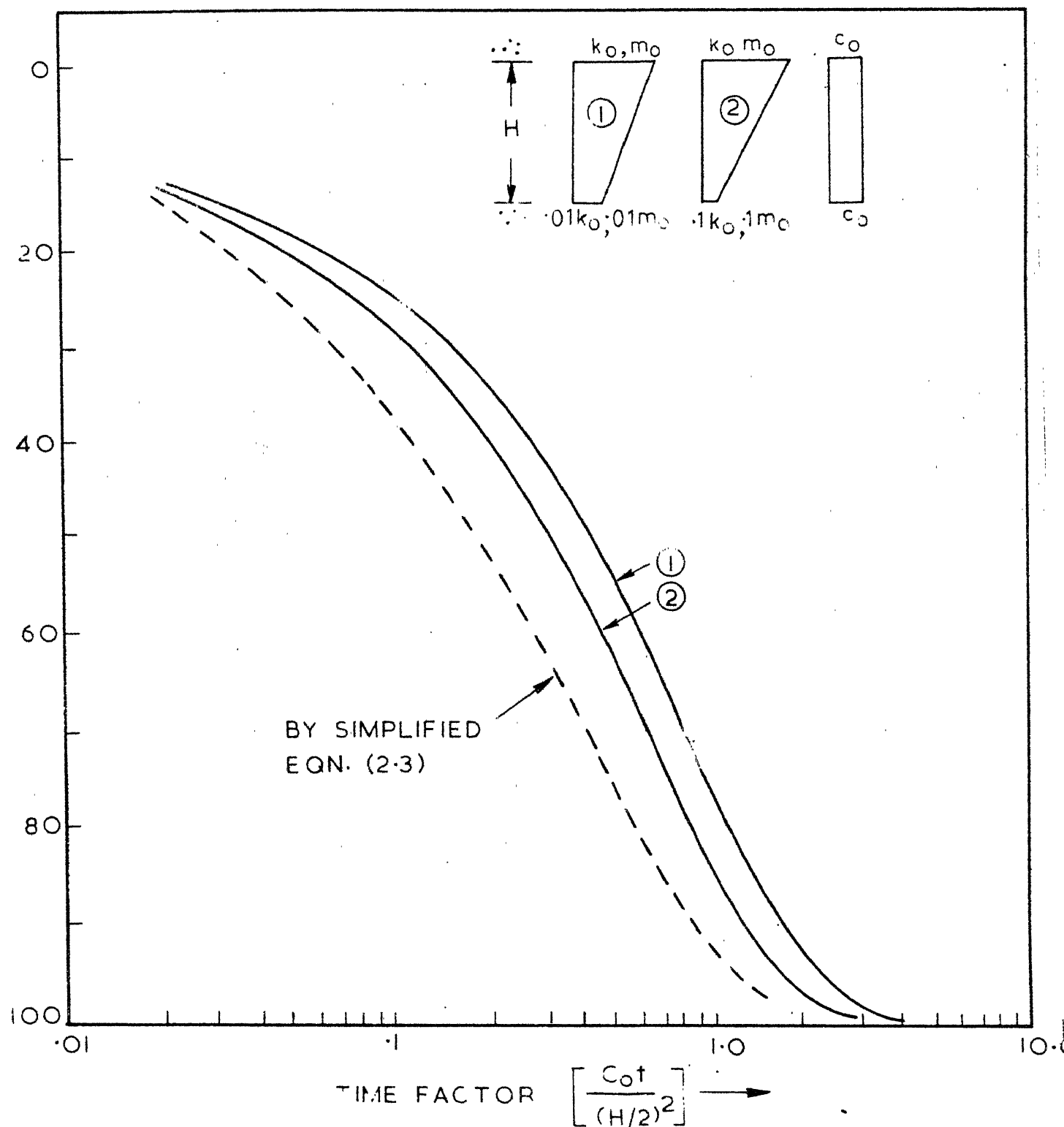


FIG. 2.9 CONSOLIDATION OF THICK LAYER WITH TWO FACE DRAINAGE

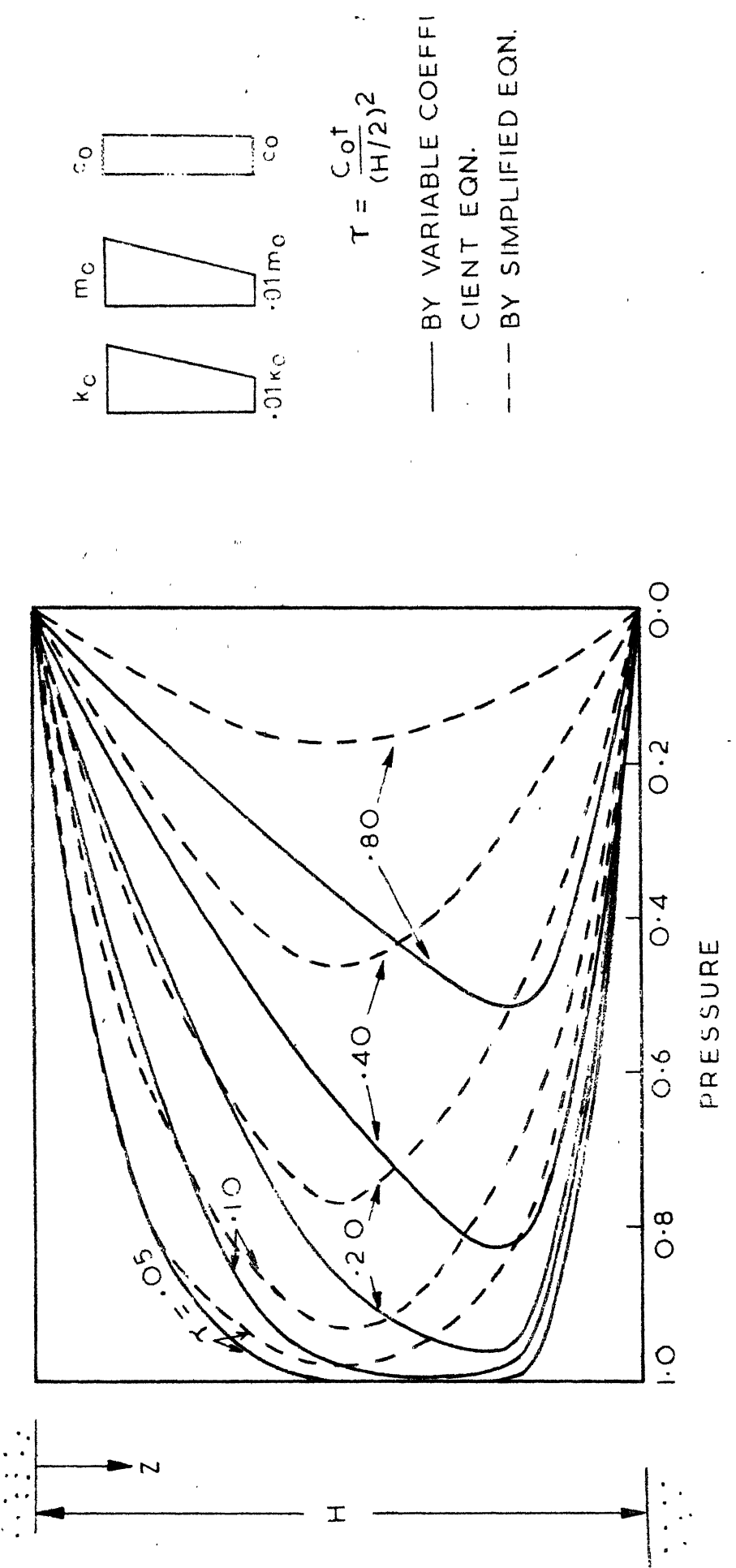


FIG. 2.10 PORE-PRESSURE DISTRIBUTION IN THICK LAYER

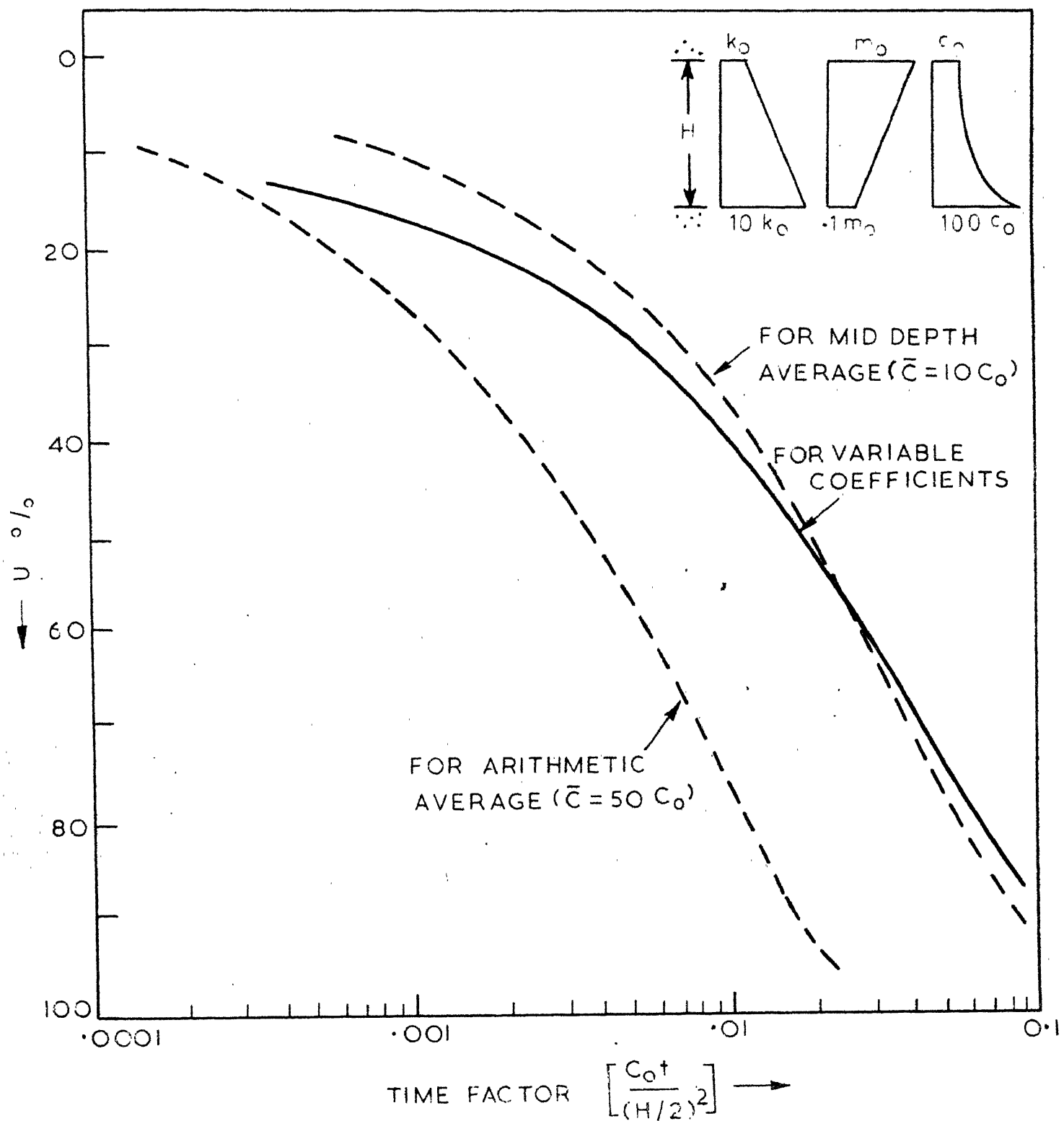


FIG. 2.11 CONSOLIDATION OF THICK LAYER WITH  
TWO FACE DRAINAGE

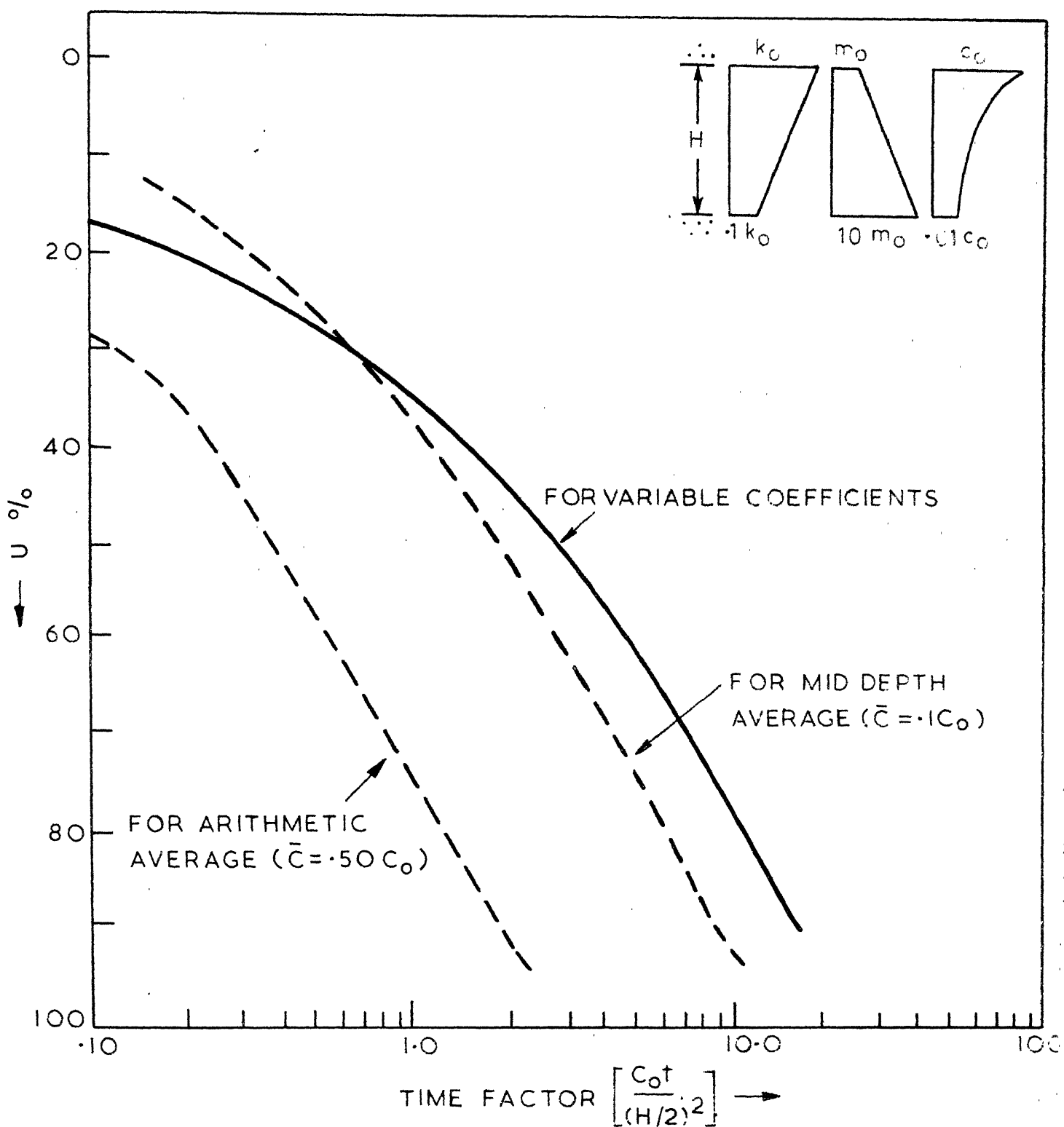


FIG. 2.12 CONSOLIDATION OF THICK LAYER WITH TWO FACE DRAINAGE

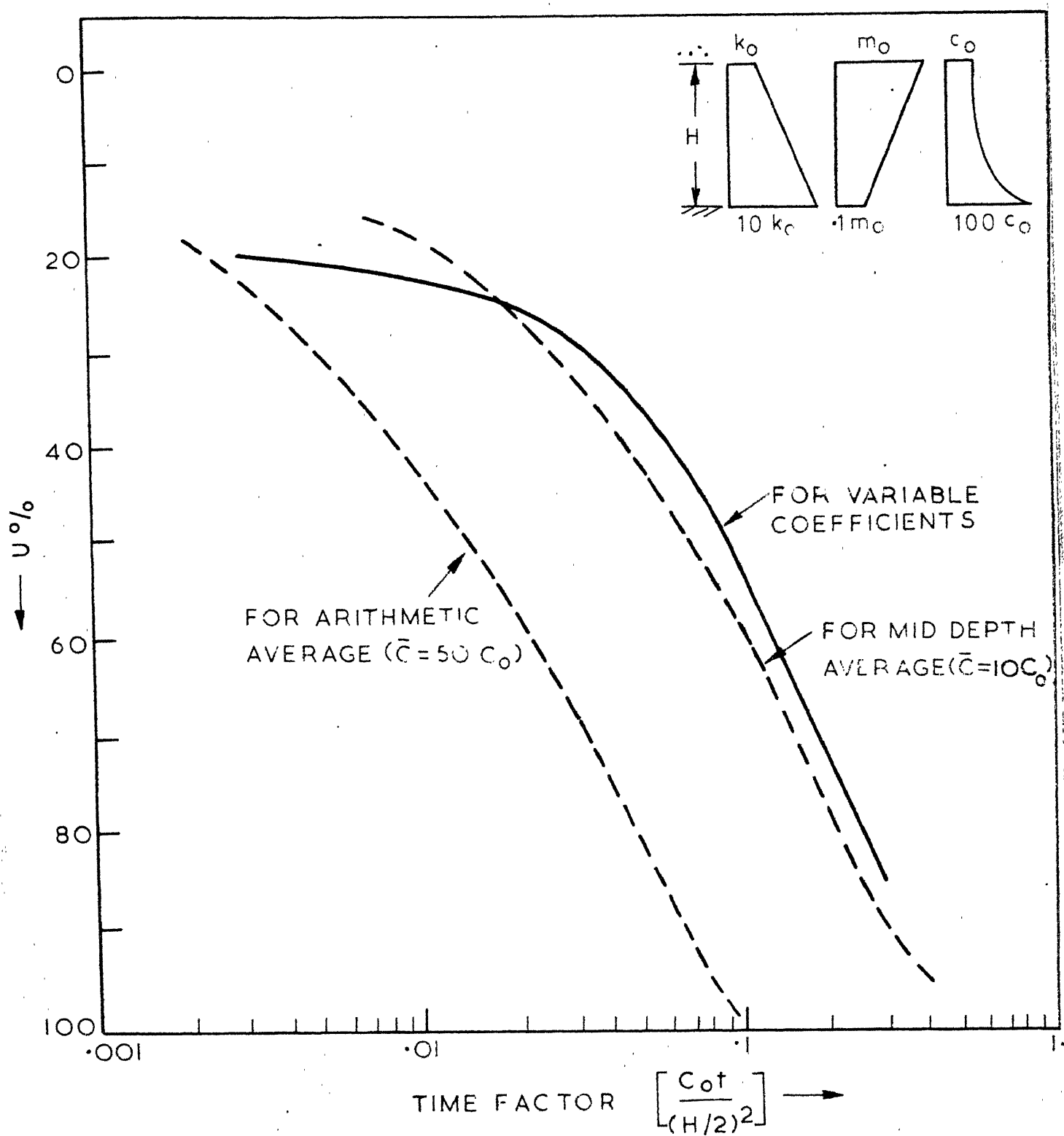


FIG. 2.13 CONSOLIDATION OF THICK LAYER WITH SINGLE FACE DRAINAGE

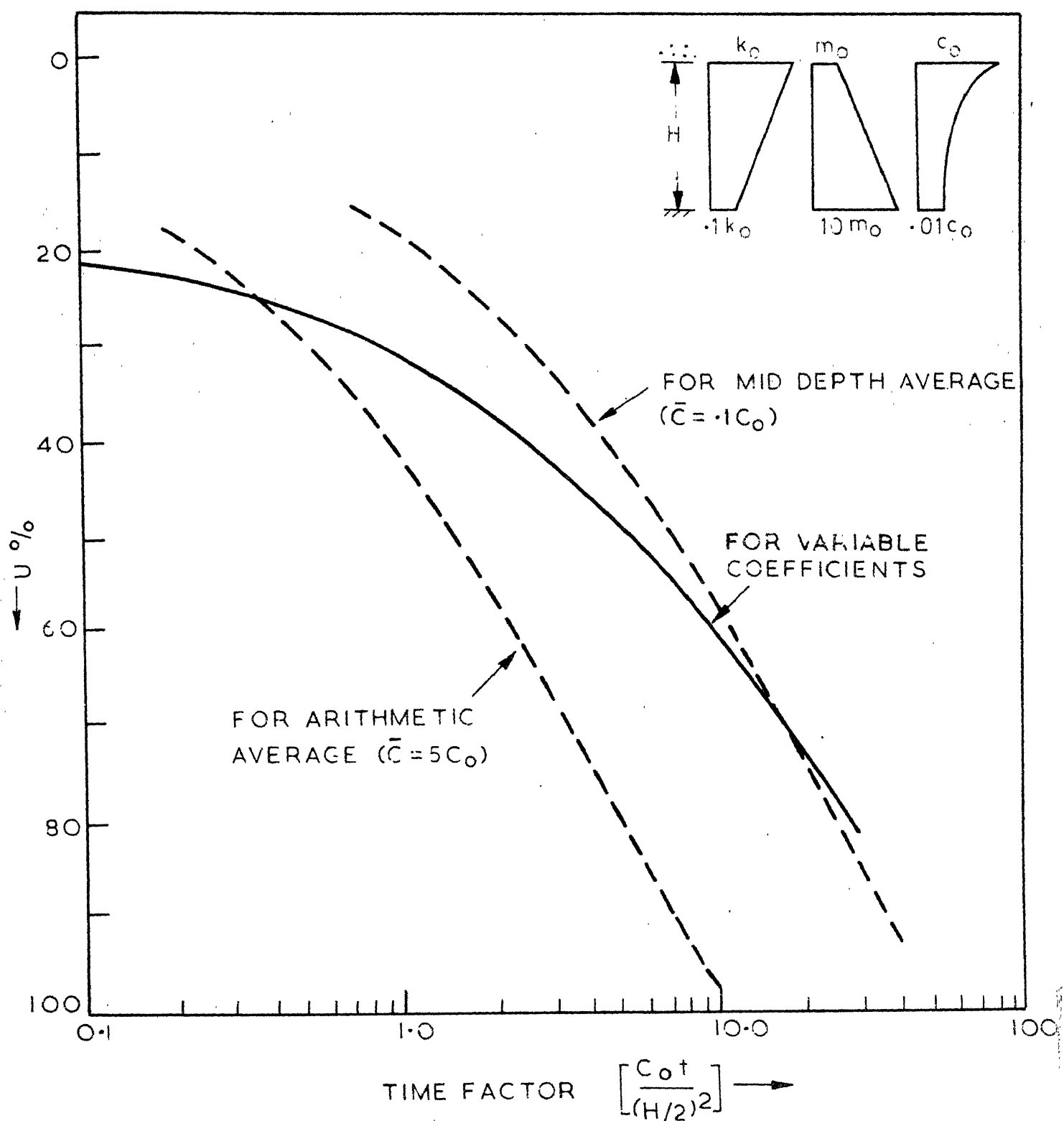


FIG. 2.14 CONSOLIDATION OF THICK LAYER WITH SINGLE FACE DRAINAGE

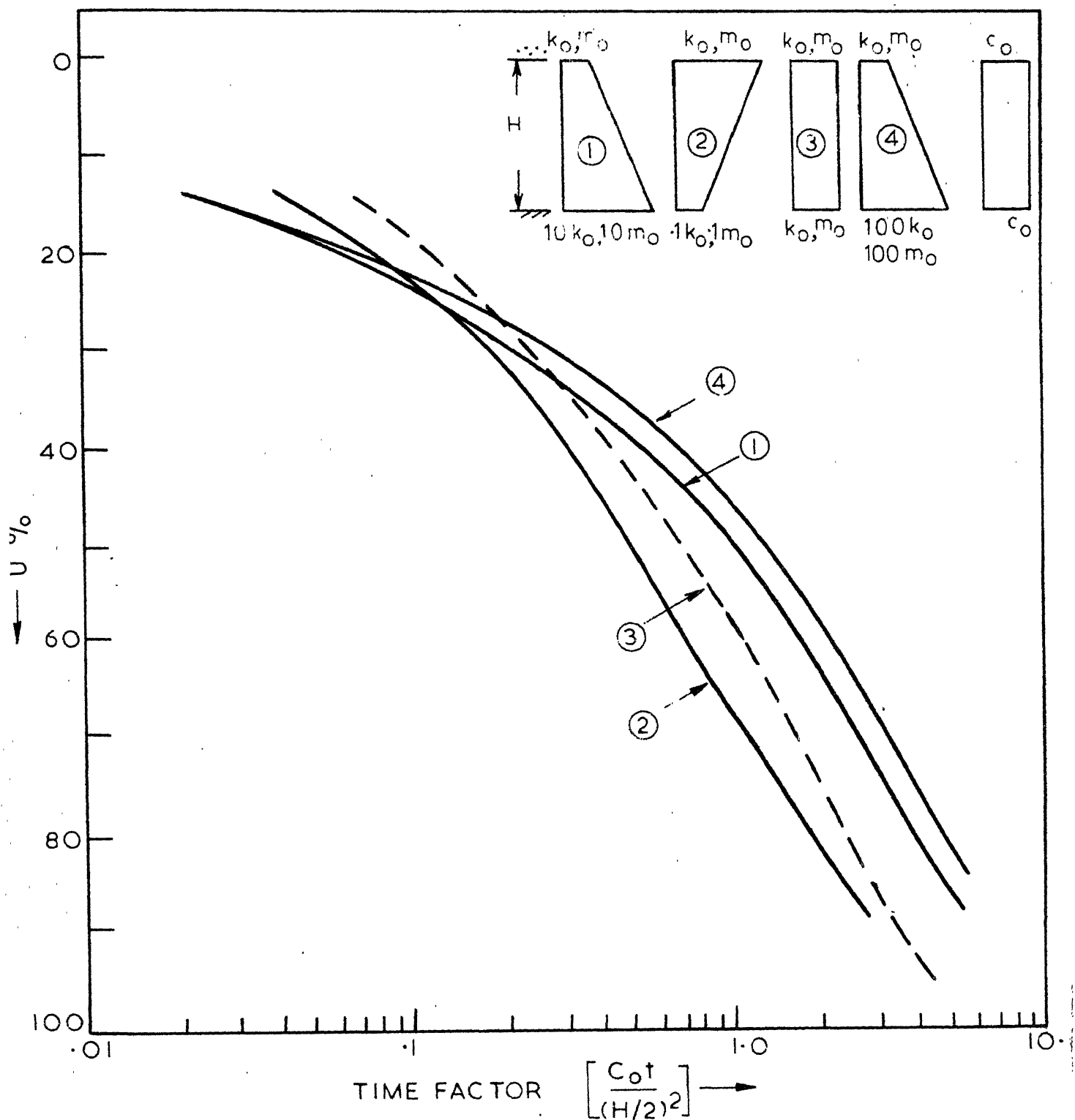


FIG. 2.15 CONSOLIDATION OF THICK LAYER WITH SINGLE FACE DRAINAGE

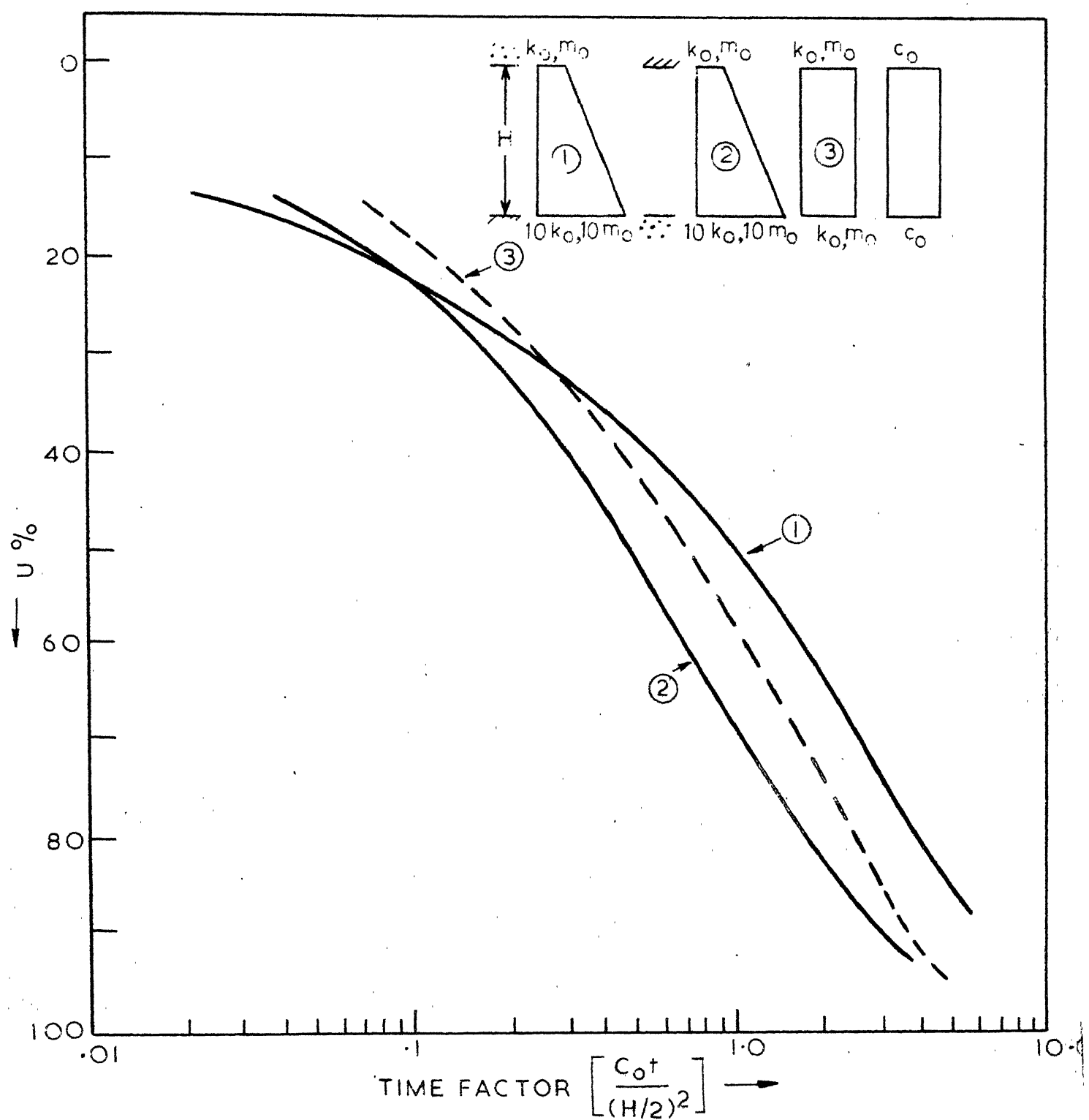


FIG. 2·16 CONSOLIDATION OF THICK LAYER WITH SINGLE FACE DRAINAGE

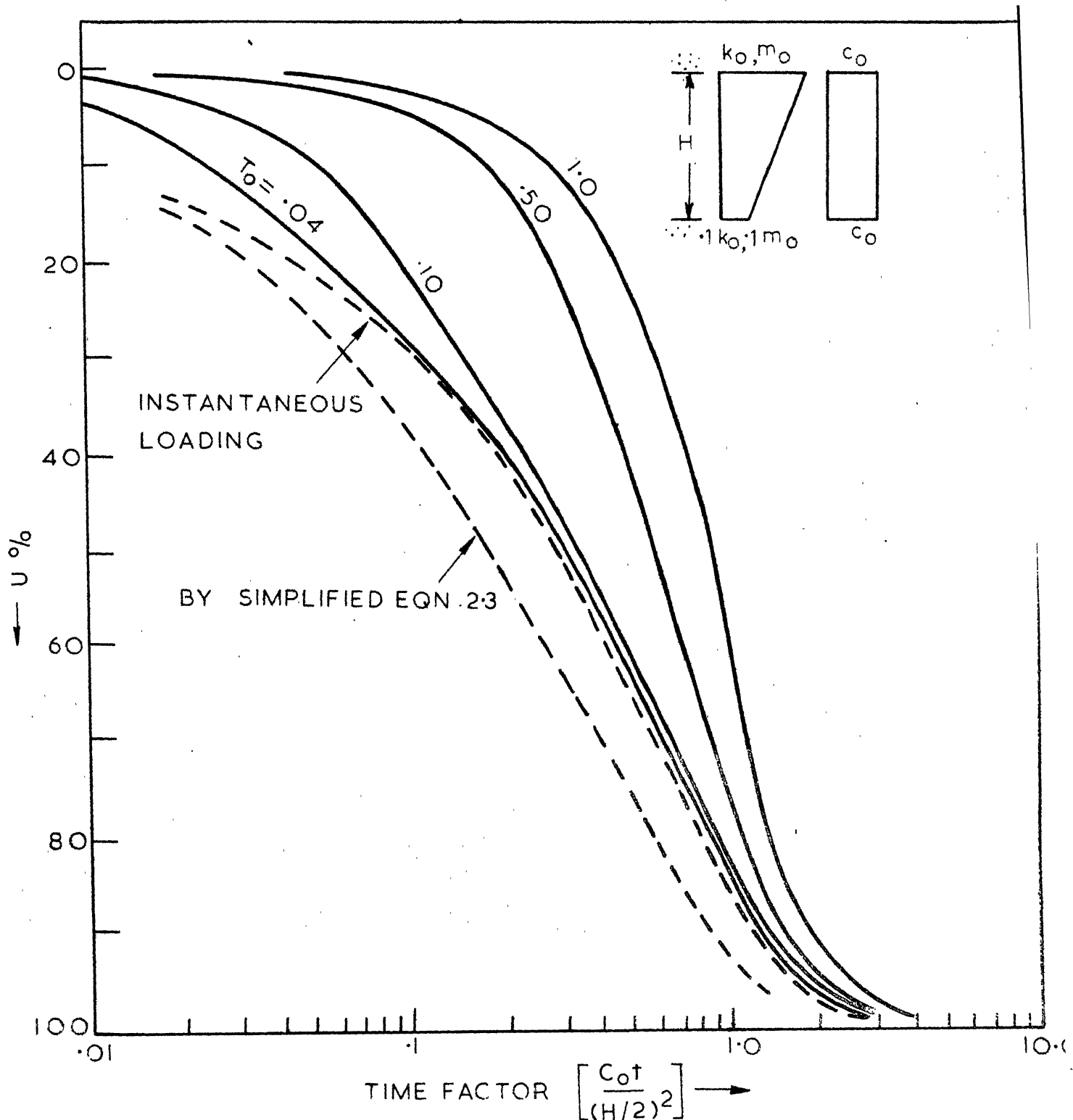


FIG. 2.17 CONSOLIDATION OF THICK LAYER UNDER CONSTRUCTION LOADING

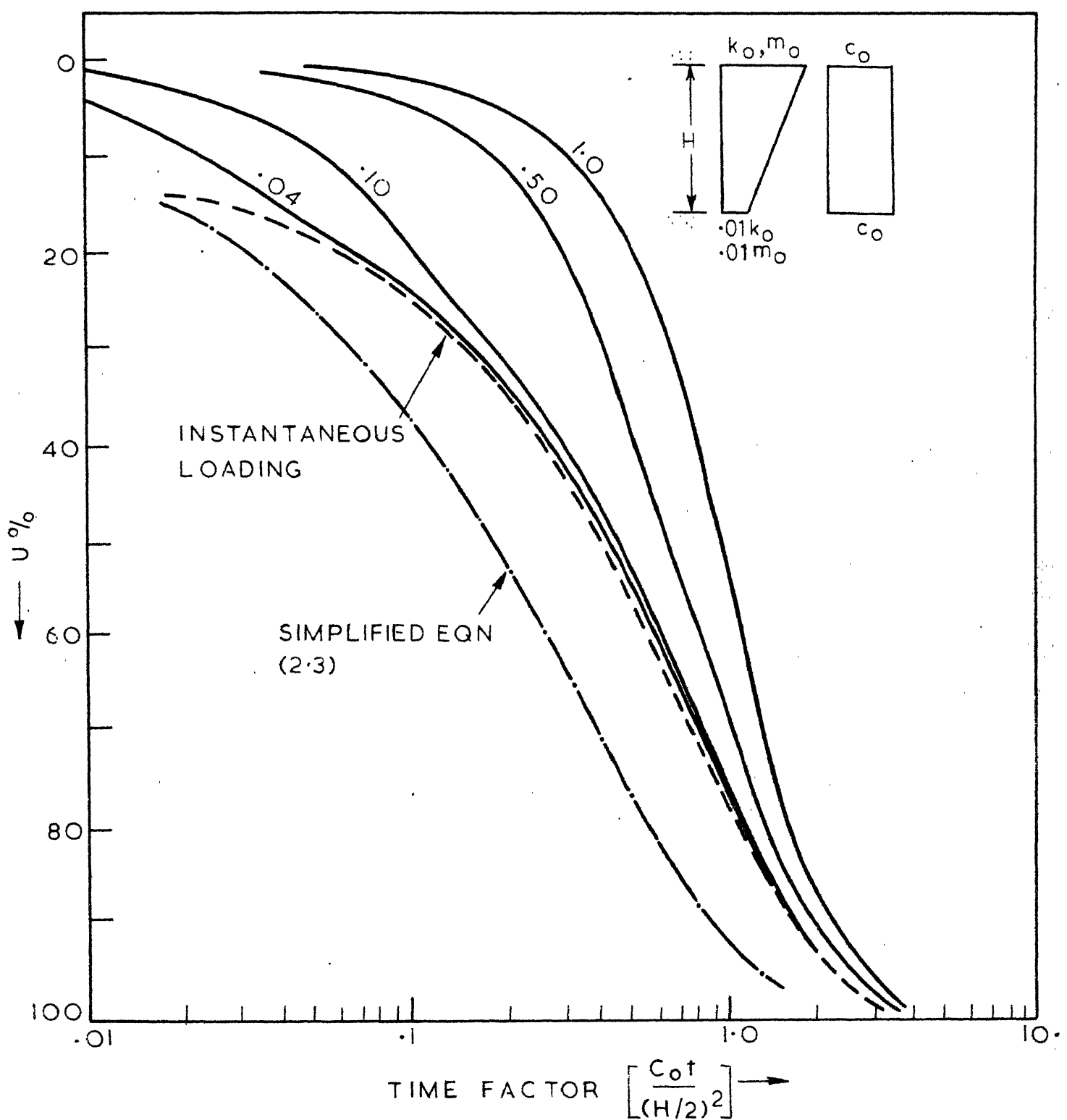


FIG. 2.18 CONSOLIDATION OF THICK LAYER UNDER CONSTRUCTION LOADING

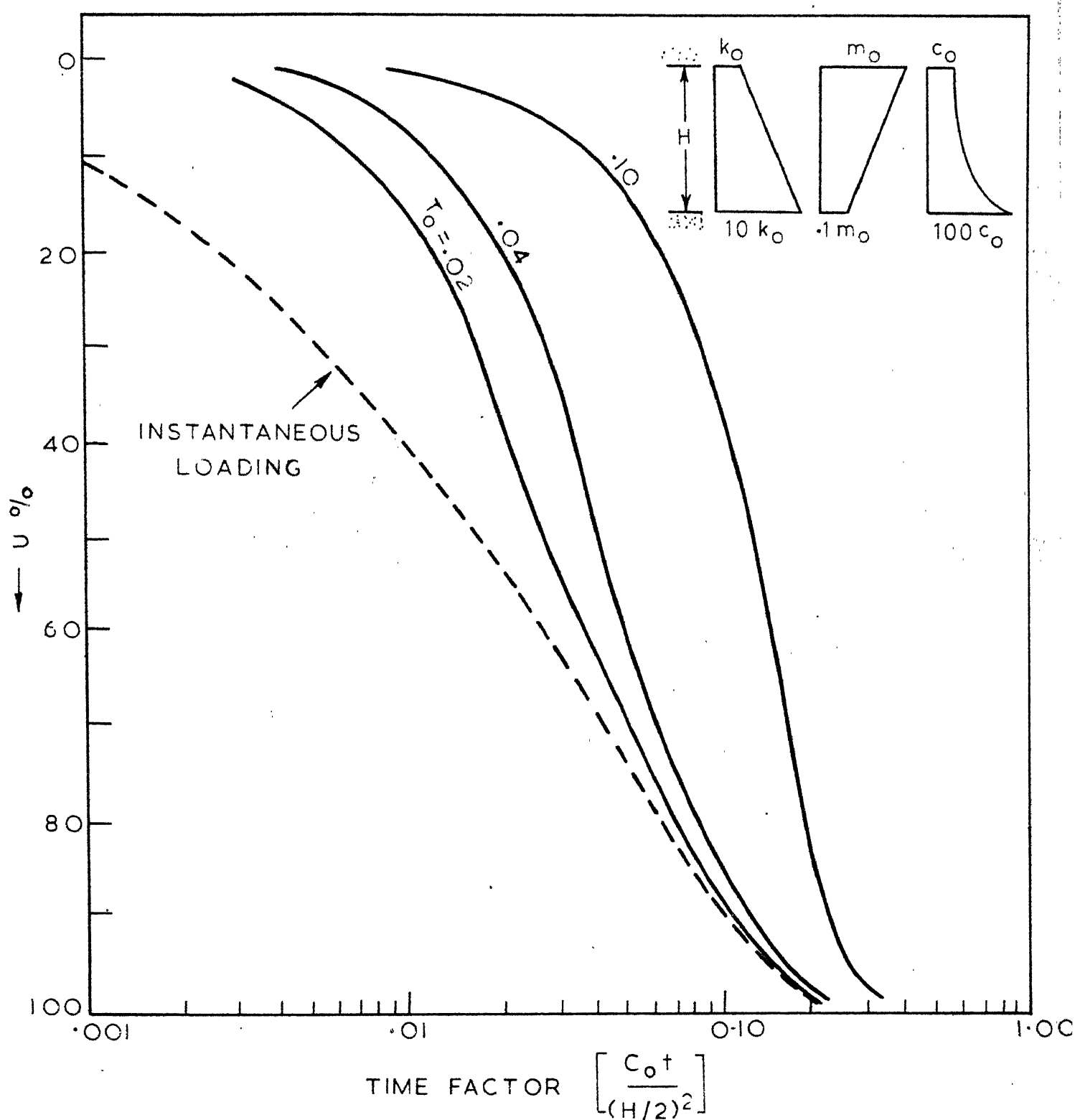


FIG. 2.19 CONSOLIDATION OF THICK LAYER UNDER CONSTRUCTION LOADING

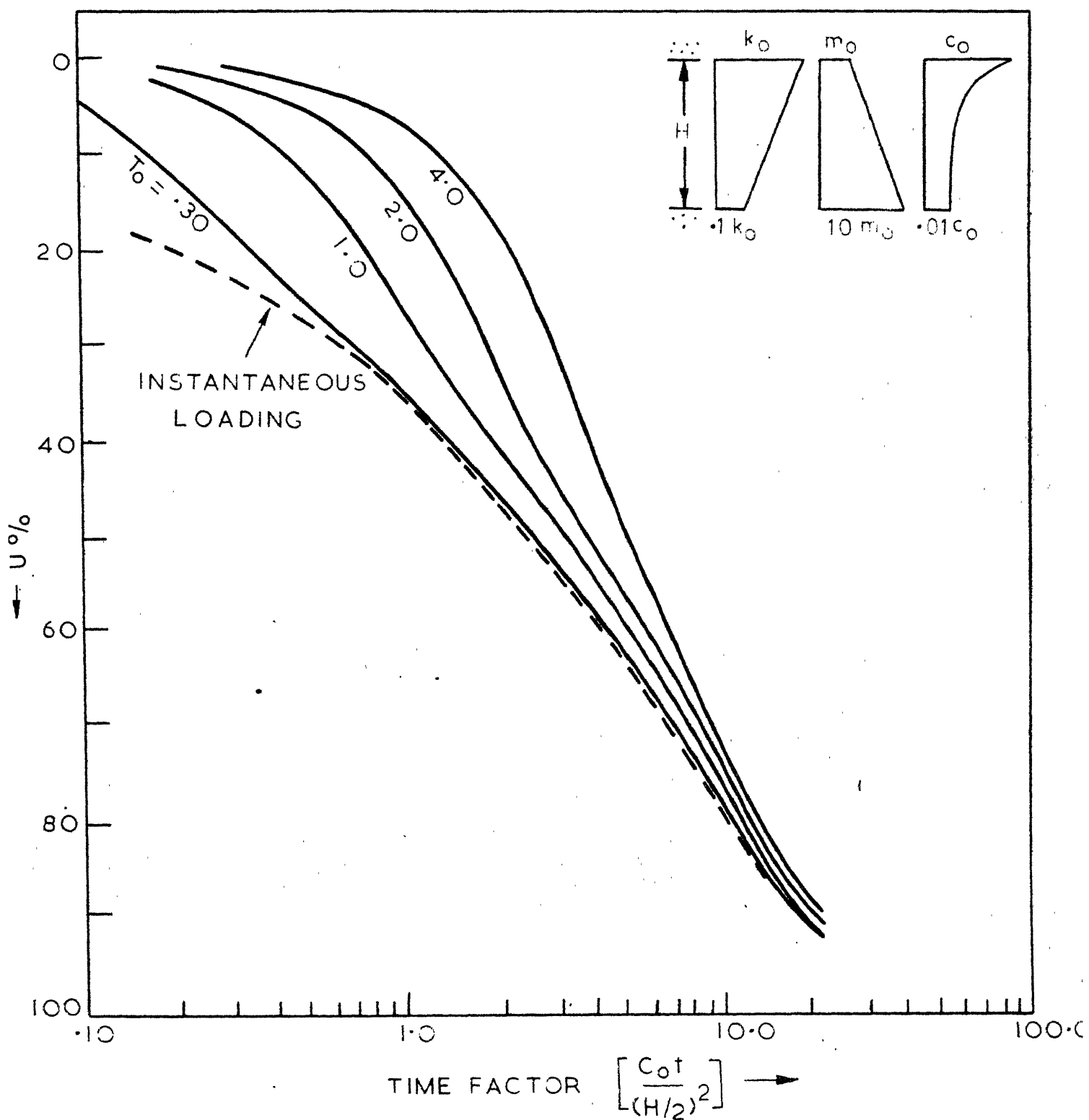


FIG. 2.20 CONSOLIDATION OF THICK LAYER UNDER CONSTRUCTION LOADING

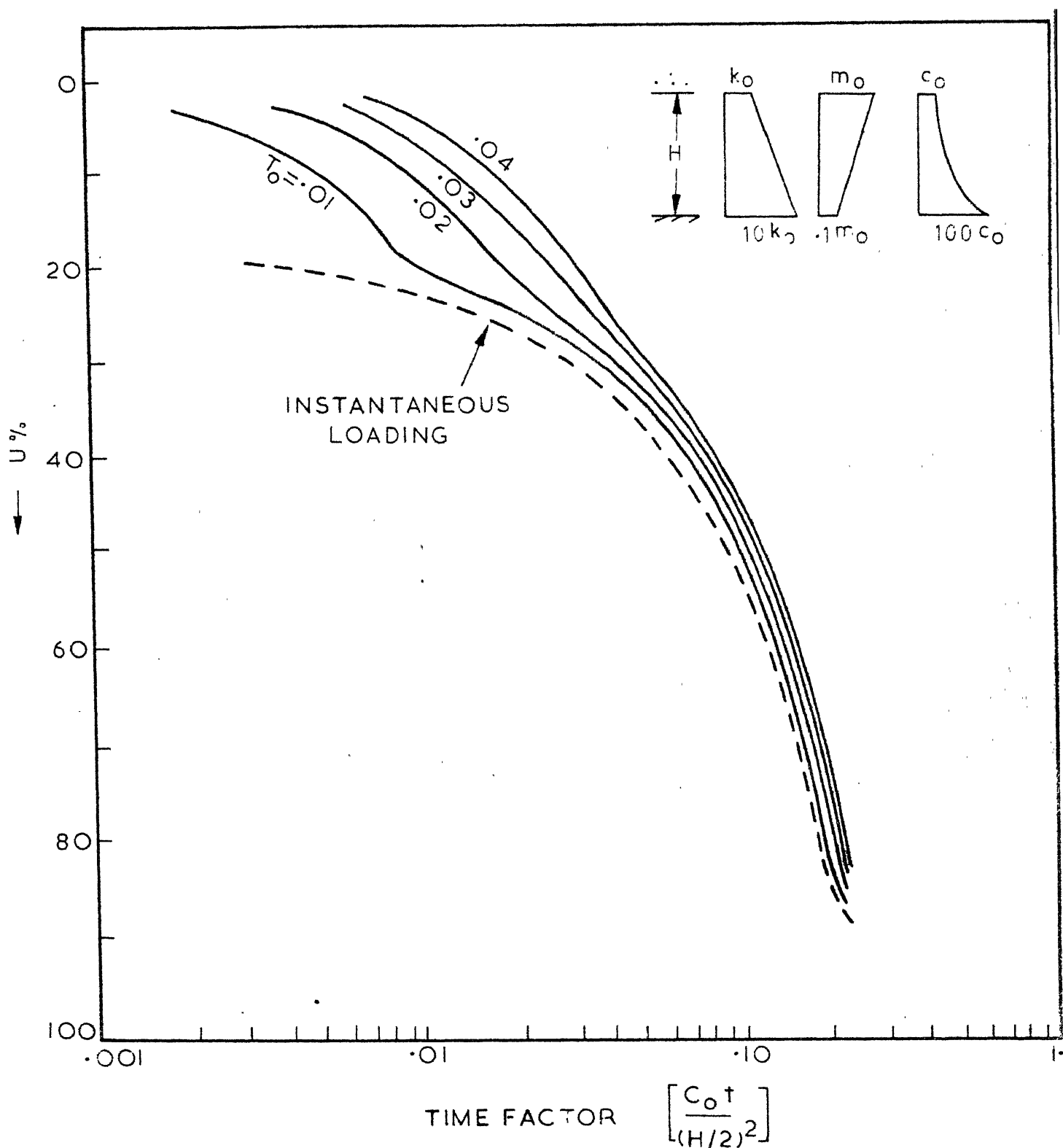


FIG. 2-21 CONSOLIDATION UNDER CONSTRUCTION LOADING - THICK LAYER

L. N. NARLIKAR,  
GENERAL LIBRARY.

Ref. No.

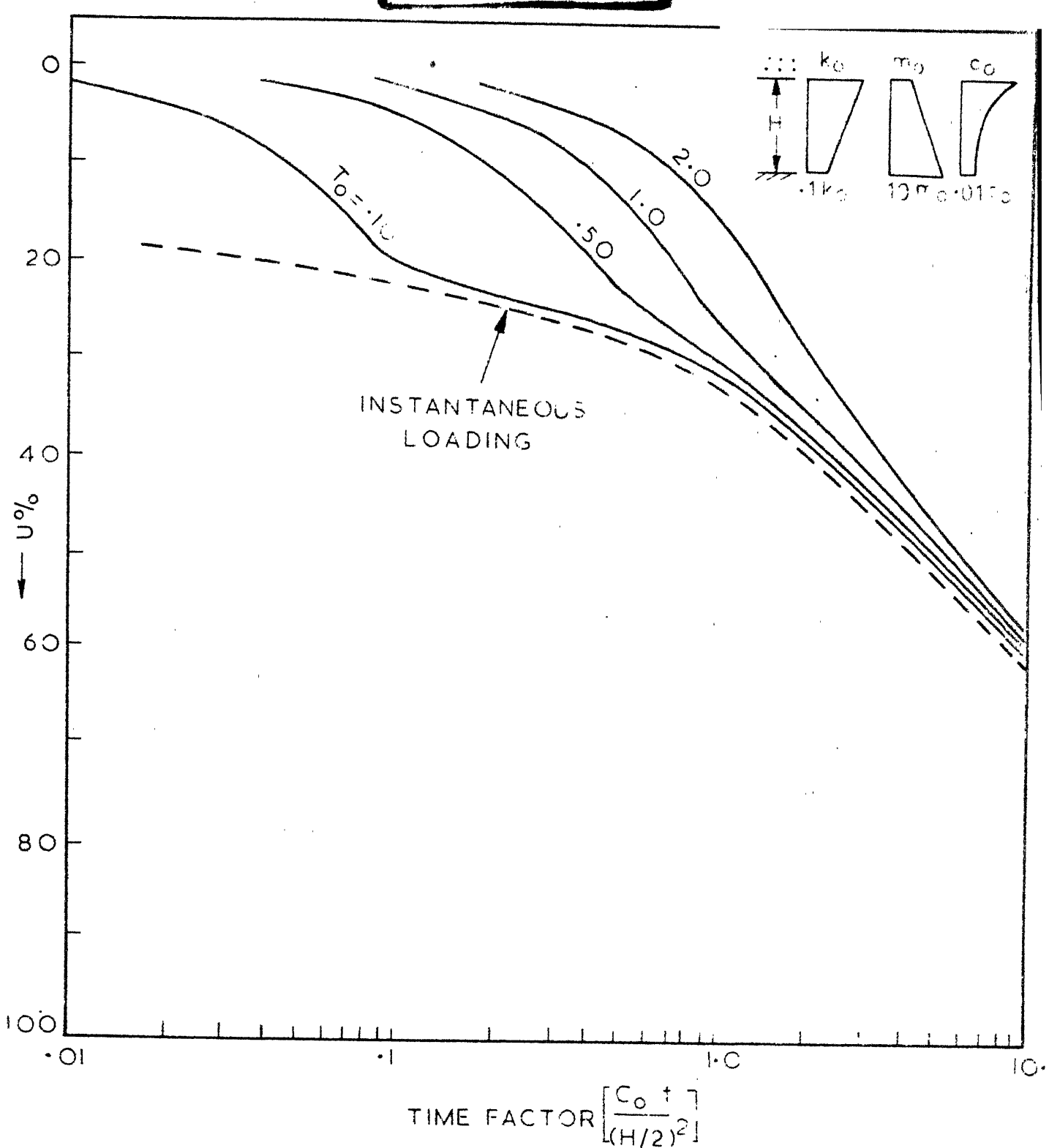


FIG. 2.22 CONSOLIDATION UNDER CONSTRUCTION LOADING-  
THICK LAYER

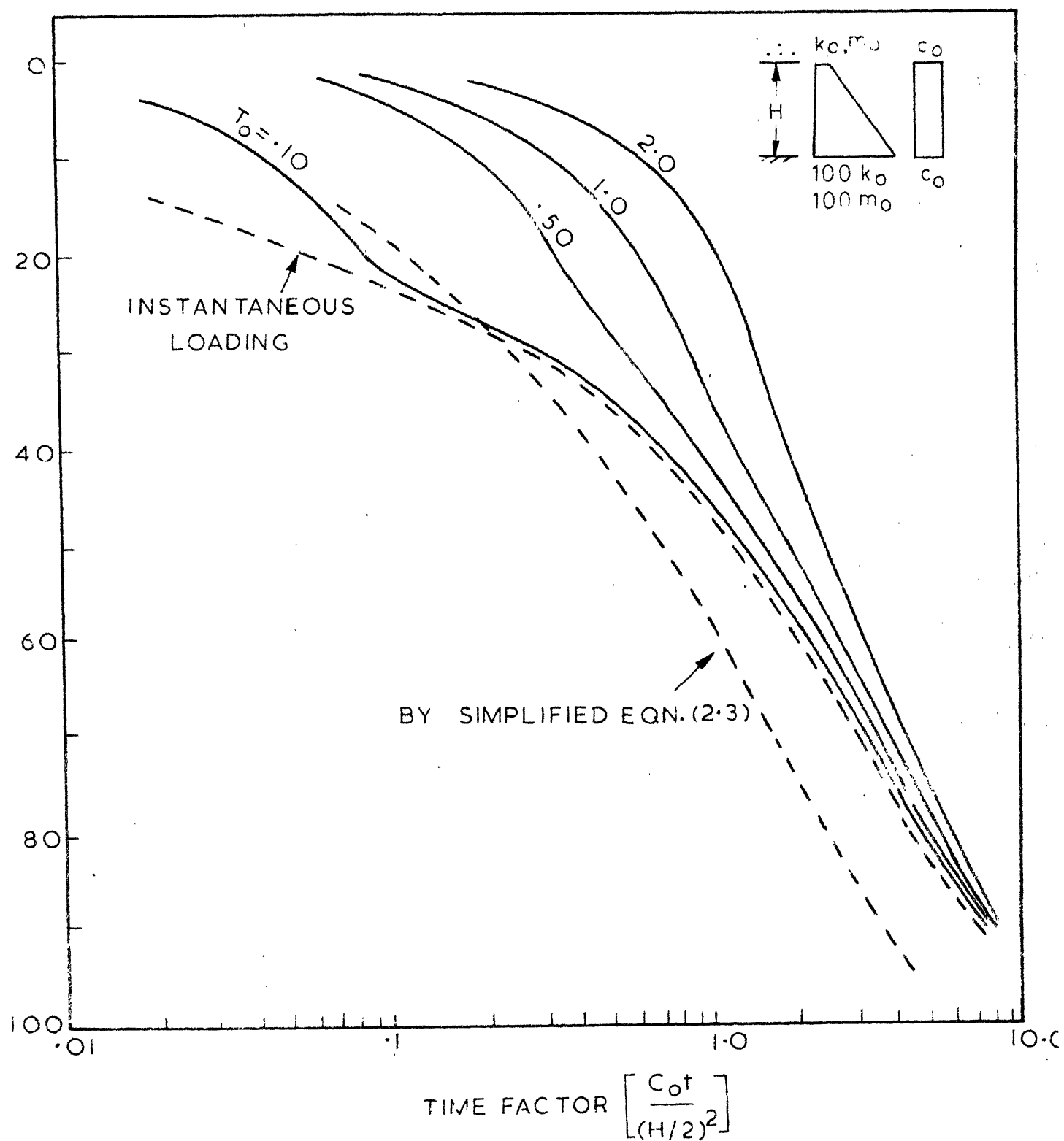


FIG. 2.24 CONSOLIDATION UNDER CONSTRUCTION LOADING - THICK LAYER

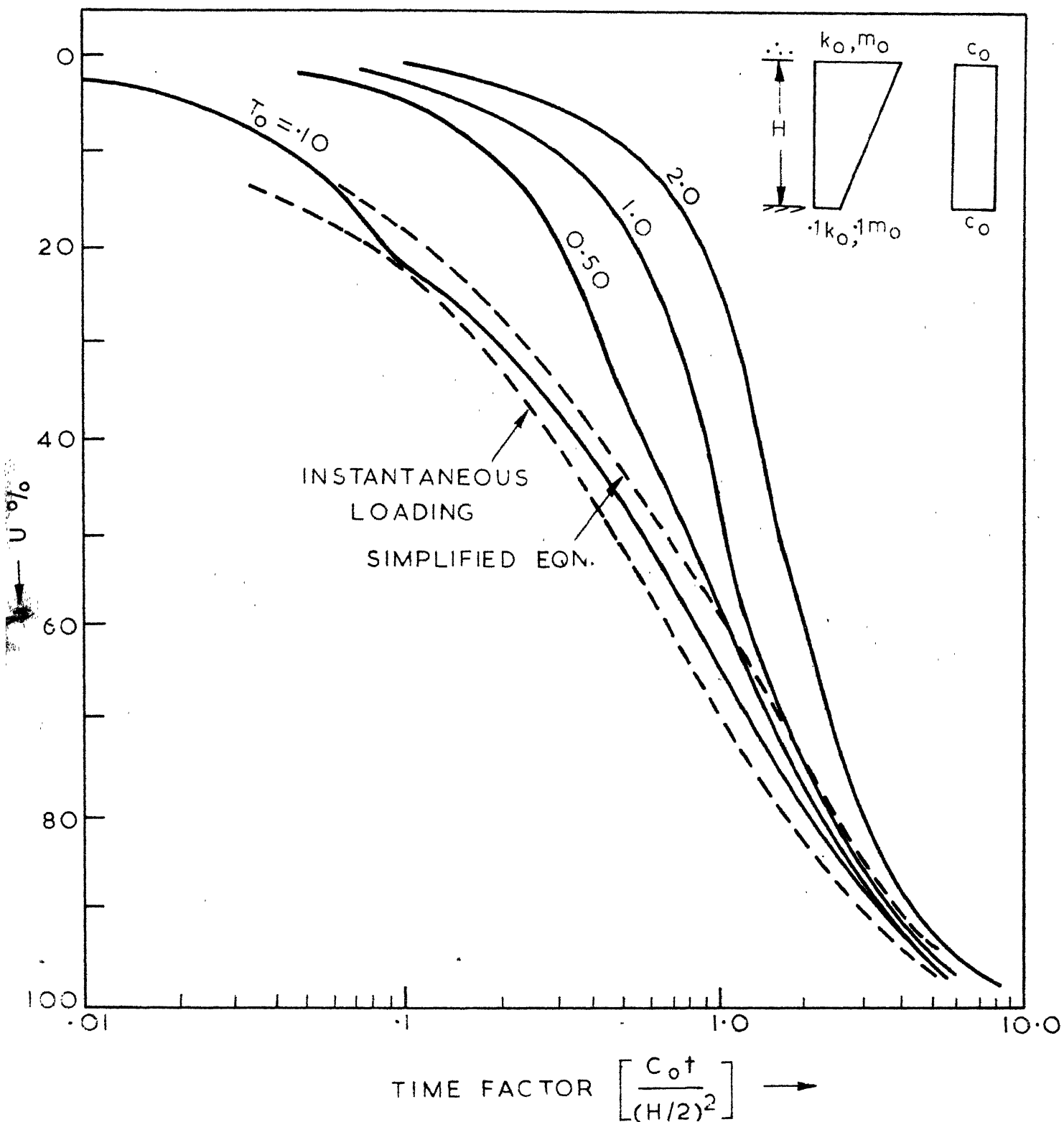


FIG. 2.25 CONSOLIDATION OF THICK LAYER UNDER CONSTRUCTION LOADING

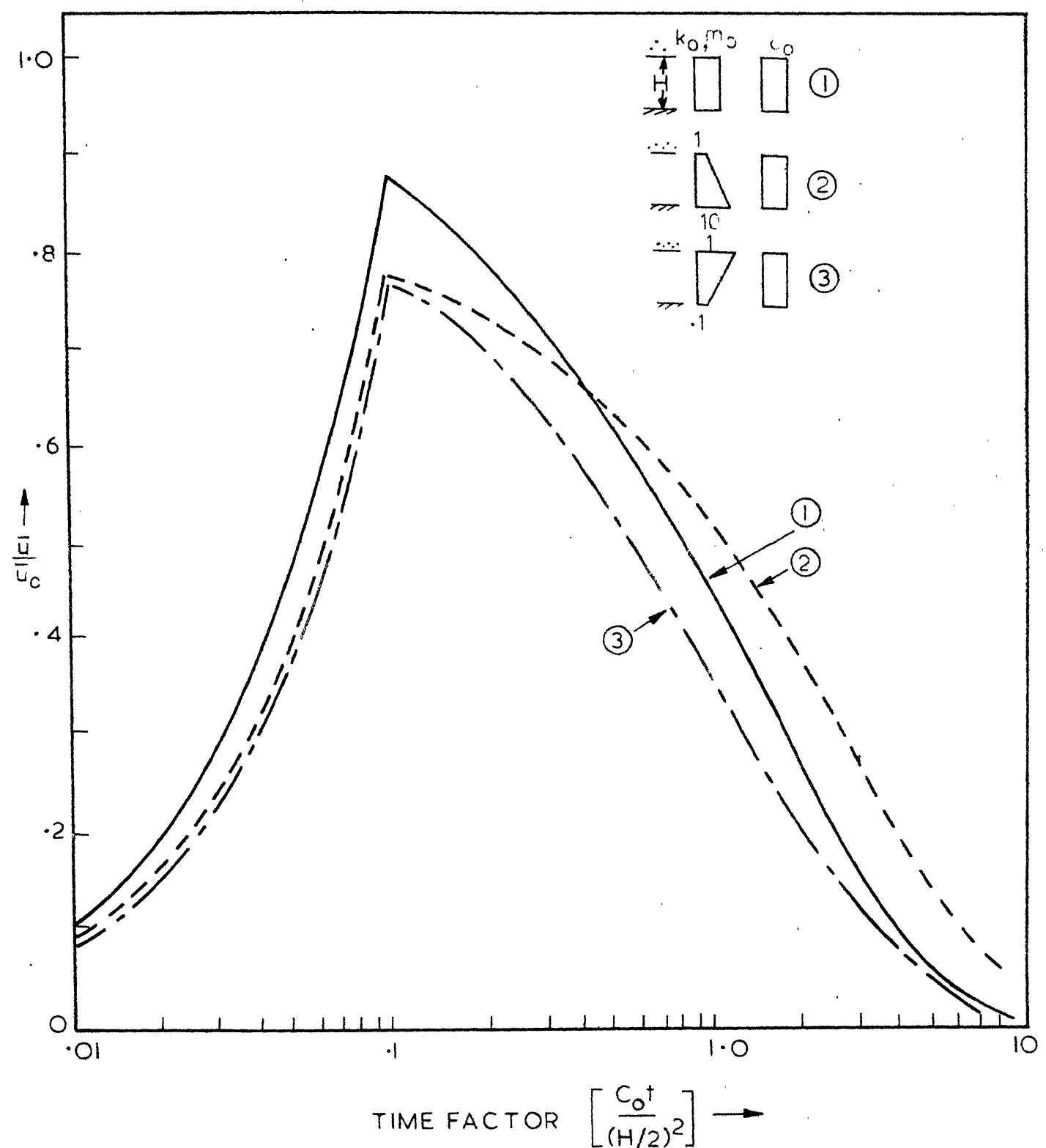


FIG. 2.26 AVERAGE PCRE-PRESSURE RATIOS UNDER CONSTRUCTION LOADING

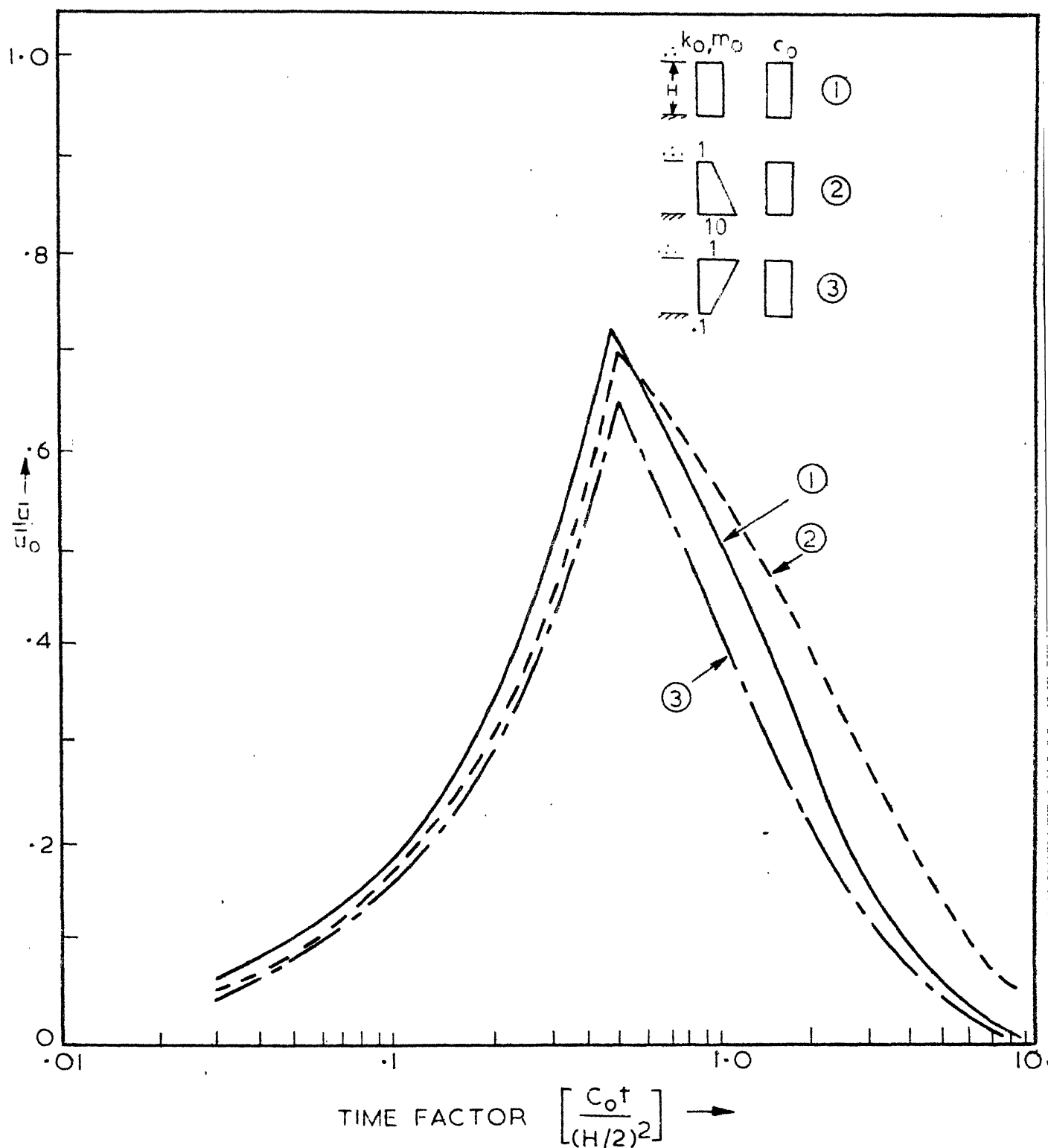


FIG. 2-27 AVERAGE PORE PRESSURE RATIOS UNDER CONSTRUCTION LOADING

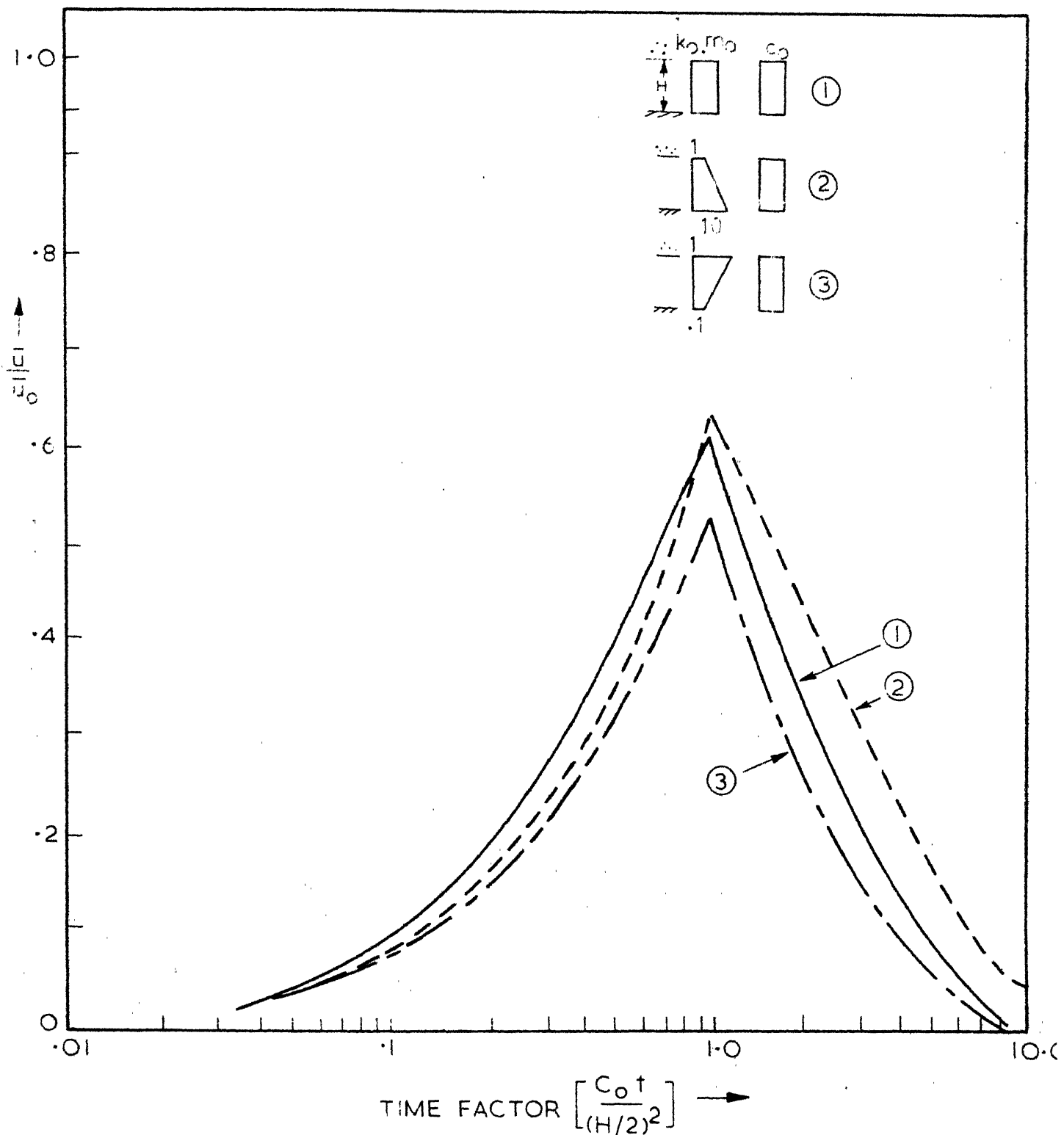


FIG. 2-28 AVERAGE PORE PRESSURE RATIOS UNDER CONSTRUCTION LOADING

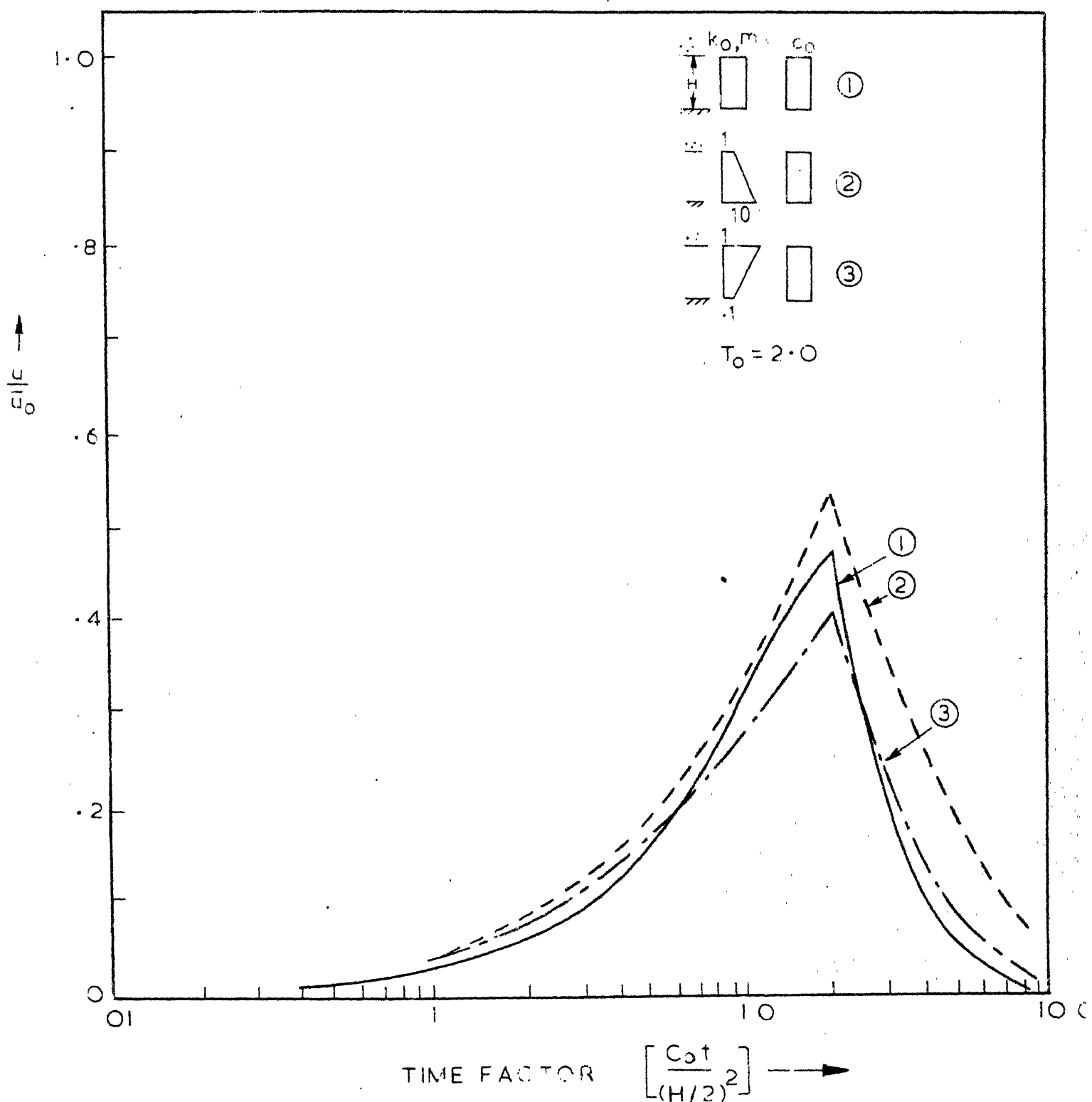


FIG. 2.29 AVERAGE PORE PRESSURE RATIOS UNDER CONSTRUCTION  
LOADING

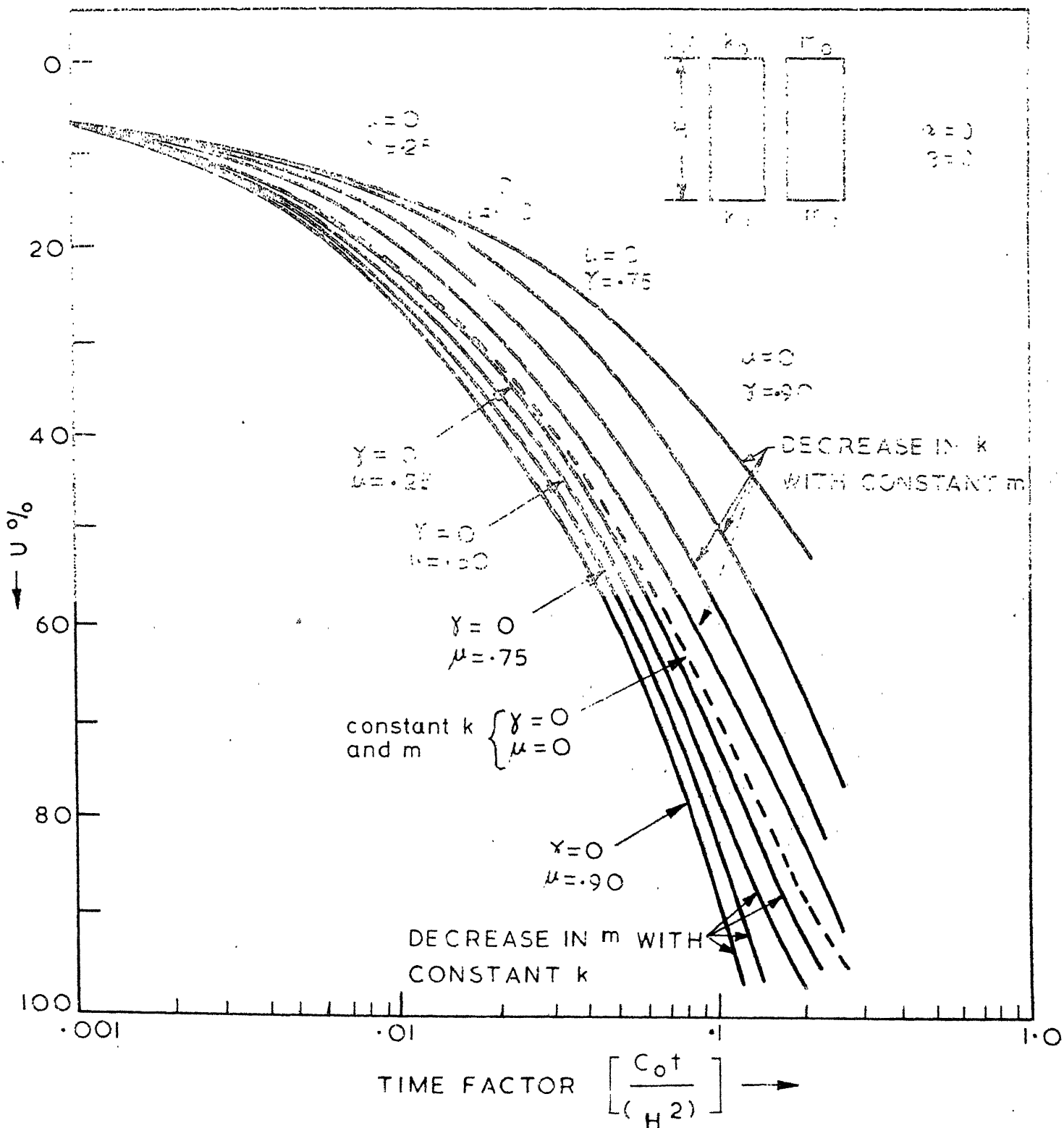


FIG. 2-30 EFFECT OF INDIVIDUAL DECREASE OF  $k$  AND  $m$  WITH PORE PRESSURE

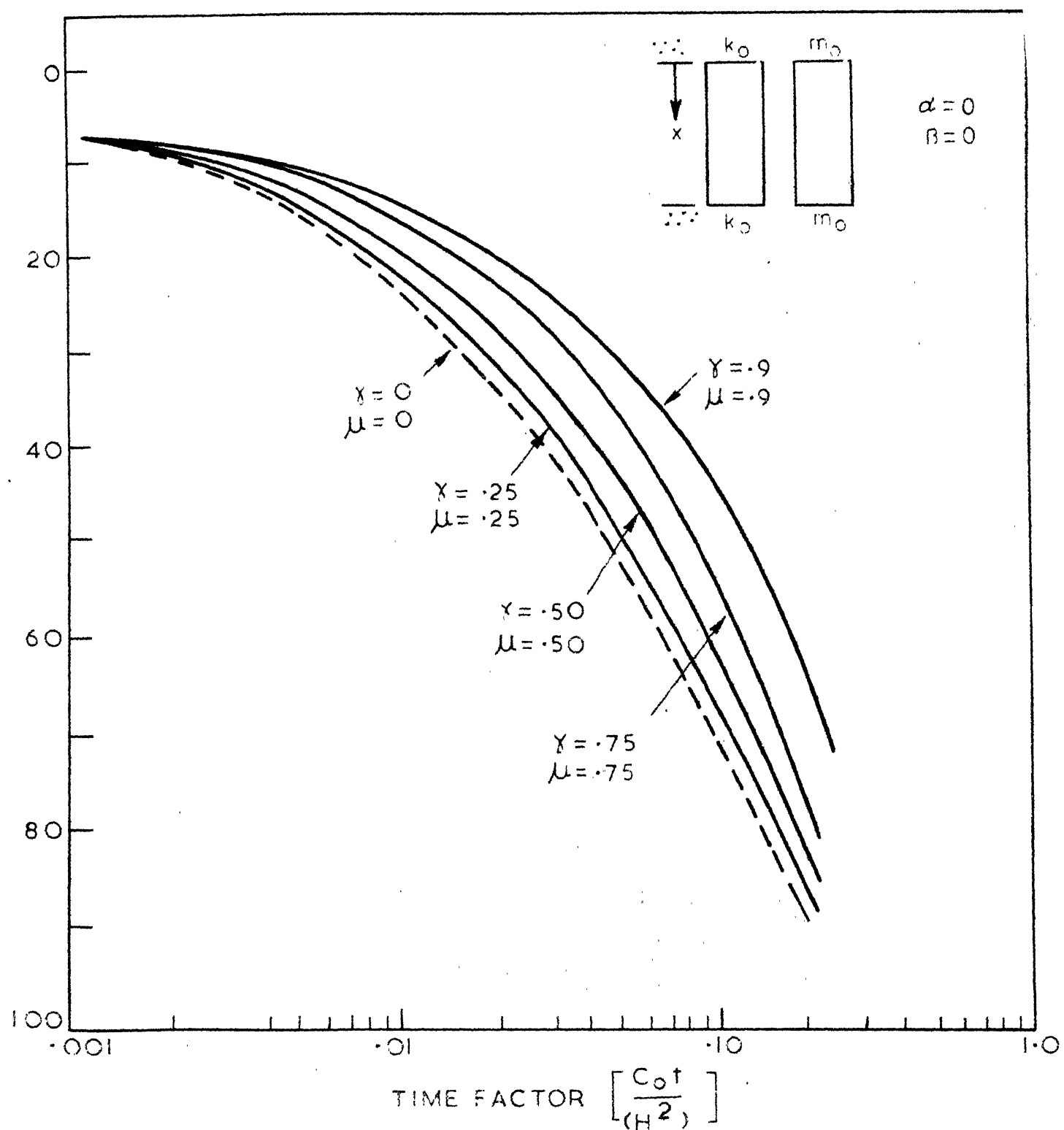


FIG. 2-31 EFFECT OF DECREASE OF  $k$  AND  $m$  WITH PORE-PRESSURE

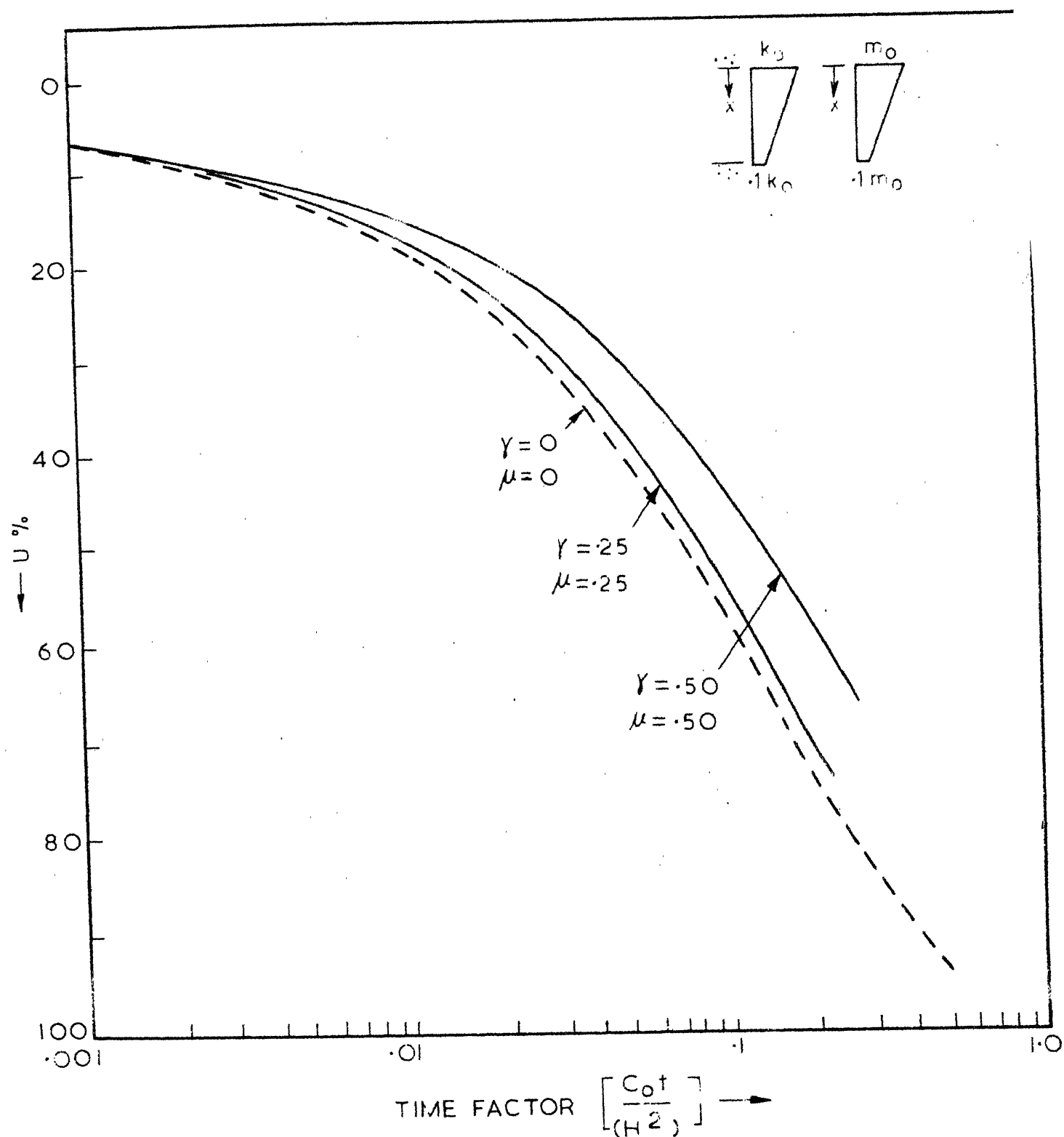


FIG. 2.32 EFFECT OF GENERAL VARIATION OF  $\gamma$  AND  $\mu$ , WITH CONSTANT  $C$

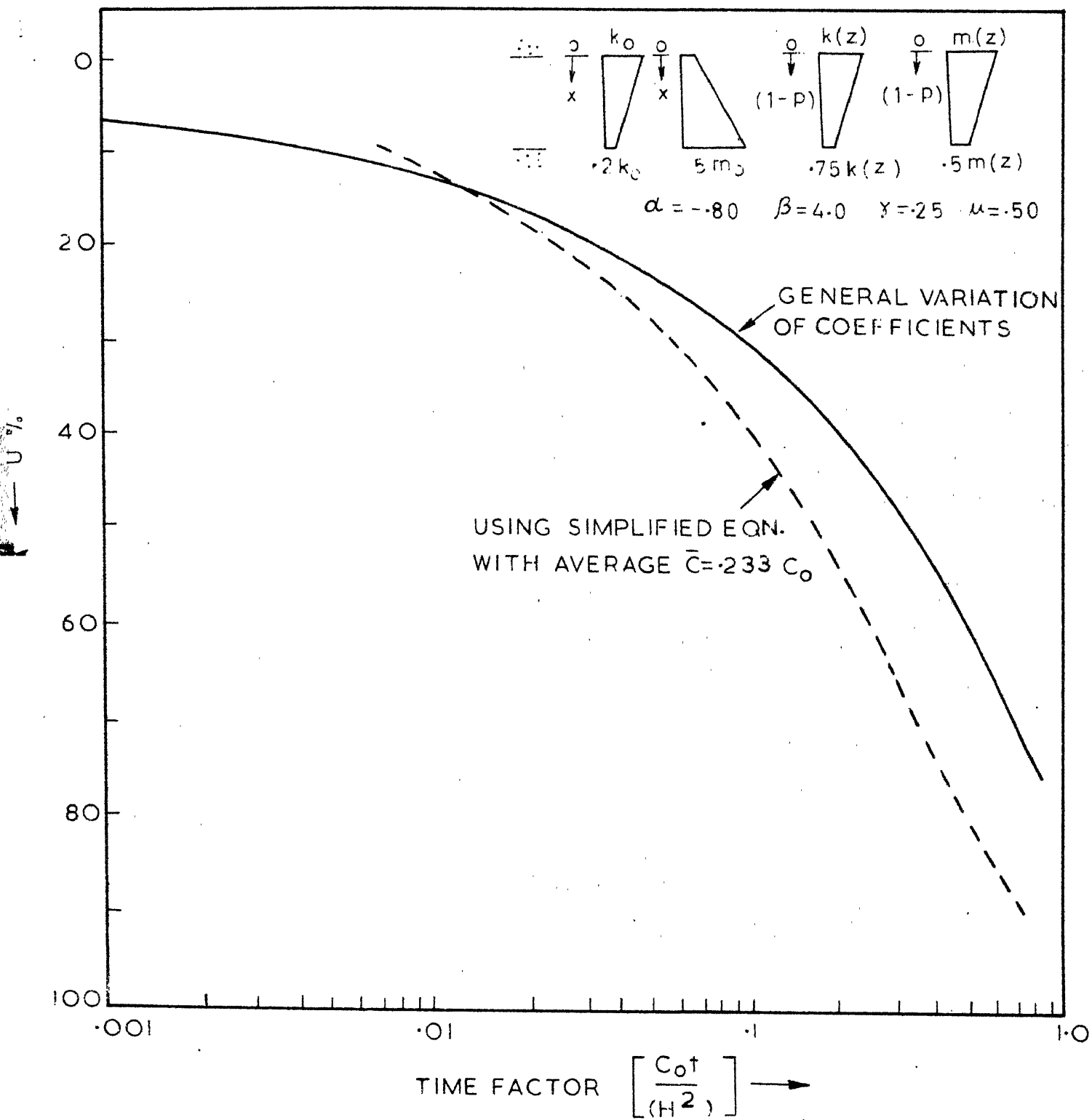


FIG. 2.33 EFFECT OF GENERAL VARIATION OF  $k$  AND  $m$

## CHAPTER III

### CONSOLIDATION OF LAYERED SYSTEM UNDER INSTANTANEOUS LOADING

#### INTRODUCTION

The effect of several variables on the prediction of time rate of settlement using Terzaghi's original formulation has engaged the attention of many research workers in the past. However, the layered systems which are common occurrences in field have received only limited attention. Several empirical approaches aimed at the use of transformed sections or averaging the soil properties yield approximate estimates, (22), (28), (39). The only closed form solution for a two-layer system was presented by Gray (14). Analytical approach for more than two layers is extremely difficult. However, the use of numerical technique with the help of high speed digital computers offers greater scope and facility for obtaining more dependable prediction of time rate of settlement for layered systems. Selected cases of layered systems are analysed here for possible ranges of soil properties so that their effects on the consolidation phenomenon can be studied.

#### FINITE DIFFERENCE METHOD

Abbot (1) solved a three-layer system by finite difference method for a particular configuration of the layers.

Raymond (25) used finite difference solutions to compare with his experimental results of two-layer system. Barden (3) employed the numerical method to compare the test results for radial flow in layered systems. Davis (12) gave time factor contours at fifty percent consolidation in a two-layer system. An attempt is made here to present design charts for a two-layer system. Also, typical cases of three-layer system are analysed to demonstrate the errors involved in estimation by simplified approach.

The simplified consolidation equations for layered system are:

$$c_j \frac{\partial^2 u_j}{\partial z^2} = \frac{\partial u_j}{\partial t} \quad (3.1)$$

where the subscript j denotes the layer number.

The above equation is written in the finite difference form using the mesh as shown in Fig. 3.1 as follows:

$$\frac{u_1 - u_0}{\delta t} = \frac{c_j}{(\delta z_j)^2} (u_2 - 2u_0 + u_4) \quad (3.2)$$

Therefore  $u_1 = (1-2B_j) (u_0 + B_j u_2 + B_j u_4) \quad (3.3)$

where  $B_j = \frac{c_j \delta t}{(\delta z_j)^2} \quad (3.4)$

The boundary conditions are:

- (1) At the drainage boundary  $u_1 = 0$
- (2) At the impervious boundary  $u_2 = u_4$
- (3) At the interface of the two layers

Consider the finite difference mesh on the interface boundary such that the points 0, 3 and 1 fall on the boundary and points 2 and 4 on layers A and B respectively.

In layer A: From Taylor's expansion we have:

$$u_2 = u_0 - \delta z \left( \frac{\partial u}{\partial z} \right)_{OA} + \left( \frac{\delta z}{2} \right)^2 \left( \frac{\partial^2 u}{\partial z^2} \right)_{OA} + \dots \quad (3.5)$$

where OA denotes the derivatives at the point 0 towards layer A.

Therefore:  $\left( \frac{\partial^2 u}{\partial z^2} \right)_{OA} = \frac{2}{(\delta z)^2} \left\{ u_2 - u_0 + \delta z \left( \frac{\partial u}{\partial z} \right)_{OA} \right\}$  (3.6)

The time derivative is approximated as:

$$\left( \frac{\partial u}{\partial t} \right)_{OA} = \frac{u_1 - u_0}{\delta t} \quad (3.7)$$

Substituting the Eqs. (3.6) and (3.7) in the consolidation equation:

$$C_A \frac{\partial^2 u}{\partial z^2} = -\frac{\partial u}{\partial t} \text{ in layer A} \quad (3.8)$$

$$\text{We get } \frac{2C_A}{\delta Z^2} \left\{ u_2 - u_0 + \delta Z \left( \frac{\partial u}{\partial Z} \right)_{OA} \right\} = \frac{u_1 - u_0}{\delta t} \quad (3.9)$$

$$\text{i.e. } \delta Z \left( \frac{\partial u}{\partial Z} \right)_{OA} = \frac{u_1 - u_0}{2 \frac{C_A \delta t}{\delta Z^2}} + u_0 - u_2 \quad (3.10)$$

In layer B: Similarly it can be derived in layer B,

$$-\delta Z \left( \frac{\partial u}{\partial Z} \right)_{OB} = \frac{u_1 - u_0}{2 \frac{C_B \delta t}{(\delta Z)^2}} + u_0 - u_4 \quad (3.11)$$

Now substituting the boundary conditions:

$$k_A \left( \frac{\partial u}{\partial Z} \right)_{OA} = k_B \left( \frac{\partial u}{\partial Z} \right)_{OB} \quad (3.12)$$

and thus equating the Eqs. (3.10) and (3.11) and simplifying,

$$u_1 = u_0 + \frac{2 \lambda C_A}{\frac{C_A}{k_A} + \frac{C_B}{k_B}} u_4 - \left( 1 + \frac{k_A}{k_B} \right) u_0 + \frac{k_A}{k_B} u_2 \quad (3.13)$$

where  $\lambda = \delta t / (\delta Z)^2$ .

It can be readily checked that when  $k_A = k_B$  and  $C_A = C_B$ , the Eq. (3.13) reduces to the original form of Eq. (3.2).

Alternatively this boundary condition can be derived by equating the rate of change of volume and flow in two half

sublayers, (25). The expression by this procedure is obtained as:

$$u_1 = E_{j,j+1} (u_2 - u_0) + F_{j,j+1} (u_4 - u_0) + u_0 \quad (3.14)$$

where

$$E_{j,j+1} = 2B_j m_j \delta Z_j / (m_j \delta Z_j + m_{j+1} \delta Z_{j+1}) \quad (3.15)$$

$$F_{j,j+1} = 2B_{j+1} m_{j+1} \delta Z_{j+1} / (m_j \delta Z_j + m_{j+1} \delta Z_{j+1}) \quad (3.16)$$

and the subscripts denote the layers.

The condition of Eq. (3.16) reduces to that of Eq. (3.13) for the particular case of  $\delta Z_A = \delta Z_B$ .

The above finite difference method is employed in the explicit method to solve the simultaneous difference equations obtained, noting the stability of this procedure depends upon the criteria  $(C_j \delta t / (\delta Z_j)^2) < 1/2$ . Here the computation is carried on in a partitioned manner. The time interval is divided into six parts and the space interval into ten parts. The values computed at end points of one panel is fed into the starting points of the next panel. As consolidation progresses the mesh sizes are varied to save computation time. A general programme is written to vary all the parameters.

Using the finite difference method, a few selected cases of the two and three-layer systems as shown in Fig. 3.2 to 3.5 are studied. The results of the computations of various cases are presented in the form of graphs in Figs. 3.6 to 3.35.

## TWO-LAYER SYSTEMS

### Effect of the soil parameters k, m and C

In order to study the effects of the soil parameters, a two-layer system with layers of equal thickness is taken. The ratios  $k_2/k_1$ ,  $m_2/m_1$  and  $C_2/C_1$  are varied. The pore pressure distribution along the depth at various time factors is shown in the figures.

### Layers with same compressibility

The results show that in a two-layer system with same compressibility but with unequal permeability drained on both faces, the layer with higher permeability has faster dissipation of pore pressure (Figs. 3.6 to 3.10). This behaviour can be visualised intuitively. The volume of water expelled in both the layers is same because of the equal compressibility. In the layer with higher permeability, the water has to flow faster resulting in a higher rate of consolidation. However, when one-layer has relatively larger permeability, say, of the order of hundred times or more as that of the other layer, most of the consolidation in the earlier stages is essentially within the layer with higher permeability. The rate of consolidation in this layer is very nearly the same as if it is a single layer with one way drainage. Therefore, if the rate of consolidation of a two-layer system with constant compressibility but with higher permeability ratios ( $>100$ ) is to be estimated in approximate steps it is suggested that

the initial rates be obtained simply for the layer with higher permeability for one-way drainage. The rates of settlement at longer periods can then be obtained by computing the rates for the layer with lower permeability treating it with two-way drainage, with its initial time taken at the end of the consolidation period for the layer with higher permeability.

The above approximate method is clearly demonstrated by the example shown in Fig. 3.11. The total settlement of the two layers is assumed as 10 inches so that the settlement in each of the layers is 5 inches. The graph is drawn between the settlement and the time factor.

#### Layers with same coefficient of consolidation

For a system with two layers of equal thickness and same coefficient of consolidation, with two face drainage there is no effect due to variation in  $k$  and  $m$  (Figs. 3.12 and 3.13). This is because that the interface boundary condition is unaffected as  $\partial u / \partial Z$  at the interface is zero and the flow is taking place from the centre towards the top and bottom surfaces symmetrically.

In as much as the coefficient of consolidation is the same in all the layers the normal tendency will be to treat the layer system as one single layer and use the simplified equation to obtain the rates of settlement. The fallacy in such an approach is demonstrated herein. Take for instance a two-layer system drained at the top face only with layers of equal thickness

and same coefficient of consolidation but the layer adjacent to the drainage boundary is having relatively lesser values of  $k$  and  $m$ . In such a situation the rate of consolidation in both the layers is found to be much slower than what is obtained by treating the system as a single layer (Fig. 3.14). In the figure the dotted curves are drawn as per simplified analysis assuming the layer system as a single layer with thickness equal to the total thickness of the layers. The consolidation ratios at various time factors of the individual layers are obtained from the area of the pore pressure isochrones of the time factors in the corresponding thickness. It is noted here that the volume of water expelled due to larger volume change farther from the drainage face meets with higher resistance to flow towards the drainage face through the layer with lesser permeability. This causes the retardation in the rate of consolidation.

The reverse situation occurs when the layer adjacent to the drainage boundary has relatively higher permeability and compressibility. The consolidation is found to be faster than that obtained by treating the system as single layer (Fig 3.15).

#### Layers with same permeability

In a two-layer system with a two-face drainage and layers of equal thickness and same permeability but with different compressibility, the layer with less compressibility

drains faster than the layer with higher compressibility (Figs. 3.16 and 3.17).

#### Layers with different permeability and compressibility

The combined layer action is more pronounced in a two-layer system with layers having different permeability and compressibility (Figs. 3.18 and 3.19). The pore pressure distribution shown in the figures demonstrates the combined influence of the permeability and compressibility ratios on the consolidation rates.

#### Design charts

For a two-layer system draining on both faces, an attempt is made to obtain design charts for a possible range of soil parameters. The following non-dimensional parameters are chosen for the computations:

$$\bar{\alpha} = \frac{k_2 h_1}{k_1 h_2} \quad ; \quad \bar{\beta} = \frac{c_2 h_1^2}{c_1 h_2^2}$$

The parameters  $\bar{\alpha}$  and  $\bar{\beta}$  are varied from 1 to 100. The consolidation ratios  $u_1$  and  $u_2$  of the two layers are presented in Figs. 3.20 to 3.31 at various time factors. For values of  $\bar{\alpha}$  and  $\bar{\beta}$  from 1 to .01, the position of the layers can be reversed and the same design charts can be used. Suitable interpolations can be made for any intermediate values of the parameters.

Illustration

For a case of  $\alpha = 40$  and  $\beta = 5$  the consolidation ratios obtained from the charts are given in Table 3.1

Table 3.1  
Consolidation of the two layers

$U_1\%$	$T_1$	$U_2\%$	$T_2$
11.5	.001	30.0	.08
15.0	.016	43.0	.16
19.0	.024	47.0	.24
21.5	.032	63.0	.48
81.5	.240	84.0	.80
97.0	.480	99.0	1.60

The design charts for a limited range of the parameters are presented here. Since the computation time required is very large for extreme ratios of parameters, all the ranges are not attempted.

## THREE-LAYER SYSTEM

Layers with same coefficient of consolidation

A three-layer system with two face drainage and layers of equal thickness and same coefficient of consolidation but with middle layer having relatively larger values of permeability

and compressibility is considered. In such a situation the rate of consolidation in all the three layers is found to be much slower than what is obtained by treating the system as single layer (Fig. 3.32). The drainage faces are located adjacent to the two outer layers having lower values of  $k$  and  $m$  than the middle layer. Therefore, the volume of water expected due to larger volume change farther from the drainage faces meets with higher resistance to flow towards the drainage faces through the layers with lower permeability. This causes the retardation of flow.

In a reverse situation where the top and bottom layers have values of  $k$  and  $m$  relatively larger than the middle layer the consolidation is faster (Fig. 3.33).

The above cases are also studied for a single face drainage at the top. When the middle layer has relatively higher permeability and compressibility the rates of consolidation are slower than the rates computed by simplified analysis assuming the system as a single layer (Fig. 3.34). In the reverse situation when the top bottom layers have relatively higher values of  $k$  and  $m$  than the middle layer, the rate of consolidation in the earlier stages is faster and in the latter stages slower than the rate predicted by simplified analysis assuming the system as a single layer (Fig. 3.35). The combined influence of the location of the drainage boundary and the relative values of  $k$  and  $m$  of the layers is observed here.

## CONCLUSIONS

In a two-layer system with two face drainage and layers of same thickness and compressibility, if one of the layers has relatively very large permeability, most of the consolidation in the earlier stages is essentially in the layer with higher permeability. This phenomenon is utilized in suggesting an approximate method for computing the rates of settlement in such cases.

A two-layer system with two face drainage having layers of same thickness and coefficient of consolidation can be treated as a single layer. However, if the drainage is on only one side it will be erroneous to treat this system as single layer despite the same coefficient of consolidation. The rate of consolidation in such a case will be governed by the relative values of  $k$  and  $m$  of the two layers, and the location of the drainage boundary.

Design charts for a limited range of soil parameters for a two-layer system with two way drainage are presented.

For a three-layer system with layers of same thickness and coefficient of consolidation whether draining on single or both faces it will be erroneous to resort to simplified analysis assuming the system as a single layer. In this case the rates of consolidation are governed by the relative values of permeability and compressibility of the individual layers and the location of the drainage boundary.

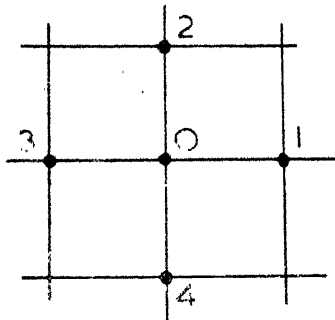


FIG. 3.1 FINITE DIFFERENCE MESH

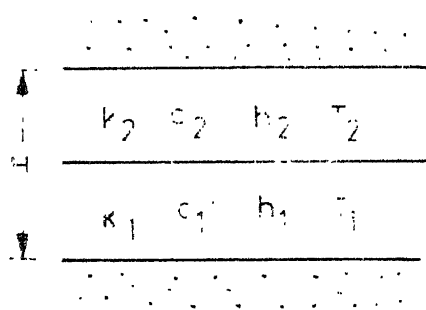


FIG. 3.2 TWO LAYER WITH -  
TWO WAY DRAINAGE

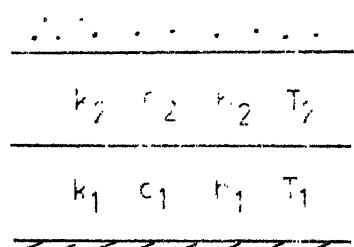


FIG. 3.3 TWO LAYER WITH -  
ONE WAY DRAINAGE

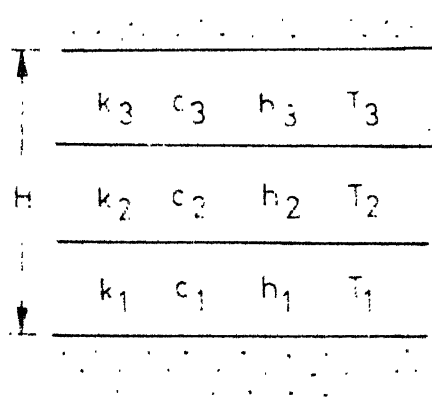


FIG. 3.4 THREE LAYER WITH  
TWO WAY DRAINAGE

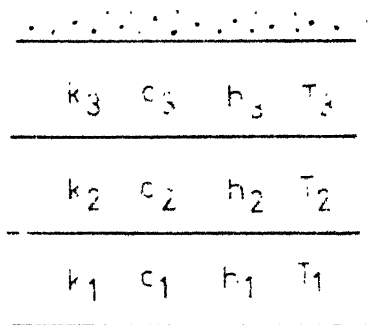


FIG. 3.5 THREE LAYER WITH  
ONE WAY DRAINAGE

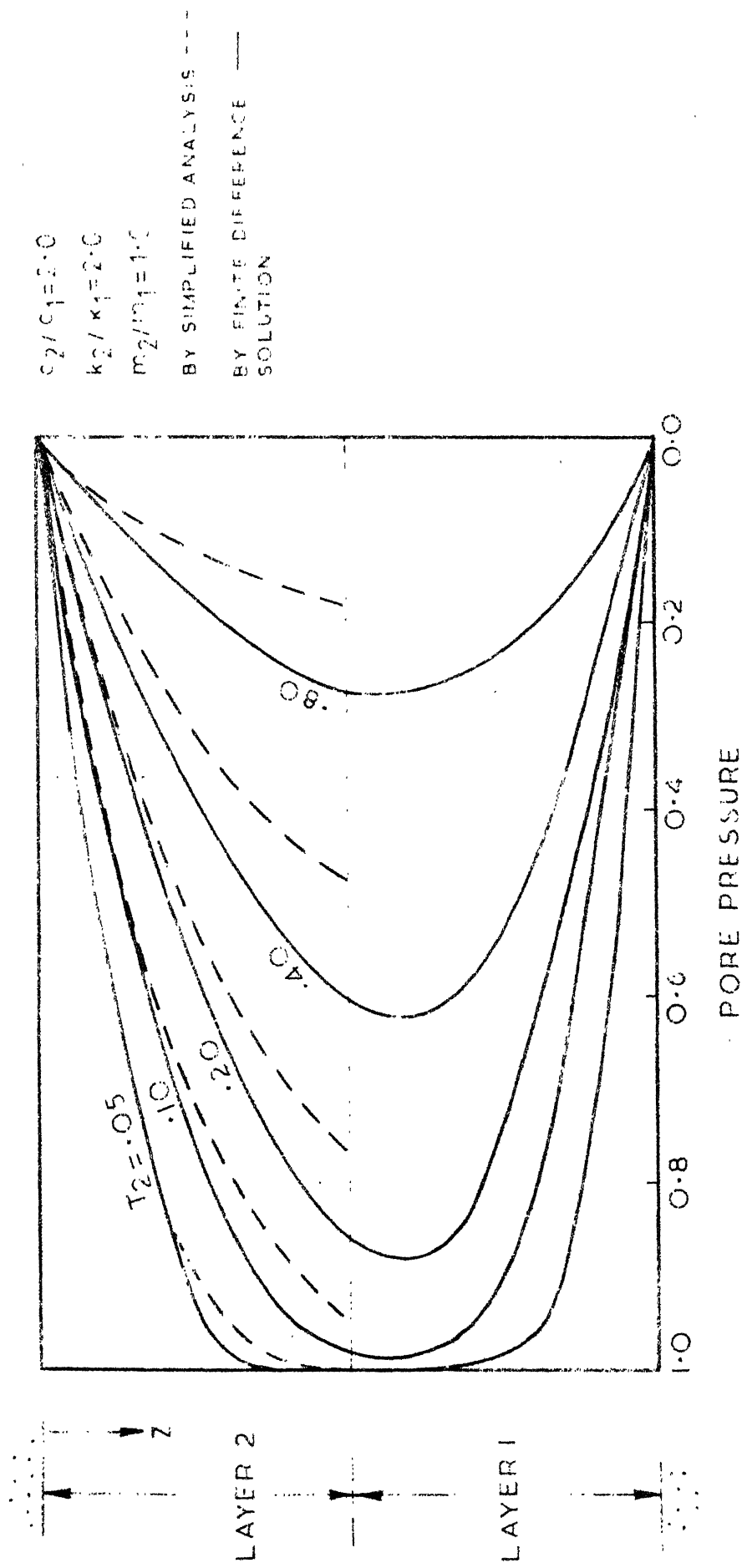


FIG. 3.6 CONSOLIDATION OF TWO LAYER SYSTEM  
WITH CONSTANT ' $m_i$ '

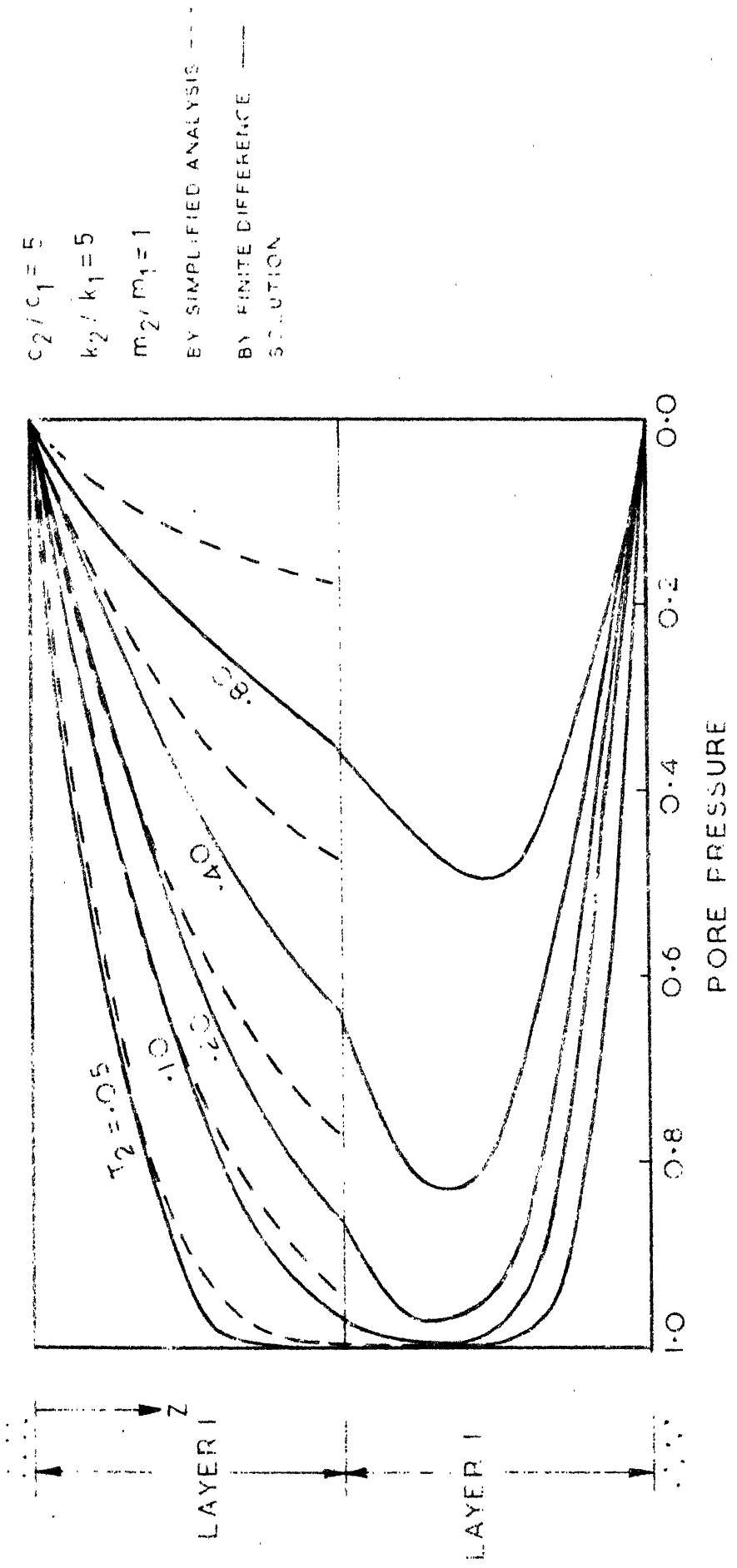


FIG. 3.7 CONSOLIDATION OF TWO LAYER SYSTEM  
WITH CONSTANT  $e_{tr}$

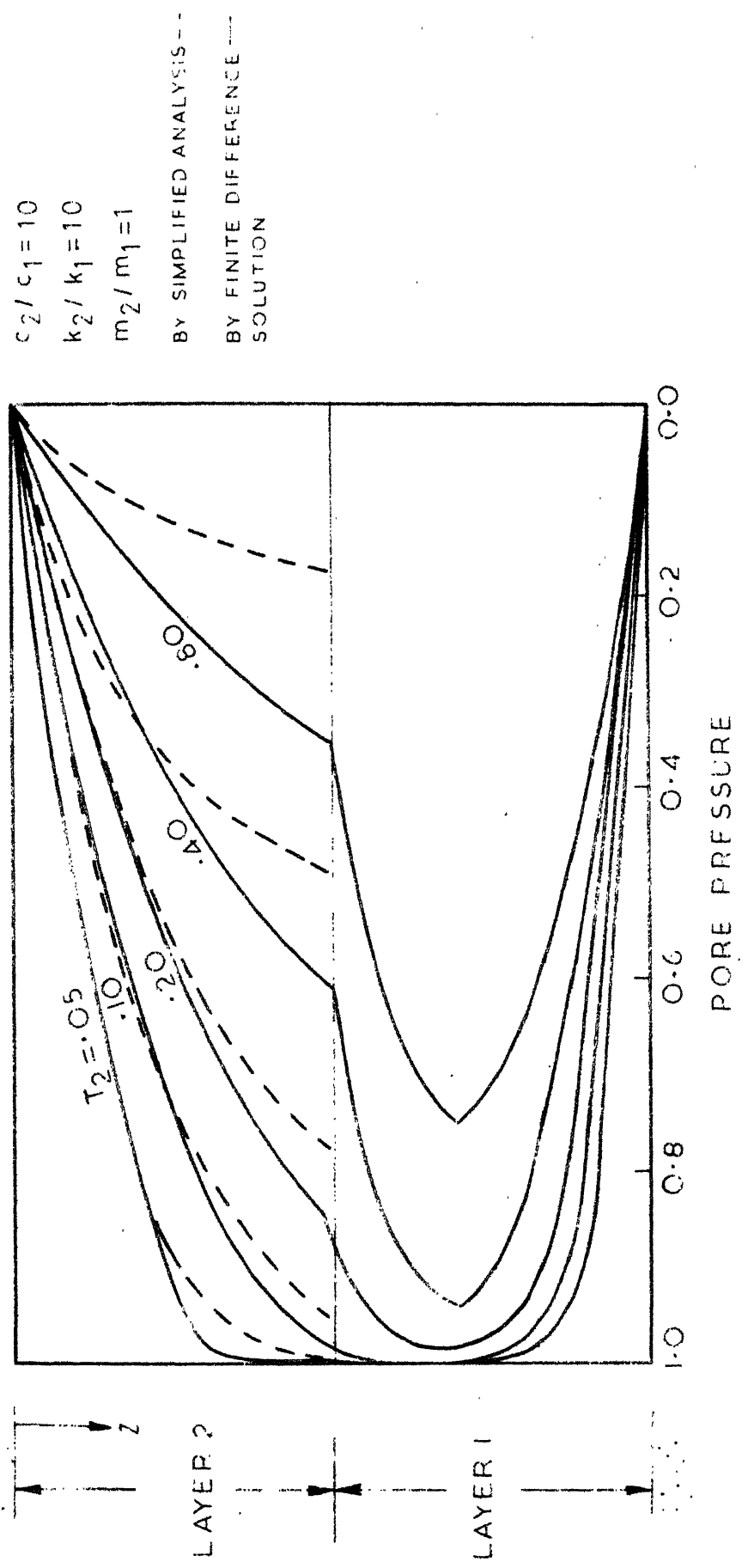


FIG. 3.8 CONSOLIDATION OF TWO LAYER SYSTEM  
WITH CONSTANT  $m_1$

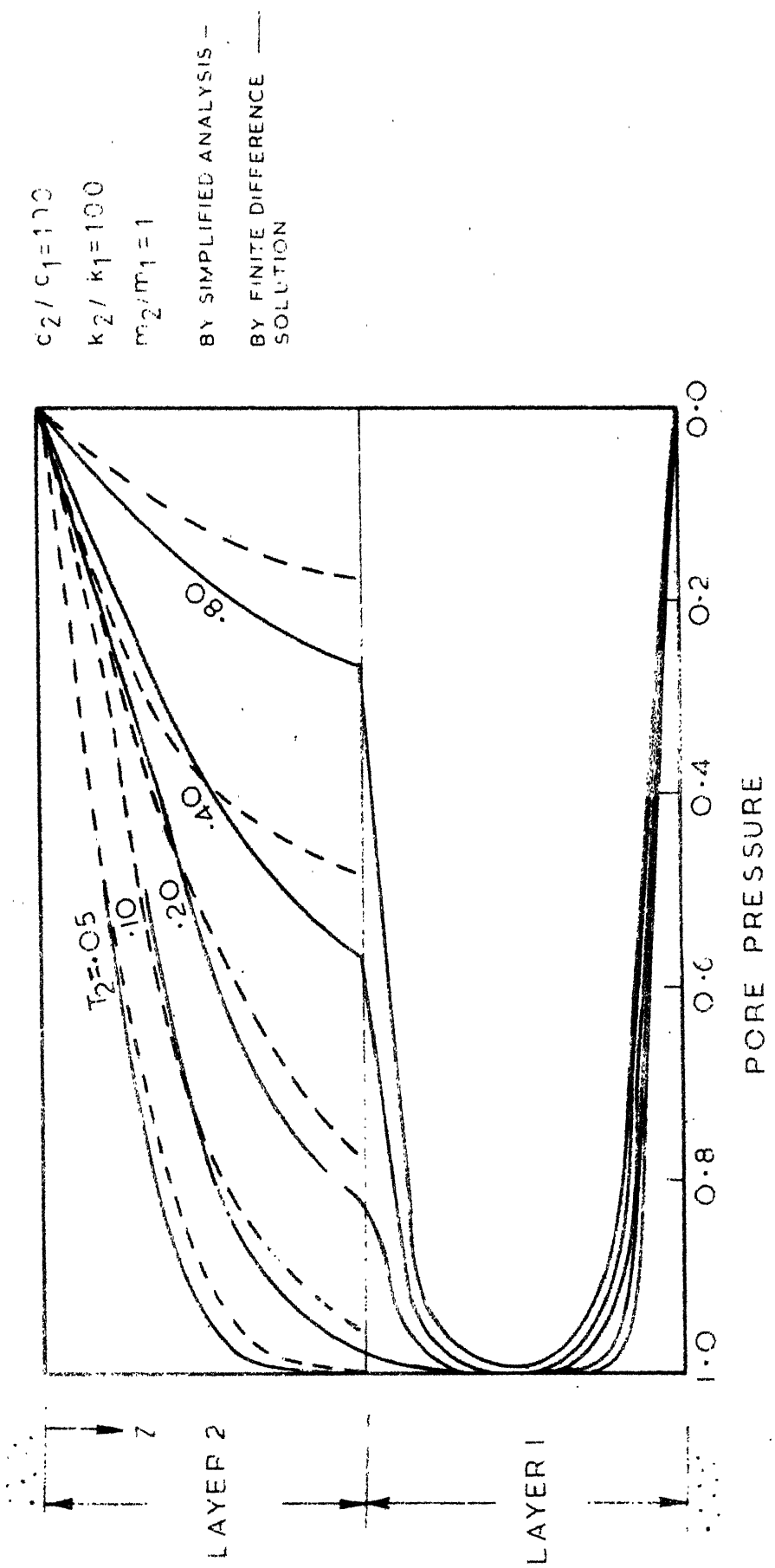


FIG. 3.9 CONSOLIDATION OF TWO LAYER SYSTEM  
WITH CONSTANT 'm'

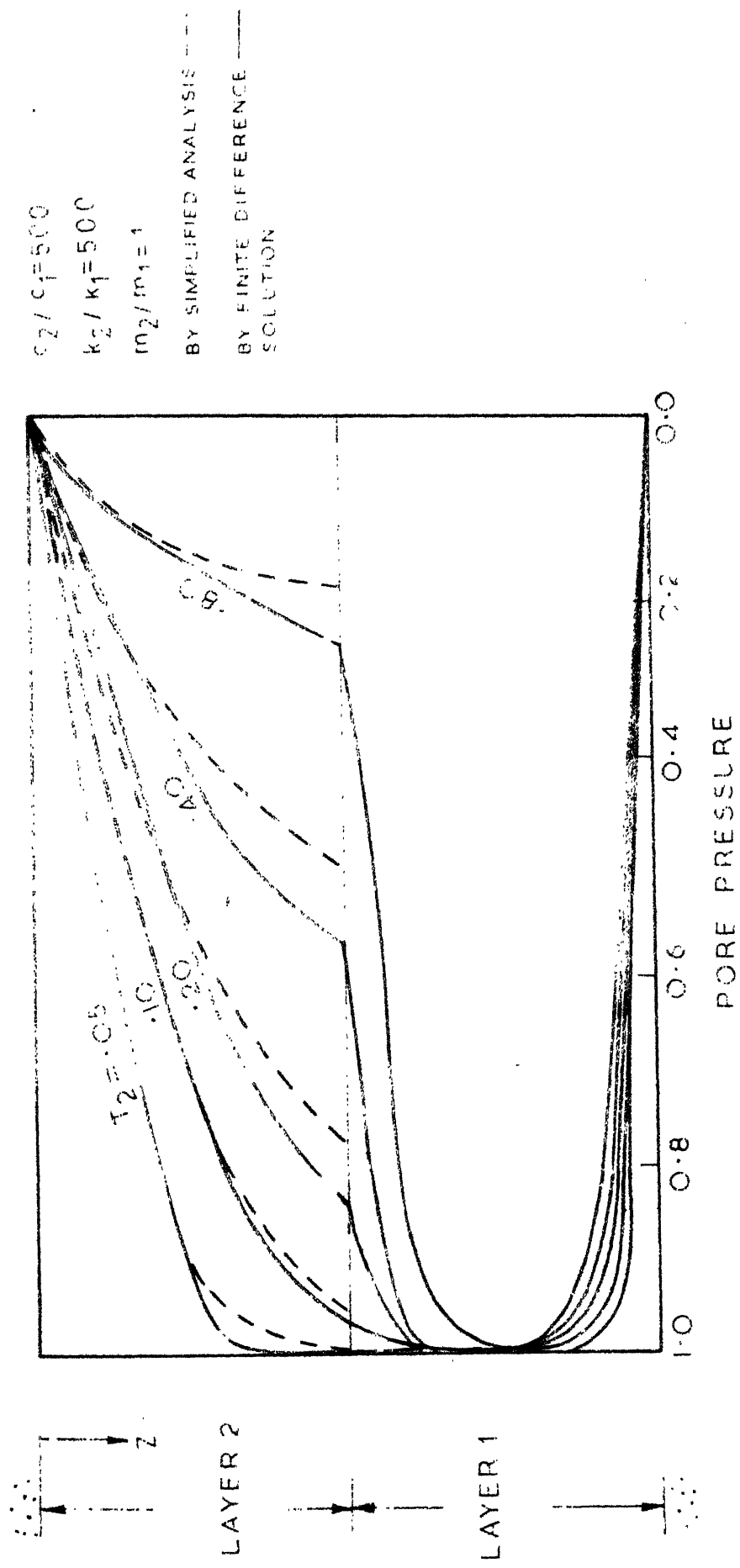


FIG. 3.10 CONSOLIDATION OF TWO LAYER SYSTEM  
WITH CONSTANT  $m_2 / m_1$

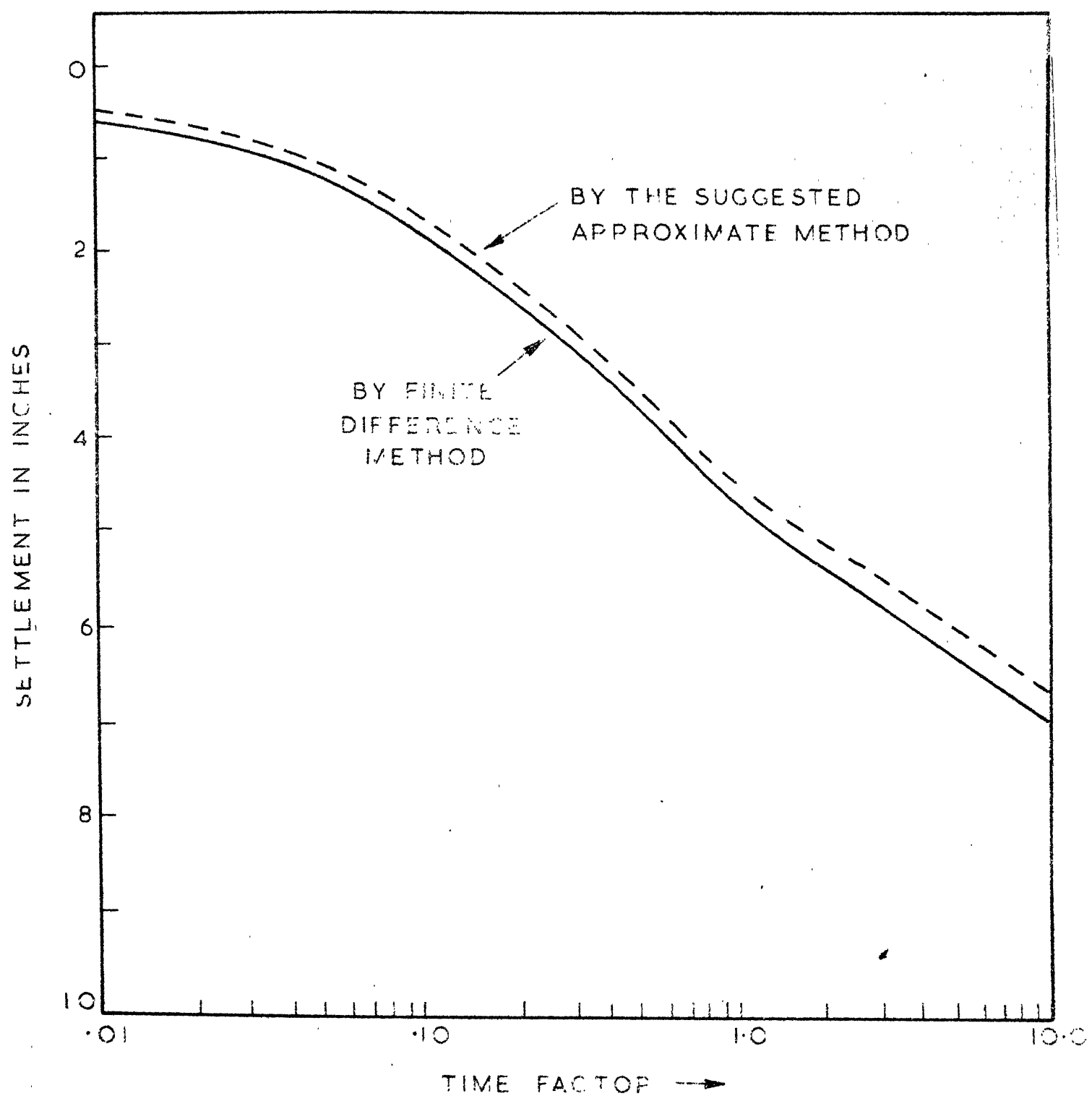


FIG. 3-II CONSOLIDATION OF TWO LAYER SYSTEM WITH TWO WAY DRAINAGE

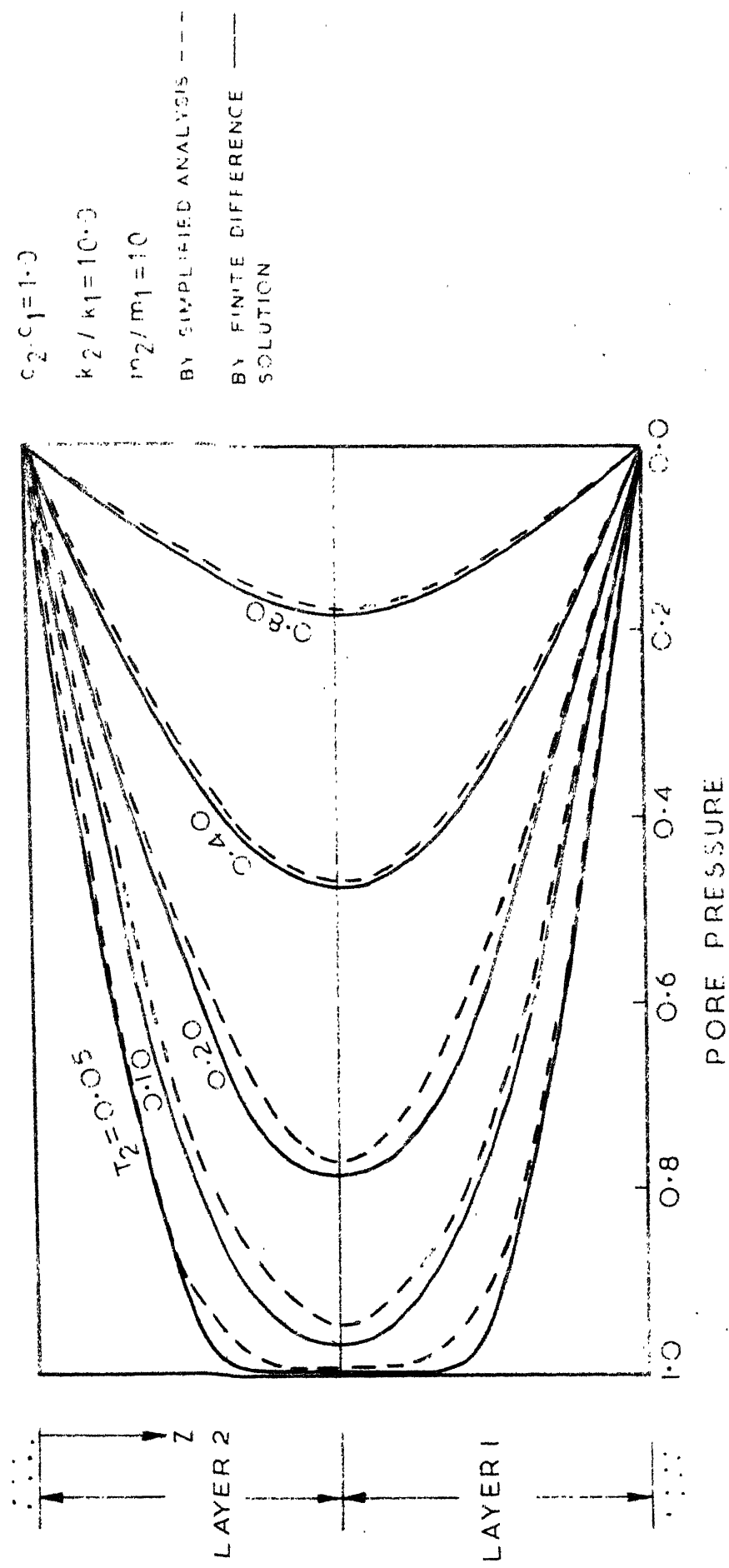


FIG. 3.12 CONSOLIDATION OF TWO LAYER SYSTEM  
WITH CONSTANT  $c$ ,

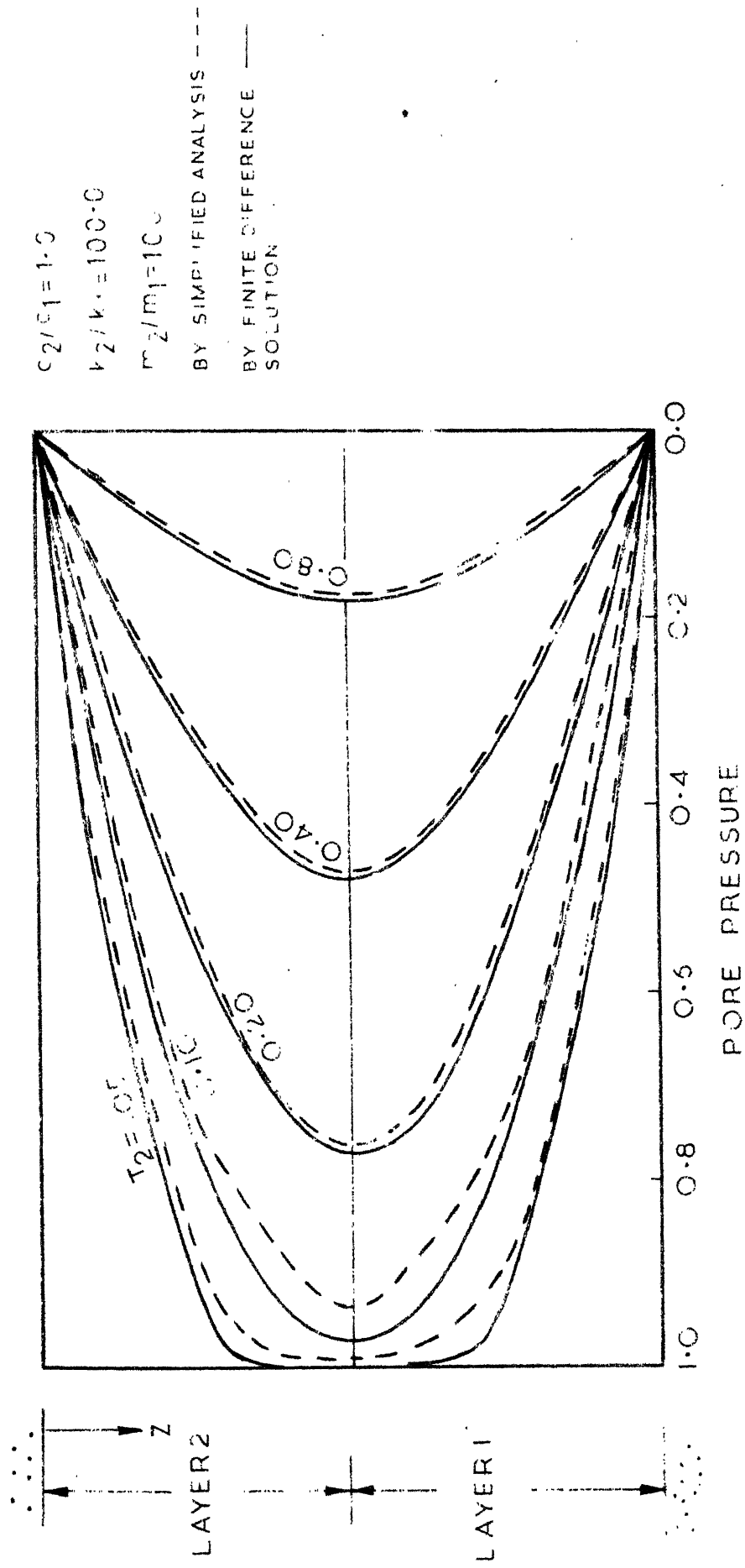
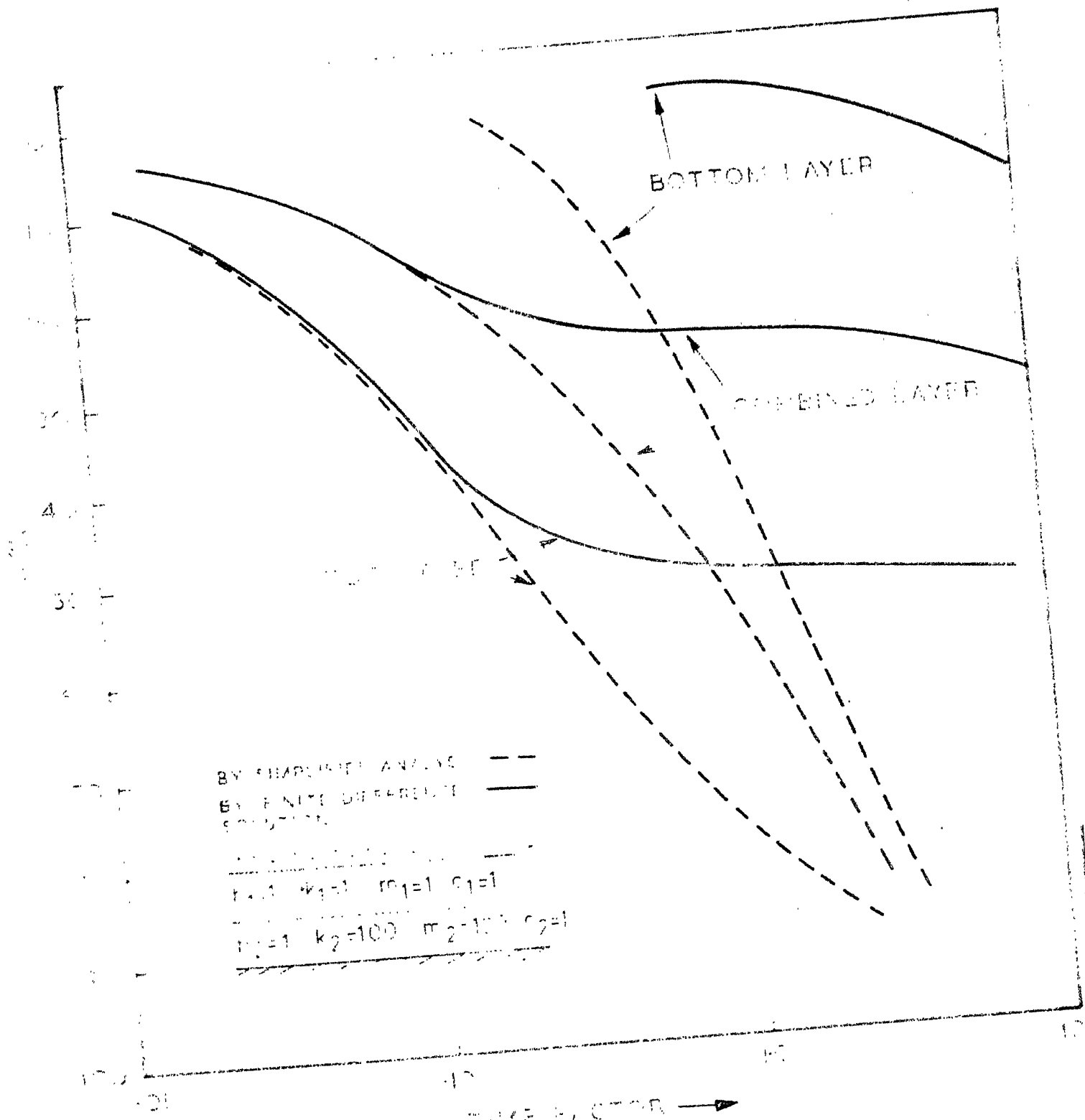


FIG. 3.13 CONSOLIDATION OF TWO LAYER SYSTEM  
WITH CONSTANT  $\tau_2$



12.3.14 021621 DA  
12.3.14 021621 DA

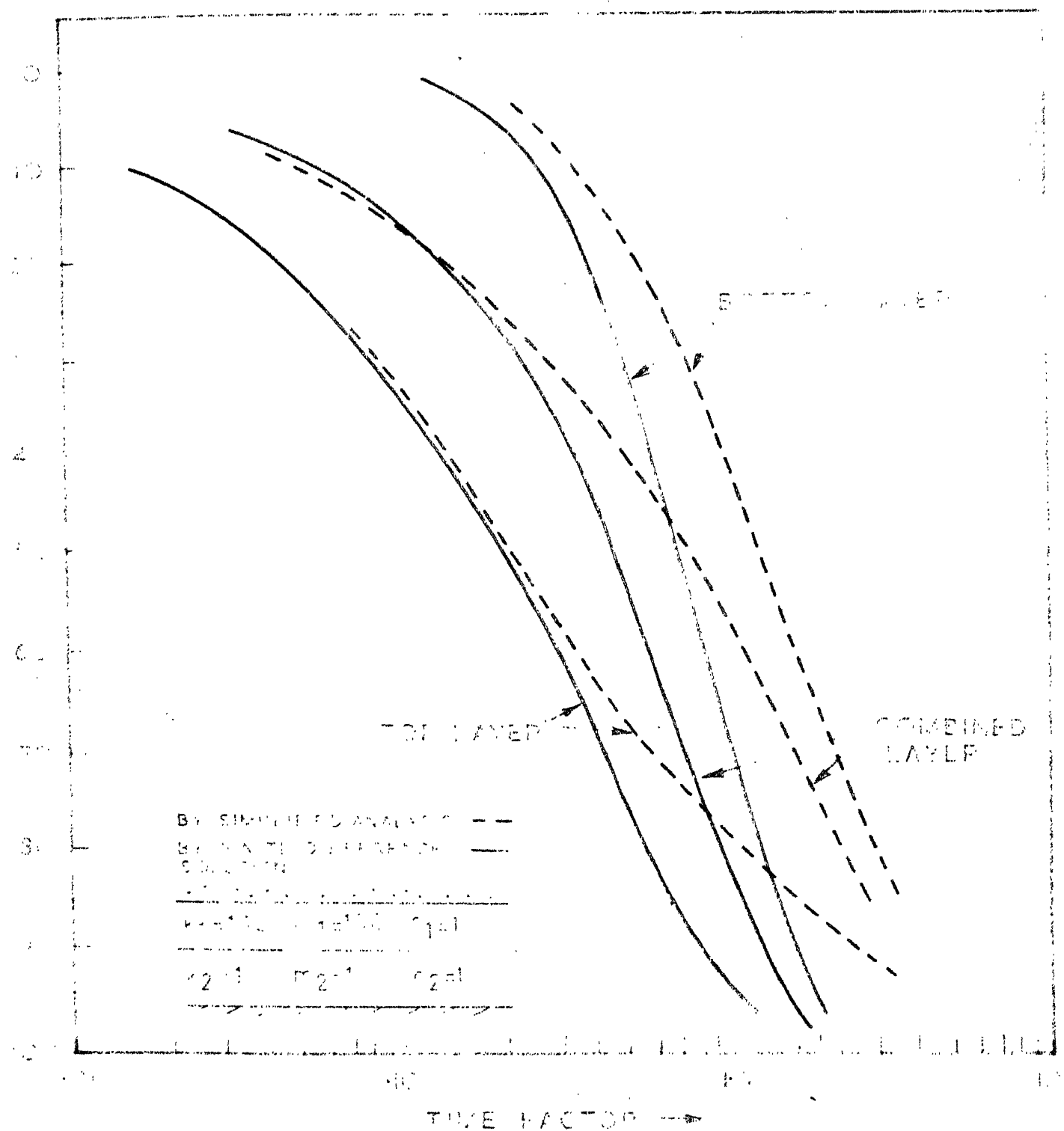


FIG. 3-15. TIME EVOLUTION OF THE LAYER MODEL FOR THE SECOND VIRIAL COEFFICIENT.

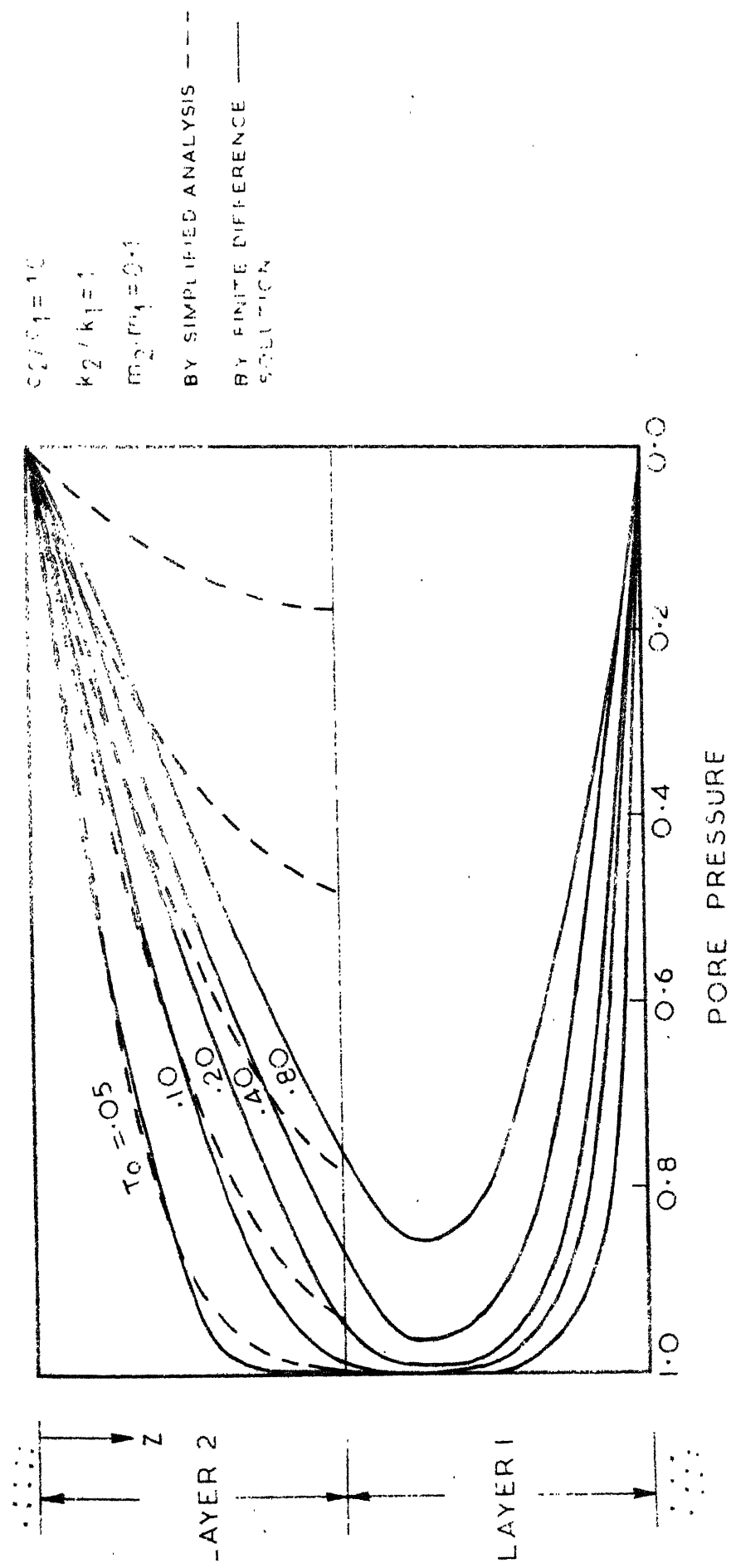


FIG. 3.16 CONSOLIDATION OF TWO-LAYER SYSTEM WITH CONSTANT  $\tau_0$

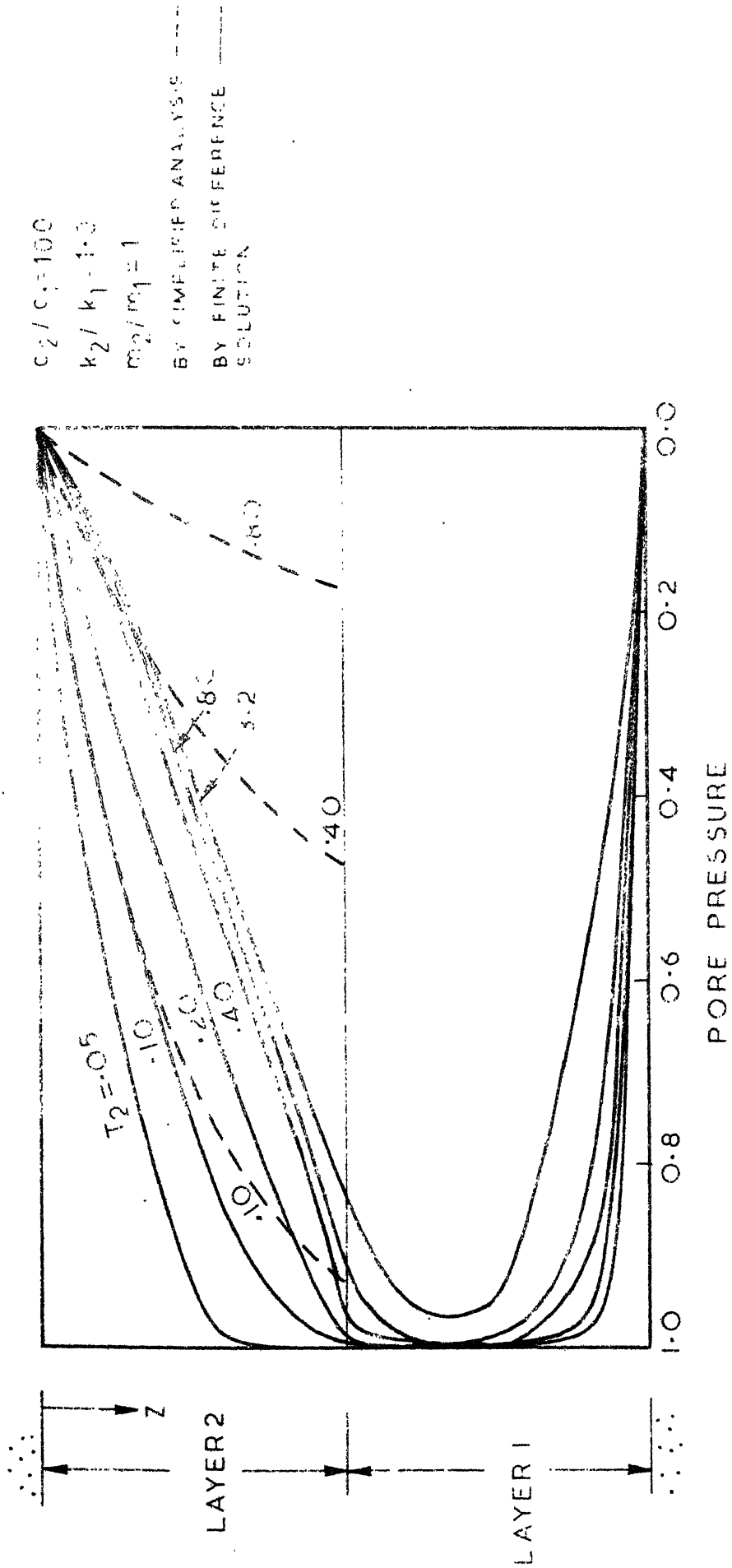


FIG. 3.17 CONSOLIDATION OF TWO LAYER SYSTEM WITH CONSTANT 'k'

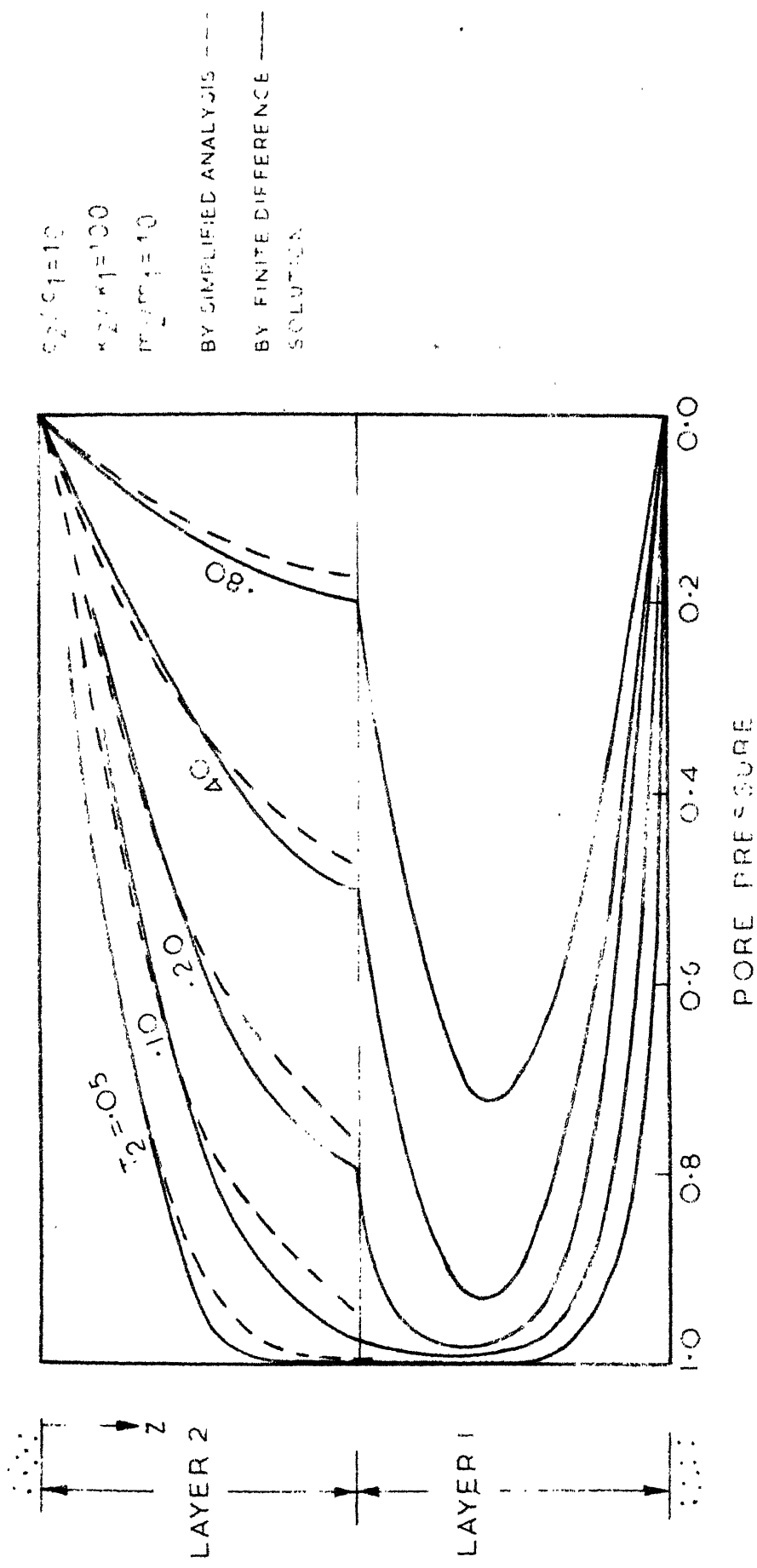


FIG. 3.18 CONSOLIDATION OF TWO LAYER SYSTEM

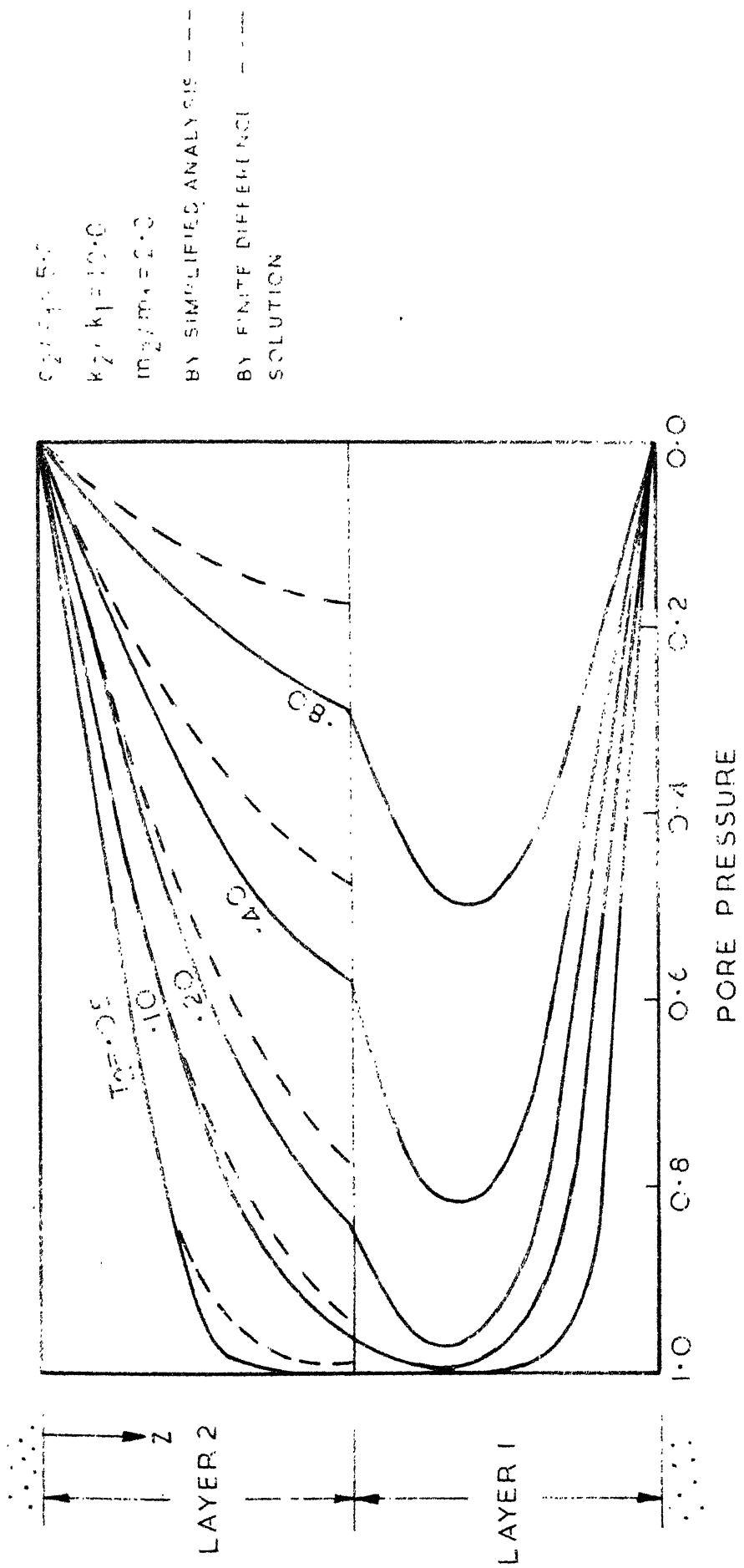


FIG. 319 CONSOLIDATION OF TWO LAYER SYSTEM

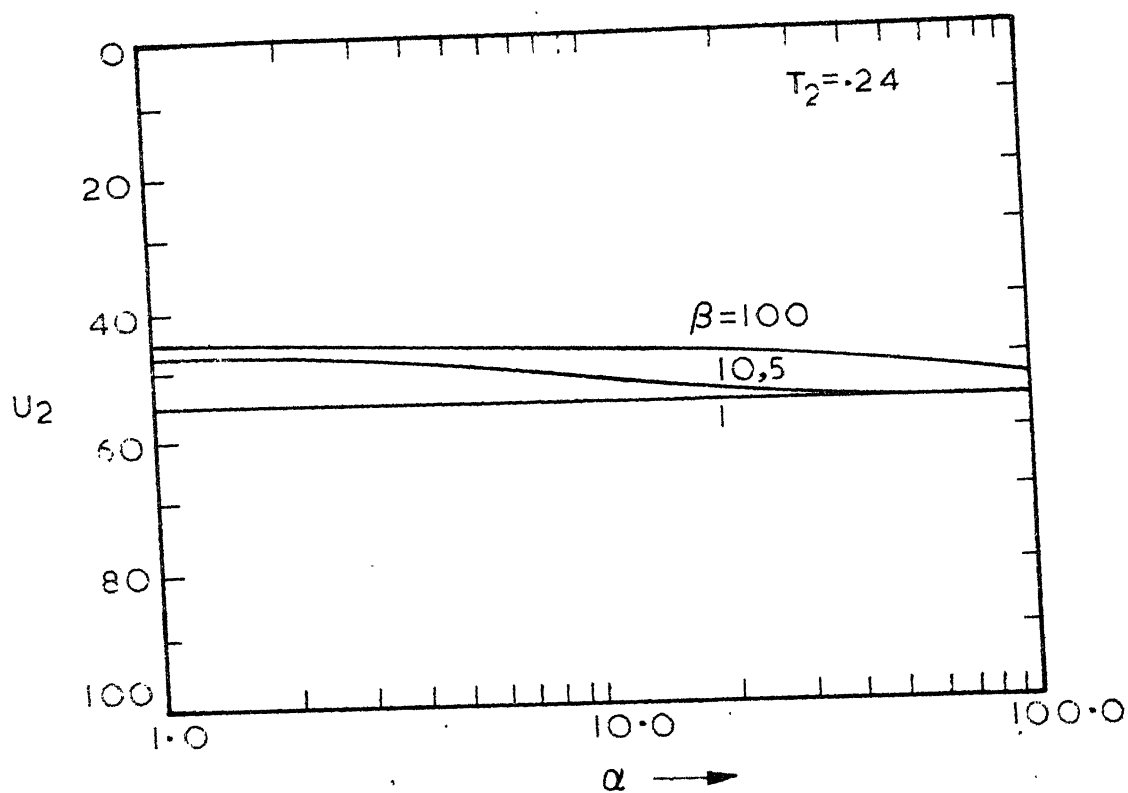


FIG.3.22 CONSOLIDATION OF BOTTOM LAYER

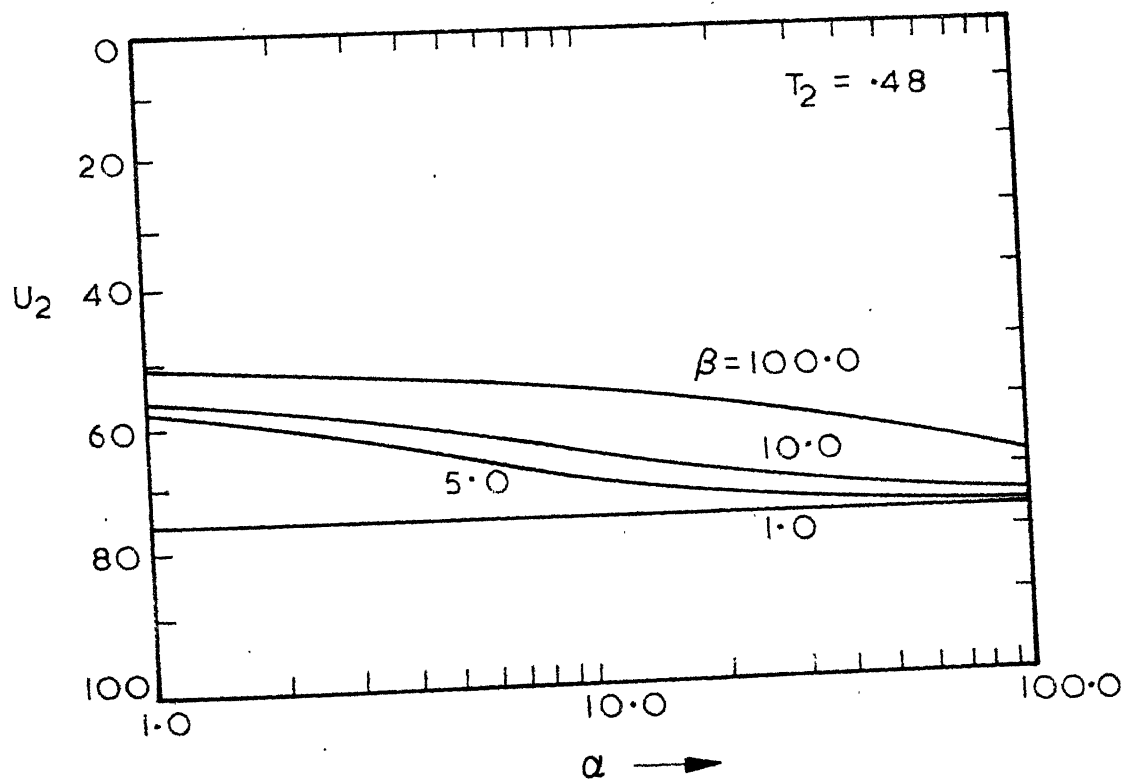


FIG.3.23 CONSOLIDATION OF BOTTOM LAYER

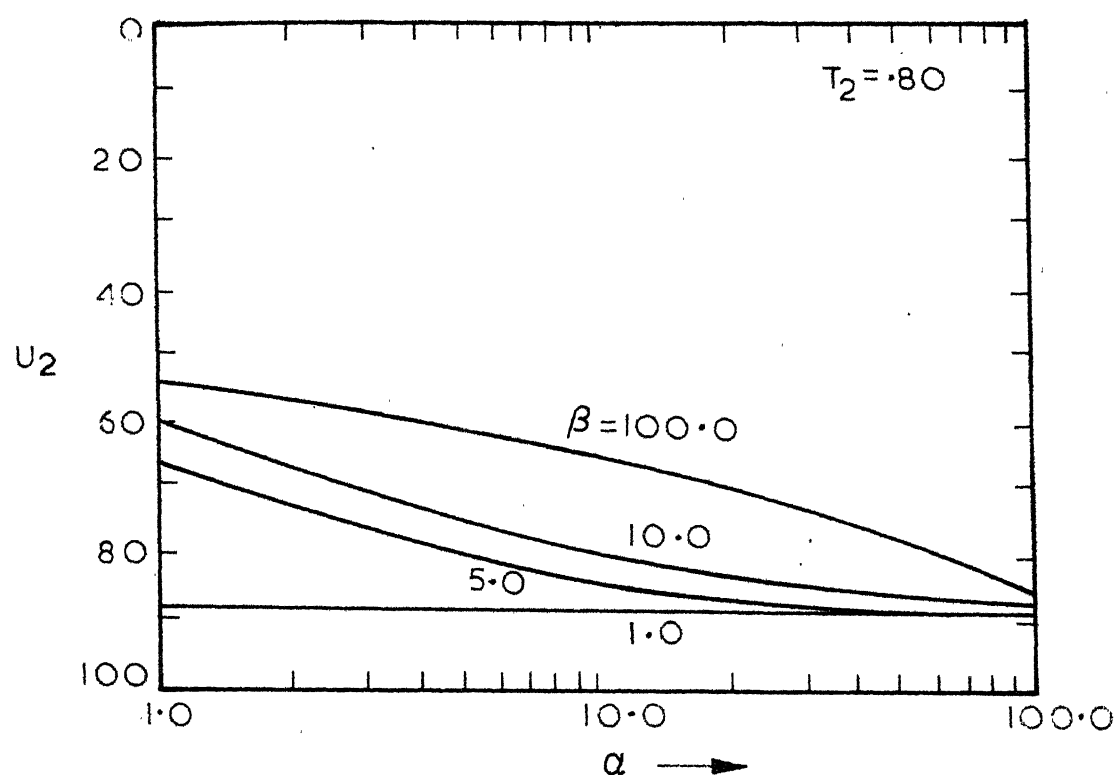


FIG.3.24 CONSOLIDATION OF BOTTOM LAYER

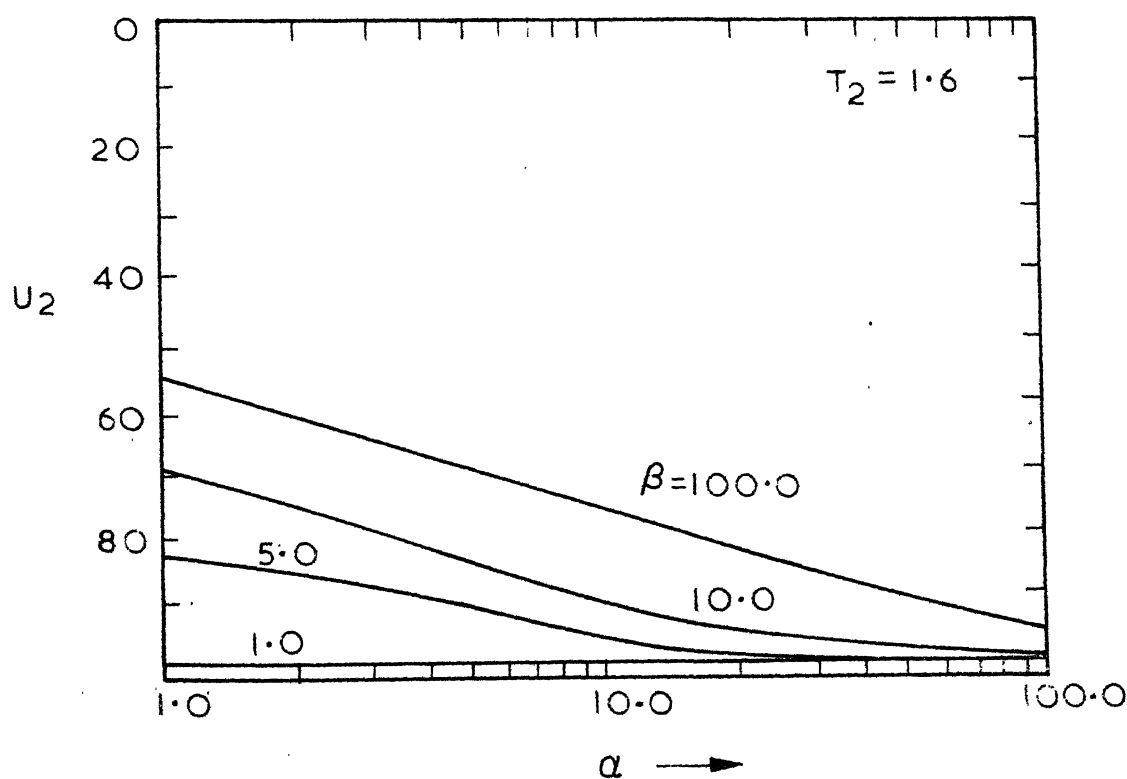


FIG.3.25 CONSOLIDATION OF BOTTOM LAYER

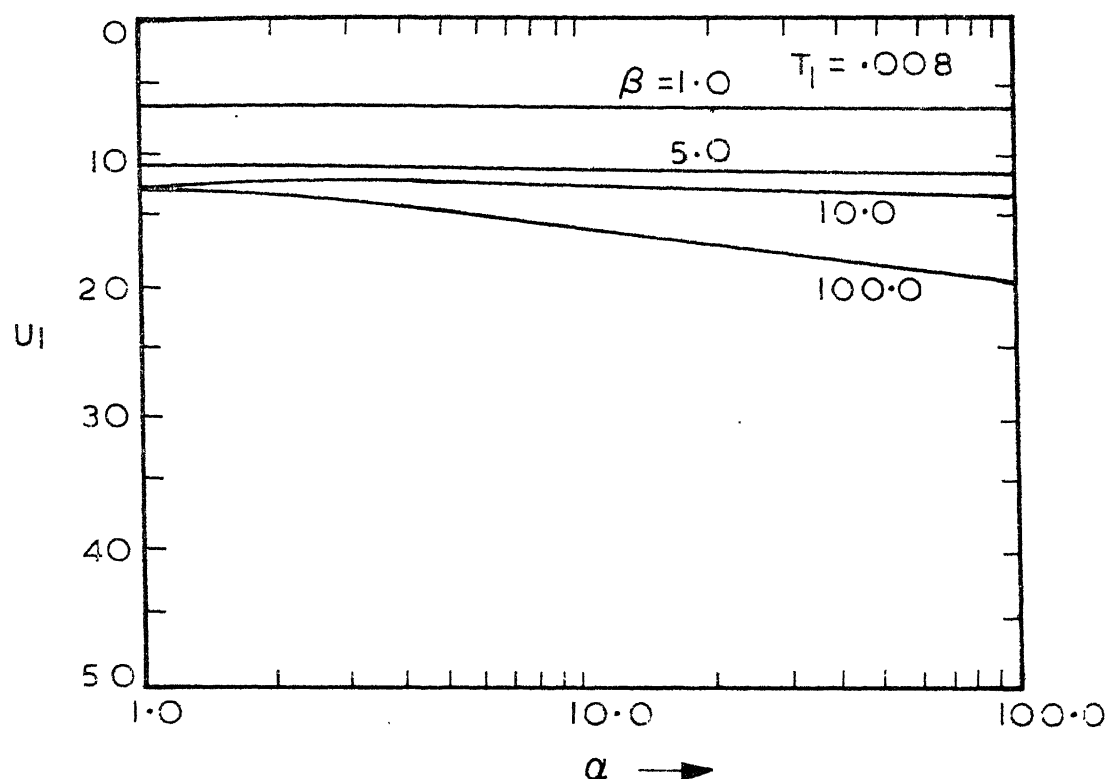


FIG. 3.26 CONSOLIDATION OF TOP LAYER

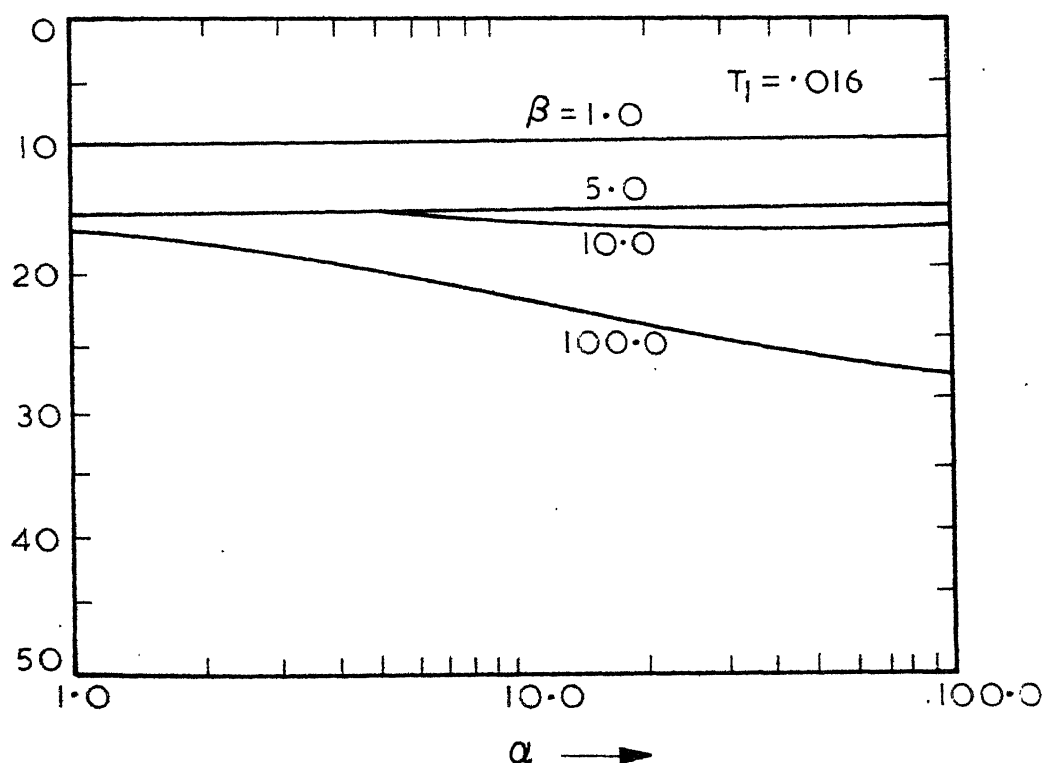


FIG. 3.27 CONSOLIDATION OF TOP LAYER

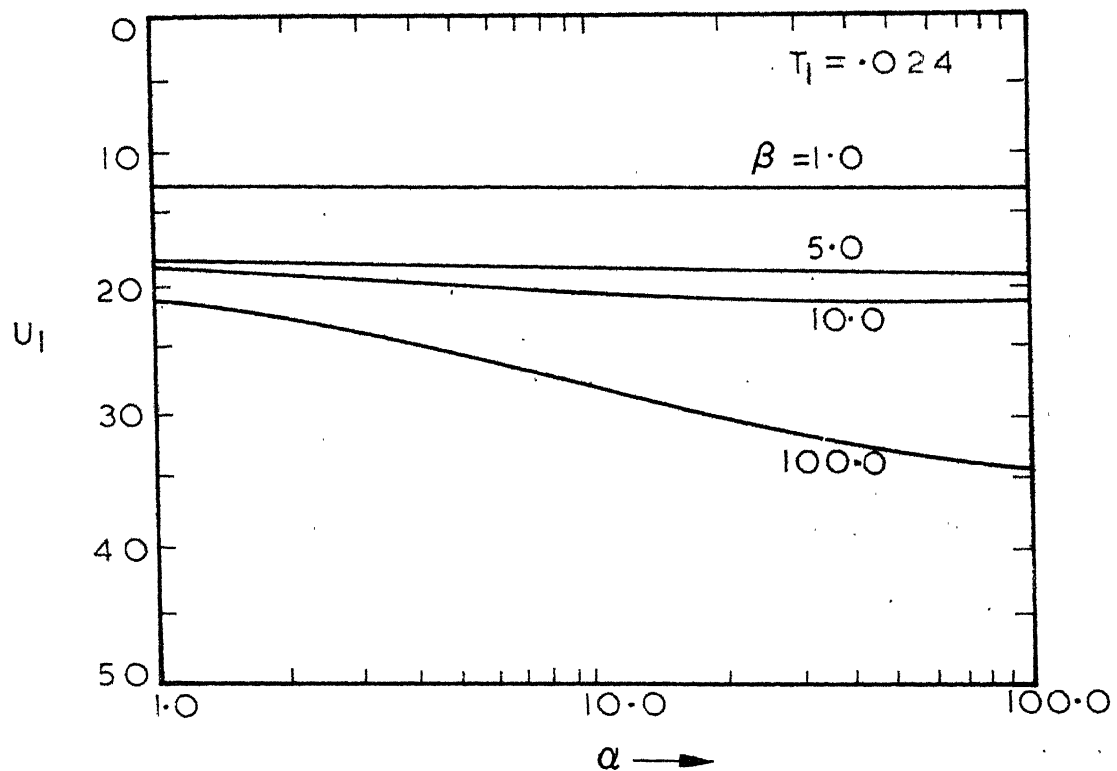


FIG.3.28 CONSOLIDATION OF TOP LAYER

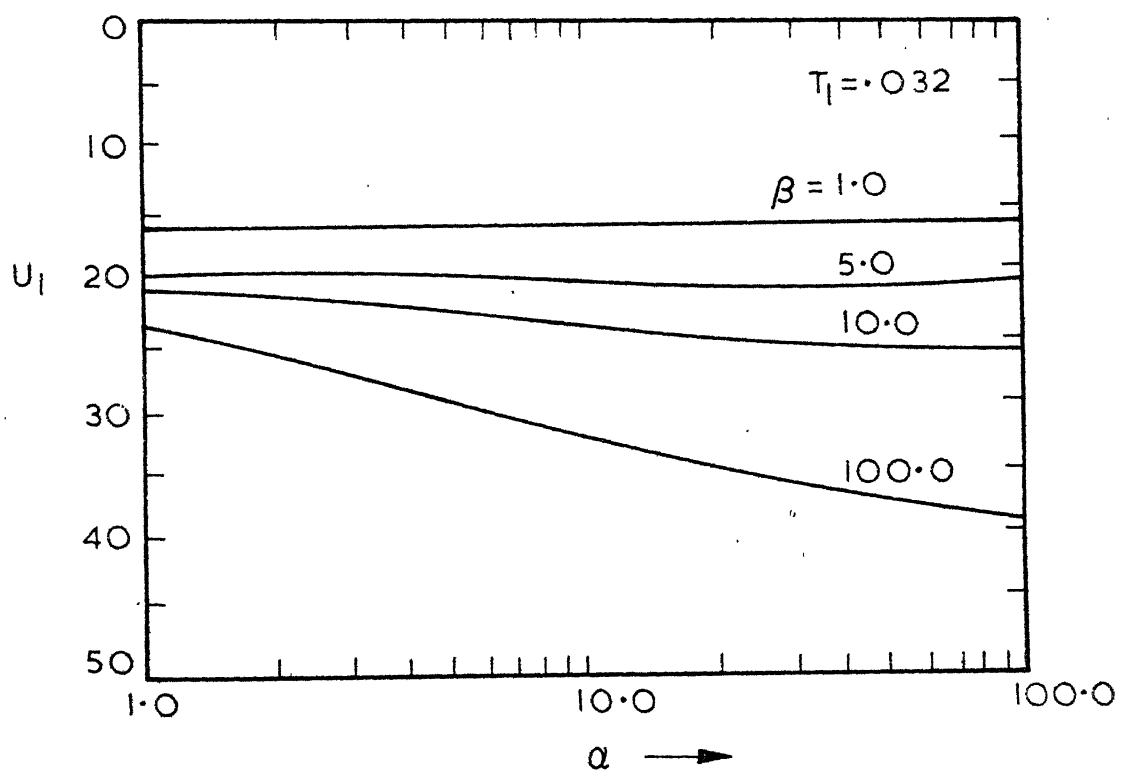


FIG.3.29 CONSOLIDATION OF TOP LAYER

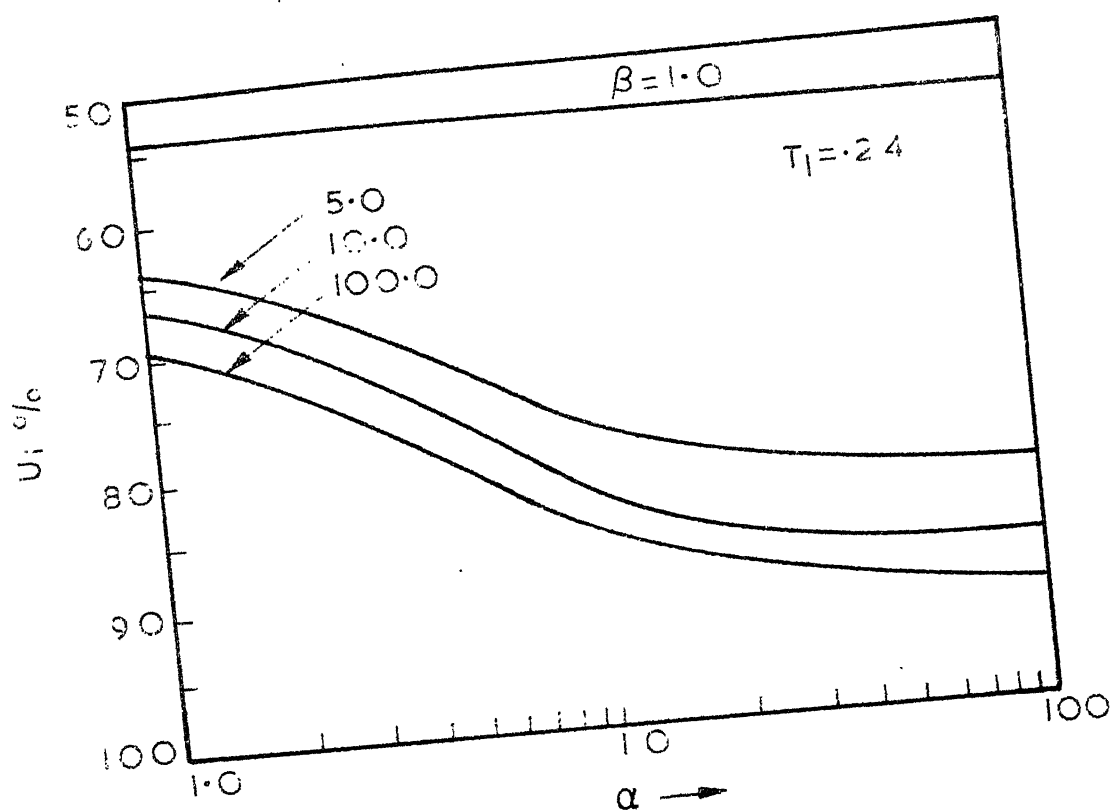


FIG. 3.30 CONSOLIDATION OF TOP LAYER

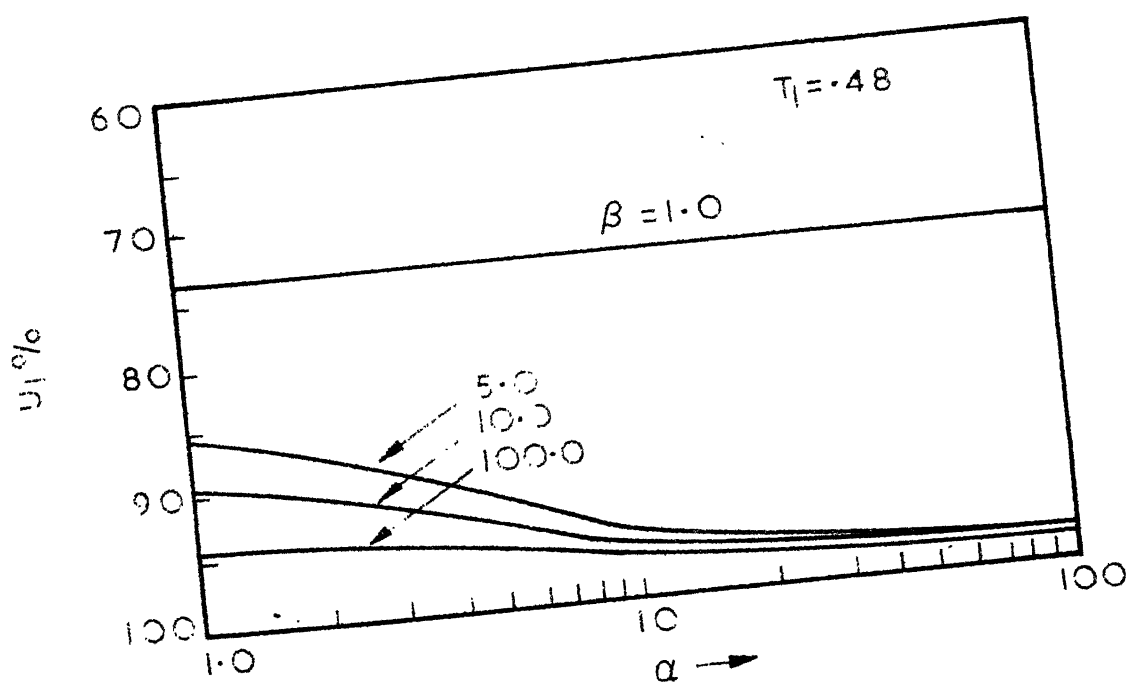


FIG. 3.31 CONSOLIDATION OF TOP LAYER

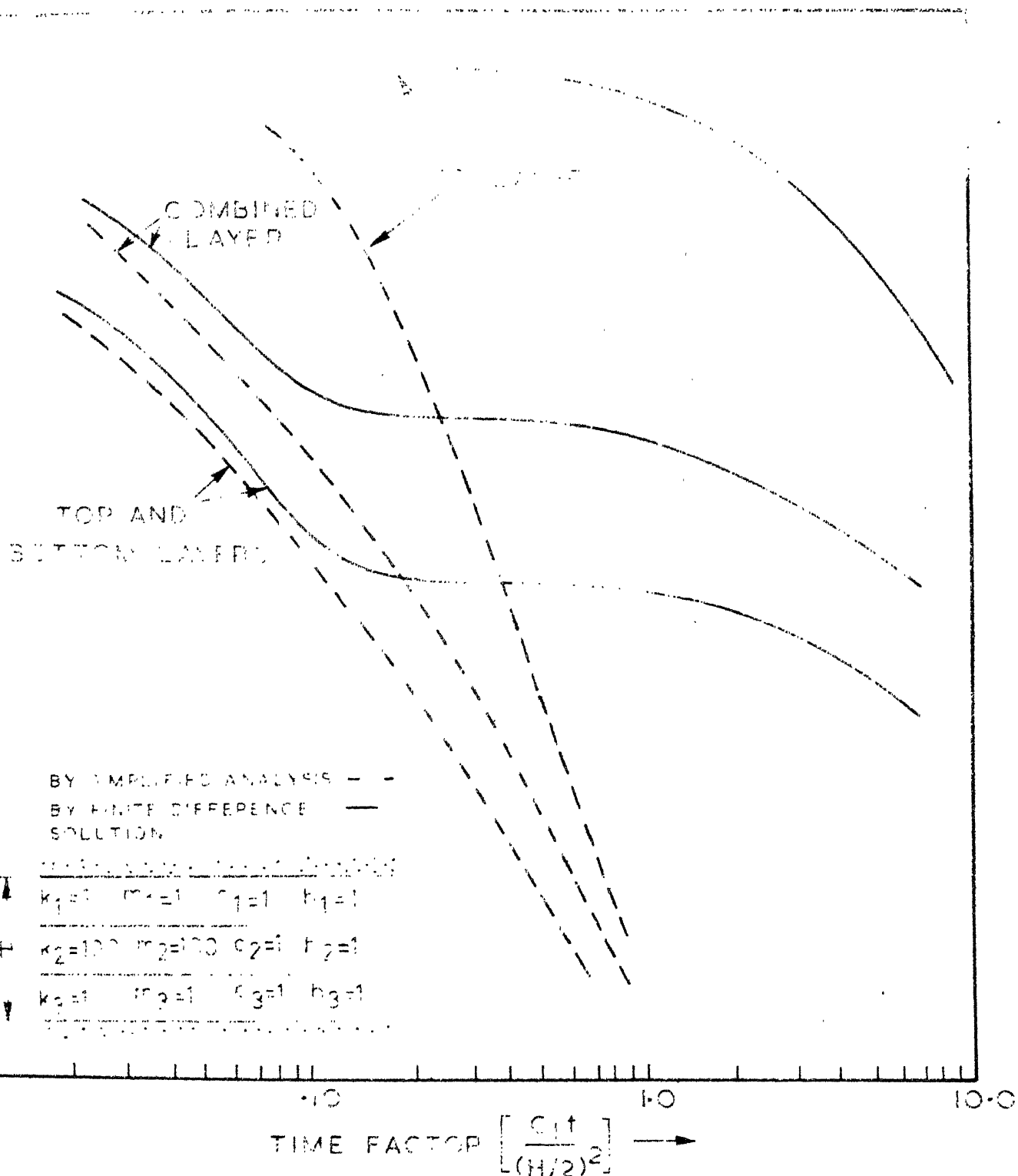


FIG. 3-32 CONSOLIDATION OF A THREE-LAYER SYSTEM

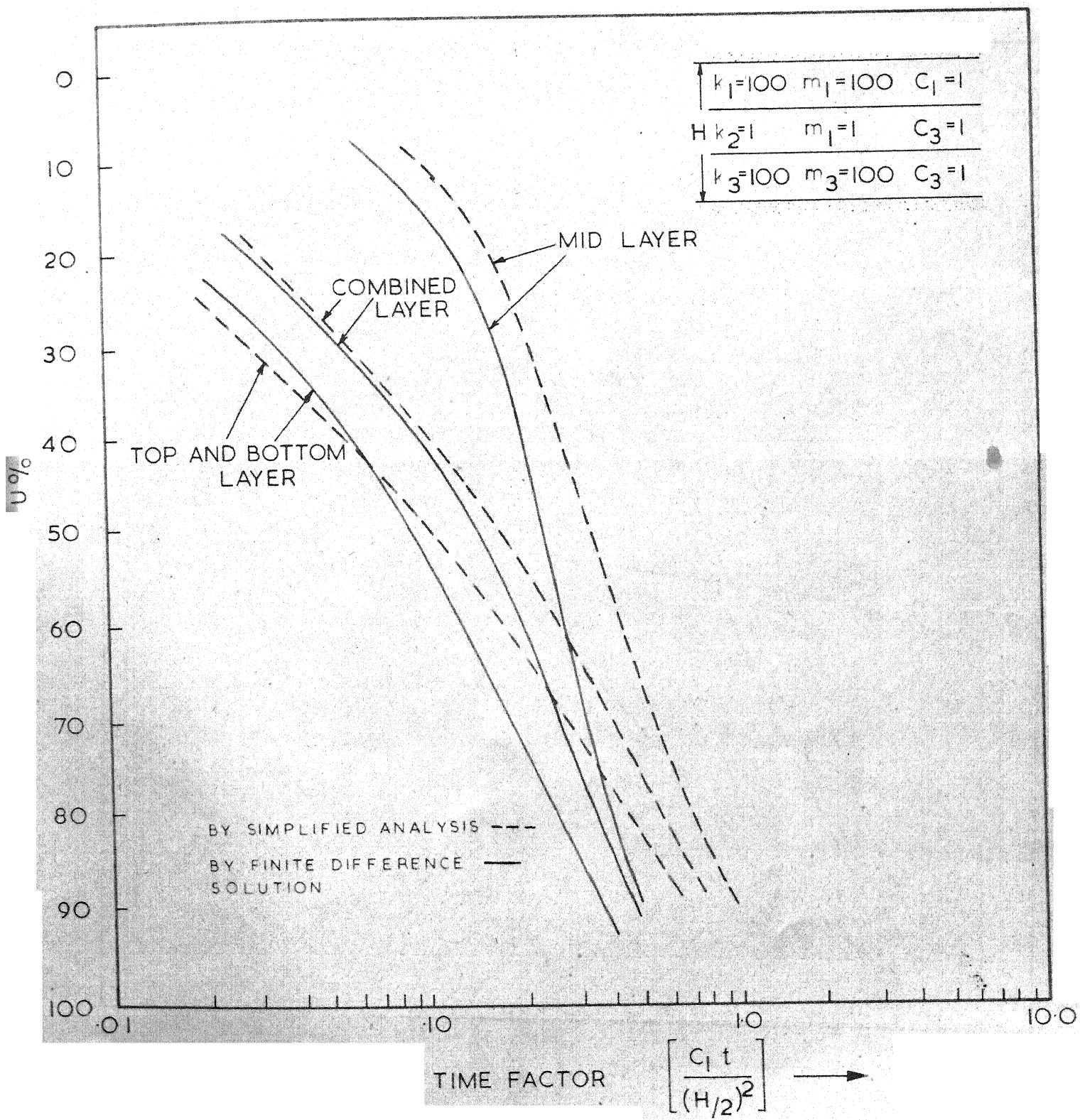


FIG. 3.33 CONSOLIDATION OF A THREE LAYER SYSTEM

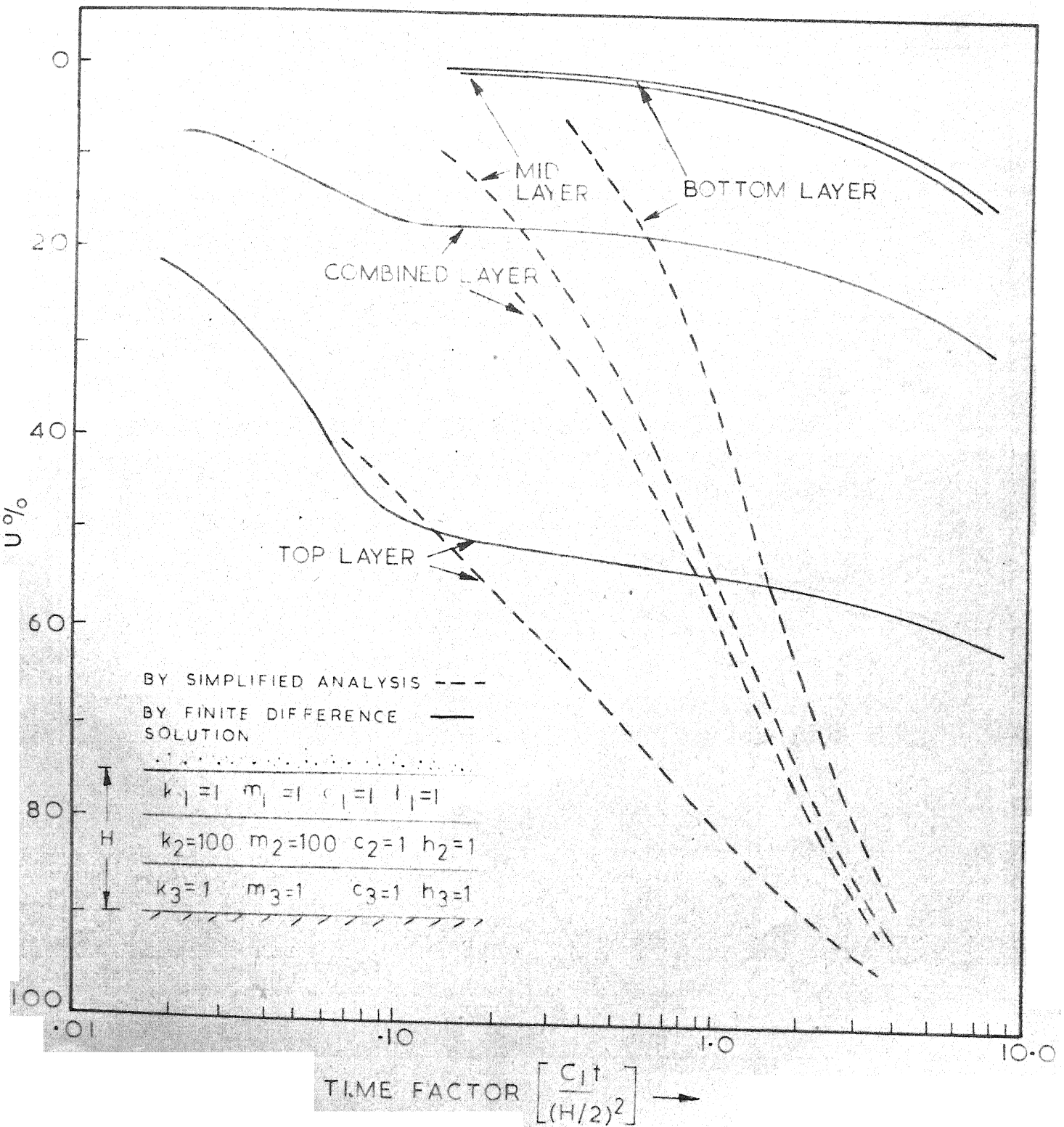


FIG. 3.34 CONSOLIDATION OF A THREE LAYER SYSTEM

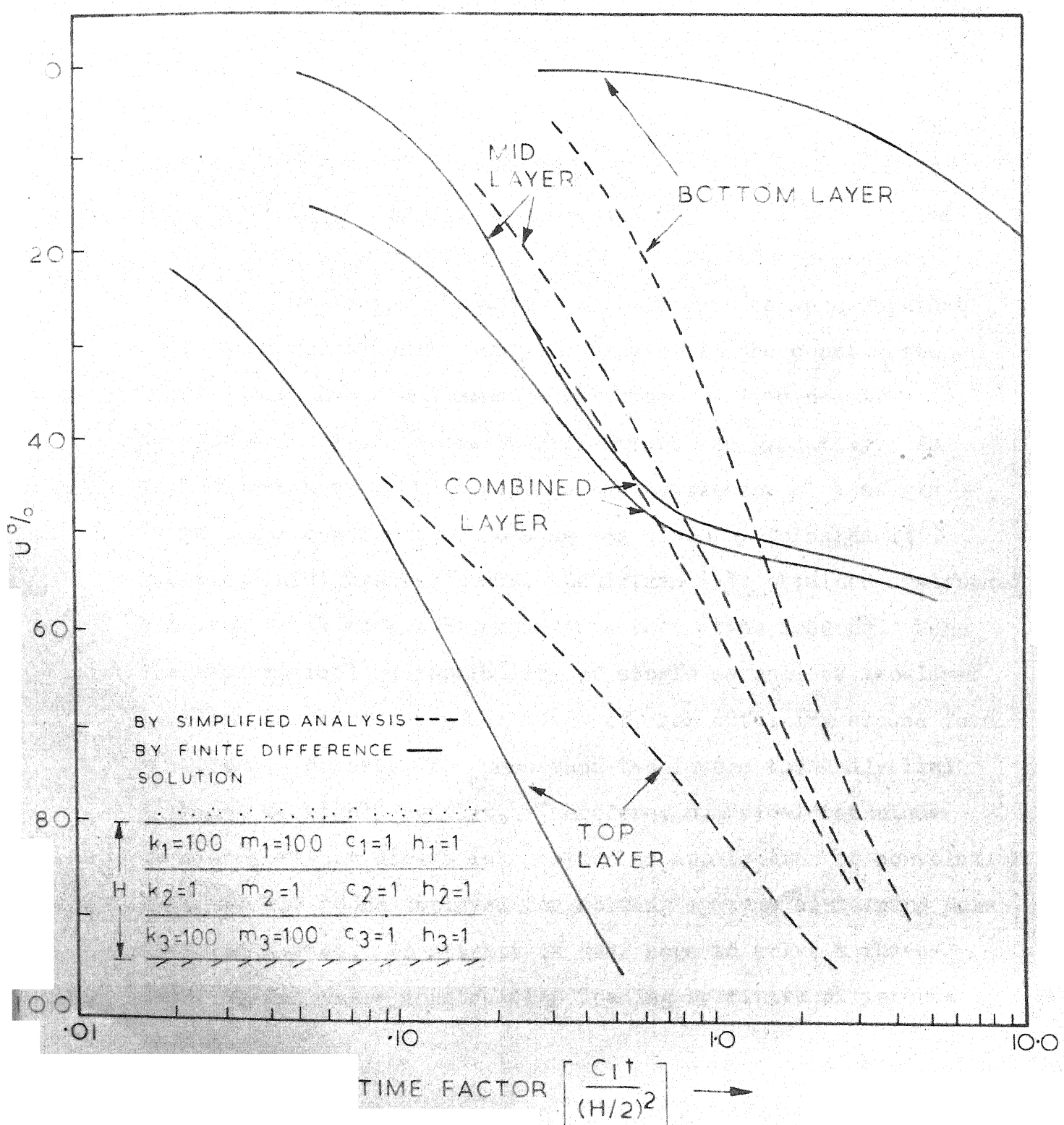


FIG. 335 CONSOLIDATION OF A THREE LAYER SYSTEM

## CHAPTER IV

### CONSOLIDATION OF LAYERED SYSTEMS UNDER TIME DEPENDENT CONSTRUCTION TYPE OF LOADING

#### INTRODUCTION

Using Terzaghi's one-dimensional consolidation theory various boundary value problems were successfully solved by many research workers in Soil Mechanics. The effect of some of the parameters involved in the consolidation phenomenon has been studied in the past. These researches were confined to instantaneous loading only. However, in the construction of buildings and embankments application of load requires considerable time and the loading progresses gradually. An approximate method of predicting the settlement of a single layer under construction loading was given by Terzaghi (41) based on intuitive arguments. Schiffman (33) obtained analytical solution for a single layer under construction loading. Here the mathematical susceptibility of single as well as two-layer problems is to be taken advantage of, for obtaining closed form solutions. However, for more than two layers the analytical approach is highly complex. Therefore, numerical technique involving either direct integration or application of convolution integral has to be employed for solving systems containing more than two layers. An attempt is made here to solve a three-layer system under construction loading by finite difference method.

## SINGLE LAYER

Analytical solution

A single layer with two way drainage is taken as shown in Fig. 4.1. The one-dimensional consolidation equation under time dependent loading is:

$$C \frac{\partial^2 u}{\partial z^2} + R = \frac{\partial u}{\partial t} \quad (4.1)$$

where  $Z$  is the space variable.

The boundary conditions are:

$$\begin{aligned} u(0, t) &= 0 & 0 \leq t \leq t_0 \\ u(2H, t) &= 0 & 0 \leq t \leq t_0 \\ u(z, 0) &= 0 & 0 \leq z \leq 2H \end{aligned} \quad (4.2)$$

where  $2H$  is the thickness of the layer and  $t_0$  is the construction period. Using the following transformations:

$$p = \frac{z}{H}; \quad T = \frac{Ct}{H^2}; \quad \text{and} \quad d = \frac{RH^2}{C}$$

Eq. (4.1) can be transformed as;

$$\frac{\partial^2 u}{\partial p^2} + d = \frac{\partial u}{\partial T} \quad (4.3)$$

To solve the Eq. (4.3) with the boundary conditions corresponding to Eq. (4.2), the following method is used (38):

$$\text{Taking the equation } \frac{\partial^2 u}{\partial p^2} = \frac{\partial u}{\partial T} \quad (4.4)$$

and using the technique of separation of variables, the solution to Eq. (4.4) which vanishes at  $p = 0$  and  $p = 2$  is:

$$u = \sum_{n=1}^{\infty} D_n \sin\left(\frac{n\pi}{2}p\right) e^{-\frac{n^2\pi^2}{4}T} \quad (4.5)$$

where  $D_n$  are constants and  $n$  are integer values.

Now the solution to Eq. (4.3) is assumed to be of the form:

$$u = \sum_{n=1}^{\infty} \phi(T) \sin\left(\frac{n\pi}{2}p\right) \quad (4.6)$$

where  $\phi(T)$  is a function of  $T$ .

$$\text{Expressing } d = \sum_{n=1}^{\infty} E_n \sin\left(\frac{n\pi}{2}p\right) \quad (4.7)$$

where  $E_n$  are the Fourier Sine coefficients evaluated as  $\frac{4d}{n\pi}$  ( $n = 1, 3 \dots$ ). Substituting Eqs. (4.6) and (4.7) in Eq. (4.3), the following ordinary differential equation is obtained:

$$\frac{d\phi(T)}{dT} + \frac{n^2\pi^2}{4} \phi(T) = \frac{4d}{n\pi} \quad (4.8)$$

Therefore:

$$\phi(T) = \frac{16d}{n^3 \pi^3} (1 - e^{-\frac{n^2 \pi^2}{4} T}), \quad n = 1, 3, \dots \quad (4.9)$$

And the solution to Eq. (4.3) is

$$u(p, T) = \frac{16 \bar{u}_o}{\pi^3 T_o} \sum_{n=1, 3, \dots} \frac{1}{n^3} (1 - e^{-\frac{n^2 \pi^2}{4} T}) \sin \frac{n \pi}{2} p \quad (4.10)$$

$$\text{where } T_o = \frac{C t_o}{H^2}$$

For the post construction period  $t_o \leq t \leq \infty$ , the consolidation equation is:

$$\frac{\partial^2 u^*}{\partial p^2} = \frac{\partial u^*}{\partial T} \quad (4.11)$$

in which  $u^*$  is the point pore pressure during the post-construction period and the boundary conditions are:

$$u^*(p, T_o) = u(p, T_o), \quad \text{Solution obtained in the previous case (as per Eq. 4.10)}$$

$$u^*(0, T) = 0$$

$$u^*(2, T) = 0 \quad (4.12)$$

The solution of Eq. (4.11) satisfying the boundary conditions of Eq. (4.12) is:

$$u^*(p, T) = \frac{16\bar{u}_o}{\pi^3 T_o} \sum_{n=1,3,\dots} \frac{1}{n^3} (1-e^{-\frac{n^2 \pi^2}{4} T}) \sin \frac{n \pi}{2} p - \frac{16\bar{u}_o}{\pi^3 T_o} \sum_{n=1,3,\dots} \frac{1}{n^3} (1-e^{-\frac{n^2 \pi^2}{4} (T-T_o)}) \sin \frac{n \pi}{2} p \quad (4.13)$$

Defining the average pore pressure values  $\bar{u}$  as the integrated value of the point pore pressure  $u(p, T)$  over the depth, the average pore pressure ratio  $\frac{\bar{u}}{u_o}$  is given by:

$$\frac{\bar{u}}{u_o} = \frac{32\bar{u}_o}{T_o \pi^4} \sum_{n=1,3,\dots} \frac{1}{n^4} (1-e^{-\frac{n^2 \pi^2}{4} T}), \quad 0 < T < T_o \quad (4.14)$$

$$\frac{\bar{u}^*}{u_o} = \frac{32\bar{u}_o}{T_o \pi^4} \sum_{n=1,3,\dots} \frac{1}{n^4} (1-e^{-\frac{n^2 \pi^2}{4} T}) - \frac{32\bar{u}_o}{T_o \pi^4} \sum_{n=1,3,\dots} \frac{1}{n^4} (1-e^{-\frac{n^2 \pi^2}{4} (T-T_o)}), \quad T_o < T < \infty \quad (4.15)$$

The solutions given by Eqs. (4.10) and (4.13) are identical with the solutions obtained by Schiffman, (33) using a different procedure. Also solutions obtained using finite difference approach yield identical results (Figs. 4.4 and 4.5).

### TWO LAYER SYSTEM WITH TWO-WAY DRAINAGE

#### Analytical solution

A two-layered system with two-way drainage as shown in Fig. 4.2 is taken. The one-dimensional consolidation equations for construction type of loading are:

$$c_1 \frac{\partial^2 u_1}{\partial z^2} + R = \frac{\partial u_1}{\partial t} \quad (4.16)$$

$$c_2 \frac{\partial^2 u_2}{\partial z^2} + R = \frac{\partial u_2}{\partial t} \quad (4.17)$$

in which the subscripts 1 and 2 denote the corresponding Soil layers 1 and 2.

Using the following transformations:

$$p = \frac{z}{h_1} ; \quad T = \frac{c_1 t}{h_1^2} ; \quad v = \frac{h_2}{h_1} ; \quad \mu^2 = \frac{c_1}{c_2} ;$$

$$\sigma = \frac{1}{\mu} \frac{k_1}{k_2} ; \quad d_1 = \frac{R h_1^2}{c_1} ; \quad d_2 = \frac{R h_1^2}{c_2}$$

the Eqs. (4.16) and (4.17) are transformed as:

$$\frac{\partial^2 u_1}{\partial p^2} + d_1 = \frac{\partial u_1}{\partial T} \quad (4.18)$$

$$\frac{\partial^2 u_2}{\partial p^2} + d_2 = \mu^2 \frac{\partial u_2}{\partial T} \quad (4.19)$$

the boundary conditions are:

$$\begin{aligned} u_1(0, T) &= 0 & 0 \leq T \leq T_0 \\ u_1(p, 0) &= 0 & 0 \leq p \leq 1 \\ u_2(p, 0) &= 0 & 1 \leq p \leq 1+ \\ u_2(1+\nu, T) &= 0 & 0 \leq T \leq T_0 \end{aligned} \quad (4.20)$$

At the interface  $p = 1$

$$u_1(p, T) = u_2(p, T)$$

$$k_1 \frac{\partial u_1}{\partial p} \Big|_{p=1\uparrow} = k_2 \frac{\partial u_2}{\partial p} \Big|_{p=1\downarrow}$$

The method of solution is given in the Appendix. The solutions of the Eqs. (4.18) and (4.19) readily satisfying the boundary conditions of Eq. (4.20) are:

$$u_1(p, T) = \sum_{i=1}^{\infty} \frac{2d_1}{A_i^2} F_i (1 - e^{-A_i^2 T}) \sin A_i p \sin A_i \mu \nu \quad (4.21)$$

$$u_2(p, T) = \sum_{i=1}^{\infty} \frac{2d_i^2}{A_i^2 \mu^2} F_i (1 - e^{-A_i^2 T}) \sin A_i \sin (1 + \psi - p) A_i \quad (4.22)$$

where  $A_i$ 's are the roots of the equation:

$$(\sigma \cos A \sin A \mu \nu + \sin A \cos A \mu \nu) = 0 \quad (4.23)$$

$$\text{and } F_i = \frac{\sigma \sin A_i \mu \nu + \sin A_i}{\mu \nu A_i \sin^2 A_i + \sigma A \sin^2 A_i} \quad (4.24)$$

Defining the average pore pressure  $\bar{u}_1$  and  $\bar{u}_2$  as the integrated value of  $u_1$  and  $u_2$  over the respective depths, the average pore pressure ratios are given by:

$$\frac{\bar{u}_1}{u_0} = \frac{1}{T_0} \sum_{i=1}^{\infty} \frac{2}{A_i^3} F_i (1 - e^{-A_i^2 T_0}) \sin A_i \mu \nu (1 - \cos A_i) \quad (4.25)$$

$$\frac{\bar{u}_2}{u_0} = \frac{1}{T_0} \sum_{i=1}^{\infty} \frac{2}{A_i^3 \mu \nu} F_i (1 - e^{-A_i^2 T_0}) \sin A_i (1 - \cos A_i \mu \nu) \quad (4.26)$$

For the post-construction period  $T_0 < T < \infty$ , the consolidation equations are:

$$\frac{\partial^2 u_1^*}{\partial p^2} = \frac{\partial u_1^*}{\partial T} \quad (4.27)$$

$$\frac{\partial^2 u_2^*}{\partial p^2} = \mu^2 \frac{\partial u_2^*}{\partial T} \quad (4.28)$$

The boundary conditions are:

$$u_1^*(p, T_0) = u_1(p, T_0) \quad \text{Solution obtained in the previous case}$$

$$u_1^*(0, T) = 0$$

$$u_2^*(1+\nu, T) = 0$$

$$u_2^*(p, T_0) = u_2(p, T_0) \quad \text{Solution obtained in the previous case}$$

At the interface  $p = 1$

$$u_1^*(p, T) = u_2^*(p, T)$$

$$k_1 \frac{\partial u_1^*}{\partial p} \Big|_{p=1\uparrow} = k_2 \frac{\partial u_2^*}{\partial p} \Big|_{p=1\downarrow} \quad (4.29)$$

The solutions of the equations (4.27) and (4.28) readily satisfying the boundary conditions given by Eq. (4.29) are:

$$u_1^*(p, T) = \sum_{i=1}^{\infty} \frac{2d_i}{A_i^2} F_i (1 - e^{-A_i^2 T}) \sin A_i p \sin A_i \mu \nu$$

$$- \sum_{i=1}^{\infty} \frac{2d_i}{A_i^2} F_i (1 - e^{-A_i^2 (T-T_0)}) \sin A_i p \sin A_i \mu \nu \quad (4.30)$$

$$\begin{aligned}
 u_2^*(p, T) = & \sum_{i=1}^{\infty} \frac{2d_2}{\frac{A_i^2}{\mu^2}} F_i (1 - e^{-A_i^2 T}) \sin A_i \sin A_i \mu (1 + \nu - p) \\
 - & \sum_{i=1}^{\infty} \frac{2d_2}{\frac{A_i^2}{\mu^2}} F_i (1 - e^{-A_i^2 (T-T_0)}) \sin A_i \sin A_i \mu (1 + \nu - p)
 \end{aligned} \tag{4.31}$$

The average pore pressure ratios are given by:

$$\begin{aligned}
 \frac{\bar{u}_1^*}{u_0} = & \frac{1}{T_0} \sum_{i=1}^{\infty} \frac{2}{\frac{A_i^3}{\mu}} F_i (1 - e^{-A_i^2 T}) \sin A_i \mu (1 - \cos A_i) \\
 - & \frac{1}{T_0} \sum_{i=1}^{\infty} \frac{2}{\frac{A_i^3}{\mu}} F_i (1 - e^{-A_i^2 (T-T_0)}) \sin A_i \mu (1 - \cos A_i)
 \end{aligned} \tag{4.32}$$

$$\begin{aligned}
 \frac{\bar{u}_2^*}{u_0} = & \frac{1}{T_0} \sum_{i=1}^{\infty} \frac{2}{\frac{A_i^3 \mu \nu}{\mu \nu}} F_i (1 - e^{-A_i^2 T}) \sin A_i (1 - \cos A_i \mu \nu) \\
 - & \frac{1}{T_0} \sum_{i=1}^{\infty} \frac{2}{\frac{A_i^3 \mu \nu}{\mu \nu}} F_i (1 - e^{-A_i^2 (T-T_0)}) \sin A_i (1 - \cos A_i \mu \nu)
 \end{aligned} \tag{4.33}$$

## TWO-LAYER SYSTEM WITH ONE-WAY DRAINAGE

Analytical solution

A two-layered system with single face drainage as shown in Fig. 4.3 is taken. Correspondingly the boundary conditions are:

$$u_1(p, 0) = 0$$

$$\left. \frac{\partial u_1}{\partial p} \right|_{p=0} = 0$$

$$u_2(1+v, T) = 0$$

$$u_2(p, 0) = 0 \quad (4.34)$$

At the interface  $p = 1$

$$u_1(p, T) = u_2(p, T)$$

$$k_1 \left. \frac{\partial u_1}{\partial p} \right|_{p=1 \uparrow} = k_2 \left. \frac{\partial u_2}{\partial p} \right|_{p=1 \downarrow}$$

The solutions of the Eqs. (4.18) and (4.19) readily satisfying the boundary conditions given by Eq. (4.34) are:

$$u_1(p, T) = \sum_{i=1}^{\infty} \frac{2d_i}{A_i^2} F_i (1 - e^{-A_i^2 T}) \cos A_i p \sin A_i \mu v \quad (4.35)$$

$$u_2(p, T) = \sum_{i=1}^{\infty} \frac{2d_i^2}{A_i^2 \mu} F_i (1 - e^{-A_i^2 T}) \cos A_i p \sin A_i \mu (1 + \nu - p) \quad (4.36)$$

where  $A_i$ 's are the roots of the equation:

$$(\sigma \sin A_i \sin A_i \mu \nu - \cos A_i \cos A_i \mu \nu) = 0 \quad (4.37)$$

$$\text{and } F_i = \frac{\cos A_i}{(\sigma A_i \sin^2 A_i \mu \nu + A_i \mu \nu \cos^2 A_i)} \quad (4.38)$$

The average pore pressure ratios are given by:

$$\frac{\bar{u}_1}{u_0} = \frac{1}{T_0} \sum_{i=1}^{\infty} \frac{2}{A_i^3} F_i (1 - e^{-A_i^2 T_0}) \sin A_i \mu \nu \sin A_i \quad (4.39)$$

$$\frac{\bar{u}_2}{u_0} = \frac{1}{T_0} \sum_{i=1}^{\infty} \frac{2}{A_i^3 \mu \nu} F_i (1 - e^{-A_i^2 T_0}) \cos A_i (1 - \cos A_i \mu \nu) \quad (4.40)$$

For post-construction period  $T_0 \leq T \leq \infty$ , the solutions of Eqs. (4.27) and (4.28) readily satisfying the boundary conditions similar to Eq. (4.29) are:

$$u_1^*(p, T) = \sum_{i=1}^{\infty} \frac{2d_i^2}{A_i^2} F_i (1 - e^{-A_i^2 T}) \cos A_i p \sin A_i \mu \nu$$

$$- \sum_{i=1}^{\infty} \frac{2d_i^2}{A_i^2} F_i (1 - e^{-A_i^2 (T-T_0)}) \cos A_i p \sin A_i \mu \nu \quad (4.41)$$

$$\begin{aligned}
 u_2^*(p, T) = & \sum_{i=1}^{\infty} \frac{2d_2}{\frac{A_i^2}{\mu} \mu} F_i (1 - e^{-A_i^2 T}) \cos A_i \sin A_i (1 + \nu - p) \mu \\
 - & \sum_{i=1}^{\infty} \frac{2d_2}{\frac{A_i^2}{\mu} \mu} F_i (1 - e^{-A_i^2 (T-T_0)}) \cos A_i \sin A_i \mu (1 + \nu - p)
 \end{aligned} \tag{4.42}$$

The average pore pressure ratios are given by:

$$\begin{aligned}
 \frac{\bar{u}_1^*}{u_0} = & \frac{1}{T_0} \sum_{i=1}^{\infty} \frac{2}{A_i^3} F_i (1 - e^{-A_i^2 T}) \sin A_i \sin A_i \mu \nu \\
 - & \frac{1}{T_0} \sum_{i=1}^{\infty} \frac{2}{A_i^3} F_i (1 - e^{-A_i^2 (T-T_0)}) \sin A_i \sin A_i \mu \nu
 \end{aligned} \tag{4.43}$$

$$\begin{aligned}
 \frac{\bar{u}_2^*}{u_0} = & \frac{1}{T_0} \sum_{i=1}^{\infty} \frac{2}{A_i^3 \mu \nu} F_i (1 - e^{-A_i^2 T}) \cos A_i (1 - \cos A_i \mu \nu) \\
 - & \frac{1}{T_0} \sum_{i=1}^{\infty} \frac{2}{A_i^3 \mu \nu} F_i (1 - e^{-A_i^2 (T-T_0)}) \cos A_i (1 - \cos A_i \mu \nu)
 \end{aligned} \tag{4.44}$$

### Illustration

The solutions for a two-layer system with single face drainage are illustrated by the following problem.

The soil parameters used for the computations are:

$$\frac{c_1}{c_2} = 16 ; \frac{h_2}{h_1} = 5 \quad \text{and} \quad \frac{k_1}{k_2} = 8;$$

For these values Eqs. (4.39), (4.40), (4.43) and (4.44) are evaluated using IBM 7044 digital computer and the results are presented in Figs. 4.6 to 4.9.

Solutions obtained by analytical as well as finite difference methods for a two-layer system with two face drainage as given in Figs. 4.10 and 4.11, show very good agreement between the two methods.

#### COMPARISON OF TERZAGHI'S METHOD WITH RIGOROUS ANALYTICAL SOLUTION FOR SINGLE LAYER

Terzaghi's method is based on the intuitive argument that the settlement at the end of construction period is equal to the settlement which would have occurred at half of the construction period if the total load had been applied instantaneously at the starting. Similar arguments can be extended to any time  $t$  and the settlement  $S_t$  is found as follows:

$$S_t = \frac{t}{t_0} S_{t/2} \quad 0 \leq t \leq t_0 \quad (4.45)$$

$$S_t = S_{(t-t_0/2)} \quad t_0 \leq t \leq \infty \quad (4.46)$$

The average pore pressure ratios of the analytical solution are converted to settlement ratios as follows:

$$\frac{S_t}{S_\infty} = \left( \frac{t}{t_0} - \frac{\bar{u}}{\bar{u}_0} \right) \quad 0 \leq t \leq t_0 \quad (4.47)$$

$$\frac{S_t}{S_\infty} = \left( 1 - \frac{\bar{u}}{\bar{u}_0} \right) \quad t_0 \leq t \leq \infty \quad (4.48)$$

The results of Terzaghi's approximate method and the rigorous analytical solution are compared in Fig. 4.12. For practical usage Terzaghi's method proves to be a good approximation of the analytical solutions. However, deviations occur for higher construction periods ( $T_0 > .4$ ).

### THREE-LAYER SYSTEM

#### Finite difference method

The one-dimensional consolidation equation for layered system under construction loading is:

$$C_j \frac{\partial^2 u_j}{\partial z^2} + R = \frac{\partial u_j}{\partial t} \quad (4.49)$$

Where the subscript j denotes the layer number. There will be as many number of the above equations as there are layers. The above equations can be transformed into the difference equations using the finite difference mesh as shown in Fig. 3.1 as follows:

$$u_1 = (1 - 2B_j) u_0 + B_j (u_2 + u_4) + \frac{\bar{u}_0}{\delta t} \quad (4.50)$$

where  $B_j = \frac{C_j \delta t}{(\delta z)^2}$

The boundary conditions are:

1. At the drainage boundary  $u_1 = 0$
2. At the impervious boundary  $u_2 = u_4$

3. At the interface of the layers:

As given in Chapter III,

$$u_1 = E_{j,j+1} (u_2 - u_0) + F_{j,j+1} (u_4 - u_0) + u_0 + \delta t \frac{\bar{u}_0}{t_0} \quad (4.51)$$

where  $E_{j,j+1} = 2(B_j m_j \delta z_j) / (m_j \delta z_j + m_{j+1} \delta z_{j+1})$

$$F_{j,j+1} = 2(B_{j+1} m_{j+1} \delta z_{j+1}) / (m_j \delta z_j + m_{j+1} \delta z_{j+1})$$

Using the above finite difference method a three-layer system is solved for the following case (Fig. 3.4):

$$\frac{k_2}{k_1} = 10 ; \frac{C_2}{C_1} = \frac{1}{10} ; \frac{h_2}{H} = \frac{1}{3}$$

$$\frac{k_3}{k_1} = 20 ; \frac{C_3}{C_1} = \frac{1}{2} ; \frac{h_3}{H} = \frac{1}{3}$$

$$H = h_1 + h_2 + h_3 ; T = C t / (H/2)^2$$

The average pore pressure ratios vs time factor is shown in Fig. 4.13 for a particular  $T_0 = .50$ . Similar curves can be obtained for different time factors  $T_0$  corresponding to the construction periods  $t_0$ . However, it is to be noted here that computation time will be enormous if extreme ratios of the parameters of the layers are encountered. Because very small time intervals are to be taken to satisfy the stability criteria in order to get converging results.

## CONCLUSIONS

In evaluating the consolidation characteristics of soils, it is more realistic to assume time dependent construction type of loading. The closed form solutions presented here for a single as well as two-layer system will be helpful in predicting the time rate of settlement for field conditions. The computer involvement in evolving the final series of the analytical solutions is negligible compared to the time required for the finite difference method. When extreme ratios of soil parameters of the layers are encountered the computation time by the finite difference method is enormous.

For systems of more than two layers the finite difference method is the only method which can be easily employed for evaluating the consolidation characteristics.

Terzaghi's approximate method of estimating the time rate of settlement for a single layer under construction loading proves to be a good approximation of the rigorous solutions.

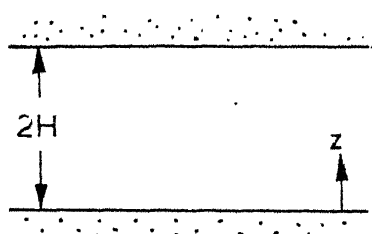


FIG.4.1 SINGLE LAYER WITH TWO WAY DRAINAGE

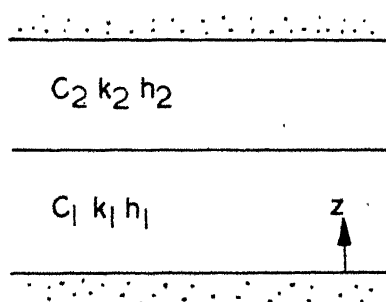


FIG.4.2 TWO LAYERED SYSTEM WITH TWO WAY DRAINAGE

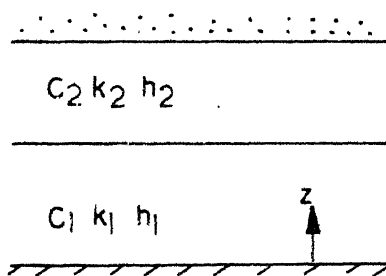


FIG. 43 TWO LAYERED SYSTEM WITH ONE WAY DRAINAGE

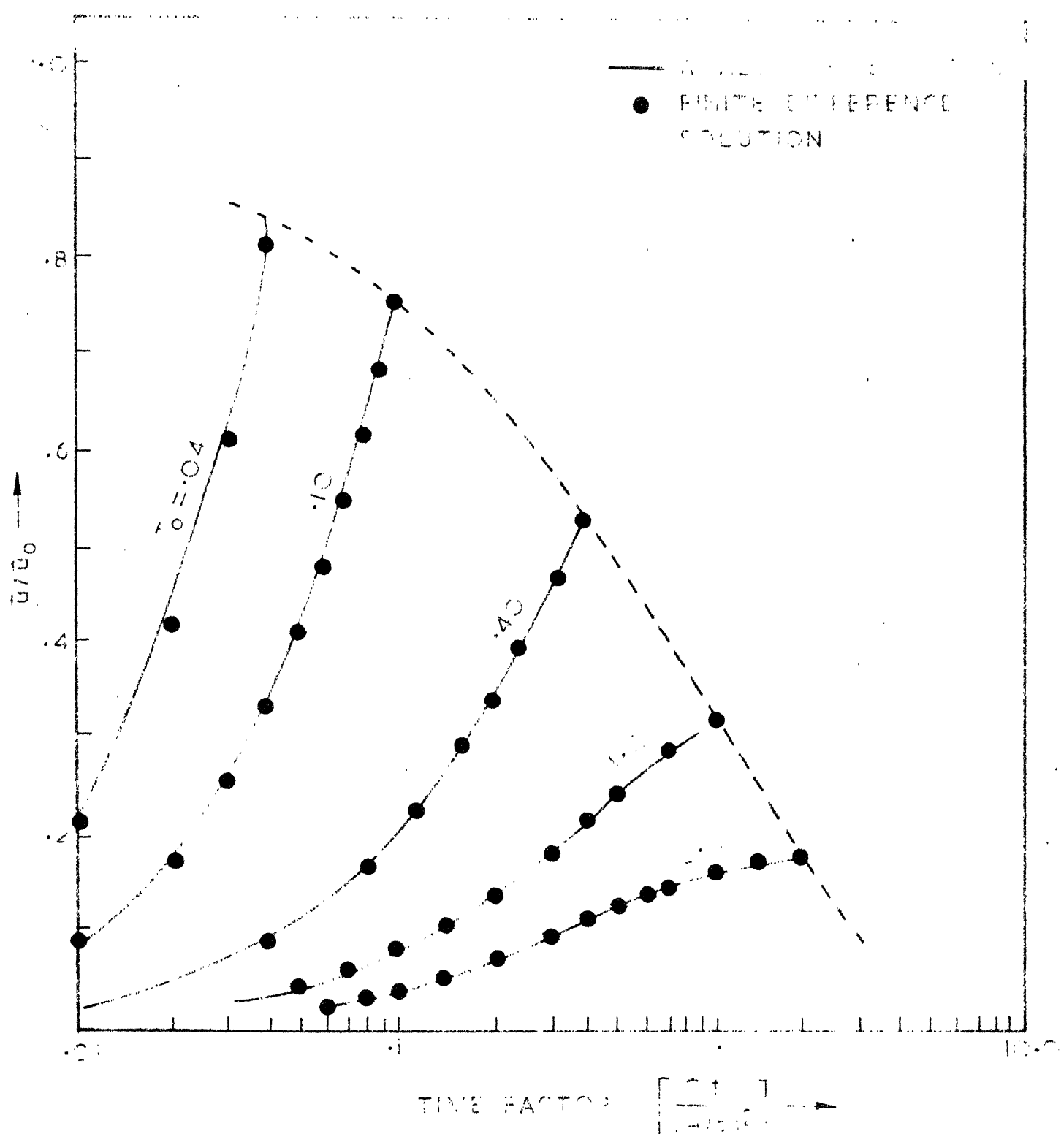


FIG. 4.4 COMPARISON OF FINITE DIFFERENCE AND ANALYTICAL SOLUTIONS FOR A TRANSIENT HEAT TRANSFER PROBLEM.

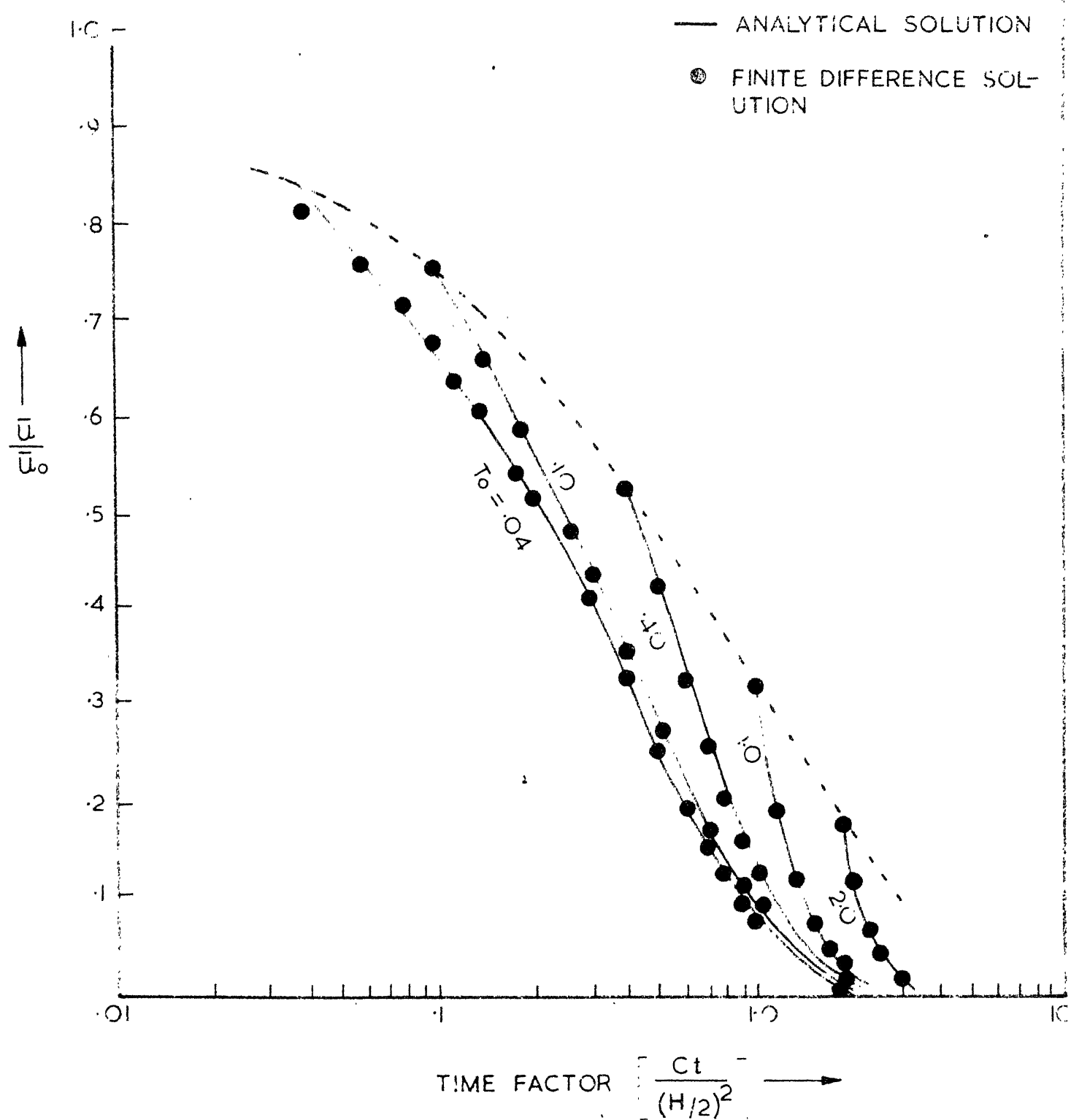


FIG. 4.5 COMPARISON OF FINITE DIFFERENCE AND ANALYTICAL SOLUTIONS FOR A DIFFUSION PROBLEM

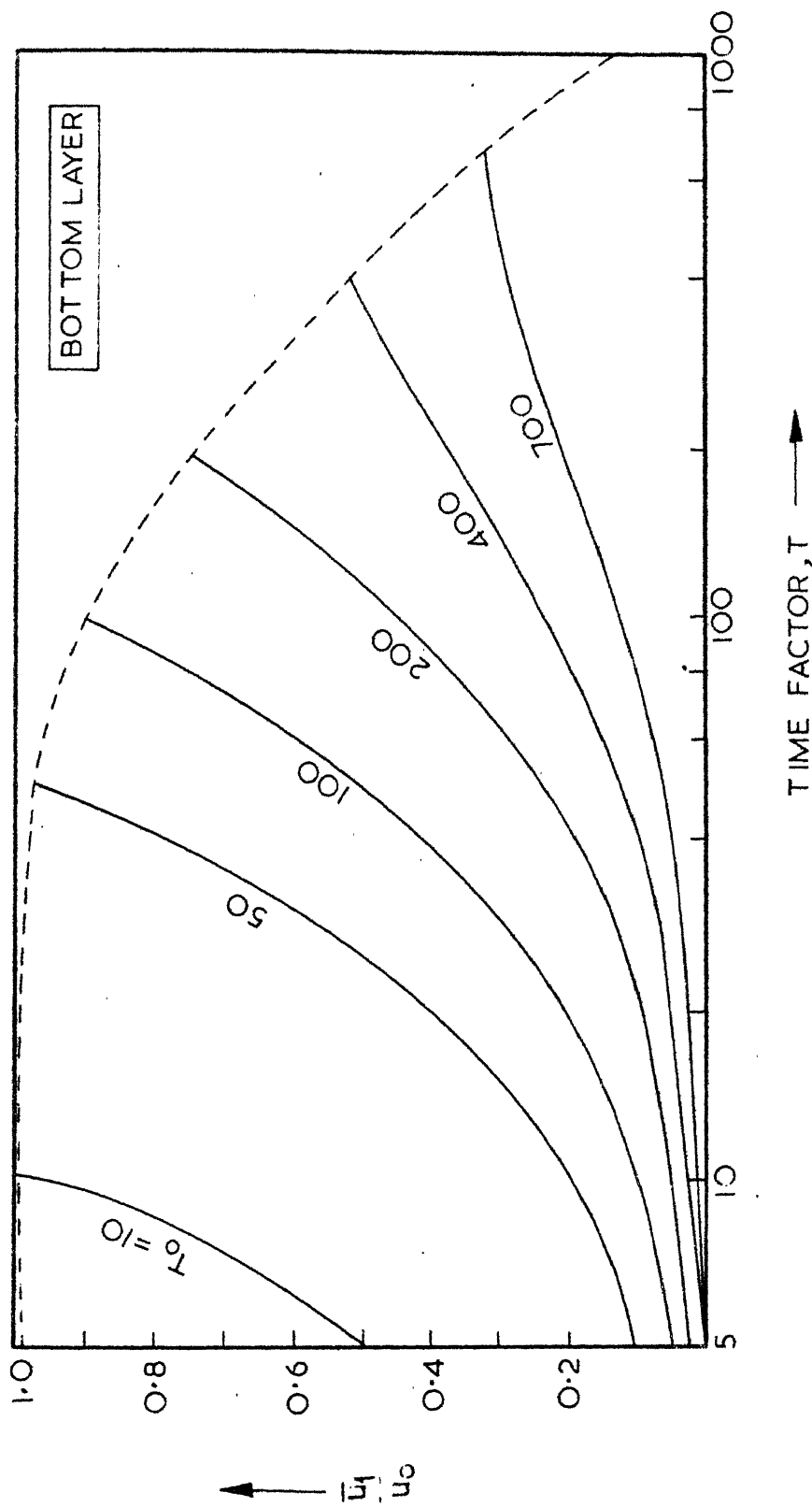


FIG. 4.6 AVERAGE PORE PRESSURE RATIOS FOR A TWO LAYERED SYSTEM WITH ONE WAY TOP DRAINAGE DURING CONSTRUCTION

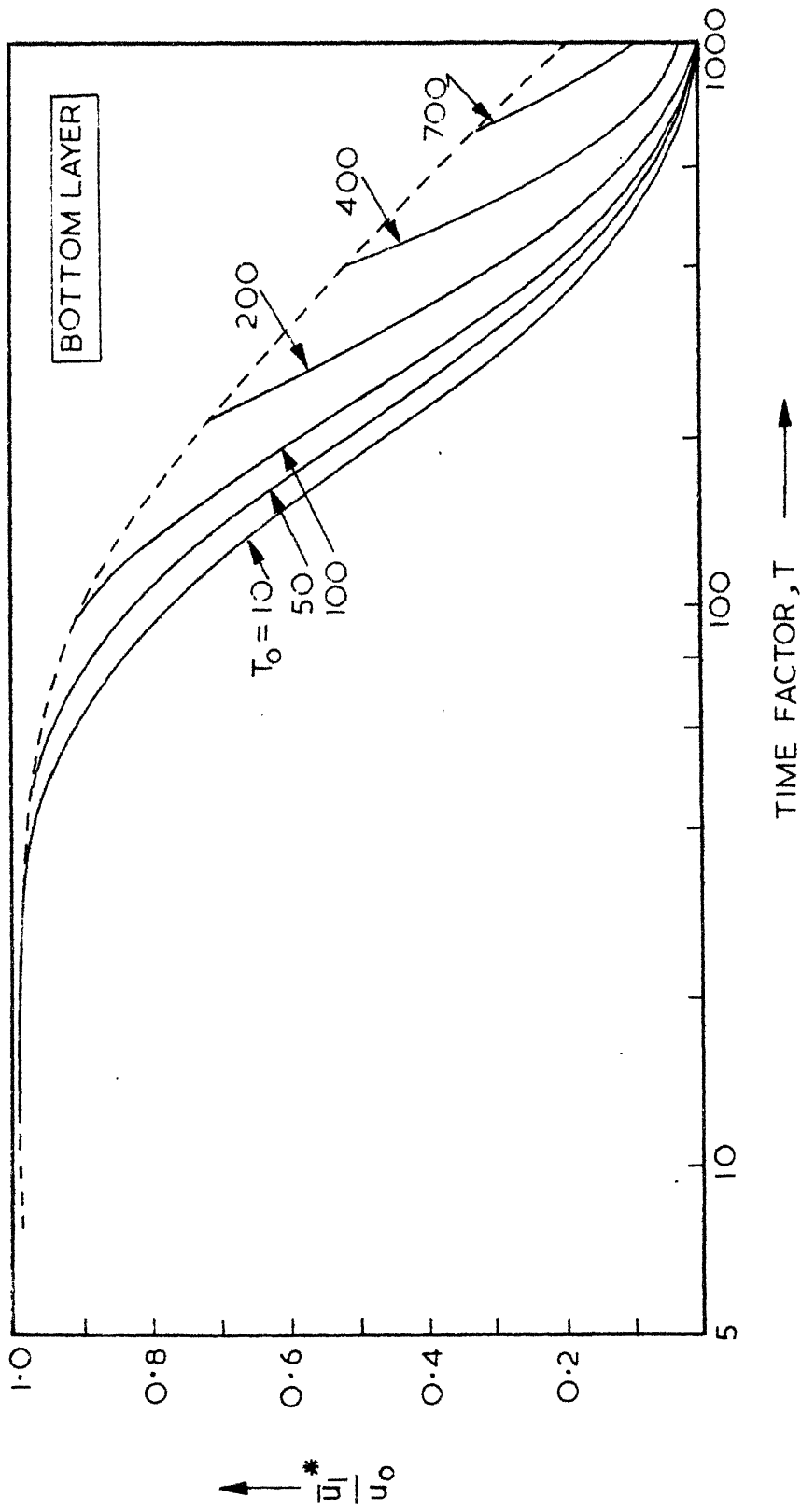


FIG. 4.7 AVERAGE PORE PRESSURE RATIOS FOR A TWO LAYERED SYSTEM WITH ONE WAY TOP DRAINAGE DURING POST CONSTRUCTION PERIOD

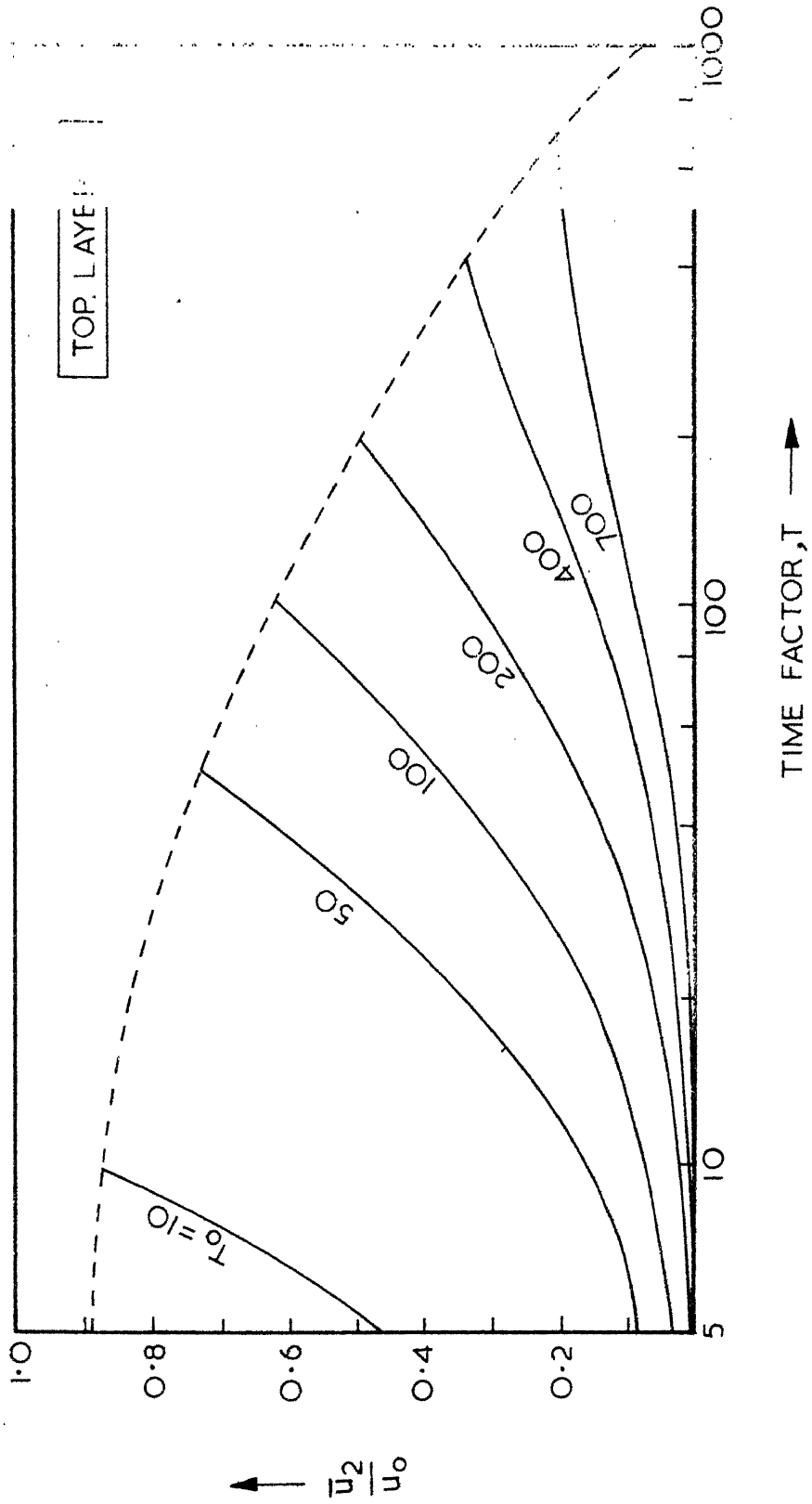


FIG. 4.8 AVERAGE PORE PRESSURE RATIOS FOR A TWO LAYERED SYSTEM WITH ONE WAY TOP DRAINAGE DURING CONSTRUCTION

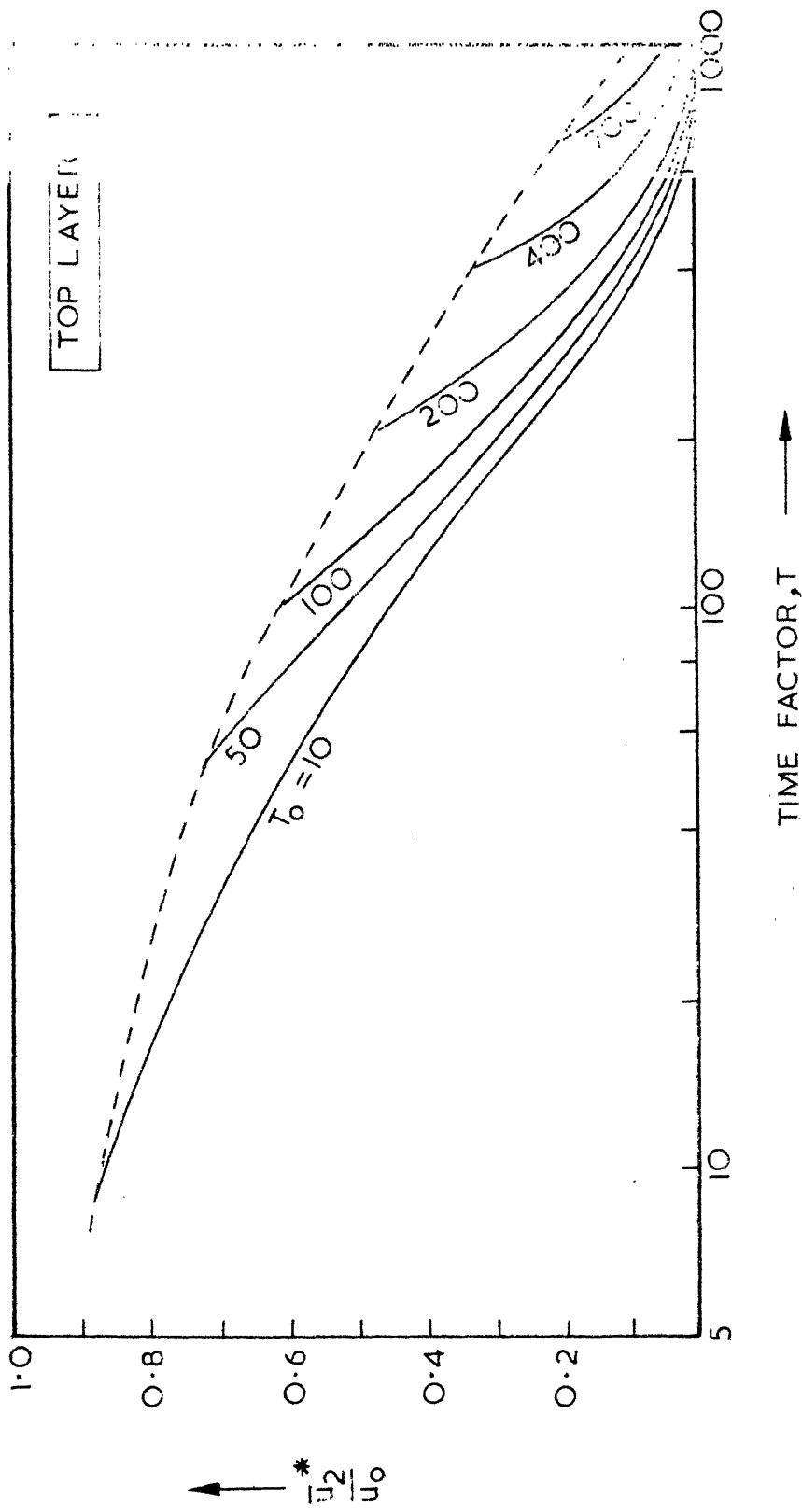


FIG. 4.9 AVERAGE PORE PRESSURE RATIOS FOR A TWO LAYERED SYSTEM WITH ONE WAY TOP DRAINAGE DURING POST CONSTRUCTION PERIOD

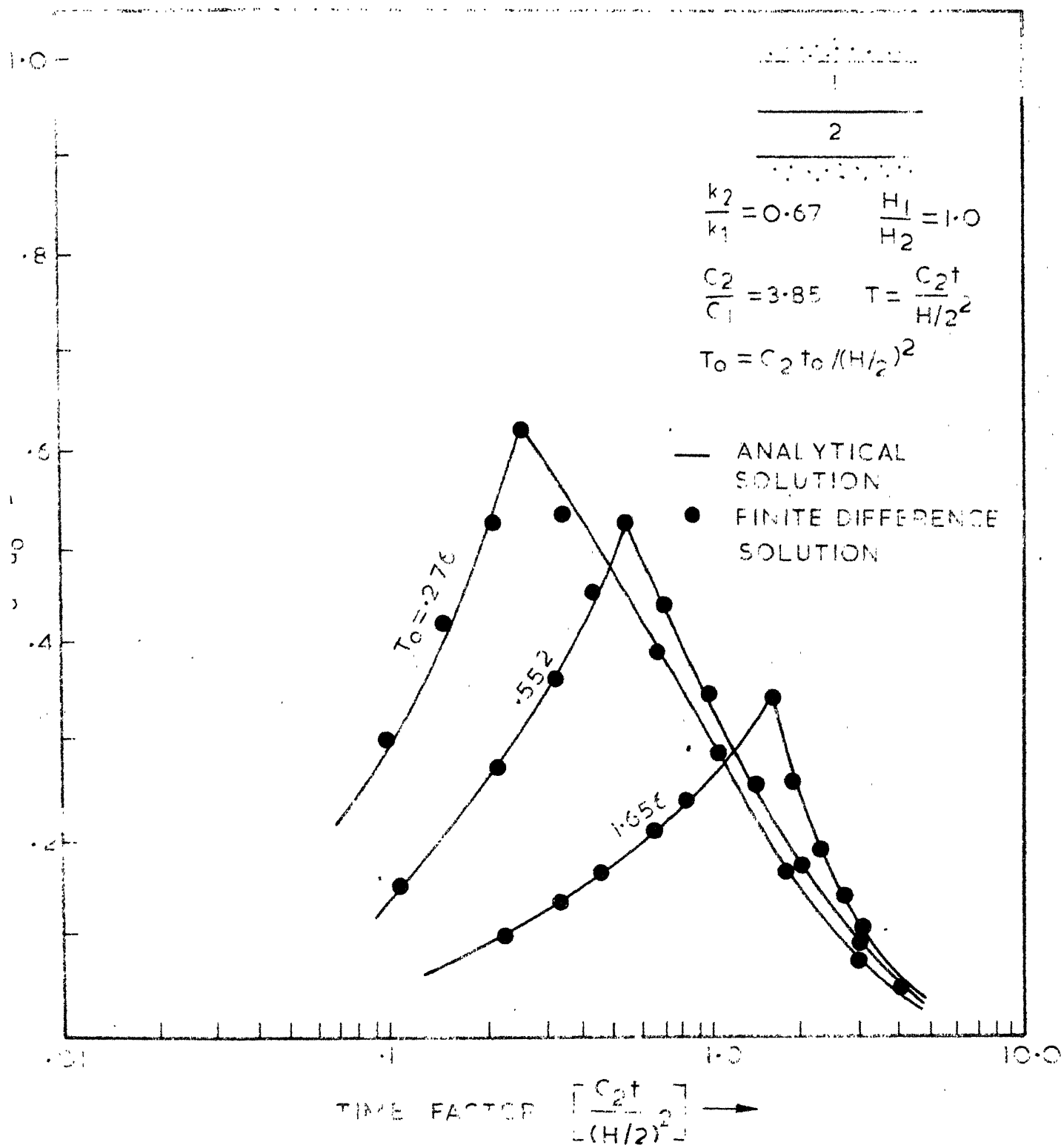


FIG. 4.10 COMPARISON OF FINITE DIFFERENCE SOLUTION AND ANALYTICAL SOLUTION FOR TWO LAYER SYSTEM-TWO WAY DRAINAGE FOR CONSTRUCTION LOADING-LAYER 2

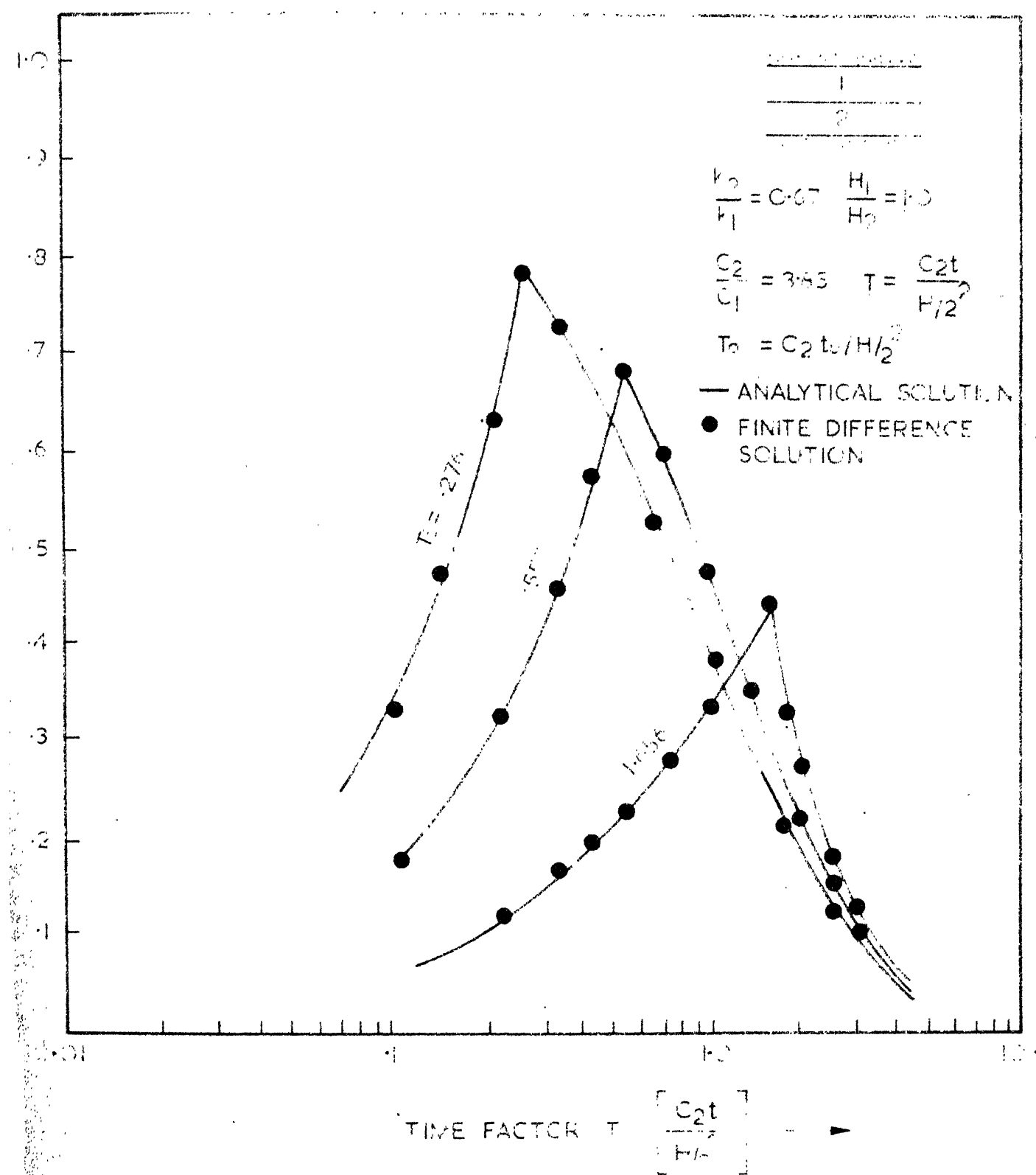
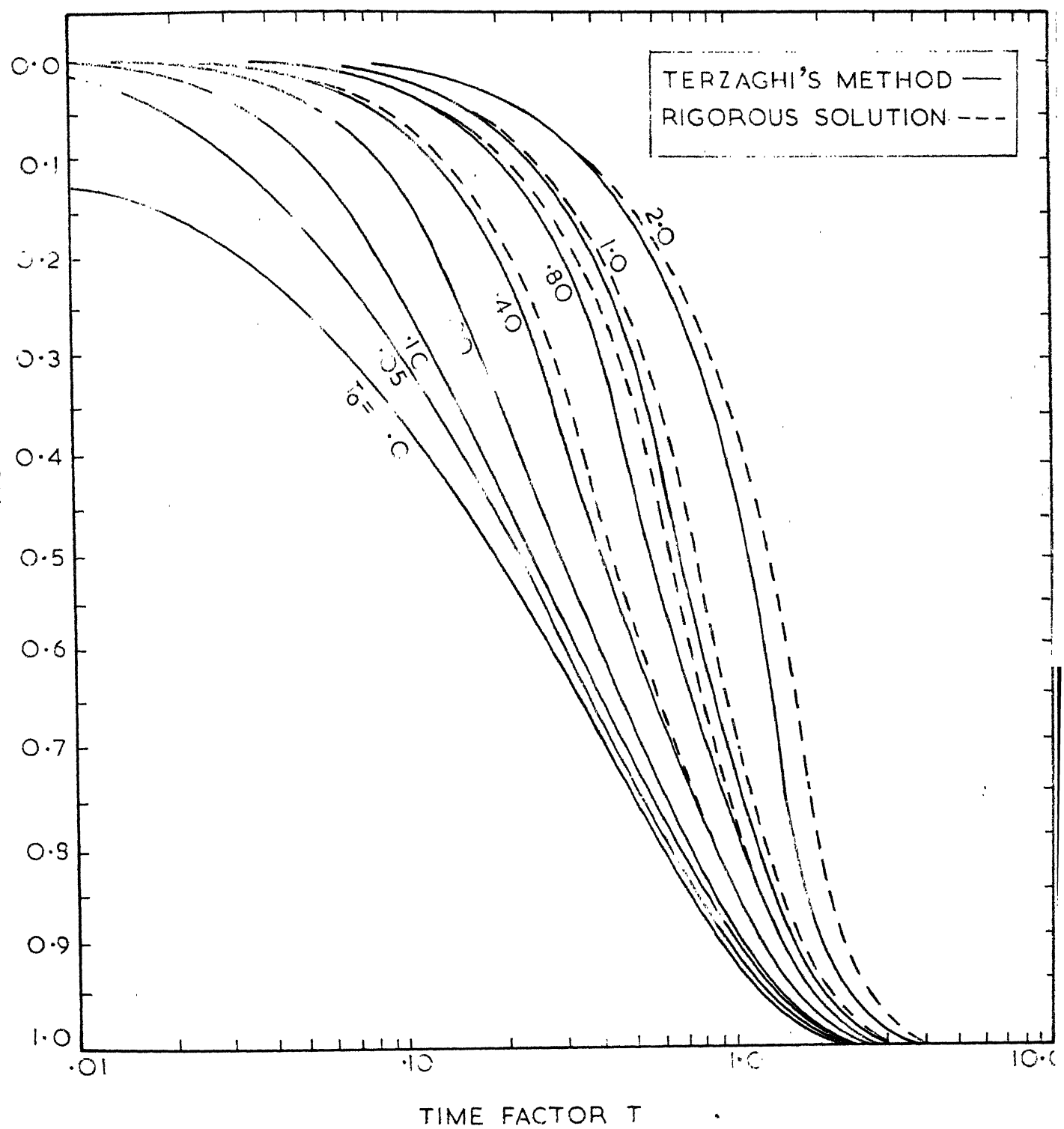


FIG.4.11 COMPARISON OF FINITE DIFFERENCE SOLUTION AND ANALYTICAL SOLUTION FOR TWO LAYER SYSTEM-TWO WAY DRAINAGE FOR CONCRETE STONE-LIMESTONE-LAYER 2



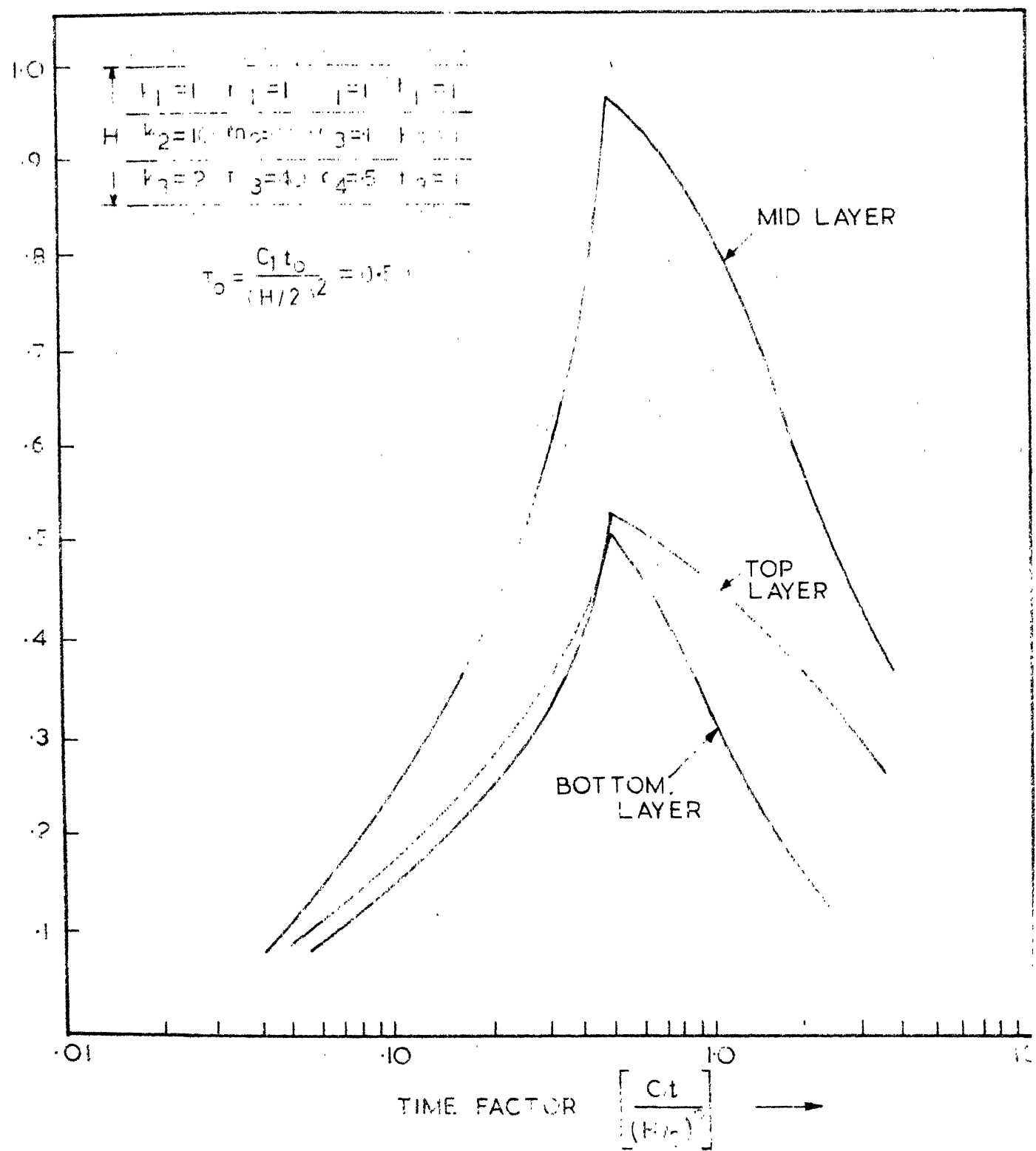


FIG. 4.13 CONSOLIDATION IN A THREE-LAYER SYSTEM

### EXPERIMENTAL SET-UP

A consolidation apparatus where the loading is applied by lever system is used. Special 3 inches dia. and  $\frac{5}{4}$  inch high brass fixed type eoedometer rings, with grooves cut in the rings, so that one can seat over the other exactly, as shown in Fig. 5.1, are used. The instantaneous loading is applied by placing weights at one end of the lever arm. A gradual increase in loading at the end of the lever arm is accomplished by a continuous increase of water level in a plastic container at the end of the lever arm as shown in Fig. 5.2. A supply tank maintains constant head for uniform flow. The rate of flow is regulated by means of a control valve fixed in the supply tank. This arrangement typically represents a gradually applied construction type of loading in one-dimensional consolidation tests.

### SOILS TESTED

Four different soils are used as layers in the experiments. They are locally available Kanpur clay, commercial Bentonite, Kaolinite and a mixture of Kanpur and Bentonite clay called Tabo clay. The properties of these soils are given in Table 5.1. The grain size distribution curves are shown in Fig. 5.3.

Table 5.1  
Soil properties

Soil	L.L.	P.I.	Sp. Gr.	Casagrande classification
Kanpur clay	44	24	2.60	CL
Bentonite	680	632	2.85	CH
Kaolinite	53	23	2.62	CL
Table clay	92	64	2.68	CH

#### TESTING PROCEDURE

The soil samples are prepared in the form of thick slurry. Thin filter papers are placed at the interface of the layers. To ensure complete saturation the soil samples are left with small back pressures for one day. To minimise the effects of side friction high graded silicon grease is applied on the sides of the oedometer rings. Two of the important limitations of the testing procedure are:

1. the temperature effect, and
2. the secondary effect

The effects of temperature variation is minimised by conducting all tests in an air-conditioned room where the variation of temperature is between  $18^{\circ}$  and  $22^{\circ}\text{C}$ . The secondary effect especially in the case of Bentonite and Table clay are bound to be predominant. However, for the purpose of this study

the consolidation parameters obtained from the test results of a single layer is assumed to be applicable to the same soil when it is part of a multi-layer system. The interpretation of test results are based on this approximation

## RESULTS

The consolidation characteristics of the soils used are found out by routine one-dimensional consolidation tests. The variation of the coefficient of consolidation with stress levels are shown in Fig. 5.4. The void ratio-pressure curves of the soils are given in Fig. 5.5. Using the coefficient of compressibility,  $a_v$ , obtained from the slope of the void ratio pressure curve, at various stress levels, the coefficients of permeability are calculated and are presented in Table 5.2. These values are subsequently used to obtain the analytical and numerical solutions of the various cases tested for the appropriate stress levels.

Table 5.2

Permeability values k cm/min.

Stress level T/Sq.ft.	Table clay	Kaolinite	Kanpur clay	Bentonite
0.25	$7.50 \times 10^{-6}$	$6.10 \times 10^{-5}$	$2.10 \times 10^{-4}$	$2.00 \times 10^{-6}$
0.50	$2.30 \times 10^{-6}$	$2.04 \times 10^{-5}$	$0.72 \times 10^{-4}$	$1.00 \times 10^{-6}$
1.00	$0.90 \times 10^{-6}$	$0.44 \times 10^{-5}$	$0.23 \times 10^{-4}$	$0.41 \times 10^{-6}$
2.00	$0.36 \times 10^{-6}$	$0.17 \times 10^{-5}$	$0.09 \times 10^{-4}$	$0.20 \times 10^{-6}$
4.00	$0.25 \times 10^{-6}$	$0.07 \times 10^{-5}$	$0.04 \times 10^{-4}$	$0.15 \times 10^{-6}$

In the case of layered systems under instantaneous loading the experimental time-consolidation curves are compared with those obtained by approximate method as well as by more rigorous analysis outlined in Chapter III. The approximate method is based on transforming the thickness of individual layers (39) as follows:

$$H'_j = H_j \sqrt{\frac{C_1}{C_j}}$$

where  $H'_j$  is the transformed thickness of jth layer,

$H_j$  is the original thickness of jth layer,

$C_1$  and  $C_j$  are the coefficients of consolidation of the first and jth layers respectively.

The total thickness  $H = \sum_{j=1}^n H'_j$  is assumed to consolidate as

single layer with coefficient of consolidation  $C_1$ .

#### CASES STUDIED

For the various cases discussed in the previous chapters, certain idealised assumptions regarding the relative values of the parameters  $k$ ,  $m$  and  $C$  were made with a view to study the effects of the variables either individually or jointly on the consolidation characteristics of layered systems. While the analytical study is valuable to provide a basic understanding of the effects of the variation of the parameters and the use

of different interpretation technique, it is not possible to strictly duplicate the idealised extreme situations in laboratory. However, certain general trends and conclusions obtained from the analytical study can be meaningfully verified from the laboratory tests using the available soils. The following cases are taken up for the study:

1. Single layer under construction loading
2. Two-layer system under instantaneous loading
3. Two-layer system under construction loading
4. Three-layer system under instantaneous loading
5. Three-layer system under construction loading

#### DISCUSSIONS

##### Construction loading

Single layer: The test results of single layer with two face drainage under construction loading are given in Figs. 5.6 to 5.14 by dotted lines. The tests are conducted for various rate of loading as denoted by  $T_0$ , the time factor corresponding to the loading time  $t_0$ . Theoretical solutions of these cases by the methods outlined in Chapter IV for the corresponding  $T_0$  values are shown by solid lines in these figures.

Reasonable agreement of the test results with the theoretical prediction is seen (Figs. 5.6 to 5.10). However, noticeable deviation occur in Bentonite (Fig. 5.10). In this test the total imposed pressure is 2.9 T/sq.ft. It is found

that the value of C under instantaneous loading itself varies from 9.9 to  $5.7 \times 10^{-4} \text{ cm}^2/\text{min}$ . Therefore, taking these values of C, theoretical curves are drawn as shown in this figure. The test results are seen to fall within the limiting theoretical curves.

In Figs. 5.11 to 5.14 curves are drawn between the average pore pressure ratios  $\frac{\bar{u}}{u_0}$  (obtained from measured settlement ratios) and the time factor T at various  $T_0$ . These figures demonstrate the building up and decay characteristics of the pore pressure under construction loading.

Two and three-layer systems: The results of the two and three layer systems under construction loading are shown in Figs. 5.15 to 5.23. The analytical solutions of the various cases as given in Chapter IV are shown in all the figures for comparison. The laboratory experiments are conducted for various rates of loading. The results obtained are shown for the  $T_0$  values corresponding to the loading period  $t_0$ .

The comparison presented here in all the figures shows the amount of error involved in predicting the rate of settlement of layered systems under construction loading by theoretical procedure. However, the general trends of consolidation characteristics of layered systems under construction loading obtained by mathematical analyses are within reasonable error as seen in all the above experimental verifications.

### Instantaneous loading

Two and three layer systems: A number of interesting trends and some fallacies in computing the time rates of settlement were demonstrated in Chapter III relating the effects of location of drainage boundary to the relative values of permeability and compressibility coefficients in two and three-layer systems. Due to experimental limitations it has not been possible to demonstrate these trends. It would have been interesting to obtain settlements of individual layers even though it will be nearly impossible to control the individual consolidation parameters of the layers. However, a comparison of the total system in experiment with the analytical results is useful to demonstrate the trends.

The results of two and three layer systems under instantaneous loading are presented in Fig. 5.24 to 5.30. In all the cases it is seen that the analytical solution obtained by numerical method compares more favourably than the transformation method with the experimental results. In some cases the transformation method yields very crude results (Figs. 5.26, 5.27 and 5.28).

### CONCLUSIONS

A simple experimental set-up is devised for applying gradually increasing construction type of loading in one-dimensional consolidation test. Special oedometer rings are

used to conduct tests on layered systems. Using four different types of soils, one-dimensional consolidation tests on layered systems up to three layers are conducted under instantaneous as well as construction loading.

The general trends of consolidation characteristics of layered systems under instantaneous as well as construction loading predicted by analytical procedures as discussed in the earlier chapters are found to be within reasonable limits of errors when compared with the experimental results.

A simplified method of analysis of the layered system under instantaneous loading, using the method of transformation of individual layers, results in substantial errors.

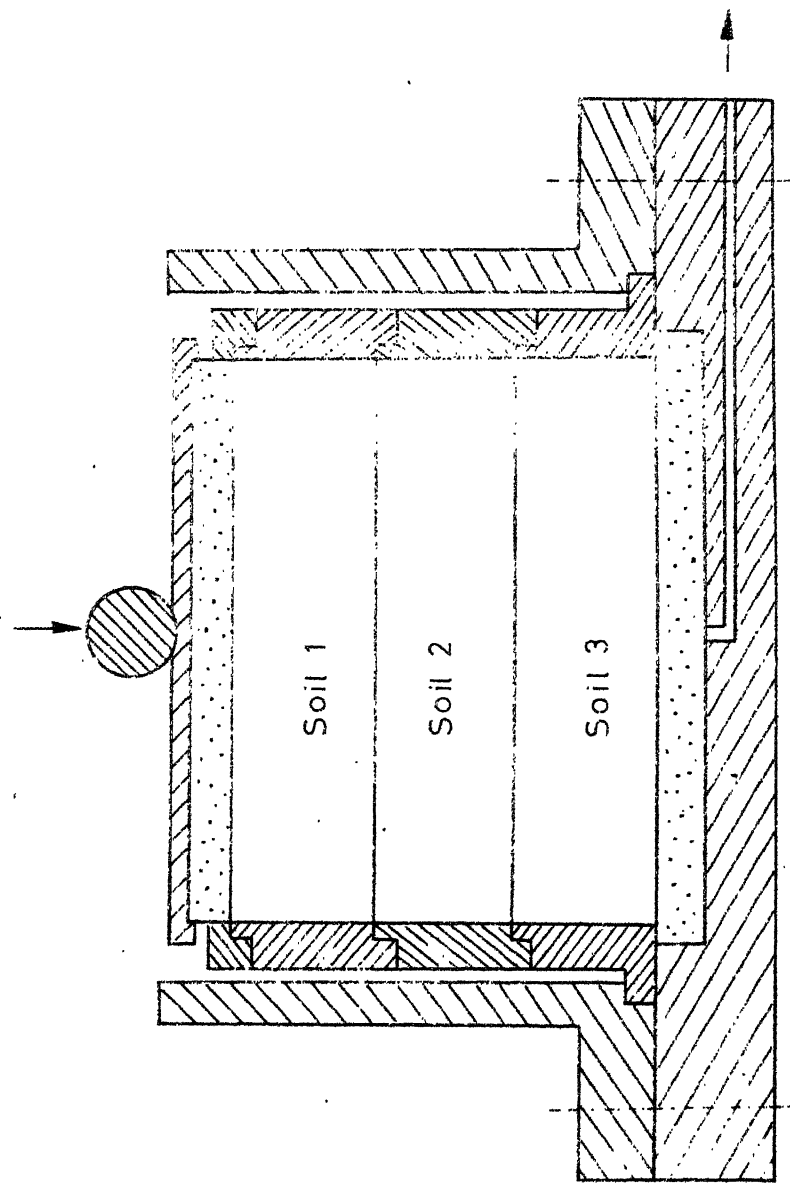
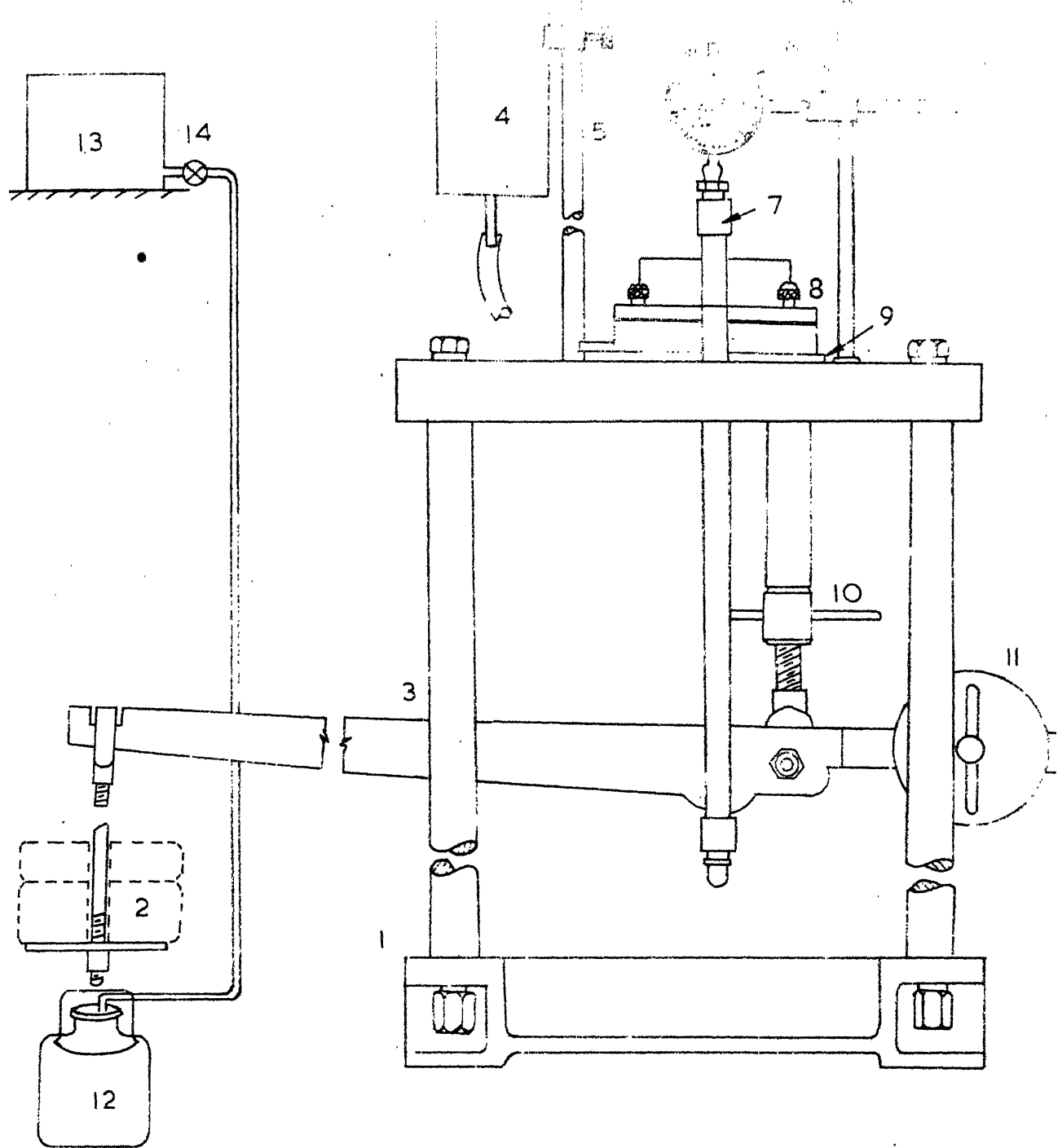


FIG. 5.1 OEDOMETER FOR MULTILAYER SYSTEM



- |                               |                   |
|-------------------------------|-------------------|
| 1 BASE                        | 8 CELL ASSEMBLY   |
| 2 WEIGHT HANGER               | 9 TOP PLATE       |
| 3 LOADING LEVER               | 10 CAPSTAN        |
| 4 WATER RESERVOIR             | 11 COUNTER WEIGHT |
| 5 RESERVOIR SUPPORT<br>PILLAR | 12 PLASTIC BUCKET |
| 6 DIAL GAUGE AND SUPPORT      | 13 SUPPLY TANK    |
| 7 LOADING YOKE                | 14 CONTROL VALVE  |

FIG. 5.2 CONSOLIDATION APPARATUS

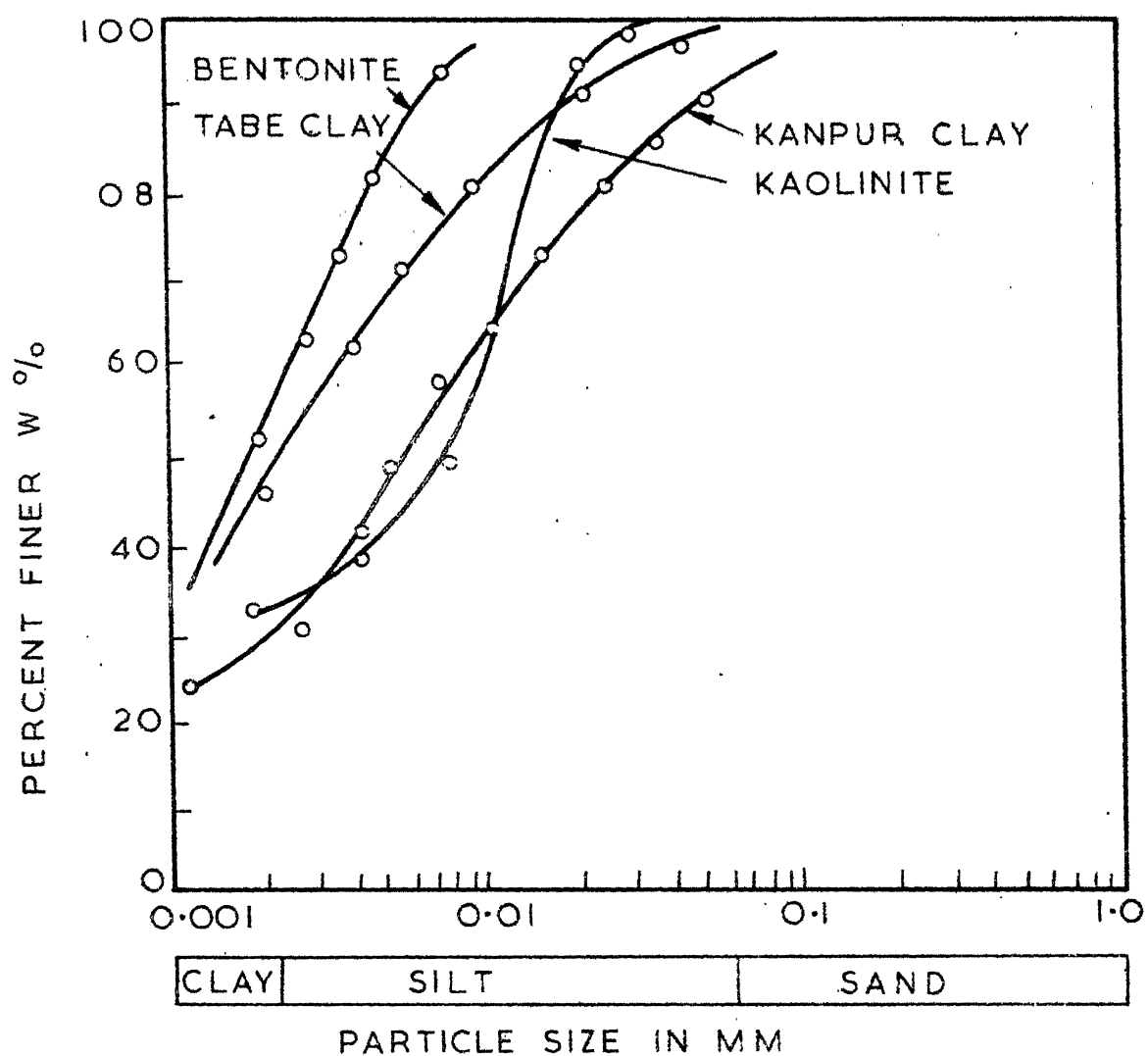


FIG. 5.3 GRAIN SIZE DISTRIBUTION CURVES

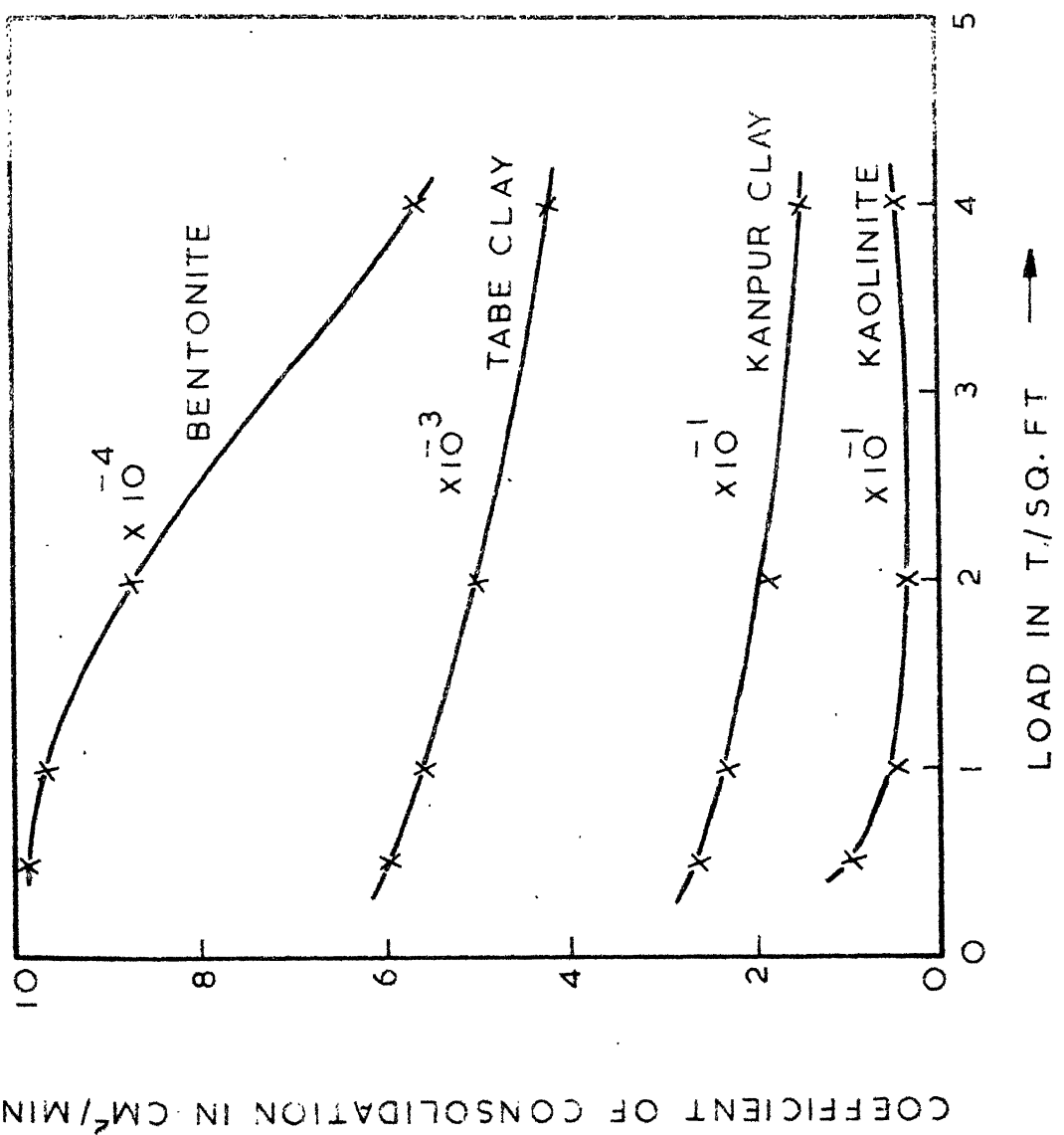


FIG. 5.4 COEFFICIENT OF CONSOLIDATION

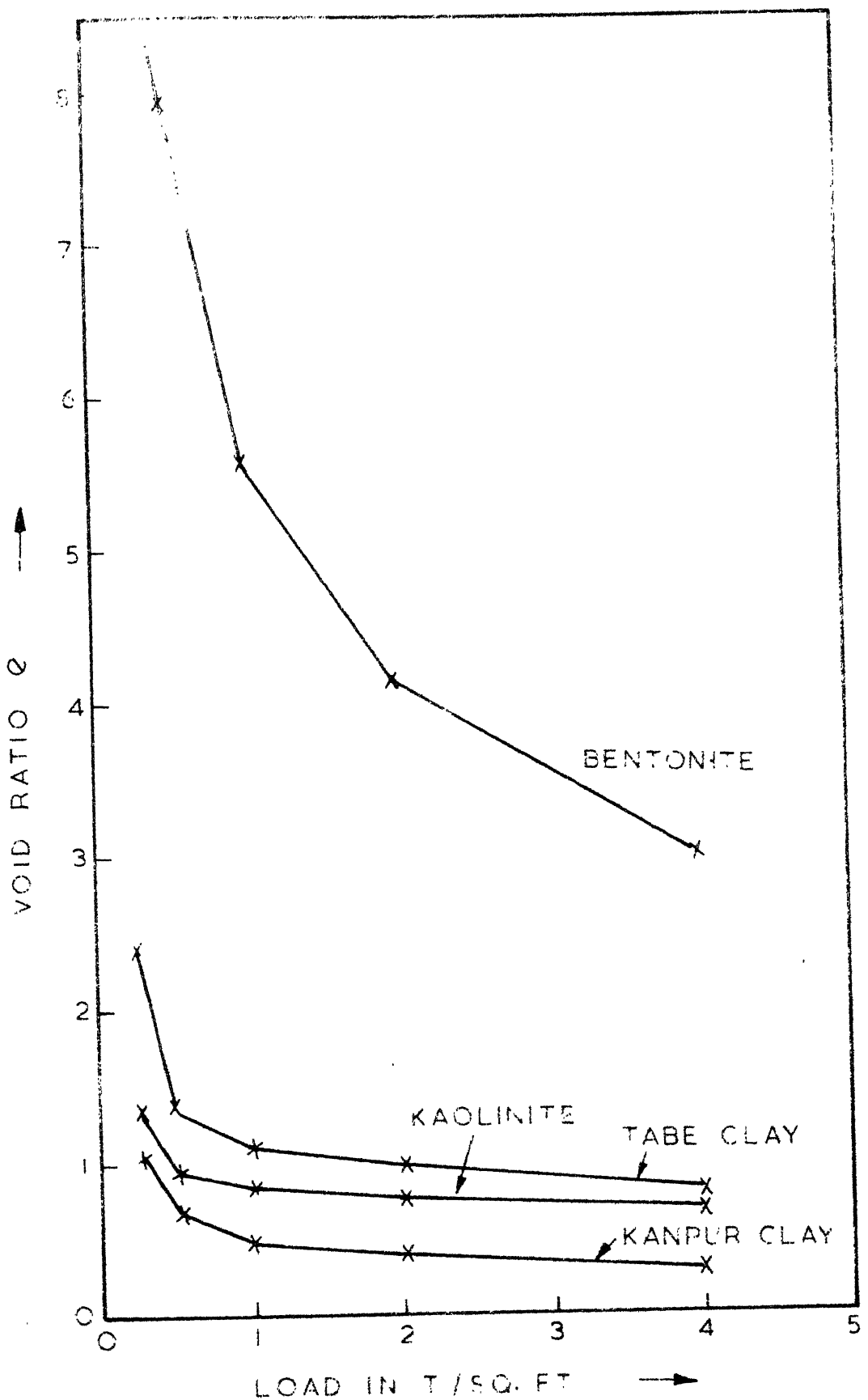


FIG. 5.5 VOID RATIO PRESSURE CURVE

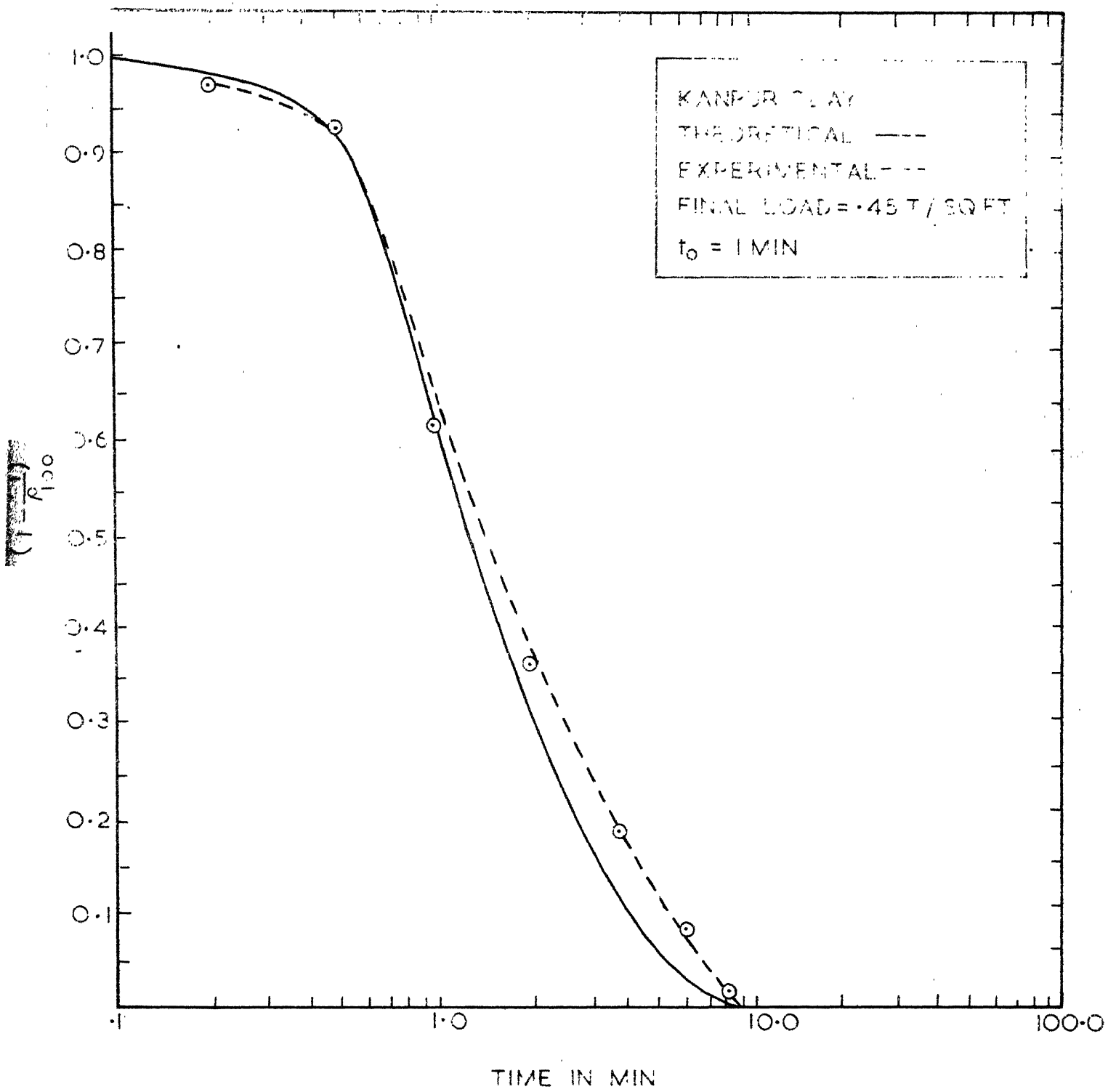


FIG. 5.6 CONSOLIDATION OF SINGLE LAYER UNDER CONSTRUCTION LOADING

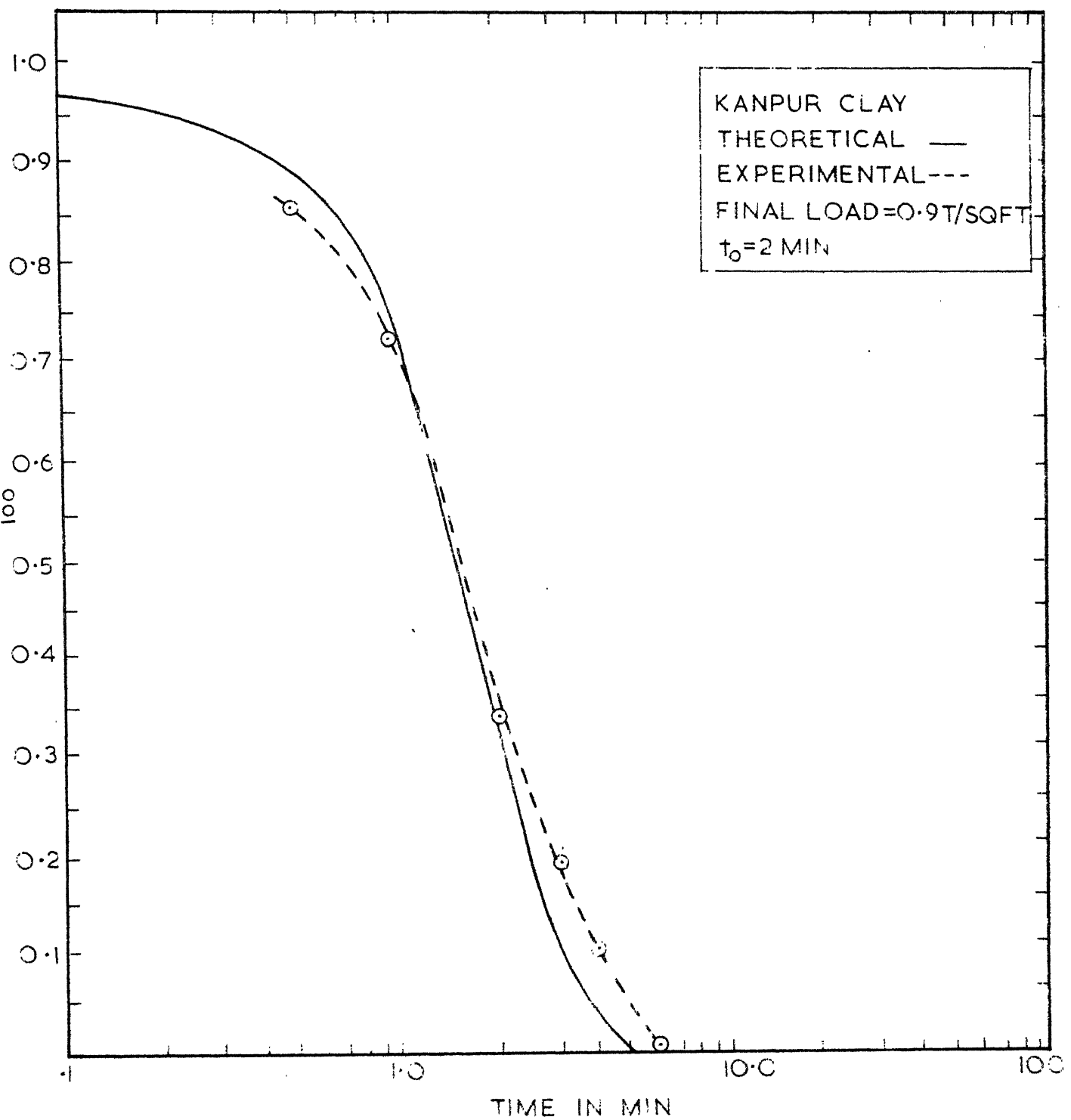


FIG. 5.7 CONSOLIDATION OF SINGLE LAYER UNDER CONSTRUCTION LOADING

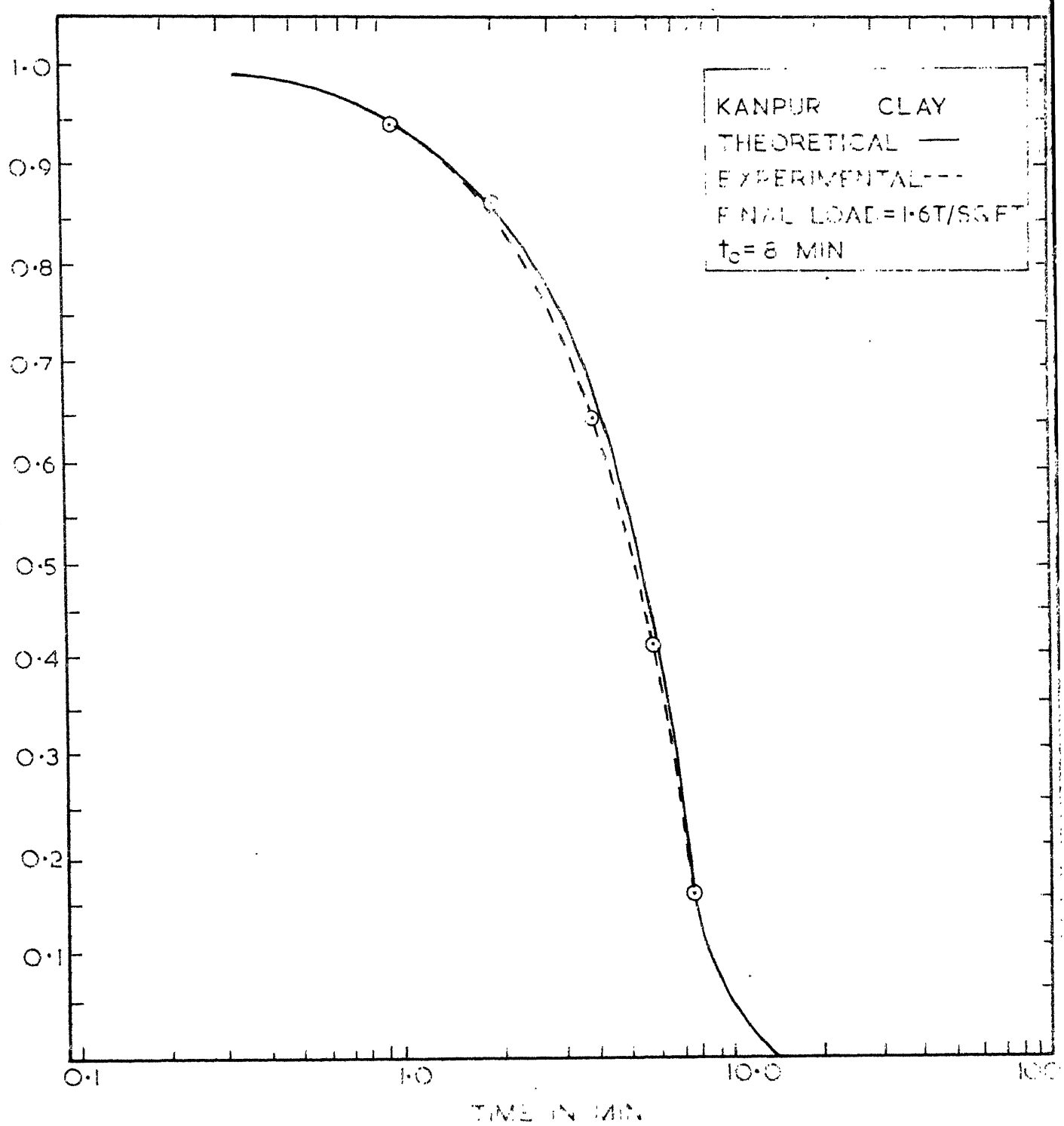


FIG. 5.8 CONSOLIDATION OF SINGLE LAYER UNDER CONSTRUCTION LOADING

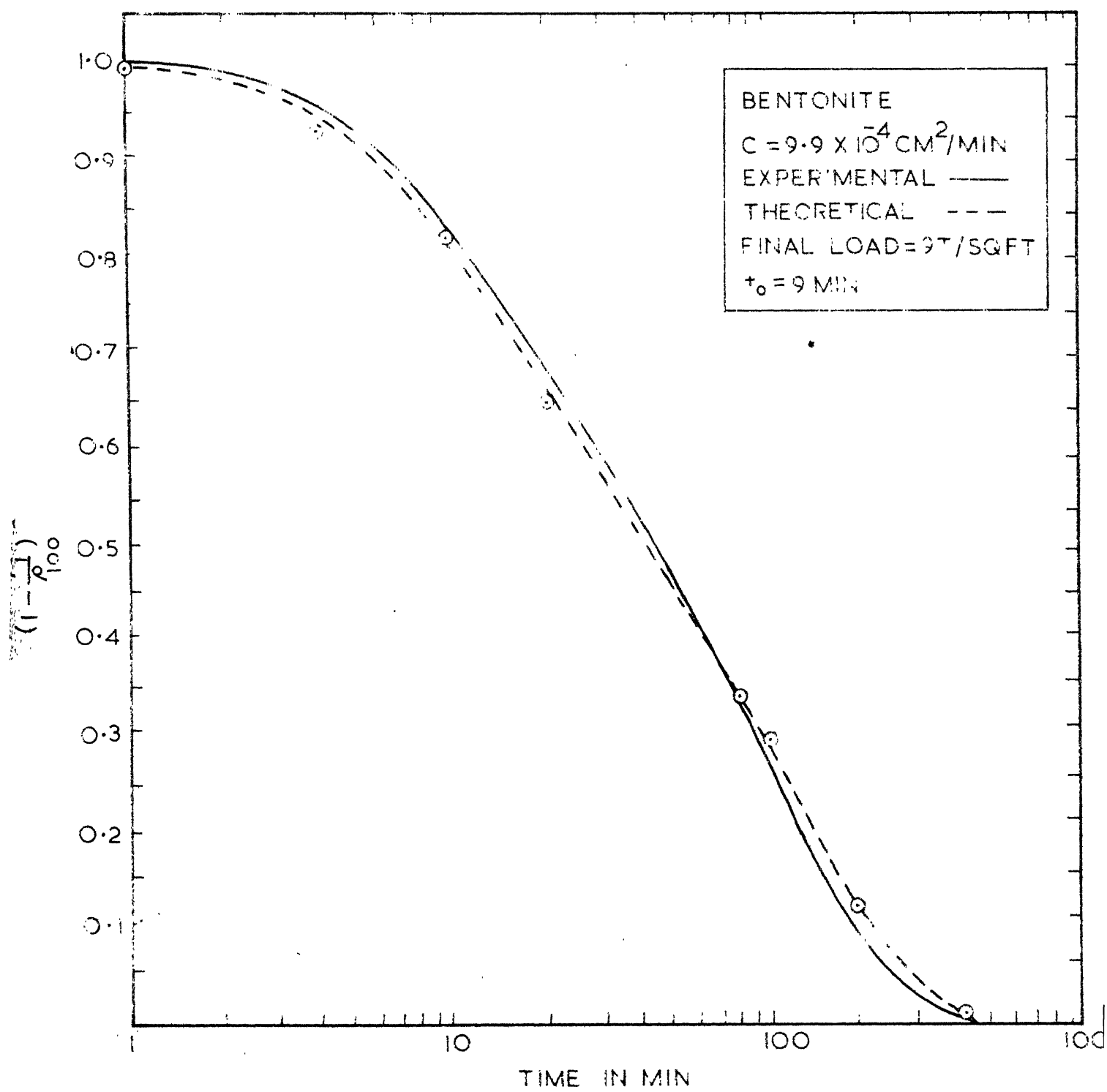


FIG. 5.9 CONSOLIDATION OF SINGLE LAYER UNDER CONSTRUCTION LOADING

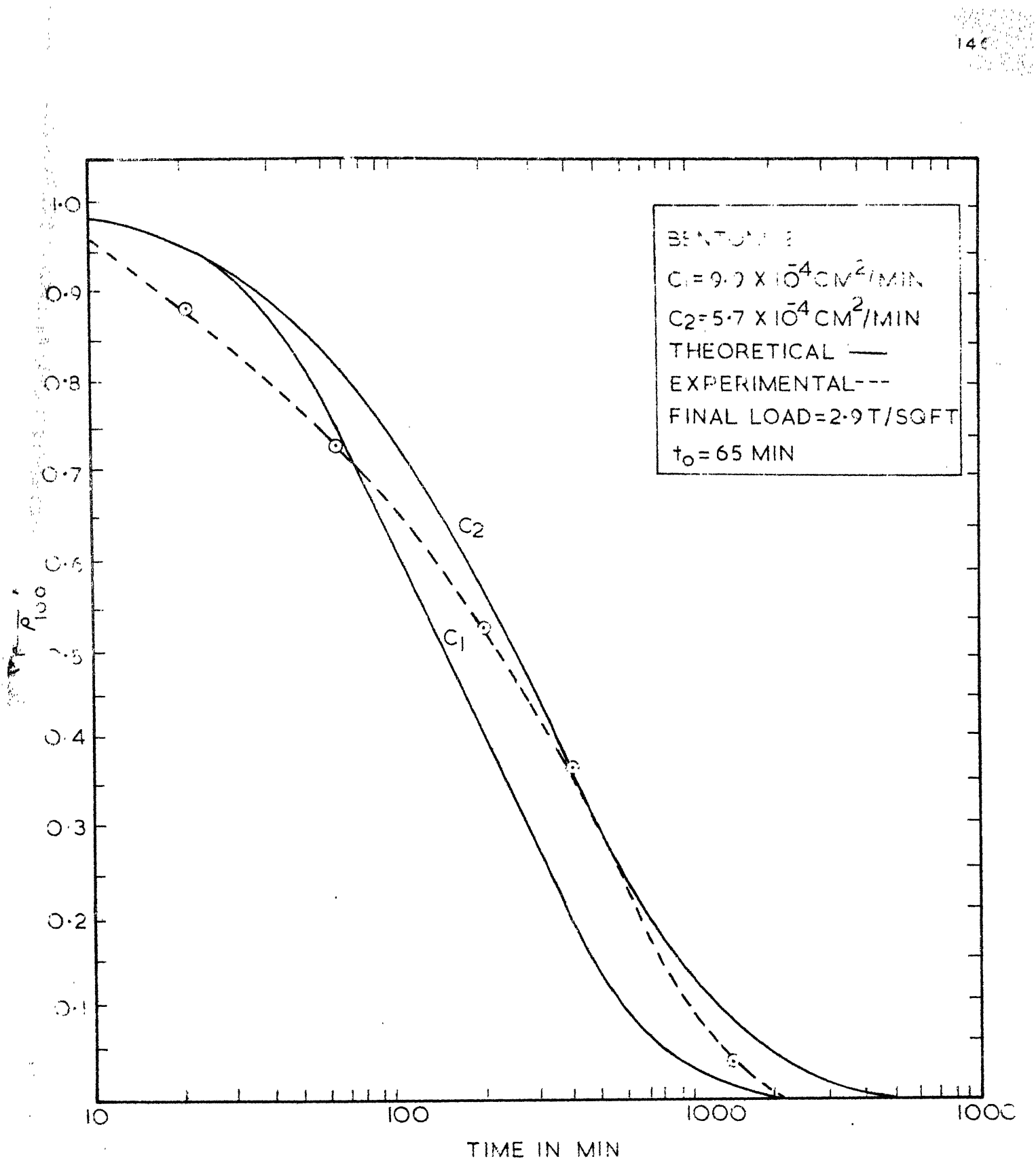


FIG. 5.10 CONSOLIDATION OF SINGLE LAYER UNDER CONSTRICITION LOADING

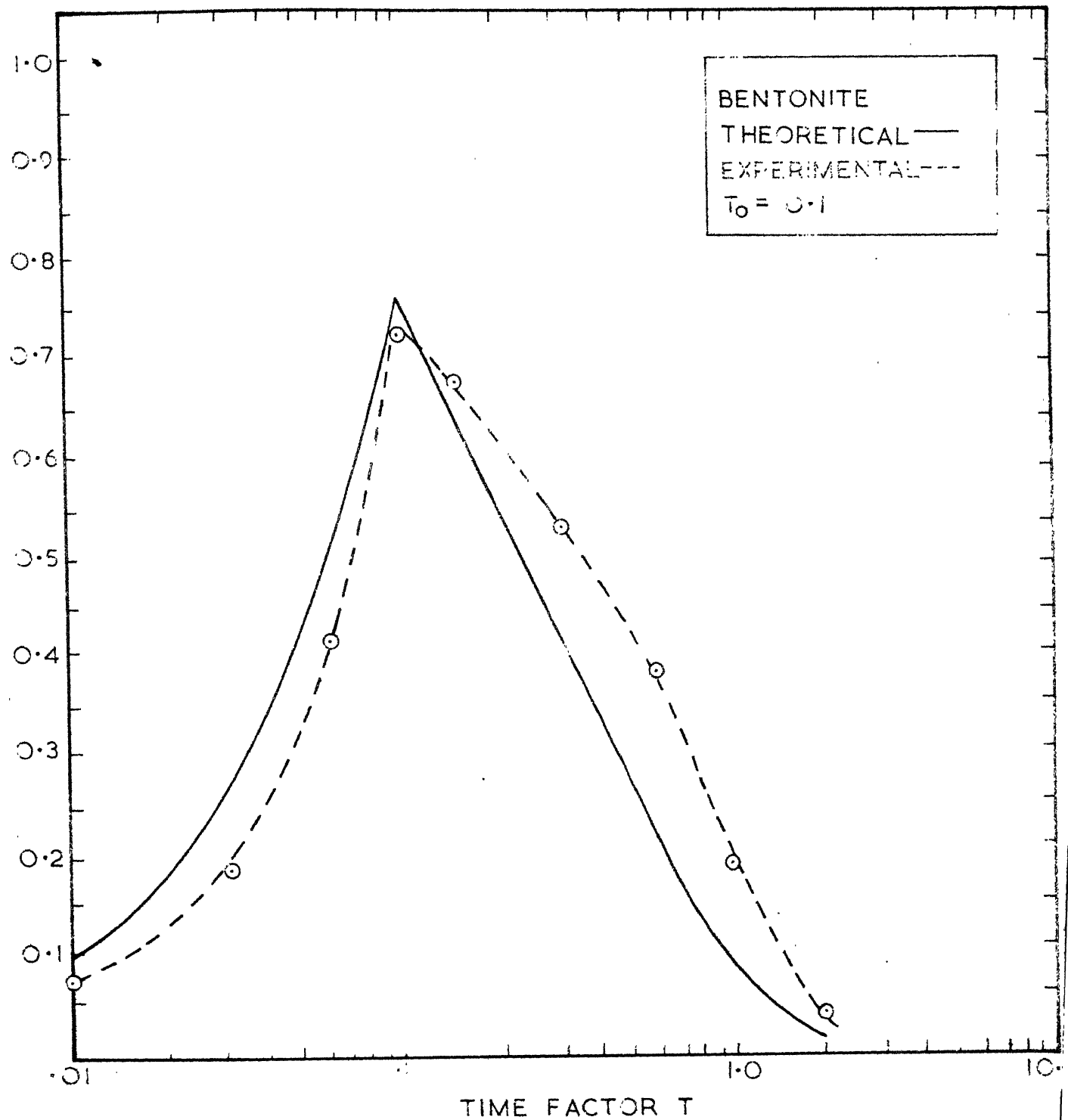


FIG.5-II AVERAGE PORE PRESSURE RATIOS IN A SINGLE LAYER UNDER CONSTRUCTION LOADING

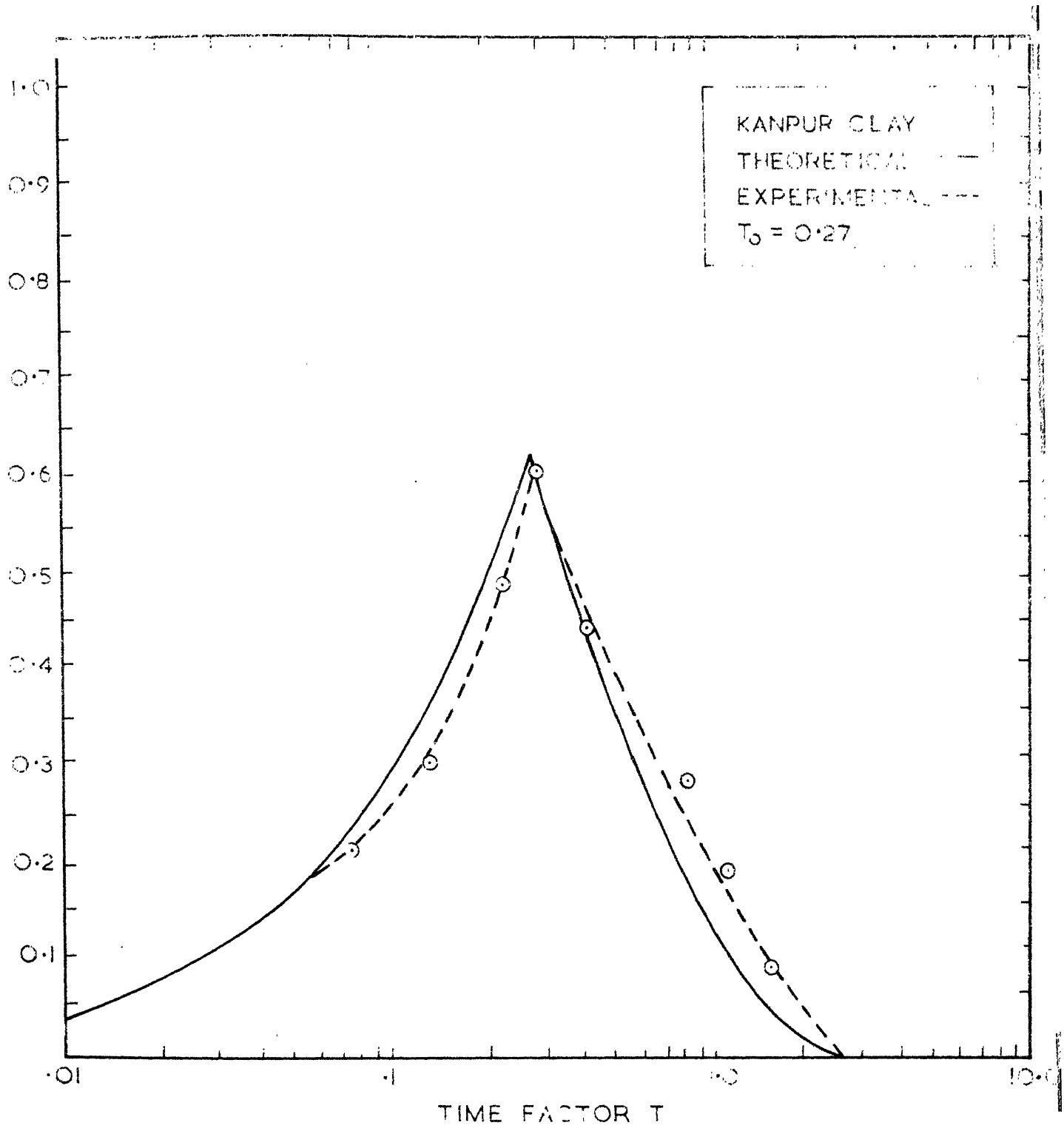


FIG. 5.12 AVERAGE PORE-PRESSURE RATIOS IN A SINGLE LAYER UNDER CONSTRUCTION LOADING

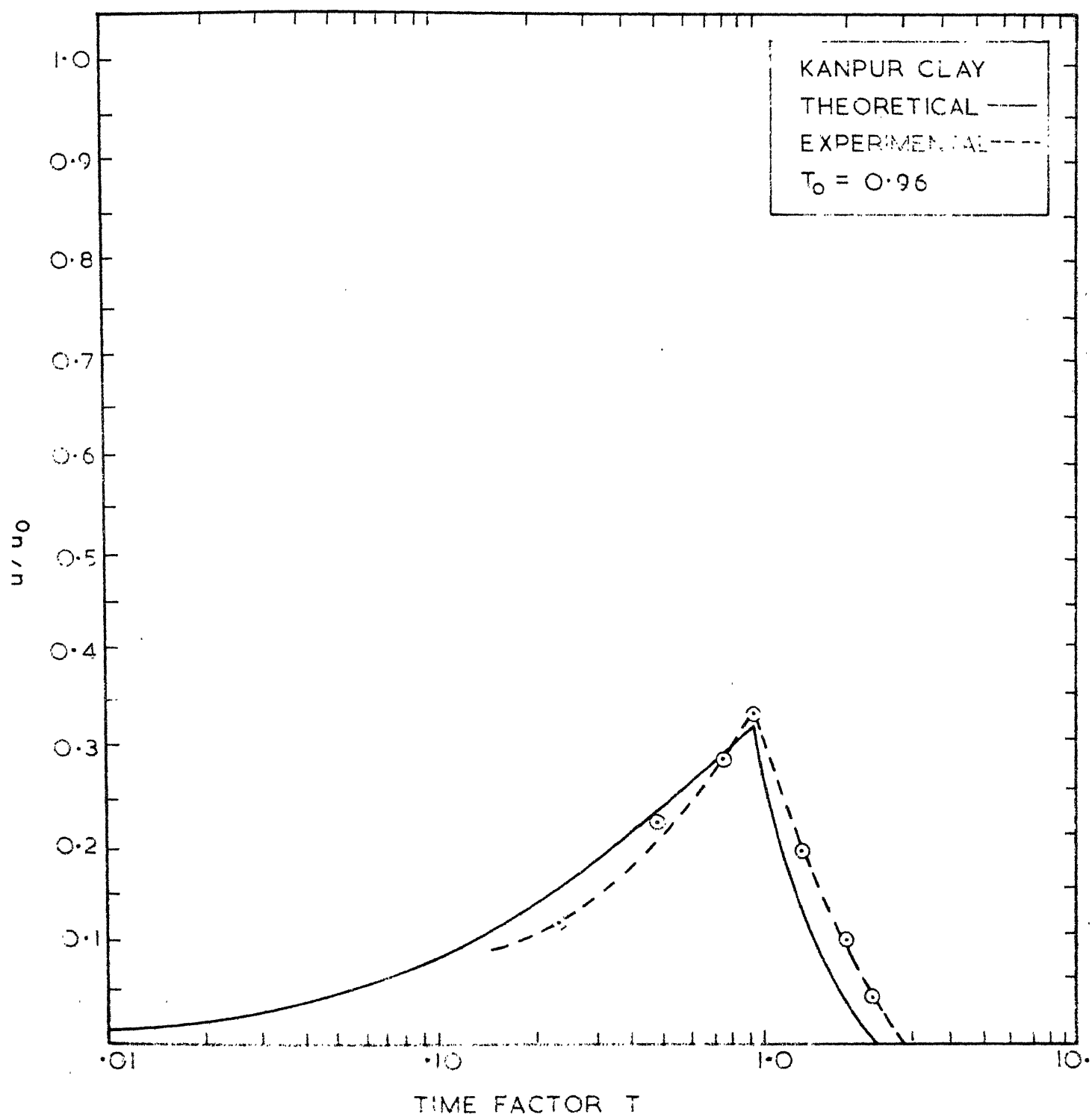


FIG. 5.13 AVERAGE PORE-PRESSURE RATIOS IN A SINGLE LAYER UNDER CONSTRUCTION LOADING

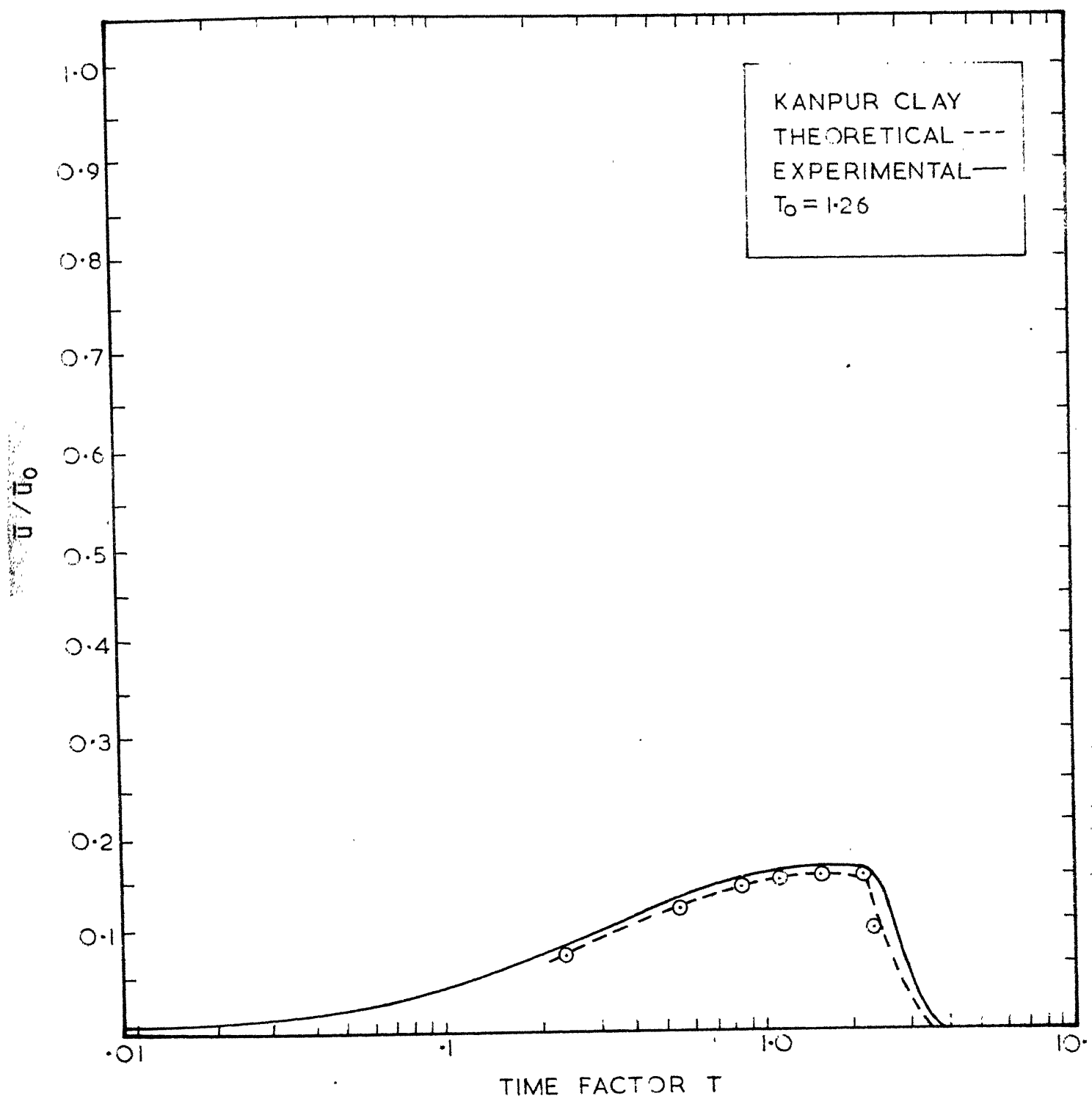


FIG. 5.14 AVERAGE PORE PRESSURE RATIOS IN A SINGLE LAYER UNDER CONSTRUCTION LOADING

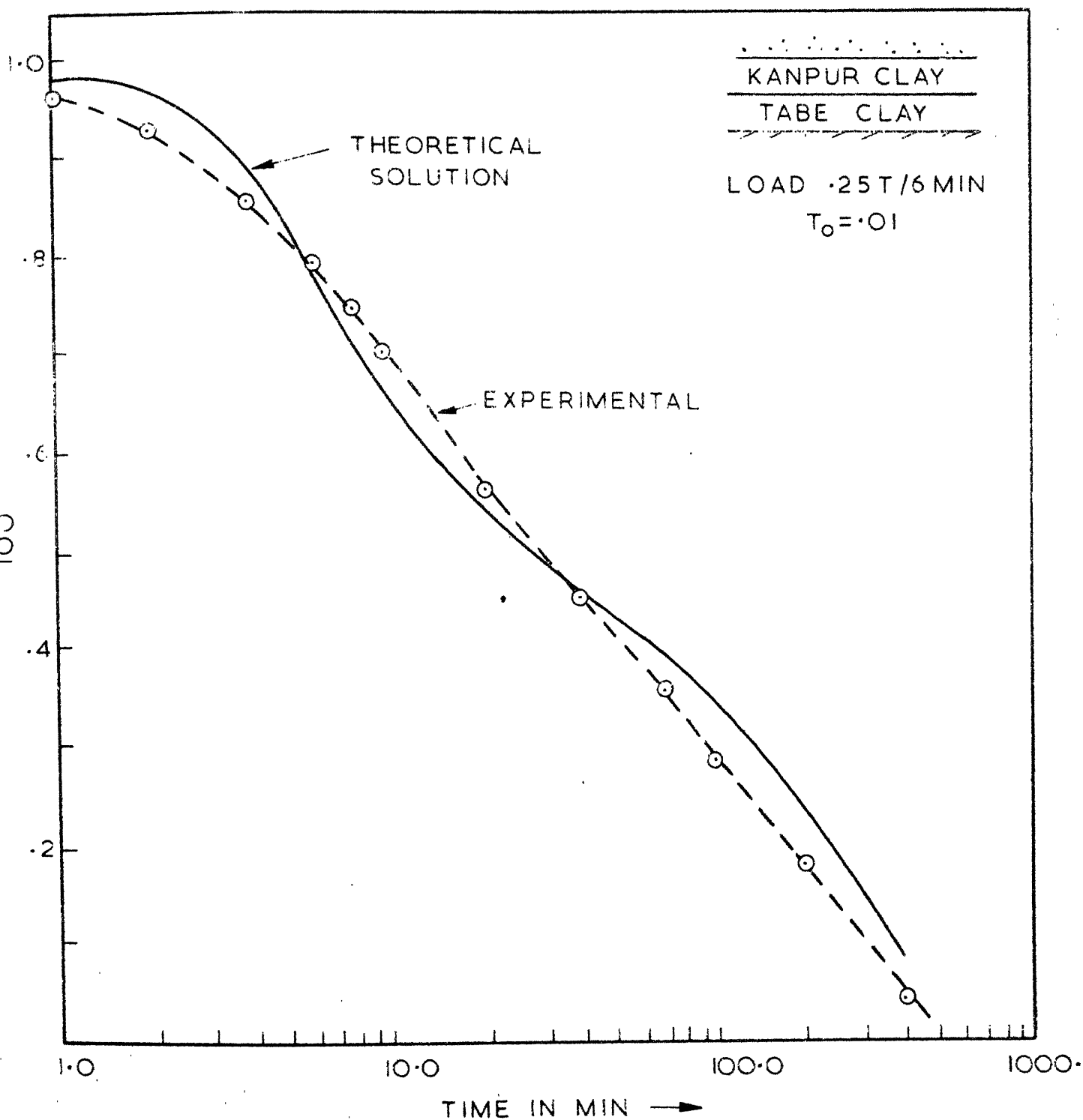


FIG. 5.15 CONSOLIDATION OF TWO LAYER SYSTEM UNDER CONSTRUCTION LOADING

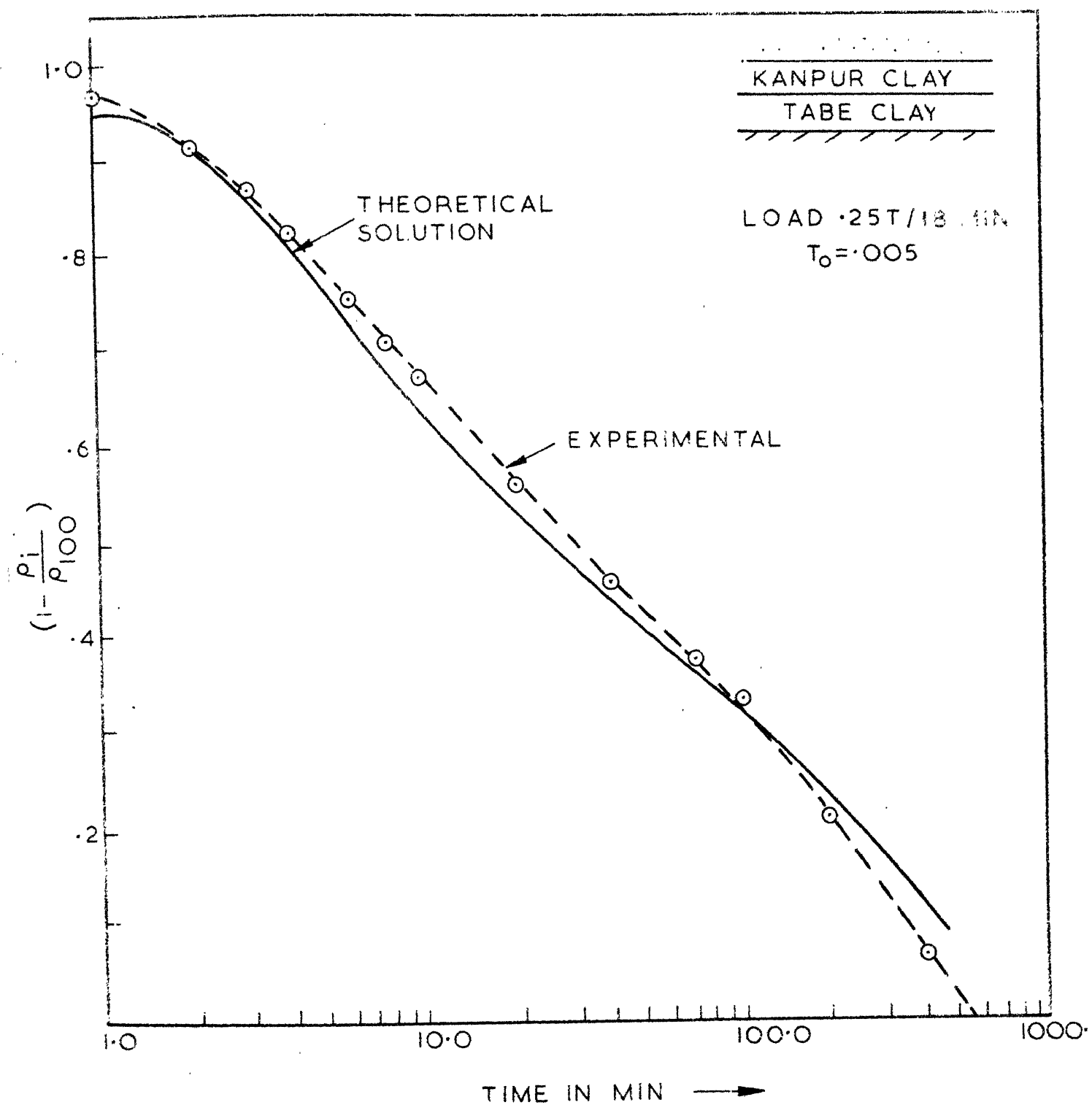


FIG. 5.16 CONSOLIDATION OF TWO LAYER UNDER CONSTRUCTION  
LOADING

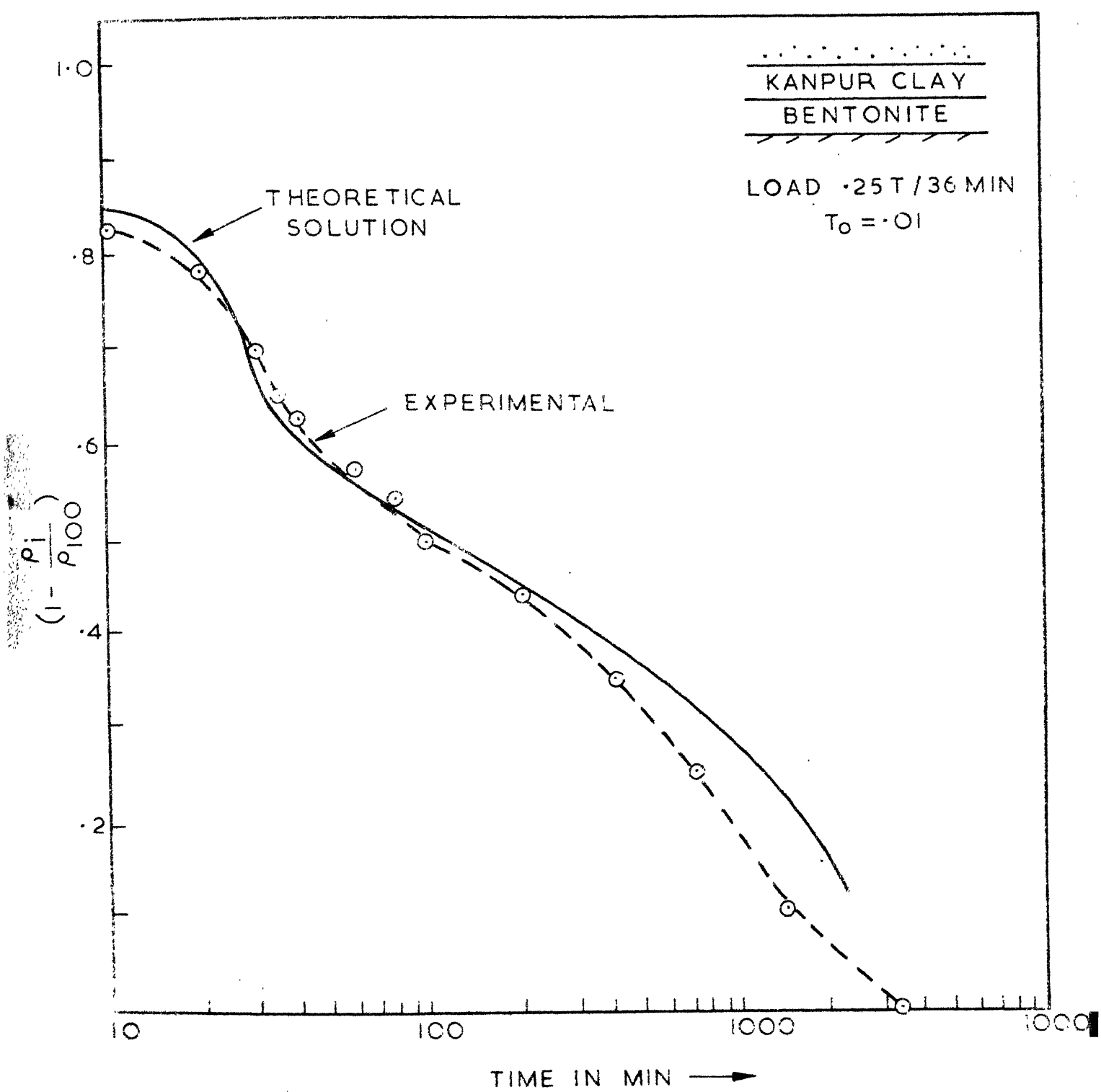


FIG. 5-17 CONSOLIDATION OF TWO LAYER SYSTEM UNDER CONSTRUCTION LOADING

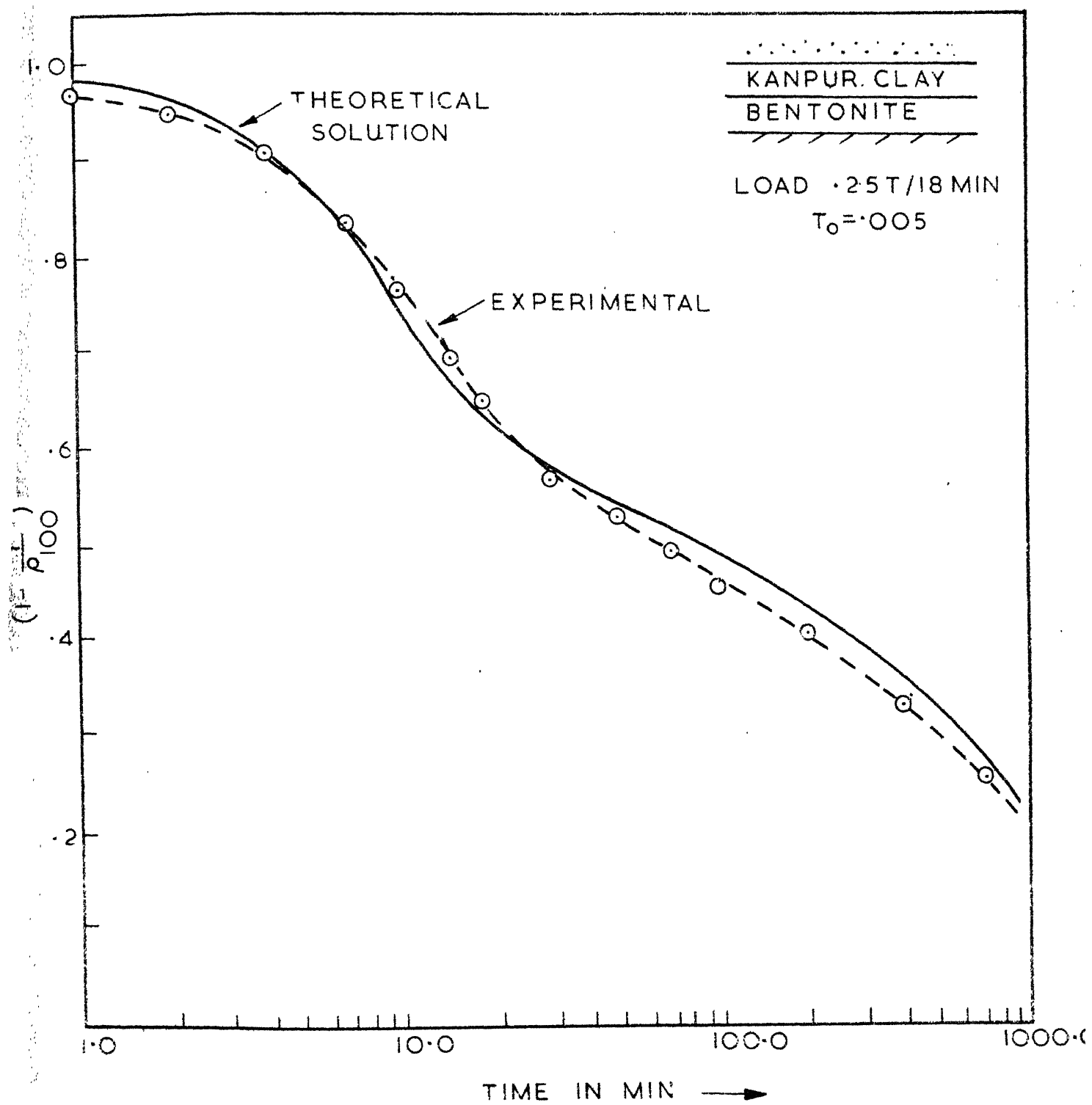


FIG. 5.18 CONSOLIDATION OF TWO LAYER SYSTEM UNDER CONSTRUCTION LOADING

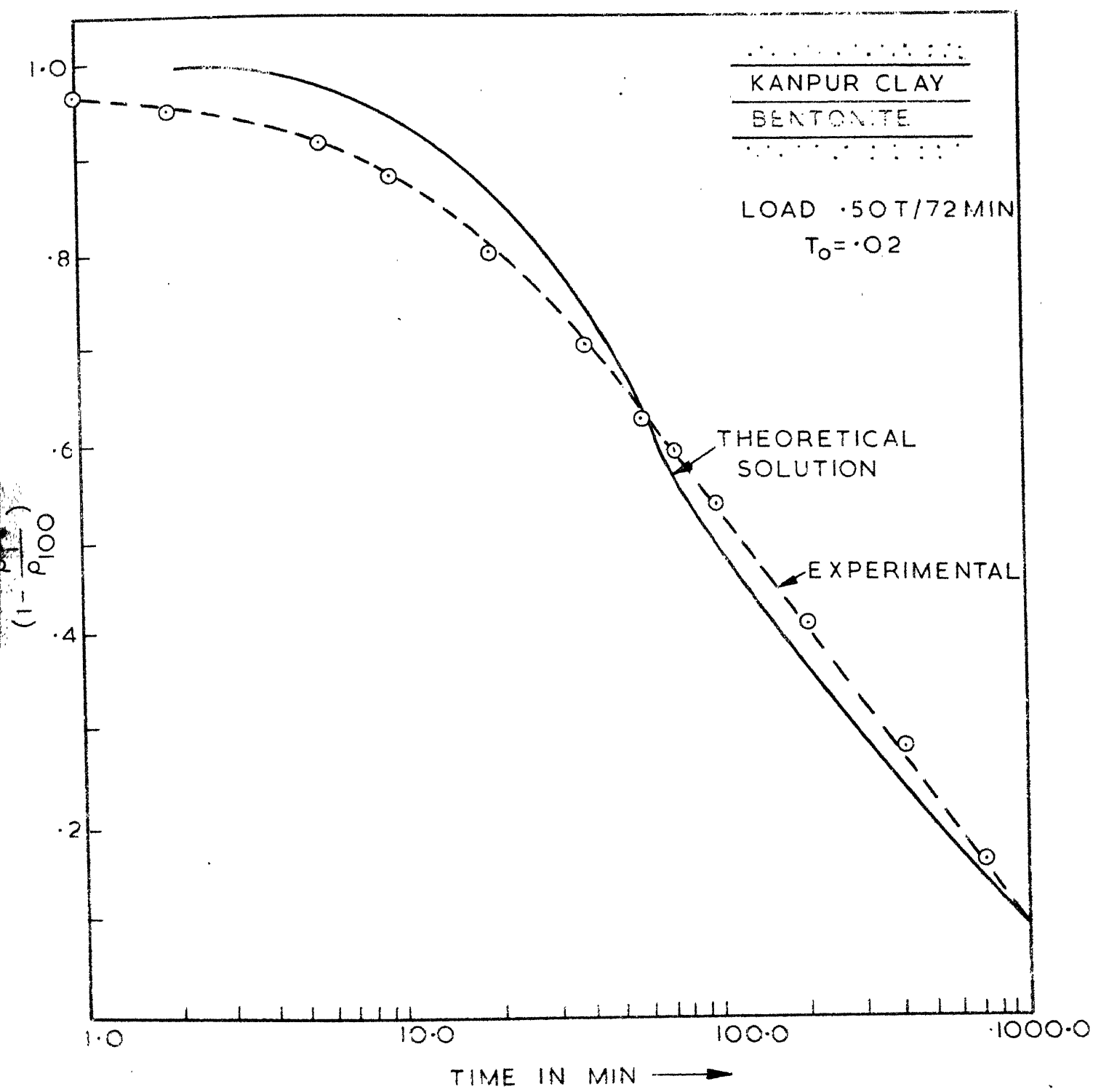


FIG. 5.19 CONSOLIDATION OF TWO LAYER SYSTEM UNDER CONSTRUCTION LOADING

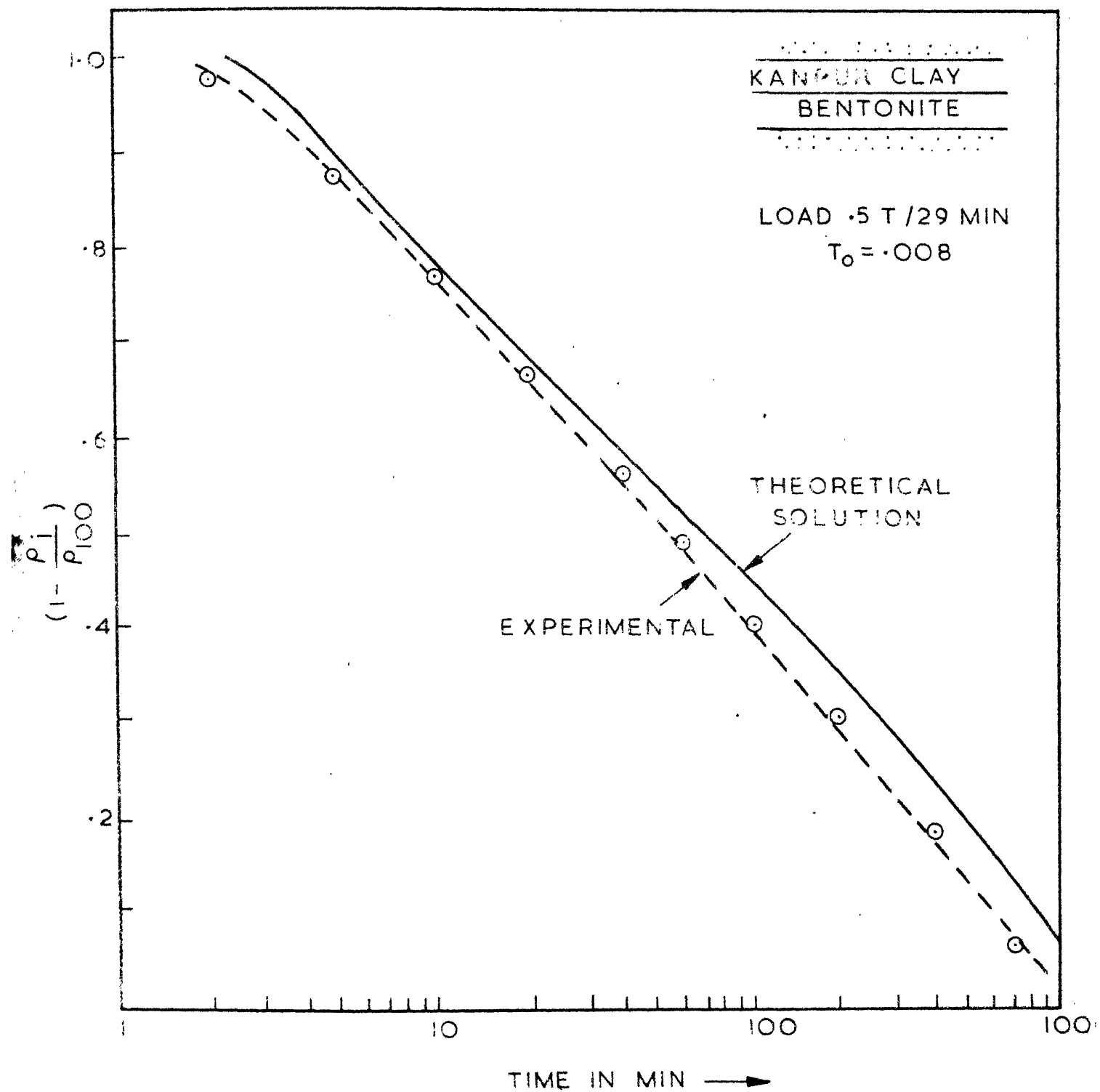


FIG. 5.20 CONSOLIDATION OF TWO LAYER UNDER CONSTRUCTION  
 LOADING

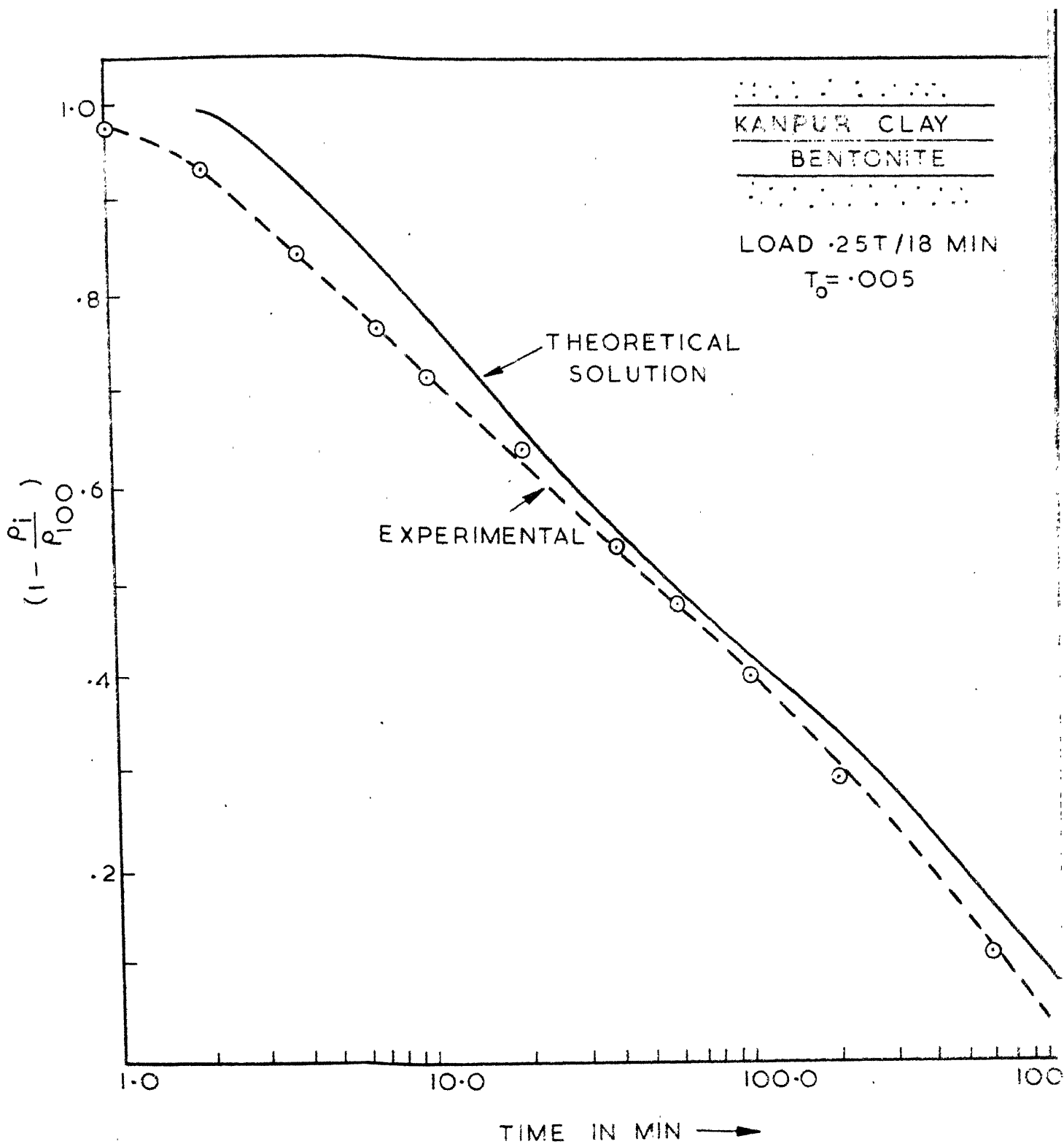


FIG. 5.21 CONSOLIDATION OF TWO LAYER SYSTEM UNDER COMPRESSION LOADING

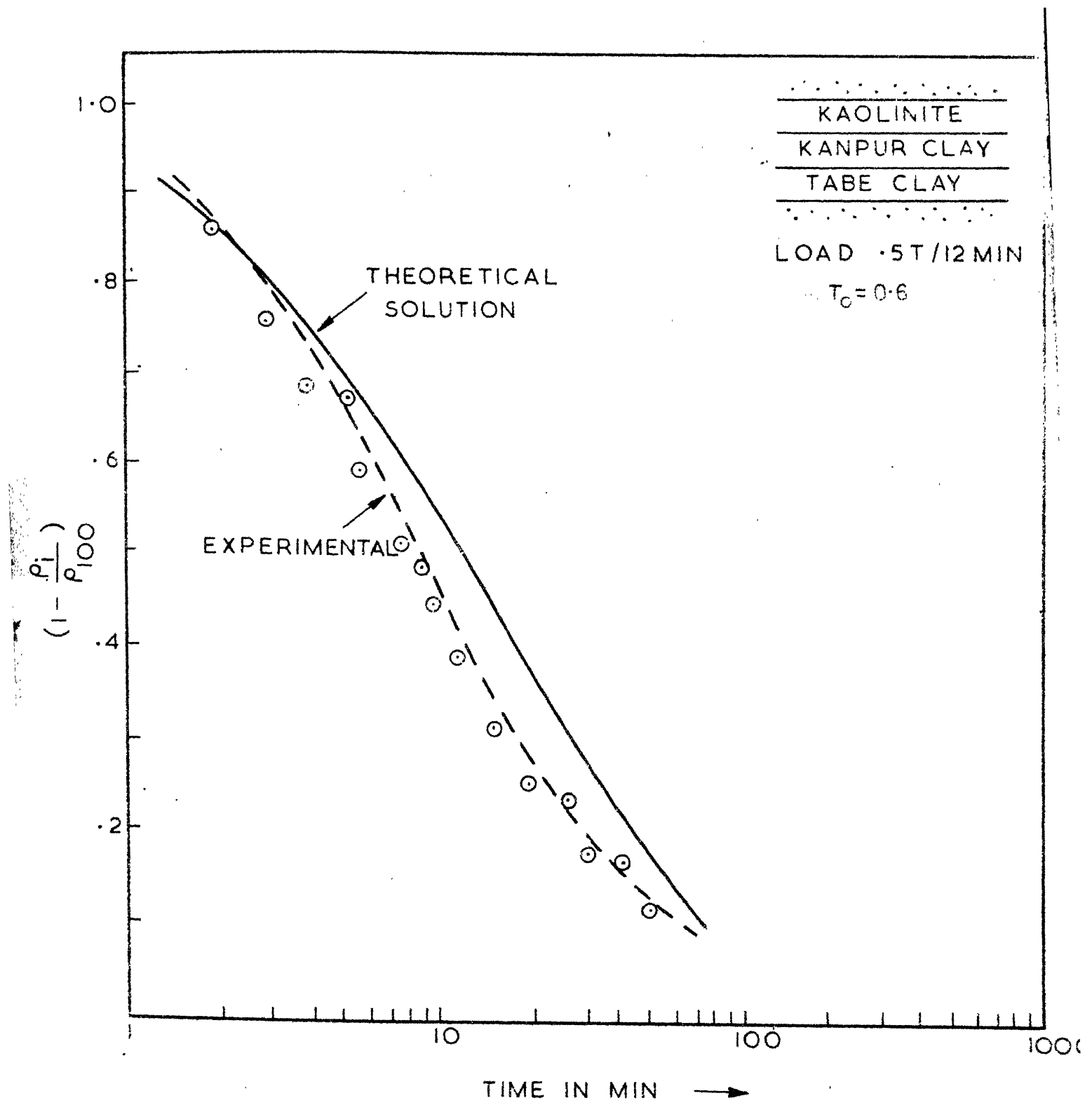


FIG. 5.22 CONSOLIDATION OF THREE LAYER SYSTEM UNDER CONSTRUCTION LOADING

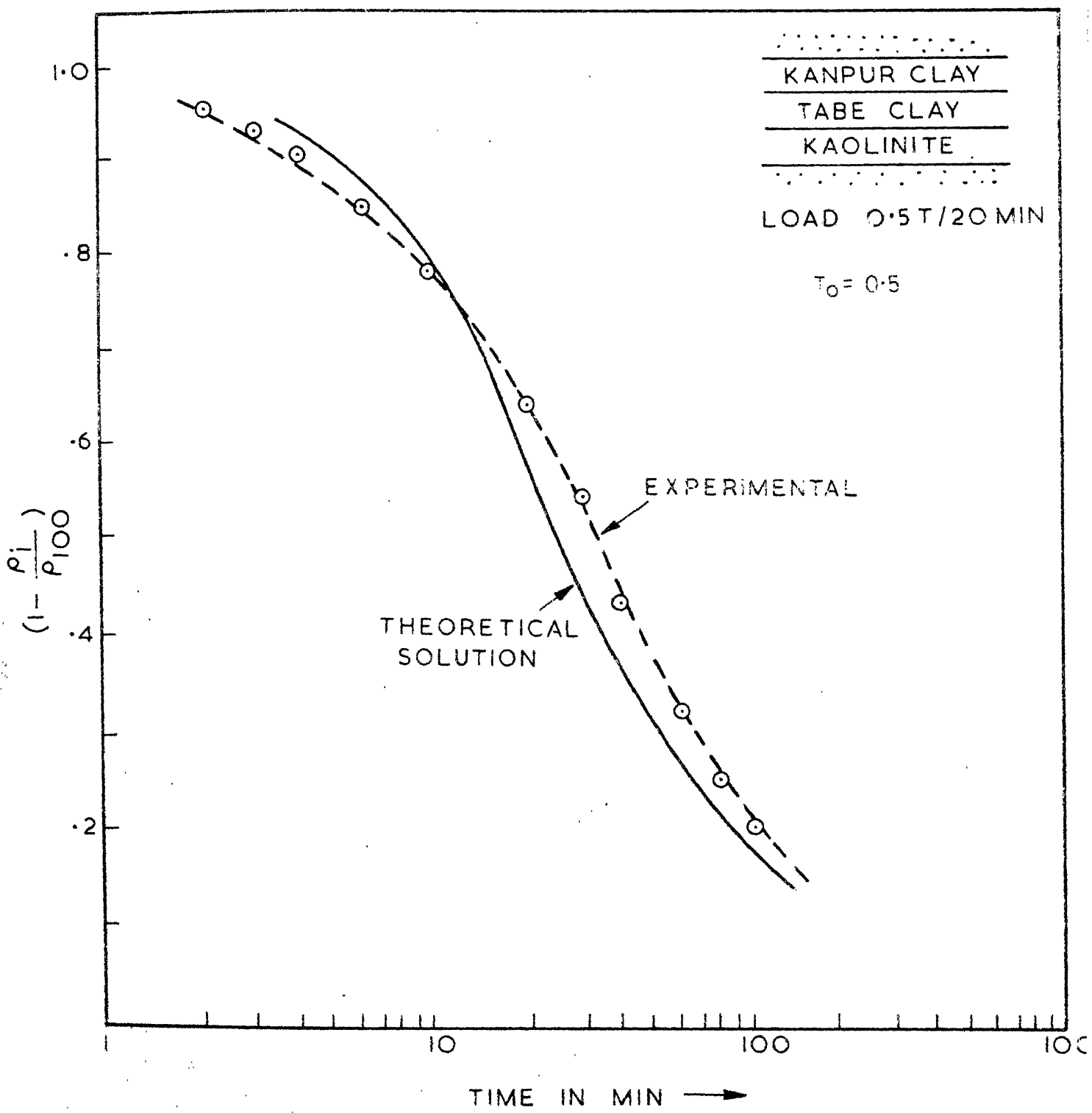


FIG. 5.23 CONSOLIDATION OF THREE LAYER SYSTEM UNDER CONSTRUCTION LOADING

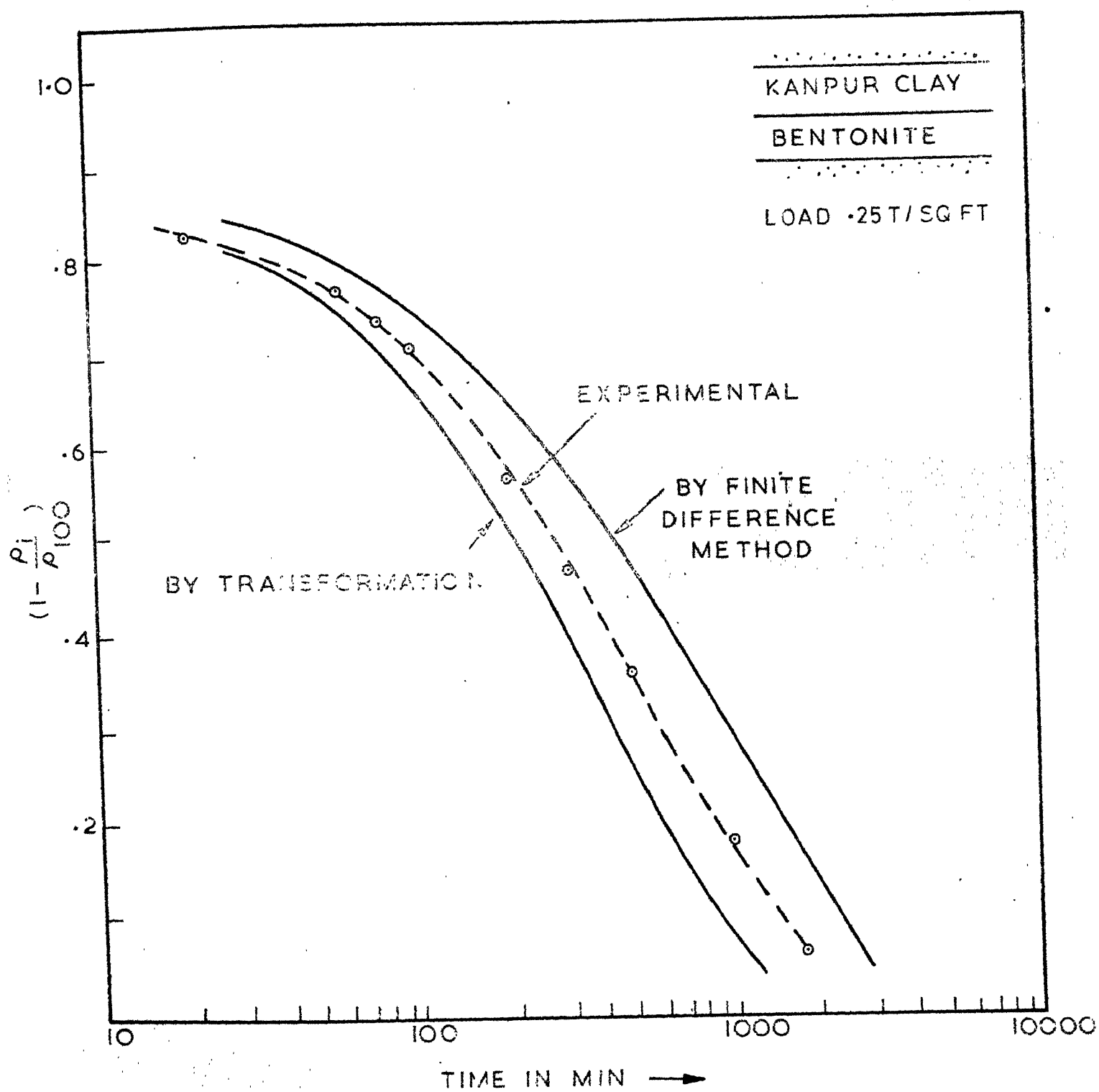


FIG.5.24 CONSOLIDATION OF TWO LAYER SYSTEM -  
INSTANTANEOUS LOADING

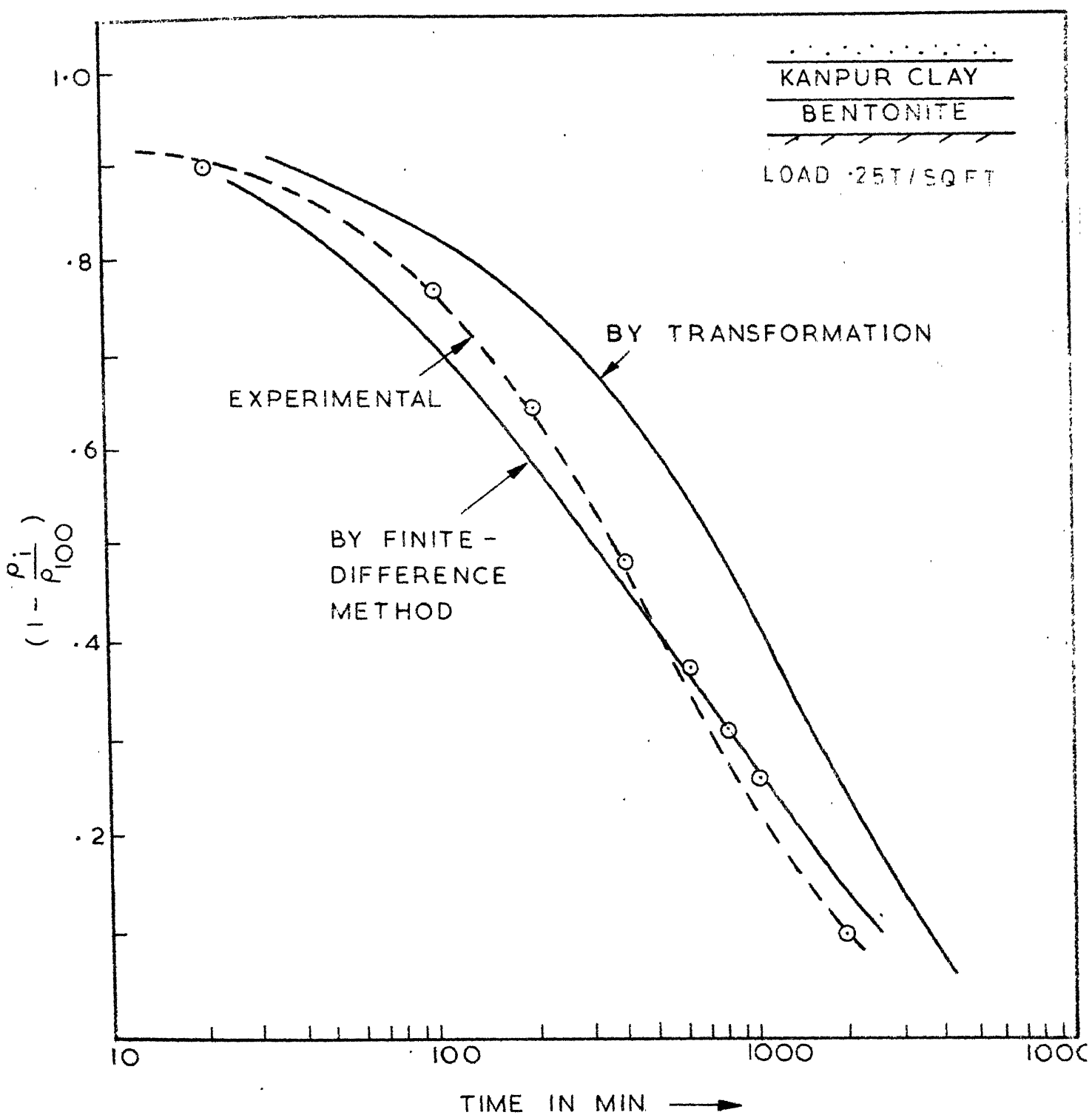


FIG. 5-25 CONSOLIDATION OF TWO LAYER SYSTEM-  
 INSTANTANEOUS LOADING

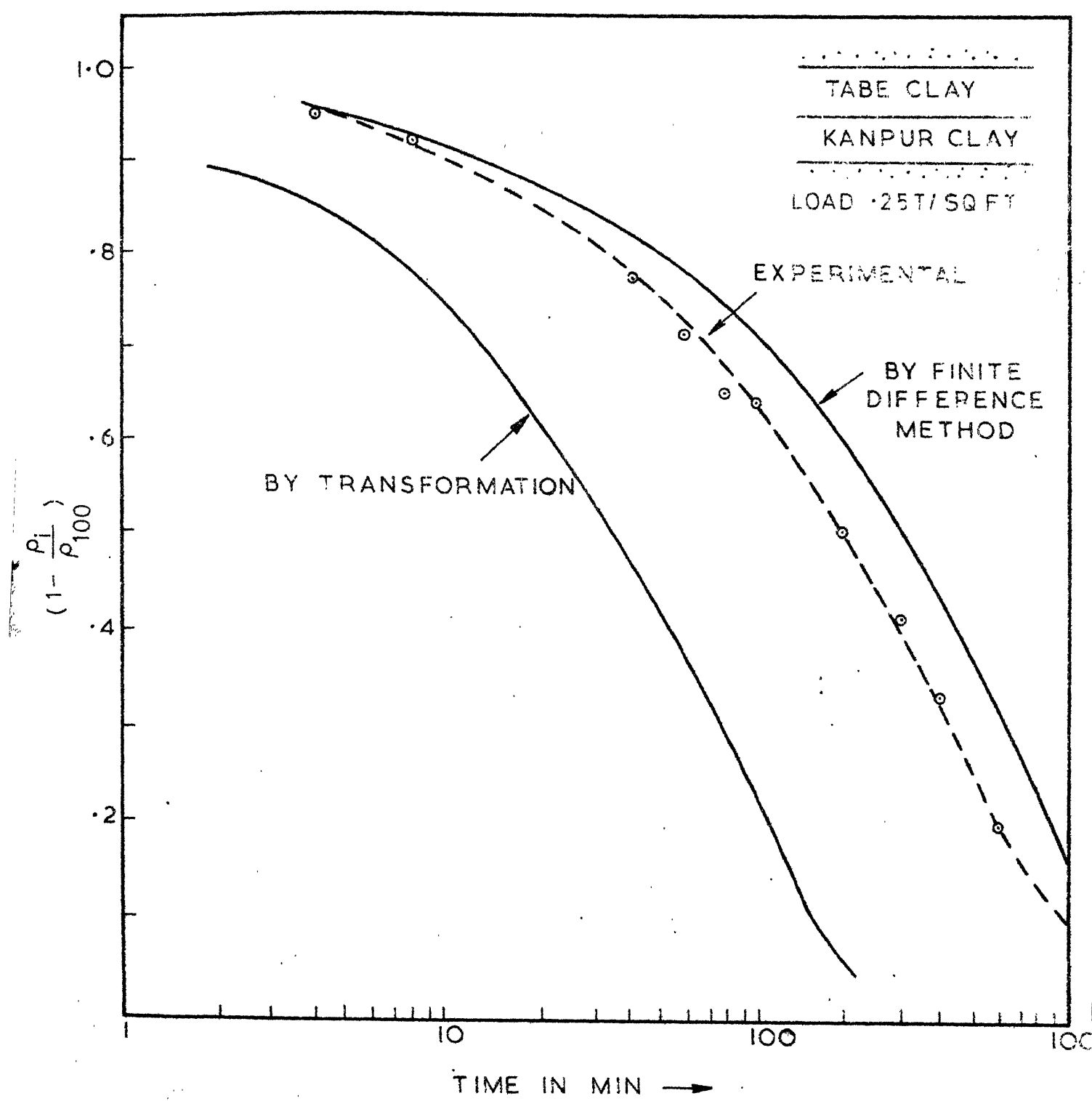


FIG.5.26 CONSOLIDATION OF TWO LAYER SYSTEM-  
INSTANTANEOUS LOADING

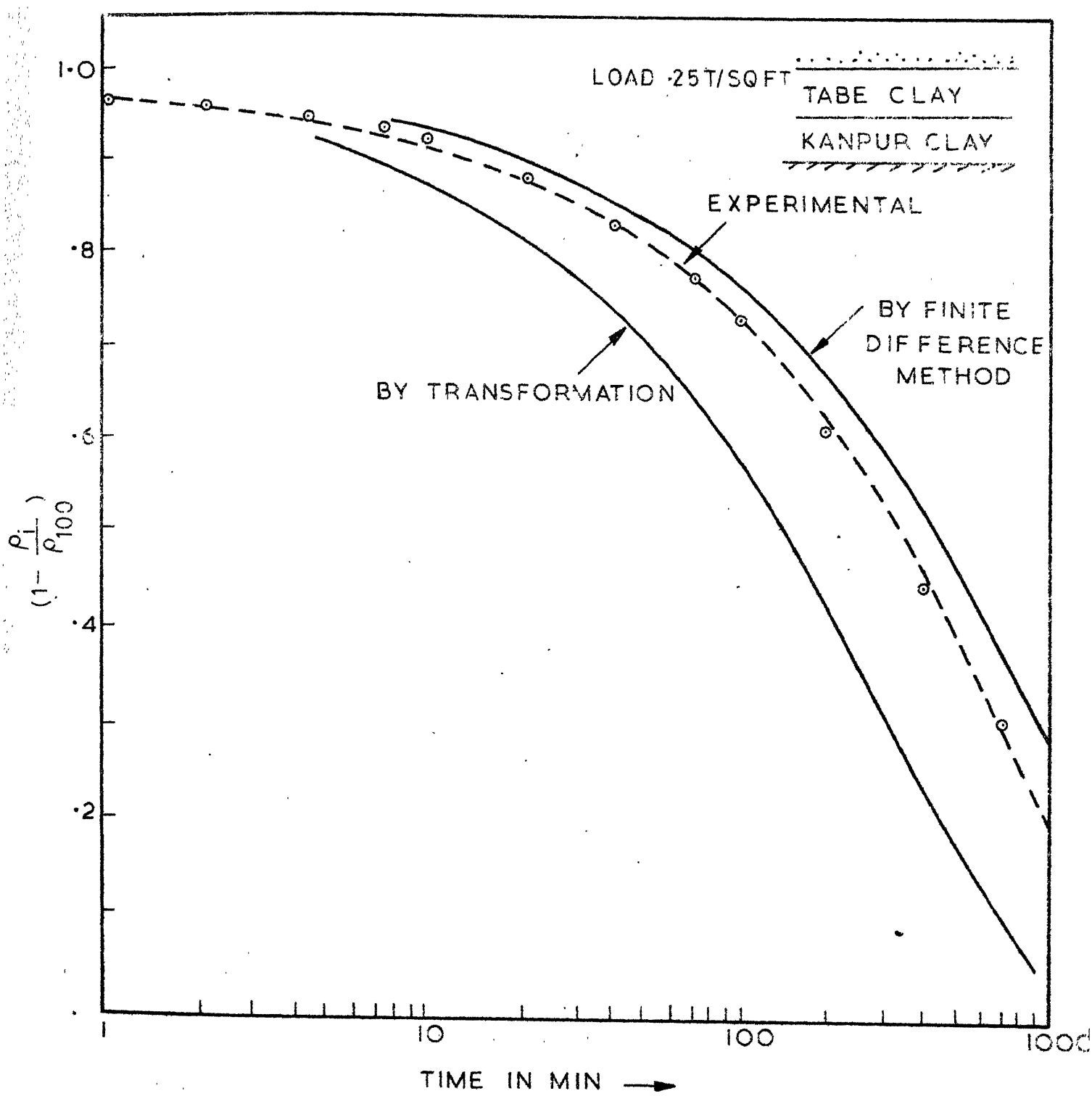


FIG. 5.27 CONSOLIDATION OF TWO LAYER SYSTEM-  
INSTANTANEOUS LOADING

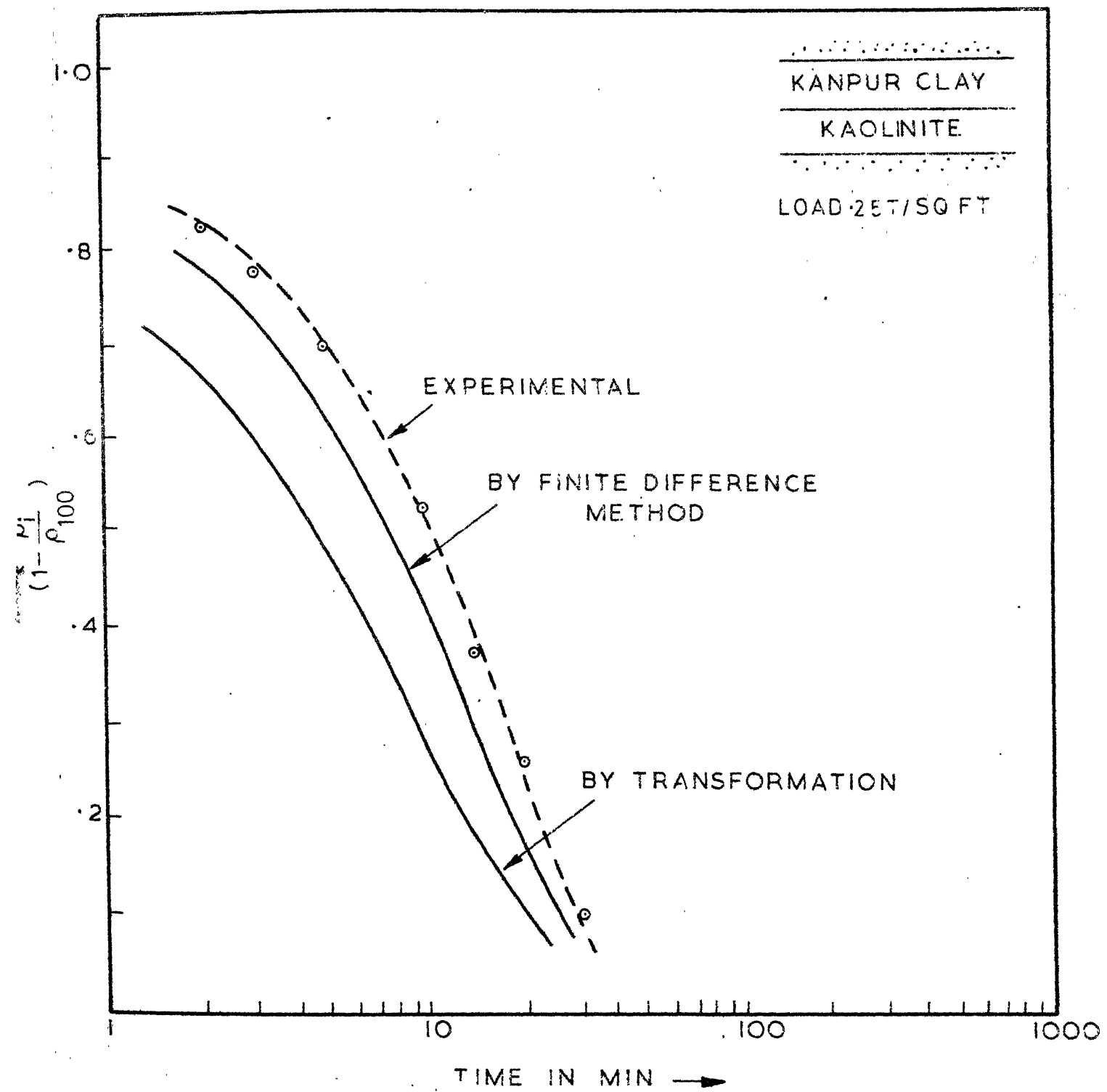


FIG. 5.28 CONSOLIDATION OF TWO LAYER SYSTEM-  
INSTANTANEOUS LOADING

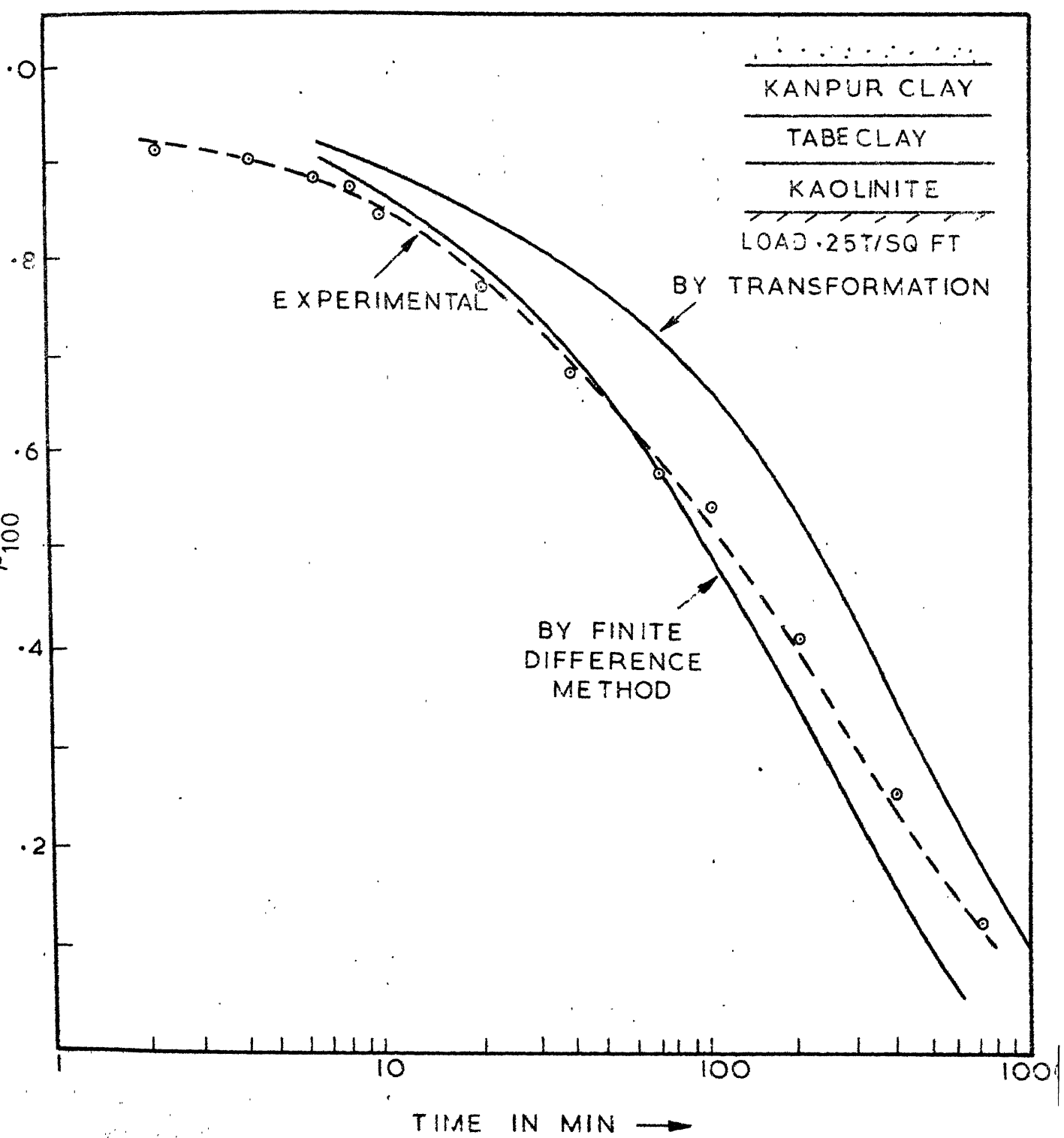


FIG. 5.29. CONSOLIDATION OF THREE LAYER SYSTEM-  
INSTANTANEOUS LOADING

## CHAPTER VI

### CONCLUSIONS AND RECOMMENDATIONS

#### CONCLUSIONS

An attempt is made in this research to obtain solutions to several complex field conditions and loading environments so as to arrive at certain general conclusions on the consolidation behaviour of soils subject to these conditions. A limited number of laboratory experiments duplicating some of the above situations have been conducted and the results are compared with the analytical solutions. The following conclusions summarise the findings of this investigation:

For a thick clay layer even though the coefficient of consolidation C is constant throughout the depth, the rate of consolidation is very much affected by the individual variation of k and m with respect to depth.

The location of the drainage boundary has significant influence on the consolidation characteristics of thick clay layer with single face drainage. The consolidation is faster when the drainage boundary is located on the side of higher k and m values.

A set of design charts for a thick clay layer under construction type of loading are presented. If appropriate field situations could be idealised under the various cases

presented, the design charts will be useful in predicting the field settlement.

A new formulation taking into account of the general variation of the consolidation parameters is presented. This forms a non-linear theory of a consolidating non-homogeneous thick clay layer with the parameters  $k$  and  $m$  varying during the process of consolidation. The solution is obtained by step-by-step numerical integration.

The effect of decrease of  $k$  during consolidation is found to be more than that of  $m$ .

Even though the coefficient of consolidation is constant throughout the depth and during consolidation, the rate of consolidation is influenced by the individual variation of  $k$  and  $m$ .

In layered systems the effects of extreme ranges of parameters of individual layers are studied. It is noted that a total dependence on the value of  $C$  for evaluating the consolidation characteristics of layered system will result in erroneous estimations. The relative magnitudes of  $k$  and  $m$  have much effects on the consolidation behaviour of layered systems. Therefore a layered system with layers of same coefficient of consolidation cannot be treated as single layer always.

A set of design charts in a two-layer system for a limited range of soil parameters is presented. This will be of use to predict the settlement rates in the field.

Closed form solutions are presented for single and two layer system under construction type of loading for single face as well as two face drainage. A three-layer system under construction loading is analysed by finite difference method. The solutions are illustrated with examples.

A simple experimental set-up is devised for testing layered systems under construction type of loading. Using four different types of soils, one-dimensional consolidation tests on layered systems up to three layers are conducted. The general trends of consolidation characteristics of layered systems under instantaneous as well as construction loading predicted by analytical procedures are found to be within reasonable limits of errors when compared with the experimental results.

In general, the simplified analysis yield very approximate estimates as compared with the more refined analysis presented here.

#### RECOMMENDATIONS

The following topics are recommended for further investigation.

Study of the variation of the consolidation parameters assuming more generalised functions such as:

$$k = k_0 \left\{ 1 + \alpha x \right\}^N \left\{ 1 - \gamma (1-p) \right\}^M$$

$$m = m_0 \left\{ 1 + \beta x \right\}^R \left\{ 1 - \mu (1-p) \right\}^S$$

where N, M, R and S are constants.

Experimental study in field to correlate the actual variation of consolidation parameters.

Experimental study on the consolidation behaviour of individual layers in layered systems with pore pressure measurements reflecting the effect of the location of drainage boundaries, the relative magnitudes of the consolidation parameters,

## LIST OF REFERENCES

1. Abbot, M.B., (1960),  
"One Dimensional Consolidation of Multilayered Soils",  
Geotechnique, Vol. 10, pp 151-165.
2. Anandakrishnan, M., (1960),  
"A Study of Some of the Variables of Consolidation  
Theory as Applied to Vertical Sand Drain Design",  
Ph.D. Thesis, University of Minnesota.
3. Barden, L. and Younan, N.A., (1969),  
"Consolidation of Layered Clays", Canadian Geotechnical  
Journal, 6, p.p. 413-429.
4. Bernt Jacobson, (1955),  
"Isotropy of Clays", Geotechnique, Vol. 5, p.p. 23.
5. Biot, M.A., (1941),  
"General Theory of Three Dimensional Consolidation",  
Journal of Applied Physics, Vol. 12, p.p. 155-164.
6. Biot, M.A., (1956),  
"General Solutions of Equations of Elasticity and  
Consolidation for a Porous Material", Trans. Journal  
of Applied Mechanics, A.S.M.E., Vol. 12, p.p. 521-541.
7. Brice Carnahan, Luther, H.A. and James O. Wilkes, (1969),  
"Applied Numerical Methods" - Wiley.
8. Carslaw, H.S., (1921),  
"The Cooling of Solid Sphere with a Concentric Core  
of Differential Material", Proc. Camb. Phil. Soc.,  
Vol. XX, p.p. 399.
9. Carslaw, H.S. and Jaeger, J.C., (1959),  
"Conduction of Heat in Solids", Oxford Univ. Press,  
London.
10. Churchill, R.V., (1936),  
"Temperature Distribution in a Slab", Duke Math.  
Journal, 2, p.p. 405.

11. Crawford, C.B., (1964),  
"Interpretation of Consolidation Test", Journal of  
the Soil Mechanics and Foundations Division, ASCE,  
Vol. 90, No. SM5, Proc. Paper 4056, p.p.87-101.
12. Davis, E.H. and Lee, I.K., (1969),  
"One Dimensional Consolidation of Layered Soils",  
Proc. VII International Conference of Soil Mechanics  
and Foundation Engineering, Mexico, p.p. 65-72.
13. Davis, E.H. and Poulos, H.B., (1968),  
"The Use of Elastic Theory for Settlement Prediction  
under Three Dimensional Conditions", Geotechnique,  
Vol. 18, p.p. 67-91.
14. Gray, Hamilton, (1945),  
"Simultaneous Consolidation of Contiguous Layers of  
Unlike Compressible Soils", Trans. ASCE, Vol. 110,  
p.p. 1327-1344.
15. Lambe, T.W., (1964),  
"Methods of Estimating Settlement", Proc. Journal of  
Soil Mechanics and Foundations Division, ASCE, Vol.  
90, SM5, p.p. 47-71.
16. Leonards, G.A. and Altchaeffl, A.G., (1964),  
"Compressibility of Clays", Proc. Journal of Soil  
Mechanics and Foundations Division, ASCE, Vol. 90,  
p.p. 133-155.
17. Mansur, C.L. and Dietrich, R.J., (1965),  
"Pumping Tests to Determine Permeability Ratio",  
Journal of Soil Mechanics and Foundations Division,  
ASCE, p.p. 151.
18. McNamee, J. and Gibson, R.E., (1960),  
"Displacement Functions and Linear Transforms Applied  
to Diffusion Through Porous Elastic Media", Quart.  
Journal of Mech. and App. Maths, Vol. 13, p.p. 98-111.
19. McNamee, J. and Gibson, R.E., (1960),  
"Plane Strain and Axially Symmetric Problems of  
Consolidation of a Semi-infinite Clay Stratum", Quart  
Journal of Mech. and App. Maths., Vol. 13, p.p.  
210-227.

20. Mitchell, J.K., (1964),  
Shearing Resistance of Soil as a Rate Process", Journal  
of Soil Mechanics and Foundations Division, ASCE, SM1,  
p.p. 29-61.
21. Moore, J. Peter and Spencer, K. Graham, (1969),  
"Settlement of Building on Deep Compressible Soil",  
Journal of Soil Mechanics and Foundations Division,  
ASCE, SM3, p.p. 769-790.
22. Palmer, L.A. and Brown, P.P., (1957),  
"Settlement Analysis for Areas of Continuing Subsidence",  
Proc. IV International Conference of Soil Mechanics and  
Foundation Engineering, Mexico, Vol. 1, p.p. 395-398.
23. Poskitt, T.T., (1969),  
"The Consolidation of Saturated Clay with Variable  
Permeability and Compressibility", Geotechnique, 19,  
No. 2, p.p. 234-252.
24. Raymond, G.P., (1965),  
"The Consolidation of Some Normally Consolidated Fine  
Grained Soils Subjected to Large Load Ratios and One  
Dimensional Drainage", O.J.H.R.P. Report No. 103,  
Queen's University, Canada.
25. Raymond, G.P. and Chou, H.T., (1966),  
"The Consolidation of Multilayered Soils Subjected to  
Large Load Ratios and One Dimensional Drainage",  
O.J.H.R.P. Report No. 104, Queen's University, Canada.
26. Raymond, G.P., (1969),  
"Consolidation of Deep Deposits of Homogeneous Clay",  
Geotechnique, 19, No. 4, p.p. 478-494.
27. Rendulic, L., (1935),  
"Ein Beitrag Zur Bestimmung der Gleitsicherheit", Der  
Bauingenien, No. 19/120.
28. Richart, F.E., (1957),  
"Review of the Theories for Sand Drains", Proc. ASCE,  
Vol. 109, p.p. 1155-1181.
29. Salvadori, M.G., and Baron, M.L., (1952),  
"Numerical Methods in Engineering" - Prentice-Hall.

30. Seed, H.B., (1964),  
"Settlement Analysis, A Review of Theory and Testing Procedure", Journal of Soil Mechanics and Foundations Division, ASCE, SM2, p.p. 39-48.
31. Scott, R.F., (1963),  
"Principles of Soil Mechanics" - Addison Wesley.
32. Schiffman, R.L., (1958),  
"Consolidation of Soil under Time Dependent Loading and Varying Permeability", Proc. H.R.B., Washington, Vol. 37, p.p. 584-617.
33. Schiffman, R.L., (1960),  
"Field Applications of the Consolidation of Soil under Time Dependent Loading and Varying Permeability", Bulletin 248, H.R.B., Washington.
34. Schiffman, R.L. and Gibson, R.E., (1964),  
"Consolidation of Non-homogeneous Clay Layers", Journal of Soil Mechanics and Foundations Division, ASCE, Vol. 90, SM5, p.p. 1-30.
35. Schiffman, R.L., Ladd and Chen, (1964),  
"The Secondary Consolidation of Clay", Paper Presented for the International Union of Theoretical and Applied Mechanics Symposium on Rheology and Soil Mechanics, Springer-Verlag.
36. Schiffman, R.L., Chen, A.T.F. and Jordan, J.C., (1969),  
"An Analysis of Consolidation Theories", Journal of Soil Mechanics and Foundations Division, ASCE, SM1, p.p. 285-312.
37. Smith, R.D. and Wahls, H.E., (1969),  
"Consolidation under Constant Rates of Strain", Journal of Soil Mechanics and Foundations Division, ASCE, SM2, p.p. 519-539.
38. Sneddon, I., (1957),  
"Elements of Partial Differential Equations", McGraw-Hill.
39. Sridharan, A. and Nagaraj, T.S., (1962),  
"One Dimensional Consolidation of Layered Soils", Journal of Institution of Engineers, India, 42, No. 11, p.p. 616-625.

40. "Symposium on Consolidation Testing of Soils", Special Technical Publication No. 126, ASCE, 195
41. Taylor, D.W., (1964),  
"Fundamentals of Soil Mechanics" - Asia Publishing.
42. Taylor, D.W., (1942),  
"Research on Consolidation of Clays", Publication of Dept. of Civil and Sanitary Engg., M.I.T.
43. Terzaghi, K., (1943),  
"Theoretical Soil Mechanics", John Wiley.
44. Tschebotarioff, G.P., (1936),  
"Comparison Between Consolidation, Elastic and other Soil Properties Established from Laboratory Tests and from Observations of Structures in Egypt", Proc. I International Conference of Soil Mechanics and Foundation Engineering, Vol. 1, p.p. 33-36.
45. Verigin, N.N., (1964),  
"Soil Consolidation under the Influence of an External Load Normal to the Boundary of Half Space", Rheology and Soil Mechanics, International Union of Theoretical and Applied Mechanics, Symp. Springer Verlag, p.p.231-234.
46. Verigin, N.N., (1965),  
"Consolidation of Saturated Soil upon the Action of External Load Normal to Boundary Half Space", Proc. VI International Conference of Soil Mechanics and Foundation Engineering, Vol. 1, p.p. 398-401.
47. Wahls, H.E., (1962),  
Analysis of Primary and Secondary Consolidation", Journal of Soil Mechanics and Foundations Division, ASCE, Vol.88, SM6, p.p. 207-231.
48. Wu, T, H, Reseudiz, D. and Nenbirchnen, R.J., (1966),  
"Analysis of Consolidation by Rate Process Theory", Journal of Soil Mechanics and Foundations Division, ASCE, SM6.
49. Zeevaert, (1949),  
"Results of Laboratory Investigation of the Organic Soft Clay Deposits of New Haven Harbour, Connecticut", Unpublished Report to Highway Department, State of Connecticut.

## APPENDIX

CONVERGENCE OF THE NUMERICAL RESULTS  
OF THE NON-LINEAR EQUATION 2.30

The numerical computation of the non-linear equation 2.30 for the particular case discussed, the convergence of the results are obtained as follows:

For:  $\alpha = -0.80$

$\beta = 4.00$

$\gamma = 0.50$

$\mu = 0.25$

At time factor  $T = 0.01$

At Depth X	VALUE OF PORE PRESSURE RATIO	
	For time interval = .0001	For time interval = .001
0	.000000	.000000
0.1	.636742	.645151
0.2	.925340	.93517
0.3	.991553	.994327
0.4	.999446	.999755
0.5	.999977	.999995
0.6	.999999	1.000000
0.7	.999988	.999993
0.8	.999600	.999703
0.9	.987463	.988543
1.0	.000000	.000000

Steps in solving two layer system  
under construction loading

The equations to be solved are:

$$\frac{\partial^2 u_1}{\partial p^2} + d_1 = \frac{\partial u_1}{\partial T} \quad (1)$$

$$\frac{\partial^2 u_2}{\partial p^2} + d_2 = \mu^2 \frac{\partial u_2}{\partial T} \quad (2)$$

The boundary conditions are as given by Eq. 4.20.

Using the Laplace Transformation defined as:

$$L\{u_1\} = \int_0^\infty e^{-st} u_1 dt = v_1 \quad (3)$$

$$L\{u_2\} = \int_0^\infty e^{-st} u_2 dt = v_2 \quad (4)$$

The Eqs. (1) and (2) are transformed as:

$$\frac{d^2 v_1}{dp^2} + \frac{d_1}{s} = s v_1 \quad (5)$$

$$\frac{d^2 v_2}{dp^2} + \frac{d_2}{s} = \mu^2 s v_2 \quad (6)$$

Now the transformed boundary conditions to be satisfied by the Eqs. (5) and (6) are:

$$\text{At } p = 0 \quad v_1 = 0 \quad (7)$$

$$p = 1 + v \quad v_2 = 0 \quad (8)$$

$$p = 1 \quad v_1 = v_2 \quad (9)$$

$$k_1 \frac{\partial v_1}{\partial p} = k_2 \frac{\partial v_2}{\partial p} \quad (10)$$

The solutions of the ordinary differential equations (5) and (6) satisfying the boundary conditions (7) and (8) only are:

$$v_1 = \frac{d_1}{s^2} \left\{ 1 - \cos h \sqrt{s} p + M \sin h \sqrt{s} p \right\} \quad (11)$$

$$v_2 = \frac{d_1}{s^2} \left\{ 1 - \cos h (1+v-p) \sqrt{s} + N \sin h (1+v-p) \sqrt{s} \right\} \quad (12)$$

Where  $M$  and  $N$  are constants to be evaluated satisfying the boundary conditions (9) and (10).

Using the notation  $A = \sqrt{s}$  and substituting the boundary conditions (9) and (10):

$$M = \frac{-\sigma \sin h A \sin h A \mu v + \cos h A \cos h A \mu v - 1}{\sin h A \cos h A \mu v + \cos h A \sin h A \mu v} \quad (13)$$

$$N = \frac{\sigma \cos h A \cos h A \mu v - \sin h A \sin h A \mu v - \sigma}{\sin h A \cos h A \mu v + \cos h A \sin h A \mu v} \quad (14)$$

Therefore,

$$v_1 = \frac{d_1}{A^4} \left\{ 1 - \cosh A p + \frac{-\sigma \sinh A \sinh A \mu v + \cosh \cosh A \mu v - 1}{\sinh A \cosh A \mu v + C \cosh A \sinh A \mu v} \sinh A p \right\} \quad (15)$$

To find out the final solution, the Inversion Theorem of the Laplace Transformation is used:

$$v_1(T) = \frac{1}{2\pi i} \int_{\zeta-i\infty}^{\zeta+i\infty} e^{st} v_1(s) ds \quad (16)$$

Where  $\zeta$  is to be so large to include all the singularities of the integrand in Eq. (16).

The line integral of Eq. (16) is found out by using the well-known Residue Theorem.

The integrand as per Eq. (14). has simple poles at  $s = 0$ , and  $s = -A_i^2$  where  $A_i$  are the roots of the following equation

$$\sin A \cos A \mu v + \sigma \cos A \sin A \mu v = 0 \quad (17)$$

Also the above equation has all roots real and simple (8, 9, 10). Therefore:

$$v_1(T) = \frac{1}{2\pi i} \times 2\pi i \left\{ \text{Res}_{s=0} + \text{Res}_{s=-A_i^2} \right\} \quad (18)$$

To find the residues:

The denominator is obtained as:

$$ds(\sin A \cos A\mu\nu + \sigma \cos A \sin A\mu\nu) \quad (19)$$

$$\begin{aligned} &= A \left\{ \mu\nu \sin A \sin A\mu\nu - \cos A \cos A\mu\nu \right. \\ &\quad \left. - \sigma \mu\nu \cos A \cos A\mu\nu + \sin A \sin A\mu\nu \right\} \\ &= A\mu\nu \left\{ \sin A \sin A\mu\nu - \sigma \cos A \cos A\mu\nu \right\} \\ &\quad - A \left\{ -\sigma \sin A \sin A\mu\nu + \cos A \cos A\mu\nu \right\} \end{aligned}$$

Using Eq. (22) the above expression is simplified as follows:

$$\begin{aligned} &= A\mu\nu \left\{ \sin A \sin A\mu\nu + \frac{\cos^2 A\mu\nu \sin A}{\sin A\mu\nu} \right\} \\ &\quad - A \left\{ \frac{\sin^2 A \cos A\mu\nu}{\cos A} + \cos A \cos A\mu\nu \right\} \\ &= \frac{A\mu\nu}{\sin A} \sin A - A \frac{\cos A\mu\nu}{\cos A} \\ &= \frac{A\mu\nu}{\sin A\mu\nu} \sin A + A \frac{\sin A\mu\nu}{\sin A} \\ &= \frac{A}{\sin A \sin A\mu\nu} \left\{ \mu\nu \sin^2 A + \sigma \sin^2 A\mu\nu \right\} \quad (20) \end{aligned}$$

The Numerator is obtained as:

The contribution by the first two terms of the Eq. (15) is zero, so the remaining terms are:

$$\left\{ -\sigma \sin A \sin A\mu\nu + \cos A \cos A\mu\nu - 1 \right\} \sin A \quad (21)$$

Using the Eq.(16) and the expression (20), the Residue when  $s = 0$  i.e. obtained as:

$$\Sigma \frac{2d_1}{A^3} \frac{\sigma \sin^2 A\mu v + \sin A \sin A\mu v}{\mu v \sin^2 A + \sigma \sin^2 A\mu v} \sin Ap \quad (22)$$

And the Residue at  $s = -A_i^2$  is obtained as:

$$\Sigma \frac{2d_1}{A^3} \cdot \frac{\sigma \sin^2 A\mu v + \sin A \sin A\mu v}{\mu v \sin^2 A + \sigma \sin^2 A\mu v} \sin Ap e^{-A^2 T} \quad (23)$$

Therefore, the final solution  $v_1(p, T)$  is put in the form as given in Eq. 4.21.

## VITA

T. Kuppusamy was born on 27th April, 1940, at Pondicherry. He was married to Rajeswari in July 1962 and has two sons, Mohan and Gandhiraj.

He was awarded Bachelor's Degree in Civil Engineering from Madras University in 1962, and Master's Degree in Soil Mechanics and Foundation Engineering from Indian Institute of Technology, Madras, in 1967. He is a member of Indian National Society of Soil Mechanics and Foundation Engineering.

He was working in Public Works Department, Pondicherry during 1962-1964 and in the faculty of Motilal Nehru Polytechnic, Pondicherry during 1964-1965.

